

# PRECISION MEDICINE IN NON-SMALL CELL LUNG CANCER

Improving dosing strategies

René J. Boosman



PRECISION MEDICINE  
IN NON-SMALL CELL  
LUNG CANCER  
Improving dosing strategies

René J. Boosman

The research described in this thesis was performed at the Department of Pharmacy & Pharmacology, the Netherlands Cancer Institute – Antoni van Leeuwenhoek Hospital, Amsterdam, The Netherlands, in collaboration with other institutes.

Printing of this thesis was financially supported by the Oncology Graduate School Amsterdam.

ISBN: 978-94-6458-024-2

**Cover design and layout**

© evelienjagtman.com

**Print**

Ridderprint

© René J. Boosman, 2022

# PRECISION MEDICINE IN NON-SMALL CELL LUNG CANCER

## Improving dosing strategies

**Precisiegeneeskunde in niet-kleincellig longkanker**

Het verbeteren van de doseerstrategieën

(met een samenvatting in het Nederlands)

### **Proefschrift**

ter verkrijging van de graad van doctor aan de Universiteit Utrecht  
op gezag van de rector magnificus, prof. dr. H.R.B.M. Kummeling,  
ingevolge het besluit van het college voor promoties  
in het openbaar te verdedigen op

maandag 30 mei 2022 des middags te 2.15 uur

door

**René Johan Boosman**

geboren op 23 juli 1994  
te Assen

**Promotoren:**

Prof. dr. A.D.R. Huitema

Prof. dr. J.H. Beijnen

**Copromotoren:**

Dr. N. Steeghs

Dr. R. ter Heine

## TABLE OF CONTENTS

Preface and thesis outline	9
<b>Part 1 - Introduction</b>	<b>15</b>
<b>Chapter 1</b> Optimized dosing: the next step in precision medicine of non-small cell lung cancer <i>Drugs. 2021;82(1):15-32</i>	17
<b>Part 2 - Boosting drugs to enhance exposure or diminish resistance to therapy</b>	<b>47</b>
<b>Chapter 2.1</b> Cytochrome P450 3A4, 3A5 and 2C8 expression in breast, prostate, lung, endometrial and ovarian tumors: relevance for resistance to taxanes <i>Cancer Chemother Pharmacol. 2019;84(3):487-499</i>	49
<b>Chapter 2.2</b> Ritonavir-boosted exposure of kinase inhibitors: an open label, single-arm pharmacokinetic proof-of-concept trial with erlotinib <i>Pharm Res. 2022 [Epub ahead of print]</i>	73
<b>Part 3 - Prediction of pharmacokinetics</b>	<b>87</b>
<b>Chapter 3.1</b> Optimization of chemotherapy in the era of immunotherapy <i>Eur Respir J. 2018;52(4):1801698</i>	89
<b>Chapter 3.2</b> Rethinking the application of pemetrexed for patients with renal impairment: a pharmacokinetic analysis <i>Clin Pharmacokinet. 2021;60(5):649-654</i>	95
<b>Chapter 3.3</b> Optimized versus standard dosing of pemetrexed – a randomized controlled trial <i>Submitted</i>	115
<b>Chapter 3.4</b> Prediction of the pharmacokinetics of pemetrexed with a low test dose: a proof-of-concept study <i>Submitted</i>	129
<b>Chapter 3.5</b> Is age just a number? A population pharmacokinetic study of gemcitabine <i>Cancer Chemother Pharmacol. 2022 [Epub ahead of print]</i>	141
<b>Part 4 - Exposure-response relationships</b>	<b>157</b>
<b>Chapter 4.1</b> Exposure-response analysis of osimertinib in EGFR mutation positive non-small cell lung cancer patients in a real-life setting <i>Submitted</i>	159
<b>Chapter 4.2</b> Toxicity of pemetrexed during renal impairment explained – implications for safe treatment <i>Int J Cancer. 2021;149(8):1576-1584</i>	173

<b>Chapter 4.3</b>	Cumulative pemetrexed dose increases the risk of nephrotoxicity	205
--------------------	---	-----

*Lung Cancer. 2020;146:30-35*

---

<b>Appendices</b>		221
-------------------	--	-----

---

Conclusions and future perspective		223
------------------------------------	--	-----

Summary		233
---------	--	-----

Nederlandse samenvatting		241
--------------------------	--	-----

Author affiliations		249
---------------------	--	-----

List of publications		255
----------------------	--	-----

Dankwoord		261
-----------	--	-----

Curriculum vitae		267
------------------	--	-----

---







# PREFACE AND THESIS OUTLINE



## PREFACE

In 2020, lung cancer remained the world's leading cause of cancer death and in the same year approximately 2.2 million new cases of lung cancer arose.<sup>1</sup> Since the era of precision medicine commenced, treatment strategies of non-small cell lung cancer (NSCLC) are swiftly evolving. For example, molecular profiling is now extensively used to select the drug which offers most benefit for the individual patient.<sup>2</sup> However, for most of the therapeutic options for NSCLC (small-molecule inhibitors (SMIs), cytotoxic agents and monoclonal antibodies (MAbs)) the doses are still based on a "one size fits all" approach. Nonetheless, for many of these drugs, there is a rationale to optimize the dose of the individual patient or the general population with the aim to improve efficacy, reduce toxicity, increase quality of life and/or reduce the financial burden.

First, during drug development, the recommended dose is determined in phase I studies. The methodology of these studies are currently still based on the pharmacology of the cytotoxic agents and focus mainly on toxicity rather than efficacy.<sup>3</sup> However, the pharmacological profiles of the SMIs and MAbs are essentially different, raising questions whether this dose finding approach for these drugs is valid.

Secondly, in the phase I studies, a small homogenous group of heavily pretreated patients is studied.<sup>4</sup> These patients often do not reflect the general lung cancer population. Moreover, despite the fact that during drug development manufacturers are required to investigate clinically relevant covariates for pharmacokinetics, the dose is often developed for prescriber convenience, rather than for the individual. Consequently, dosing of drugs based on variables with limited effect on the pharmacokinetics will not decrease the already high variability in pharmacokinetic drug exposure.<sup>5-7</sup> Since there is often a fine balance between exposure and response of the SMIs and cytotoxic agents, this increase in pharmacokinetic variability will inevitably lead to suboptimal treatment outcomes. For example, in patients with an impaired clearance of drugs (e.g. impaired renal or hepatic function, older age or use of interacting drugs), the current doses might yield supratherapeutic drug exposure.<sup>8</sup> Since dose adaptations are only performed in case of treatment-related adverse events, these patients are confronted with toxic levels already at the start of therapy. Meanwhile, patients with an above average clearance of drugs (e.g. higher than average renal function or use of interacting drugs) are confronted with subtherapeutic exposure, which might ultimately lead to treatment failure.<sup>9</sup>

Lastly, treatment costs for the new targeted therapies are rising faster than ever before, contributing to the financial pressure on the current public health budget.<sup>10</sup> Since there is a high incidence of NSCLC, cost-ineffective dosing based on poor predictors of systemic exposure will result in unnecessary high health care costs. Therefore, it is pivotal to tackle the current imprecisions in precision medicine. This quest can be achieved by implementation of the correct dose from the first dose onwards based on patient(group) variables and/or pharmacokinetic-guided dosing based on measured drug concentrations.

## THESIS OUTLINE

Taken all considerations into account, the current dosing strategies can be improved. This thesis focuses on the dose optimization for the current therapeutic options of NSCLC.

In **Part I, Chapter 1**, the position of dose optimizations in the current dosing strategies is addressed and the rationale behind several other potential strategies is discussed. In **Part II**, the inhibition of metabolic enzymes of anticancer drugs by protease inhibitors is described. **Chapter 2.1** addresses the intratumoral expression of taxane-metabolizing enzymes in solid tumors. In addition, it provides a rationale for concomitant intake with CYP3A4 inhibitors to boost intratumoral taxane exposure. **Chapter 2.2** illustrates a proof-of-concept study in which the effect of ritonavir on the exposure of erlotinib is studied. **Part III** focusses on predictors for the pharmacokinetic exposure of drugs. In this part, both covariate-based and pharmacokinetic-guided dosing strategies are addressed. **Chapter 3.1** provides a rationale for the inclusion of renal function on the exposure to pemetrexed. In **Chapter 3.2**, a pharmacokinetic analysis is performed to assess the impact of renal function on the pharmacokinetic exposure of pemetrexed based on phase I study data. Moreover, in **Chapter 3.3** this relationship was further evaluated in a clinical study in patients with adequate renal function. This study investigated the superiority of a renal function-based dosing versus the conventional body surface area (BSA)-based dosing of pemetrexed. To assess if pharmacokinetic-derived dosing would be an alternative dosing strategy, **Chapter 3.4** shows the relationship between the pharmacokinetics of a low dose and a therapeutic dose of pemetrexed. Finally, in **Chapter 3.5**, the impact of age on the pharmacokinetics of gemcitabine is investigated. **Part IV** illustrates the relationships between exposure to drugs and the efficacy and toxicities are described. In **Chapter 4.1**, the exposure-response relationship of osimertinib is studied. The exposure to pemetrexed and the development of hematological toxicities and nephrotoxicity are described in **Chapter 4.2 and 4.3**, respectively.

Finally, the general conclusions of the gathered work and the future perspectives arising out of them are discussed, followed by a summary of the individual chapters featured in this thesis.

## REFERENCES

1. The Global Cancer Observatory. Cancer fact sheet trachea, bronchus and lung, 2020. Accessed on 15 Dec 2021.
2. Calvayrac O, Pradines A, Pons E, Mazières J, Guibert N. Molecular biomarkers for lung adenocarcinoma. *Eur Respir J*. 2017;49(4):1601734. <https://doi.org/10.1183/13993003.01734-2016>.
3. Mathijssen RH, Sparreboom A, Verweij J. Determining the optimal dose in the development of anticancer agents. *Nat Rev Clin Oncol*. 2014;11(5):272-281. <https://doi.org/10.1038/nrclinonc.2014.40>.
4. Stronks K, Wieringa NF, Hardon A. Confronting diversity in the production of clinical evidence goes beyond merely including under-represented groups in clinical trials. *Trials*. 2013;14(1):177. <https://doi.org/10.1186/1745-6215-14-177>.
5. Herbrink M, Nuijen B, Schellens JH, Beijnen JH. Variability in bioavailability of small molecular tyrosine kinase inhibitors. *Cancer Treat Rev*. 2015;41(5):412-422. <https://doi.org/10.1016/j.ctrv.2015.03.005>.
6. Ciccolini J, Serdjebi C, Peters GJ, Giovannetti E. Pharmacokinetics and pharmacogenetics of Gemcitabine as a mainstay in adult and pediatric oncology: an EORTC-PAMM perspective. *Cancer Chemother Pharmacol*. 2016;78(1):1-12. <https://doi.org/10.1007/s00280-016-3003-0>.
7. Latz JE, Chaudhary A, Ghosh A, Johnson RD. Population pharmacokinetic analysis of ten phase II clinical trials of pemetrexed in cancer patients. *Cancer Chemother Pharmacol*. 2006;57(4):401-411. <https://doi.org/10.1007/s00280-005-0036-1>.
8. Mita AC, Sweeney CJ, Baker SD, Goetz A, Hammond LA, Patnaik A, et al. Phase I and pharmacokinetic study of pemetrexed administered every 3 weeks to advanced cancer patients with normal and impaired renal function. *J Clin Oncol*. 2006;24(4):552-562. <https://doi.org/10.1200/Jco.2004.00.9720>.
9. Chen CY, Lin JW, Huang JW, Chen KY, Shih JY, Yu CJ, et al. Estimated creatinine clearance rate is associated with the treatment effectiveness and toxicity of pemetrexed as continuation maintenance therapy for advanced nonsquamous non-small-cell lung cancer. *Clin Lung Cancer*. 2015;16(6):e131-140. <https://doi.org/10.1016/j.clcc.2015.01.001>.
10. Sussell J, Vanderpuye-Orgle J, Vania D, Goertz H, Lakdawalla D. Understanding price growth in the market for targeted oncology therapies. *Am J Manag Care*. 2019;25(6).

# PART 1



# INTRODUCTION



# CHAPTER 1

# Optimized dosing: the next step in precision medicine of non-small cell lung cancer

*Drugs. 2021;82(1):15-32*

René J. Boosman  
Jacobus A. Burgers  
Egbert F. Smit  
Neeltje Steeghs  
Anthonie J. van der Wekken  
Jos H. Beijnen  
Alwin D.R. Huitema  
Rob ter Heine

Author's contribution: R.J. Boosman designed this review, performed the literature search, wrote the first draft of the manuscript and edited the contribution of the co-authors in this manuscript.

## **ABSTRACT**

In oncology, and especially in the treatment of non-small cell lung cancer (NSCLC), dose optimization is often a neglected part of precision medicine. Many drugs are still being administered in "one dose fits all" regimens or based on parameters that are often only minor determinants for systemic exposure. These dosing approaches often introduce additional pharmacokinetic variability and do not add to treatment outcomes. Fortunately, pharmacological knowledge is increasing, providing valuable information regarding the potential of, for example, therapeutic drug monitoring. This article focuses on the evidence for the most promising and easily implemented optimized dosing approaches for the small-molecule inhibitors, chemotherapeutic agents, and monoclonal antibodies as treatment options currently approved for NSCLC. Despite limitations such as investigations having been conducted in oncological diseases other than NSCLC or the retrospective origin of many analyses, an alternative dosing regimen could be beneficial for treatment outcomes, prescriber convenience, or financial burden on healthcare systems. This review of the literature provides recommendations on the implementation of dose optimization and advice regarding promising strategies that deserve further research in NSCLC.

## INTRODUCTION

In the current era of precision medicine in oncology, treatment is mainly tailored to the individual tumor characteristics to optimize therapy outcomes.<sup>1</sup> However, the dosing of these drugs has not yet entered this era. Special patient populations, such as patients with obesity or cachexia or with drug–drug interactions, are usually not studied in clinical trials. In addition, even in a clinical trial population, high interindividual variability (IIV) in exposure, efficacy, tolerability, and safety of drugs is observed.<sup>2</sup> Consequently, it is unlikely that the approved dose for the population is the optimal dose for each individual. Moreover, assuming that toxicity is a biomarker for efficacy, the maximum tolerable dose (MTD) is targeted during clinical development of anticancer drugs. Although this may hold true for classic cytotoxic agents, whether it is the case for targeted therapies is debatable<sup>3</sup>, creating opportunities for dose optimization in this class of drugs to reach optimal systemic and tumor exposure. Implementation of dose optimization is already clinical practice for several drug classes, such as antibiotics, antiepileptics, antidepressants, and immunosuppressants.<sup>4–7</sup> However, its application in oncology is not commonplace<sup>8</sup> and this is best observed for lung cancer. Lung cancer is the leading cause of cancer-related deaths worldwide. In 2020, more than two million new cases of lung cancer arose and about 1.8 million patients with lung cancer died, accounting for 18% of the worldwide cancer-related deaths.<sup>9</sup> Therefore, even small benefits from optimized dosing will affect many patients. Over the past decade, several new treatment options for lung cancer have been approved and marketed and more are to follow.<sup>10</sup> However, most therapeutics are still used in a “one dose fits all” approach. Altogether, dose optimization remains an important but forgotten part of precision medicine in lung cancer treatment. In this review, we discuss opportunities for dose optimization of drugs currently approved by the European Medicines Agency (EMA) for treatment of non-small cell lung cancer (NSCLC).

## METHODS OF LITERATURE REVIEW

This article is not a systematic review, but a comprehensive search of the literature was performed. The Clinical Pharmacology and Biopharmaceutics Reviews of the US FDA, as well as the European Public Assessments Reports of the EMA were consulted for all of the drugs described in this review. In addition, terms related to pharmacokinetics, exposure–response analysis, and dose optimizations, in combination with the individual drugs or drug classes, were used in PubMed searches. Citation snowballing was used to find related articles.

## GENERAL

Overall, dose optimization can be based *a priori* or *a posteriori* to the first administration of a drug. *A priori* dose optimizations include the implementation of covariate-specific dosing, such as organ function (e.g., renal function) or body size (e.g., weight or body surface area (BSA)).

Table 1. Key characteristics and precision dosing strategies for the drug-based treatment options in NSCLC.

Class/drug	Target	Currently approved dose	Exposure- efficacy <sup>a</sup>	Exposure- toxicity <sup>a</sup>
<b>Small-molecule inhibitors</b>				
Erlotinib	EGFR	150 mg QD	No	Yes
Gefitinib	EGFR	250 mg QD	No	Yes
Afatinib	EGFR/HER	40 mg QD	No	Yes
Dacomitinib	EGFR/HER	45 mg QD	No	Yes
Osimertinib	EGFR	80 mg QD	No	Yes
Crizotinib	ALK, ROS1, MET	250 mg BID	Yes	No
Alectinib	ALK	600 mg BID	Yes	No
Ceritinib	ALK	450 mg QD (fed) 750 mg QD (fasted)	Positive trend	Yes
Brigatinib	ALK	90 mg QD for 7 days followed by 180 mg QD	Yes	Yes
Lorlatinib	ALK, ROS1	100 mg QD	Yes	Yes
Dabrafenib	BRAF	150 mg BID	No <sup>d</sup>	Yes <sup>d</sup>
Trametinib	MEK	2 mg QD	Yes <sup>d</sup>	No <sup>d</sup>
Larotrectinib	NTRK	100 mg BID	Inconclusive	No
Entrectinib	NTRK, ALK, ROS1	600 mg QD	Inconclusive	Inconclusive
<b>Cytotoxic agents</b>				
Cisplatin	DNA bases	75 mg/m <sup>2</sup> Q3W	Yes	Yes
Carboplatin	DNA bases	400 mg/m <sup>2</sup> Q3W	Yes	Yes
Pemetrexed	Folate pathway	500 mg/m <sup>2</sup> Q3W	Weakly positive	Yes
Docetaxel	Micro tubules	75 mg/m <sup>2</sup> Q3W	Yes	Yes
Paclitaxel	Micro tubules	175 mg/m <sup>2</sup> Q3W	Yes	Yes
Nab-paclitaxel	Micro tubules	100 mg/m <sup>2</sup> Q1W	Yes <sup>d</sup>	Yes <sup>d</sup>
Gemcitabine	Cytidine analog	1,250 mg/m <sup>2</sup> Q3W	Inconclusive	Inconclusive
Vinorelbine	β-tubulin	25 mg/m <sup>2</sup>	Inconclusive	Inconclusive
<b>Monoclonal antibodies</b>				
Nivolumab	PD-1	3 mg/kg Q2W.	No	No
Pembrolizumab	PD-1	2 mg/kg Q3W.	No	No
Durvalumab	PD-L1	10 mg/kg Q2W	No	No
Atezolizumab	PD-L1	15 mg/kg Q3W	No	No

Precision dosing			References
Directly implementable	On indication	Required additional research	
	Fixed lower dose <sup>b,c</sup>		23, 31, 34
	Fixed lower dose (e.g. on alternating days) <sup>b,c</sup>		21, 22
	Fixed lower dose <sup>b,c</sup>		40, 44
	Fixed lower dose <sup>b,c</sup>		42
	Fixed lower dose <sup>b,c</sup>		41, 45
TDM-guided dosing			56, 61, 180
TDM-guided dosing			61, 181
TDM-guided dosing		E-R analysis in NSCLC	58, 182
TDM-guided dosing		E-R analysis in NSCLC	59, 63, 183
TDM-guided dosing		E-R analysis in NSCLC	60, 184
		E-R analysis in NSCLC	67, 185
	TDM-guided dosing <sup>b,c,e</sup>	E-R analysis in NSCLC	66, 67, 186
	TDM-guided dosing <sup>b,c,e</sup>	TDM-guided dosing, Lower fixed dose	77, 187
	TDM-guided dosing <sup>b,c,e</sup>	TDM-guided dosing	76, 188
		Neutrophil count	79, 85-87
		TDM-guided dosing	91-93
		AUC-based dosing on renal function	107, 110, 116
		Neutrophil count	79, 117, 122-125
	TDM-guided dosing <sup>b,c,e</sup>		128-130, 133, 134
		Neutrophil count TDM-guided dosing	79, 118, 146, 189
	Decreased infusion rate with low dose gemcitabine <sup>f</sup>	Neutrophil count	79, 125, 139, 146
		Neutrophil count, Fixed dosing	79, 144
		Lower fixed dose	155, 160, 190
		Lower fixed dose	154, 160, 191
		Lower fixed dose	160, 192, 193
		Lower fixed dose	149, 160, 194

Table 1. Continued.

Class/drug	Target	Currently approved dose	Exposure- efficacy <sup>a</sup>	Exposure- toxicity <sup>a</sup>
Ipilimumab	CTLA-4	1 mg/kg Q6W	Yes	Yes
Ramucirumab	VEGFR	10 mg/kg Q3W in combination with docetaxel 10 mg/kg Q2W in combination with erlotinib	Yes	Yes
Bevacizumab	VEGFR	7.5-15 mg/kg Q3W	Yes	Yes

ALK: anaplastic lymphoma kinase, AUC: area under the plasma concentration-time curve, BID: twice daily, BRAF: B-Raf proto-oncogene, CrCl: creatinine clearance, CTLA-4: cytotoxic T-lymphocyte associated protein 4, EGFR: epidermal growth factor receptor, E-R: exposure-response, HER: human epidermal growth factor receptor, MEK: mitogen-activated extracellular signal-regulated kinase, MET: mesenchymal epithelial transition factor, NSCLC: non-small cell lung cancer, NTRK: neurotrophic tyrosine receptor kinase, PD-1: programmed cell death protein 1, PD-L1: programmed cell death-ligand 1, QxW: every x weeks, QD: once daily, ROS1: c-ros oncogene 1, TDM: Therapeutic drug monitoring, VEGFR: vascular endothelial growth factor receptor

For some compounds, dosing based on covariates is included in the drug label, although evidence for this is lacking. In these cases, fixed dosing might be more appropriate. For *a posteriori* dose adaptations, doses can be based on laboratory tests such as neutrophil count for toxicity-guided dosing or drug concentrations for therapeutic drug monitoring (TDM). The latter might only be considered if (1) no easily measured biomarker for response to the drug is available, (2) therapy is given over a prolonged period to allow dose adaptations, (3) a sensitive and validated bioanalytic method is available, (4) there is high IIV and relatively low interoccasional variability in pharmacokinetic exposure, (5) the drug has a narrow therapeutic range, (6) exposure-response relationships are defined or expected, and (7) dose adaptation is feasible.<sup>11</sup> For all dose optimization strategies, information regarding dose-exposure-response relationships at both an individual and a population level is crucial to ensure sufficient exposure/pharmacodynamic effects during therapy.<sup>2, 12, 13</sup> Table 1 lists the characteristics of all drug-based therapeutic options and their optimized dosing strategies for the treatment of NSCLC.

## SMALL-MOLECULE INHIBITORS

### *Where do we stand?*

In adenocarcinoma, epidermal growth factor receptor (EGFR) and KRAS<sup>G12C</sup> mutations are the most frequently detected driver mutations.<sup>14</sup> Other oncogenic drivers such as anaplastic lymphoma kinase (ALK) rearrangements, B-Raf proto-oncogene (BRAF)<sup>V600</sup> mutations, neurotrophic tyrosine receptor kinase (NTRK) fusion genes, hepatocyte growth factor receptor gene (MET), and exon skipping or transfection gene (RET) rearrangements are present in lower frequencies. In the last decade, several small-molecule inhibitors (SMIs) have been developed to target these driver mutations. Currently, all these SMIs have been developed according to the “one dose fits all”

Precision dosing			References
Directly implementable	On indication	Required additional research	
		Tolerability-guided dosing	160, 170, 172, 173
		Fixed dosing	195, 196
			160, 177, 178, 197

<sup>a</sup> found for the current dosing regimens.

<sup>b</sup> in case of toxicity.

<sup>c</sup> in case of PK based drug-drug interactions which cannot be prevented.

<sup>d</sup> in other indication than NSCLC.

<sup>e</sup> in case of no efficacy.

<sup>f</sup> based on the preference of patient/prescribe.

paradigm. However, since they are notoriously subject to high IIV, fixed doses might lead to under- and/or overexposure.<sup>15</sup> Several reviews have advocated the implementation of TDM as a tool to minimize toxicities while maintaining efficacy<sup>11, 16</sup>, but this has not generally been accepted.

#### Epidermal growth factor receptor inhibitors

Erlotinib and gefitinib are first-generation EGFR SMIs.<sup>17</sup> Acquired resistance due to mutations has fueled the development of the second- and third-generation EGFR SMIs afatinib, dacomitinib, and osimertinib.<sup>18-20</sup>

#### *Dose individualization of EGFR SMIs*

Overall, it has become evident that the approved doses (Table 1) of EGFR SMIs are higher than necessary for maximal efficacy. A lower dose of these drugs might minimize toxicities and increase tolerability while maintaining efficacy and making treatment available for a larger group, e.g., frail patients (under the condition that exposure-response relationships for both efficacy as toxicity are similar to those in the non-frail population).

#### *First-generation EGFR SMIs*

Erlotinib and gefitinib are both reversible inhibitors of EGFR. An exposure-response relationship might be expected, since the equilibrium of the bound and unbound drug will play a major role in the target occupancy. However, as shown in Table 1, in the current dosing regimens of both drugs, no relationship between plasma exposure and response has been found.<sup>21-24</sup> Interestingly, lower doses of erlotinib and gefitinib (25-100 mg once daily (QD) and 250 mg on alternating days, respectively) were noninferior to the approved dose of erlotinib 150 mg QD and gefitinib 250 mg QD gefitinib.<sup>24-29</sup> Unfortunately, no exposure-response analyses were performed in these patients. However, these dose-response analyses showed that low doses of these first-generation SMIs were indeed as effective as and less



toxic than the currently approved doses, indicating that extrapolation from non-frail to frail patients would be reasonable until new data arise.<sup>24-29</sup> Moreover, in lung cancer cell lines, half-maximal inhibition ( $IC_{50}$ ) values for erlotinib have been reported to be in the order of 10-40 nM<sup>30</sup>, which is a concentration approximately 1,000-fold lower than the observed steady-state concentrations of erlotinib 150 mg QD.<sup>31</sup> Naturally, differences in target exposure between *in vivo* and *in vitro* experiments (e.g., the differences in partition coefficient) and additional factors such as protein binding, for which *in vivo*  $IC_{50}$  values are probably higher than those reported for *in vitro* experiments, should be considered. Still, these data together suggest that exposure is much higher at the approved doses than required for target inhibition and is at the plateau of the exposure-efficacy curve. Although data are scarce and conflicting<sup>32</sup>, one preclinical study in mice advocated that lower doses (5-15 mg/kg) of at least gefitinib might result in a more rapid acquired resistance than higher doses (25-50 mg/kg).<sup>33</sup> However, solid evidence in humans (with the equivalent doses) is missing.

At the approved dose, associations between systemic drug exposure and the development of rash and diarrhea have been reported.<sup>22, 34</sup> The development of these adverse events was observed to be far less for erlotinib 25-100 mg QD or gefitinib 250 mg on alternating days.<sup>24-29, 35</sup> Reported frequencies of 7-30% of patients discontinuing treatment because of side effects<sup>36, 37</sup> indicate that treatment may be optimized by the administration of lower doses.

#### *Second- and third-generation EGFR SMIs*

For the irreversible inhibitors of EGFR (afatinib, dacomitinib and osimertinib), the use of TDM is even more debatable. EGFRs have been found to be completely renewed every one to five days *in vitro*.<sup>38</sup> Afatinib, dacomitinib, and osimertinib all have elimination half-lives > 36 hours, are dosed daily, and display low  $IC_{50}$  values for binding to mutated EGFR (steady-state trough concentrations are approximately 40- to 150-fold higher than the reported (protein-unbound)  $IC_{50}$  values).<sup>39-42</sup> Therefore, only low daily doses are necessary for binding and pharmacodynamic effects may hold on longer than systemic exposure indicates. Indeed, a semi-mechanistic model for osimertinib showed that a daily dose for two weeks led to a delayed onset of tumor growth when compared to a single dose of osimertinib.<sup>43</sup> This indicates that, despite the irreversible binding of these drugs, lowering the dose frequency is not desirable because of the EGFR turnover time. Exposure-efficacy relationships with regard to afatinib, dacomitinib, and osimertinib in their current dosing schedule have not been found,<sup>40-42</sup> whereas clear associations were found between exposure (in terms of area under the plasma concentration-time curve (AUC), trough concentrations, or average plasma concentrations) and the development of rash and diarrhea.<sup>40, 42, 44</sup> <sup>45</sup> Similar to erlotinib and gefitinib, it can be hypothesized that lower doses of afatinib, dacomitinib and osimertinib could be sufficient for efficacy and will decrease toxicity. Indeed, for osimertinib and afatinib, preliminary results suggested that low-dose treatments (50% of the approved dose) resulted in efficacy similar to that with the approved dose.<sup>46-49</sup>

In summary, EGFR SMIs seem to be dosed higher than necessary for maximal efficacy in EGFR-mutated NSCLC. Dose adjustments are not recommended, and more clinical studies are warranted to assess whether fixed lower doses of these drugs are indeed as effective as and less toxic than the standardized doses, without triggering faster acquired resistance.

### *KRAS<sup>G12C</sup> inhibitors*

Currently, no effective SMIs to target the KRAS<sup>G12C</sup> mutation are approved by the EMA. However, the FDA recently granted accelerated approval to sotorasib<sup>50</sup>, and this drug is expected to also receive approval in the EU. Data are currently insufficient to support dose individualization of this drug. The current dose approved by the FDA is 960 mg QD, and the license holder is currently investigating the efficacy of 240 mg QD as an FDA postmarketing requirement.<sup>51</sup>

### *Anaplastic lymphoma kinase inhibitors*

Three generations of ALK SMIs have been approved by the EMA. Crizotinib, which also inhibits c-ros oncogene 1 (ROS1) and MET, was the first ALK SMI to be approved.<sup>52</sup> Alectinib, ceritinib, and brigatinib form the second-generation and lorlatinib the third-generation ALK SMI.<sup>53-55</sup> Positive exposure-efficacy relationships have already been observed in the clinical development studies of most ALK SMIs.<sup>56-60</sup> For some of these drugs, positive exposure-toxicity relationships were also found<sup>59, 60</sup>, as well as high IIV (ranging from 30 to 60%) in exposure.<sup>56-60</sup> Moreover, the current standardized dosing of these drugs is based on the MTD found in clinical studies. However, it has been reported that, for at least crizotinib and alectinib, only 50-60% of the population in clinical practice reaches target exposure for efficacy<sup>61</sup>, indicating a narrow therapeutic window for this drug class and showing the potential for dose individualization by means of TDM. Several (translational) studies and reviews have already proposed the optimal target concentrations or doses for the ALK inhibitors.<sup>16, 56, 61-64</sup> Thus, for this class of drugs, implementation of TDM is necessary to improve treatment outcomes with ALK SMIs.

### *B-Raf proto-oncogene/mitogen-activated extracellular signal-regulated kinase inhibitors*

Combination therapy with dabrafenib plus trametinib has been approved for lung adenocarcinoma harboring BRAF<sup>V600</sup> mutation as oncogenic driver.<sup>65</sup> For NSCLC, the exposure-response relationships for the combination of dabrafenib and trametinib are unknown. For trametinib in patients with melanoma, a relationship between median trough concentrations and efficacy outcomes was found, and high IIV (24-36%) in exposure was observed.<sup>66, 67</sup> Although a formal exposure-safety analysis has not yet been performed, mitogen-activated extracellular signal-regulated kinase (MEK) inhibitors are well known to have a small therapeutic window because of their limited sensitivity towards BRAF-mutant cells over BRAF-wildtype cells.<sup>68, 69</sup> Therefore, the use of TDM for trametinib would be a rational choice. For dabrafenib, no exposure-response relationship has been established in melanoma, so the use of TDM is not substantiated. Whether these findings can be translated to NSCLC is unknown, since the pharmacokinetics and -dynamics are dependent on tumor type<sup>70, 71</sup> and IC<sub>50</sub> values have been reported as comparable to or higher for BRAF<sup>V600E</sup>-mutated NSCLC cell lines than for melanoma cells with the same driver mutation.<sup>70, 72-75</sup> Until exposure-response analyses are evaluated for NSCLC cohorts, TDM-guided dosing should not be carried out as standard care for the dabrafenib-trametinib combination in NSCLC. If treatment response is insufficient or extensive adverse effects are experienced, TDM-based dose guiding could be useful, targeting the predefined threshold of trametinib in melanoma<sup>67</sup> and the previously described population geometric mean for dabrafenib.<sup>70</sup>

### Neurotrophic tyrosine receptor kinase inhibitors

Larotrectinib and entrectinib have been approved for treatment of NSCLC with fusions in the NTRK genes. Entrectinib also inhibits ROS1 and ALK.<sup>76</sup> A remarkable observation with larotrectinib noted that patients in the highest quartile of exposure performed worse in terms of overall response rate than did those in the other quartiles. Although this was observed in a low number of patients (n = 66) with various tumor types, it could indicate that patients receive higher doses than necessary.<sup>77</sup> Although clues indicate positive exposure-efficacy relationships, the lack of exposure-response analyses prevents the implementation of TDM-guided dosing (based on the geometric observed mean trough concentration), but could be potentially useful in case of a treatment-related toxicity or inadequate response.

### Where should we go?

Generally speaking, it is critical for the relationship between exposure and response to therapy to be elucidated to optimize the dosing strategy for these drugs. One important factor is the nature of the exposure metric used in these analyses. In addition, not only the drug but also the target needs to be taken into account to inform the dose adaptations. For the EGFR inhibitors, it is important to set up prospective studies to evaluate whether (fixed) lower doses of these drugs have similar efficacy outcomes and less toxicity. All ALK inhibitors show positive exposure-efficacy relationships and high IIV in exposure. In addition, for many of these drugs, clear targets for exposure have been described and positive exposure-safety relationships mentioned, so TDM-based dosing could be implemented directly for all patients. For some ALK inhibitors, no trough levels on which TDM could be based have been reported. The geometric population mean concentrations found in registration studies are frequently reported to be in the same order of magnitude as or even lower than the actual target concentrations for efficacy.<sup>78</sup> Therefore, until the target trough concentrations are established, dosing could be based on the geometric mean reported in these clinical trials. For the BRAF/MEK and NTRK inhibitors, exposure-response analyses should be performed in NSCLC, since there are clues for the superiority of TDM-guided dosing for these drugs. Dose modifications based on TDM might be valuable in cases with lack of efficacy or with toxicity, or when pharmacokinetic-based drug-drug interactions cannot be prevented.

## **CYTOTOXIC AGENTS**

### Where do we stand?

Although SMIs and immunotherapy are currently shifting the treatment paradigm in oncology, cytotoxic chemotherapy remains a cornerstone in the treatment of metastatic NSCLC. In general, the chemotherapeutic regimens in first-line therapy consist of a platinum-based agent (cisplatin or carboplatin) in combination with another chemotherapeutic such as pemetrexed, a taxane (docetaxel or (albumin-bound (nab-)) paclitaxel), gemcitabine, or vinorelbine. All these drugs, with the exception of carboplatin, are currently dosed on BSA, although there are hints that dosing based on other parameters might be of added value. For example, dosing to neutropenia has been proposed to be a prognostic factor for treatment outcomes with almost all cytotoxic agents

(cisplatin, taxanes, gemcitabine, and vinorelbine) used in the treatment of NSCLC.<sup>79, 80</sup> Since TDM should only be considered to be beneficial if no biomarkers for drug effect are present (see Sect. 3), and since IIV in pharmacodynamic parameters are expected to be minimized with toxicity-guided dosing<sup>81</sup>, dosing on neutrophils is assumed to be superior to TDM. The specifics of this toxicity-guided dosing have been described previously.<sup>82</sup> Interestingly, dose reductions are performed for severe toxicities, but no dose increments are carried out in the absence of toxicity, despite the well-described toxicity-efficacy relationship (as summarized in Table 1). As a consequence, these patients may be receiving a subtherapeutic dose.

#### *Platinum-based agents*

Both cisplatin and carboplatin are cleared by the kidneys. The hydrolyzed active platinum metabolites bind irreversibly to proteins, so elimination is also dependent on protein turnover, which forms a non-renal elimination pathway.<sup>83, 84</sup> Given the more stable chemical structure of carboplatin compared with cisplatin, less carboplatin is hydrolyzed and undergoes bioactivation, resulting in more renal elimination of carboplatin compared with cisplatin.<sup>83</sup>

#### *Dose individualization of cisplatin*

The AUC of unbound cisplatin has been observed to be statistically significantly related to response status during therapy.<sup>85</sup> Moreover, total and free platinum peak concentrations have been related to a deterioration of renal function.<sup>86-88</sup> Controversially, the incidence of nephrotoxicity was observed not to be altered by the infusion rate of cisplatin.<sup>89</sup> Currently, dosing of cisplatin is, like many cytotoxic agents, based on BSA. However, it has been shown that 44% of the IIV in cisplatin clearance can be explained by BSA.<sup>90</sup> Until now, no better predictors for the clearance of cisplatin have been found, so BSA-based dosing remains the recommended dosing strategy.

#### *Dose individualization of carboplatin*

As for cisplatin, the approved dosing of carboplatin is based on BSA, and systemic exposure has been related to its efficacy and toxicity.<sup>91, 92</sup>

However, in clinical practice, BSA-based dosing is not routinely applied, with the dose instead individualized based on renal function according to the Calvert formula.<sup>93</sup> Glomerular filtration rate (GFR) has been generally considered to be the optimal measure for renal function. However, methods to measure this parameter are often inconvenient and time-consuming.<sup>94</sup> Alternatively, calculation of an estimated GFR (eGFR) or creatinine clearance (CrCl) using a single serum creatinine measurement has been standard practice. However, serum creatinine is subject to active secretion, so CrCl is often an overestimation of the GFR.<sup>95</sup> As carboplatin does not undergo active secretion, whether CrCl is a good predictor for carboplatin clearance remains questionable. Indeed, it has been found that the use of serum creatinine does not represent carboplatin clearance accurately in patients with adequate renal function (eGFR > 50 mL/min).<sup>96</sup> In addition, 24-h collection of urine to calculate the CrCl has also proven to be an inaccurate base for carboplatin dosing.<sup>97</sup> A flat dose (based on the mean carboplatin population clearance) of 695 mg in patients with eGFR > 50 mL/min resulted in similar variability in carboplatin exposure as serum creatinine-based

dosing.<sup>96</sup> Implementation of markers that more accurately estimate the GFR are thus warranted. The addition of cystatin C in the calculation of the eGFR was shown to reduce bias and imprecision in carboplatin clearance.<sup>98</sup> Proenkephalin, a recently developed biomarker for glomerular filtration, more accurately predicted the eGFR than serum creatinine and is even useful in unstable and critically ill patients.<sup>99</sup> Major steps toward reaching target carboplatin exposure, especially in patients with systemic inflammation, could be made by including inflammatory markers in the dose calculation.<sup>100</sup> However, this dosing regimen needs prospective evaluation in a large patient cohort before implementation in clinical practice. Since *a priori* and *a posteriori* dose optimization strategies could be synergistic, one might also argue for the additional implementation of TDM-guided dosing for carboplatin. Indeed, TDM-guided dosing of carboplatin has been used successfully in children and could therefore be promising for at least this patient group.<sup>101-103</sup> Further evaluation of this dosing strategy should be studied in an NSCLC population.

In summary, inclusion of cystatin C in the AUC-based dosing of carboplatin is feasible in clinical practice and could be employed on indication. If cystatin C is not available, a fixed carboplatin dose of 695 mg every three weeks (Q3W) in patients with CrCl > 50 mL/min could be recommended.

#### Pemetrexed

Pemetrexed is an antifolate agent that inhibits enzymes (including thymidylate synthase (TS)) in the folate pathway and consequently, the formation of DNA precursors. Upon administration, pemetrexed is effectively transported intracellularly and polyglutamylated.<sup>104</sup> This process is believed to play a pivotal role in both antitumor and toxic effects (such as nephrotoxicity and hematological toxicities), as pemetrexed pentaglutamate has a 100 times higher potency for TS inhibition than pemetrexed itself.<sup>105</sup> Measurement of the intracellular polyglutamylated forms of pemetrexed thus would be an ideal marker for its pharmacological effects. However, the development of an analytic method has proven to be challenging.<sup>106</sup> Although it is unclear how well the polyglutamylated forms of pemetrexed correlate to pemetrexed plasma concentrations, a plasma exposure-toxicity relationship has been well-established in a generally broad range of doses (126-1362 mg).<sup>107-109</sup> In addition, doses of pemetrexed 900-1,000 mg/m<sup>2</sup> did not improve efficacy of treatment compared with standard dosing of 500 mg/m<sup>2</sup> Q3W.<sup>110</sup> Based on differences in doses, dose frequencies, and efficacy in the early clinical trial<sup>111-113</sup> and based on the analogy of methotrexate<sup>114</sup>, it is expected that the exposure-efficacy relationship is AUC-driven and that the current dose might be in the flat part of the exposure-efficacy curve. Therefore, standardized lower doses might be effective; however, trials to study this lower dose might not be ethical. Pemetrexed is mainly excreted by the kidneys, and renal function contributes substantially to total pemetrexed clearance.<sup>115, 116</sup> These results suggest that inclusion of renal function in a dosing algorithm for pemetrexed could result in less IIV in pemetrexed exposure and toxicity. A pharmacokinetic study to assess the suitability of renal function-based dosing in patients with adequate renal function is ongoing (NCT03655821). In addition, another study is determining whether renal function-based dosing with additional prophylactic therapy to prevent toxicity is feasible in patients with CrCl < 45 mL/min (NCT03656549). Given all this, implementation of TDM

could also serve as a dose optimization strategy. However, since serum creatinine is part of the standard laboratory assessment during pemetrexed treatment and may be used in the dosing algorithm from the first cycle onward, renal function-based dosing is assumed to be superior to TDM as a dosing strategy.

### Taxanes

The taxanes are currently dosed based on BSA without exception. High IIV in exposure to taxanes has been observed<sup>90, 117-119</sup>, which may partly play a role in the unpredictability of treatment response and the development of toxicities.

#### *Dose individualization of docetaxel*

Results from studies of docetaxel AUC and time to progression in solid tumors (including NSCLC) have been contradictory.<sup>117, 120, 121</sup> Regarding toxicity-response relationships, it has been observed that the exposure to docetaxel is a predictor of severe toxicity, especially neutropenia, during the first course of treatment.<sup>122-124</sup> In addition, neutrophil counts are also associated with the toxicity and efficacy of docetaxel.<sup>79, 125, 126</sup> This could indicate that there is a balance in the optimal neutrophil nadir during docetaxel treatment. One could aim for an individualized dose that will both avoid severe hematological toxicities and be maximally effective.<sup>126</sup> However, as yet, no easily implemented dose individualization methods have been revealed. Neutropenia has particular potential as a prognostic marker for efficacy but cannot be implemented without solid knowledge of the efficacy and safety of toxicity-guided dosing.<sup>82</sup>

#### *Dose individualization of paclitaxel*

The time above a certain paclitaxel plasma concentration is related to clinical efficacy<sup>127, 128</sup> and the development of the primary adverse events, neutropenia<sup>127, 129, 130</sup> and polyneuropathy.<sup>131, 132</sup> Two large randomized studies in patients with NSCLC assessed the feasibility of TDM of the time above a paclitaxel toxicity threshold concentration when combined with cisplatin 80 mg/m<sup>2</sup> or carboplatin (AUC 6). They both showed that pharmacokinetic-guided paclitaxel dosing targeting 26-31 h above a concentration of 42.7 µg/L (0.05 µM) resulted in a statistically significantly lower paclitaxel dose, similar efficacy results, and reduced adverse events compared with BSA-based (175-200 mg/m<sup>2</sup>) dosing.<sup>133, 134</sup> This pharmacokinetic-guided dosing of paclitaxel has been shown to be feasible and can be based on a single sample 24 h after administration.<sup>135</sup> Since TDM is only possible after administration of a drug, a BSA-based starting dose is recommended in the first cycle, followed by a TDM-guided dose.

#### *Dose individualization of nab-paclitaxel*

During treatment with nab-paclitaxel, longer times above a total paclitaxel concentration of 720 µg/L in plasma were associated with a ≥ 50% decrease in neutrophils.<sup>118</sup> Furthermore, in patients with NSCLC, weekly 100 mg/m<sup>2</sup> was more effective and less toxic than 300 mg/m<sup>2</sup> Q3W.<sup>136</sup> Although clinical study results are scarce, the available data regarding TDM-guided or neutrophil-guided dosing provide us a valuable starting point for dose optimization of nab-paclitaxel. More studies are required to assess the feasibility of these strategies.

### Gemcitabine

After administration, gemcitabine is rapidly transported intracellularly and subsequently phosphorylated, with the most important and rate-limiting enzyme being deoxycytidine kinase (dCK).<sup>137</sup> Saturation of the dCK has been shown to decrease the intracellular disposition of the active metabolites. Current clinical practice is a 30-min infusion of gemcitabine regardless of the dose. Logically, this would result in plasma concentrations above saturable levels, where the excess of gemcitabine in plasma will be inactivated by cytidine deaminase and would not contribute to its pharmacological effect.<sup>137</sup>

Decreasing the infusion rate and/or lowering the gemcitabine dose are two easily adjusted factors that would lead to less saturation and consequently a more predictable dose-effect relationship. A meta-analysis (n = 867) found similar efficacy for the fixed dosing rate (10 mg/m<sup>2</sup>/min) and the fixed infusion duration (30 min). However, the fixed dosing rate was associated with more toxicity.<sup>138</sup> This suggests that the current dosing of gemcitabine results in intracellular concentrations well within the therapeutic range and that increased infusion rates will push the intracellular concentrations toward toxic levels. Logically, a decreased dose of gemcitabine administered over a prolonged period could result in similar efficacy and toxicity. Indeed, administration of gemcitabine 250 mg/m<sup>2</sup> over 6 h showed efficacy similar to that with 1,000 mg/m<sup>2</sup> over 30 min.<sup>139</sup> Studies to test this prolonged infusion duration of low-dose gemcitabine in combination with 75 mg/m<sup>2</sup> cisplatin found beneficial efficacy results and a different toxicity profile for gemcitabine compared with historical cohorts.<sup>140, 141</sup> Whether the reduction in drug-related costs are beneficial given the costs related to the prolonged hospital stay remains debatable. In addition, it has been reported that prolonged infusions with chemotherapy carry higher chances of extravasation, posing additional risks for this treatment schedule.<sup>142</sup>

### Vinorelbine

Vinorelbine is a vinca alkaloid that binds to  $\beta$ -tubulin, resulting in inhibition of mitosis and activation of the apoptosis pathway. Currently, vinorelbine is dosed on BSA and can be administered either orally or intravenously on a weekly basis.<sup>143</sup> Although no relationship between BSA and the pharmacokinetics of vinorelbine has been found, dosing based on this parameter might still lead to a more efficacious and tolerable treatment.<sup>144</sup> In contrast, in patients with metastatic breast cancer, fixed dosing of vinorelbine (and capecitabine) could be an alternative, safe, and effective dosing strategy.<sup>145</sup> However, an assessment of pharmacokinetic and pharmacodynamic endpoints in a large NSCLC study cohort receiving vinorelbine has not yet been reported. Until data become available, dosing on BSA remains recommended.

### Where should we go?

For many of the cytotoxic drugs, neutropenia is postulated to be a prognostic factor for treatment outcome. This has been assessed retrospectively for at least treatment regimens containing cisplatin<sup>79</sup>, docetaxel<sup>79, 125</sup>, nab-paclitaxel<sup>146</sup>, gemcitabine<sup>79, 125, 146</sup> and/or vinorelbine.<sup>79</sup> Prospective studies are necessary to evaluate whether dosing toward a certain neutrophil count is feasible and enhances treatment outcomes. For carboplatin and pemetrexed, AUC-based dosing using renal

function appears to be more rational to predict exposure to these agents. In the absence of reliable markers for renal function, a flat dose of carboplatin is feasible in patients with a relatively normal renal function. Paclitaxel could be dosed based on BSA, with subsequent cycles of therapy based on a TDM-dosing approach in case of severe toxicities or lack of efficacy.

## MONOCLONAL ANTIBODIES

### *Where do we stand?*

Two classes of monoclonal antibodies (mAbs) have been approved for the treatment of NSCLC: immune-checkpoint inhibitors and the vascular endothelial growth factor receptor (VEGFR) inhibitors, bevacizumab and ramucirumab. The immune-checkpoint inhibitors include antibodies targeting programmed cell death protein 1 (PD-1; pembrolizumab and nivolumab), programmed cell death-ligand 1 (PD-L1; atezolizumab and durvalumab), and cytotoxic T-lymphocyte antigen-4 (CTLA-4; ipilimumab). Currently, dosing regimens are effective, and flat exposure-toxicity relationships are observed in a broad dose range. However, a rationale for body weight-based dosing (as implemented for some of these drugs) is missing and further increases the high healthcare costs associated with these drugs.

### *Programmed cell death-ligand 1 antibodies*

#### *Exposure-response analyses*

As target saturation is maximal at the current dosing of PD-(L)1 mAbs<sup>147-151</sup>, it is obvious that flat exposure-response relationships are found. However, these relationships are further complicated by the dynamic relationships between baseline factors, exposure, and disease progression. For example, tumor shrinkage may influence cachexia and thus clearance of mAbs, altering exposure to the mAbs.<sup>152-154</sup> This suggests that clearance of mAbs is related to tumor size and thus to patient response status. Indeed, for at least the PD-1 antibodies, it has been shown that baseline clearance is a better predictive tool for treatment outcome than is exposure.<sup>154-158</sup> This suggests that change in clearance during treatment with these agents could be used as a biomarker for treatment response in PD-(L)1 therapy. Although data are scarce and the exact driving mechanism(s) behind this effect should be explored, some studies have advocated that clearance-based dose adjustments could be made to reduce therapy costs while maintaining efficacy.<sup>159</sup> However, if clearance is merely a parameter to distinguish between responders and non-responders, these dose adaptations should not be performed.

#### *Dose individualization*

Although roughly all PD-(L)1 antibodies were initially dosed based on body weight, fixed dosing could lead to fewer preparation errors and lower healthcare costs. However, implementation of fixed doses is not yet common in clinical practice<sup>160</sup>, or -when implemented- the fixed doses are supratherapeutic. The latter also becomes evident because no exposure-response or dose-response relationships have been found for any of the PD-(L)1 antibodies. The use of supratherapeutic doses is best illustrated for pembrolizumab, which is currently given in a 200 mg



dose. Although NSCLC is often accompanied with weight loss<sup>161, 162</sup>, this fixed dosing corresponds to the initial body weight-based dosing of a patient weighing 100 kg. In addition, the time-dependent decrease in clearance of the PD-L(1) antibodies would result in higher exposure during longer treatment. Adaptation toward a (lower) fixed dose will result in less drug being discarded during preparation and decreased healthcare costs.<sup>163</sup> In line with the flat exposure-response relationship, similar efficacy has been described in a retrospective study of low doses of nivolumab (20 or 100 mg Q3W) compared with the standard dose of 3 mg/kg Q3W in patients with NSCLC.<sup>164</sup> This indicates that lower doses of PD-L(1) antibodies could be administered, potentially saving millions per year in healthcare.<sup>165</sup> Furthermore, it is currently believed that complete inhibition of the PD-1/PD-L1 complex is necessary during treatment and that patients should be treated until progression occurs. Although data on the optimal treatment durations for PD-(L)1 antibodies are scarce, some studies have observed durable responses in patients with lung cancer treated for 1-2 years followed by an intention to treat (for at least the PD-1 antibodies).<sup>166-169</sup>

### *Ipilimumab*

Exposure-efficacy and -toxicity analyses in NSCLC are yet to be performed for ipilimumab. However, as discussed in Table 1 for other indications, positive dose-response and dose-toxicity relationships have been determined<sup>170, 171</sup>: a 10 mg/kg Q3W dose showed increased overall survival and toxicity when compared with the approved 3 mg/kg Q3W.<sup>172, 173</sup> For NSCLC, the currently approved ipilimumab dose is 1 mg/kg Q6W in combination with nivolumab 3 mg/kg Q3W and results in fewer adverse events than alternative ipilimumab regimens.<sup>174</sup> In case of toxicity, dosing is often temporarily halted or even discontinued.<sup>175</sup> Currently, nothing would indicate that the exposure-toxicity relationship would be different for NSCLC. Thus, if a positive exposure-efficacy relationship is present in NSCLC, it would be rational to adjust dosing of ipilimumab based on tolerability. Doses could be escalated in patients who do not experience adverse events and reduced in those who do. However, this strategy needs confirmation in a large number of patients (with NSCLC). Refining of the current body weight-based dosing into three weight group-based doses has been proposed. This strategy, involving using the complete contents of vials and the possibility of administering the preparation to another patient in case of treatment discontinuation, will contribute to healthcare cost savings.<sup>160</sup>

### *Vascular endothelial growth factor inhibitors*

The VEGF inhibitors ramucirumab and bevacizumab are currently dosed on body weight, although body weight has been shown to have only limited influence on the pharmacokinetics of these drugs. Hendriks *et al.* advocated the use of fixed dosing of mAbs when the effect of body weight on the clearance and volume of distribution was minimal.<sup>160</sup> In a more recent population pharmacokinetic meta-analysis of ramucirumab, the effect of body weight on both clearance and volume of distribution was around the arbitrary threshold to implement body weight-based dosing.<sup>176</sup> Based on the limited data available, no further optimization of the dosing regimen can be performed at this time. For bevacizumab, body weight has only a small effect on clearance and volume of distribution.<sup>177</sup> Positive exposure-efficacy and exposure-toxicity relationships in doses of 7.5-15 mg/kg Q3W have been observed.<sup>178</sup> Therefore, it is time to implement fixed dosing of bevacizumab in the treatment of NSCLC at a dose of 600-800 mg Q3W.

### Where should we go?

Currently, the dosing regimens for mAbs are effective and show a flat exposure-toxicity relationship in a large proportion of patients. This indicates that additional precision dosing strategies might not be necessary. For ipilimumab, the feasibility of tolerability-guided dosing should be studied before this strategy is implemented. Costs associated with all mAbs are high. Therefore, dosing strategies could be optimized to decrease the financial burden on the healthcare system. Research to evaluate the efficacy of even lower doses than postulated by the “fixed-dose studies” (see Table 1) could be helpful for this. It is important to ensure that these drugs are dosed on the plateau of the exposure-efficacy curve on an individual basis. Since pharmacokinetic variability is generally low to moderate for these drugs<sup>159, 176, 177</sup>, TDM-guided dosing would not be preferable, and only sufficiently high doses might prevent underexposure. In addition, it is not exactly known for how long and at which intervals patients should receive these mAbs, and additional research is warranted to evaluate the number of courses of treatment patients should receive for optimal outcomes.

## FINAL REMARKS

This review shows that the current dosing regimens of many of the drugs approved for the treatment of NSCLC need to be adapted to improve treatment outcomes or to restrict the ever-rising healthcare costs. However, challenges to implementing precision dosing also exist. Individualization, especially based on laboratory tests such as the monitoring of drug concentrations, is subject to time, logistics, and availability of personnel.<sup>179</sup> In addition, for many drugs approved more than a decade ago, individualization could be based on the extended knowledge gained after approval of the drug. The extra effort required, delays in adjusting labels, and reluctance to prescribe drugs in an off-label dosing regimen all led to discrepancies between knowledge and the implementation of this knowledge. However, suboptimal dosing remains highly undesirable, and the urge to implement precision dosing to improve treatment remains high (Table 1). Currently, most drugs used in the treatment of NSCLC are still dosed as one size fits all, based on BSA or body weight, despite an accumulation of evidence showing that dosing based on other parameters may improve treatment outcomes. For some drugs, precision dosing is sometimes not necessary to improve treatment outcomes. However, adaptation of the current dosing regimen might be beneficial for other factors, such as prescriber/pharmacy convenience or healthcare costs, while maintaining efficacy. This review provides an overview of studies already performed to optimize dosing in NSCLC. In addition, we provide the most promising and easily implemented dose optimization strategies. Most of these strategies can readily be rolled out in clinical practice or require further research.

## REFERENCES

1. Lyman GH. Impact of chemotherapy dose intensity on cancer patient outcomes. *J Natl Compr Canc Netw*. 2009;7(1):99-108. <https://doi.org/10.6004/jnccn.2009.0009>.
2. Maloney A. A new paradigm. "Learn - Learn More": dose-exposure-response at the center of drug development and regulatory approval. *Clin Pharmacol Ther*. 2017;102(6):942-950. <https://doi.org/10.1002/cpt.710>.
3. Mathijssen RH, Sparreboom A, Verweij J. Determining the optimal dose in the development of anticancer agents. *Nat Rev Clin Oncol*. 2014;11(5):272-281. <https://doi.org/10.1038/nrclinonc.2014.40>.
4. Rybak MJ, Le J, Lodise T, Levine D, Bradley J, Liu C, et al. Executive summary: Therapeutic monitoring of vancomycin for serious methicillin-resistant staphylococcus aureus infections: A revised consensus guideline and review of the American Society of Health-System Pharmacists, the Infectious Diseases Society of America, the Pediatric Infectious Diseases society, and the Society of Infectious Diseases Pharmacists. *J Pediatric Infect Dis Soc*. 2020;9(3):281-284. <https://doi.org/10.1093/jpids/piaa057>.
5. Hiemke C, Bergemann N, Clement HW, Conca A, Deckert J, Domschke K, et al. Consensus guidelines for therapeutic drug monitoring in neuropsychopharmacology: Update 2017. *Pharmacopsychiatry*. 2018;51(1-02):e1. <https://doi.org/10.1055/s-0037-1600991>.
6. Brunet M, van Gelder T, Åsberg A, Haufroid V, Hesselink DA, Langman L, et al. Therapeutic drug monitoring of tacrolimus-personalized therapy: Second consensus report. *Ther Drug Monit*. 2019;41(3):261-307. <https://doi.org/10.1097/ftd.0000000000000640>.
7. van Dijkman SC, Wicha SG, Danhof M, Della Pasqua OE. Individualized dosing algorithms and therapeutic monitoring for antiepileptic drugs. *Clin Pharmacol Ther*. 2018;103(4):663-673. <https://doi.org/10.1002/cpt.777>.
8. Touw DJ, Neef C, Thomson AH, Vinks AA. Cost-effectiveness of therapeutic drug monitoring: A systematic review. *Ther Drug Monit*. 2005;27(1):10-17. <https://doi.org/10.1097/00007691-200502000-00004>.
9. The Global Cancer Observatory. Cancer fact sheet trachea, bronchus and lung, 2020. Accessed on 14 Apr 2021.
10. Toschi L, Rossi S, Finocchiaro G, Santoro A. Non-small cell lung cancer treatment (r)evolution: Ten years of advances and more to come. *Ecancermedicalscience*. 2017;11:787. <https://doi.org/10.3332/ecancer.2017.787>.
11. Groenland SL, Mathijssen RHJ, Beijnen JH, Huitema ADR, Steeghs N. Individualized dosing of oral targeted therapies in oncology is crucial in the era of precision medicine. *Eur J Clin Pharmacol*. 2019;75(9):1309-1318. <https://doi.org/10.1007/s00228-019-02704-2>.
12. Maloney A. Personalized dosing = approved wide dose ranges + dose titration. *Clin Pharmacol Ther*. 2021;109(3):566-567. <https://doi.org/10.1002/cpt.1997>.
13. Lyauk YK, Jonker DM, Lund TM. Dose finding in the clinical development of 60 US Food and Drug Administration-approved drugs compared with learning vs. Confirming recommendations. *Clin Transl Sci*. 2019;12(5):481-489. <https://doi.org/10.1111/cts.12641>.
14. Salgia R, Pharaon R, Mambetsariev I, Nam A, Sattler M. The improbable targeted therapy: KRAS as an emerging target in non-small cell lung cancer (NSCLC). *Cell Rep Med*. 2021;2(1):100186. <https://doi.org/10.1016/j.xcrm.2020.100186>.
15. de Wit D, Guchelaar HJ, den Hartigh J, Gelderblom H, van Erp NP. Individualized dosing of tyrosine kinase inhibitors: Are we there yet? *Drug Discov Today*. 2015;20(1):18-36. <https://doi.org/10.1016/j.drudis.2014.09.007>.
16. Verheijen RB, Yu H, Schellens JHM, Beijnen JH, Steeghs N, Huitema ADR. Practical recommendations for therapeutic drug monitoring of kinase inhibitors in oncology. *Clin Pharmacol Ther*. 2017;102(5):765-776. <https://doi.org/10.1002/cpt.787>.
17. Urata Y, Katakami N, Morita S, Kaji R, Yoshioka H, Seto T, et al. Randomized phase III study comparing gefitinib with erlotinib in patients with previously treated advanced lung adenocarcinoma: WJOG 5108L. *J Clin Oncol*. 2016;34(27):3248-3257. <https://doi.org/10.1200/jco.2015.63.4154>.
18. Li D, Ambrogio L, Shimamura T, Kubo S, Takahashi M, Chirieac LR, et al. BIBW2992, an irreversible EGFR/HER2 inhibitor highly effective in preclinical lung cancer models. *Oncogene*. 2008;27(34):4702-4711. <https://doi.org/10.1038/onc.2008.109>.
19. Park K, Tan EH, O'Byrne K, Zhang L, Boyer M, Mok T, et al. Afatinib versus gefitinib as first-line treatment of patients with EGFR mutation-positive non-small-cell lung cancer (LUX-Lung 7): A phase 2B, open-label, randomised controlled trial. *Lancet Oncol*. 2016;17(5):577-589. [https://doi.org/10.1016/s1470-2045\(16\)30033-x](https://doi.org/10.1016/s1470-2045(16)30033-x).

20. Wu YL, Cheng Y, Zhou X, Lee KH, Nakagawa K, Niho S, et al. Dacomitinib versus gefitinib as first-line treatment for patients with EGFR-mutation-positive non-small-cell lung cancer (ARCHER 1050): A randomised, open-label, phase 3 trial. *Lancet Oncol*. 2017;18(11):1454-1466. [https://doi.org/10.1016/s1470-2045\(17\)30608-3](https://doi.org/10.1016/s1470-2045(17)30608-3).
21. Xin S, Zhao Y, Wang X, Huang Y, Zhang J, Guo Y, et al. The dissociation of gefitinib trough concentration and clinical outcome in NSCLC patients with EGFR sensitive mutations. *Sci Rep*. 2015;5:12675. <https://doi.org/10.1038/srep12675>.
22. Food and Drug Administration. Center for Drug Evaluation and Research. Clinical pharmacology and biopharmaceutics review(s) NDA 206995 Review - Gefitinib. 2014.
23. European Medicines Agency. Tarceva: EPAR-Scientific discussion. 2005.
24. Miyamoto S, Azuma K, Ishii H, Bessho A, Hosokawa S, Fukamatsu N, et al. Low-dose erlotinib treatment in elderly or frail patients with EGFR mutation-positive non-small cell lung cancer: A multicenter phase 2 trial. *JAMA Oncol*. 2020;6(7):e201250. <https://doi.org/10.1001/jamaoncol.2020.1250>.
25. Lampson BL, Nishino M, Dahlberg SE, Paul D, Santos AA, Jänne PA, et al. Activity of erlotinib when dosed below the maximum tolerated dose for EGFR-mutant lung cancer: Implications for targeted therapy development. *Cancer*. 2016;122(22):3456-3463. <https://doi.org/10.1002/cncr.30270>.
26. Lind JS, Postmus PE, Heideman DA, Thunnissen EB, Bekers O, Smit EF. Dramatic response to low-dose erlotinib of epidermal growth factor receptor mutation-positive recurrent non-small cell lung cancer after severe cutaneous toxicity. *J Thorac Oncol*. 2009;4(12):1585-1586. <https://doi.org/10.1097/JTO.0b013e3181bbb2b9>.
27. Yeo WL, Riely GJ, Yeap BY, Lau MW, Warner JL, Bodio K, et al. Erlotinib at a dose of 25 mg daily for non-small cell lung cancers with EGFR mutations. *J Thorac Oncol*. 2010;5(7):1048-1053. <https://doi.org/10.1097/JTO.0b013e3181dd1386>.
28. Satoh H, Inoue A, Kobayashi K, Maemondo M, Oizumi S, Isobe H, et al. Low-dose gefitinib treatment for patients with advanced non-small cell lung cancer harboring sensitive epidermal growth factor receptor mutations. *J Thorac Oncol*. 2011;6(8):1413-1417. <https://doi.org/10.1097/JTO.0b013e31821d43a8>.
29. Kwok WC, Ho JCM, Tam TCC, Lui MMS, Ip MSM, Lam DCL. Efficacy of gefitinib at reduced dose in EGFR mutant non-small cell lung carcinoma. *Anticancer Drugs*. 2019;30(10):1048-1051. <https://doi.org/10.1097/cad.0000000000000849>.
30. Hirano T, Yasuda H, Tani T, Hamamoto J, Oashi A, Ishioka K, et al. In vitro modeling to determine mutation specificity of EGFR tyrosine kinase inhibitors against clinically relevant EGFR mutants in non-small-cell lung cancer. *Oncotarget*. 2015;6(36):38789-38803. <https://doi.org/10.18632/oncotarget.5887>.
31. European Medicines Agency. Tarceva: EPAR-Product information. 2019.
32. Foo J, Chmielecki J, Pao W, Michor F. Effects of pharmacokinetic processes and varied dosing schedules on the dynamics of acquired resistance to erlotinib in EGFR-mutant lung cancer. *J Thorac Oncol*. 2012;7(10):1583-1593. <https://doi.org/10.1097/JTO.0b013e31826146ee>.
33. Hayakawa H, Ichihara E, Ohashi K, Ninomiya T, Yasugi M, Takata S, et al. Lower gefitinib dose led to earlier resistance acquisition before emergence of T790M mutation in epidermal growth factor receptor-mutated lung cancer model. *Cancer Sci*. 2013;104(11):1440-1446. <https://doi.org/10.1111/cas.12284>.
34. Fiala O, Hosek P, Pesek M, Finek J, Racek J, Stehlik P, et al. Serum concentration of erlotinib and its correlation with outcome and toxicity in patients with advanced-stage NSCLC. *Anticancer Res*. 2017;37(11):6469-6476. <https://doi.org/10.21873/anticancer.12102>.
35. Yamada K, Miyamoto S, Azuma K, Ishii H, Bessho A, Fukamatsu N, et al. A multicenter phase II study of low-dose erlotinib in frail patients with EGFR mutation-positive, non-small cell lung cancer: Thoracic oncology research group (TORG) trial 1425. *J Clin Oncol*. 2018;36:9063.
36. Timmers L, Boons CC, Moes-Ten Hove J, Smit EF, van de Ven PM, Aerts JG, et al. Adherence, exposure and patients' experiences with the use of erlotinib in non-small cell lung cancer. *J Cancer Res Clin Oncol*. 2015;141(8):1481-1491. <https://doi.org/10.1007/s00432-015-1935-0>.
37. Ding PN, Lord SJ, GebSKI V, Links M, Bray V, Gralla RJ, et al. Risk of treatment-related toxicities from EGFR tyrosine kinase inhibitors: A meta-analysis of clinical trials of gefitinib, erlotinib, and afatinib in advanced EGFR-mutated non-small cell lung cancer. *J Thorac Oncol*. 2017;12(4):633-643. <https://doi.org/10.1016/j.jtho.2016.11.2236>.
38. Greig MJ, Niessen S, Weinrich SL, Feng JL, Shi M, Johnson TO. Effects of activating mutations on EGFR cellular protein turnover and amino acid recycling determined using silac mass spectrometry. *Int J Cell Biol*. 2015;2015:798936. <https://doi.org/10.1155/2015/798936>.

39. Engelman JA, Zejnullahu K, Gale CM, Lifshits E, Gonzales AJ, Shimamura T, et al. PF00299804, an irreversible pan-ERBB inhibitor, is effective in lung cancer models with EGFR and ERBB2 mutations that are resistant to gefitinib. *Cancer Res.* 2007;67(24):11924-11932. <https://doi.org/10.1158/0008-5472.Can-07-1885>.
40. Food and Drug Administration. Center for Drug Evaluation and Research. Clinical pharmacology and biopharmaceutics review(s) NDA 201292 Review – Afatinib 2012.
41. Brown K, Comisar C, Witjes H, Maringwa J, de Greef R, Vishwanathan K, et al. Population pharmacokinetics and exposure-response of osimertinib in patients with non-small cell lung cancer. *Br J Clin Pharmacol.* 2017;83(6):1216-1226. <https://doi.org/10.1111/bcp.13223>.
42. Food and Drug Administration. Center for Drug Evaluation and Research. Clinical pharmacology and biopharmaceutics review(s) NDA 211288 Review – Dacomitinib. 2018.
43. Yates JW, Ashton S, Cross D, Mellor MJ, Powell SJ, Ballard P. Irreversible inhibition of EGFR: Modeling the combined pharmacokinetic-pharmacodynamic relationship of osimertinib and its active metabolite AZ5104. *Mol Cancer Ther.* 2016;15(10):2378-2387. <https://doi.org/10.1158/1535-7163.Mct-16-0142>.
44. Nakao K, Kobuchi S, Marutani S, Iwazaki A, Tamiya A, Isa S, et al. Population pharmacokinetics of afatinib and exposure-safety relationships in Japanese patients with EGFR mutation-positive non-small cell lung cancer. *Sci Rep.* 2019;9(1):18202. <https://doi.org/10.1038/s41598-019-54804-9>.
45. Food and Drug Administration. Center for Drug Evaluation and Research. Clinical pharmacology and biopharmaceutics review(s) NDA 208065 Review – Osimertinib. 2015.
46. Sonobe S, Taniguchi Y, Saijo N, Naoki Y, Tamiya A, Omachi N, et al. 1381 - the efficacy of a reduced dose (40mg) of osimertinib with T790M-positive advanced non-small-cell lung cancer (427P). *Esmo Asia.* 2017.
47. Fang W, Huang Y, Gan J, Shao YW, Zhang L. Durable response of low-dose afatinib plus cetuximab in an adenocarcinoma patient with a novel EGFR exon 20 insertion mutation. *J Thorac Oncol.* 2019;14(10):e220-e221. <https://doi.org/10.1016/j.jtho.2019.05.023>.
48. Nakamura A, Tanaka H, Saito R, Suzuki A, Harada T, Inoue S, et al. Phase II study of low-dose afatinib maintenance treatment among patients with EGFR-mutated non-small cell lung cancer: North Japan Lung Cancer Study Group Trial 1601 (NJLCC1601). *Oncologist.* 2020;25(10):e1451-e1456. <https://doi.org/10.1634/theoncologist.2020-0545>.
49. Yokoyama T, Yoshioka H, Fujimoto D, Demura Y, Hirano K, Kawai T, et al. A phase II study of low starting dose of afatinib as first-line treatment in patients with EGFR mutation-positive non-small-cell lung cancer (KTORG1402). *Lung Cancer.* 2019;135:175-180. <https://doi.org/10.1016/j.lungcan.2019.03.030>.
50. Food and Drug Administration. FDA grants accelerated approval to sotorasib for KRAS G12C mutated NSCLC. Available via <https://fda.gov>. Accessed on 12 July 2021.
51. Amgen. Press release, Amgen Provides Updated Information On LUMAKRAS™ (Sotorasib) Dose Comparison Study. Available via <https://amgen.com>. Accessed on 12 July 2021.
52. Shaw AT, Kim DW, Nakagawa K, Seto T, Crinó L, Ahn MJ, et al. Crizotinib versus chemotherapy in advanced ALK-positive lung cancer. *N Engl J Med.* 2013;368(25):2385-2394. <https://doi.org/10.1056/NEJMoa1214886>.
53. Peters S, Camidge DR, Shaw AT, Gadgeel S, Ahn JS, Kim DW, et al. Alectinib versus crizotinib in untreated ALK-positive non-small-cell lung cancer. *N Engl J Med.* 2017;377(9):829-838. <https://doi.org/10.1056/NEJMoa1704795>.
54. Soria JC, Tan DSW, Chiari R, Wu YL, Paz-Ares L, Wolf J, et al. First-line ceritinib versus platinum-based chemotherapy in advanced ALK-rearranged non-small-cell lung cancer (ASCEND-4): A randomised, open-label, phase 3 study. *Lancet.* 2017;389(10072):917-929. [https://doi.org/10.1016/S0140-6736\(17\)30123-X](https://doi.org/10.1016/S0140-6736(17)30123-X).
55. Solomon BJ, Besse B, Bauer TM, Felip E, Soo RA, Camidge DR, et al. Lorlatinib in patients with ALK-positive non-small-cell lung cancer: Results from a global phase 2 study. *Lancet Oncol.* 2018;19(12):1654-1667. [https://doi.org/10.1016/s1470-2045\(18\)30649-1](https://doi.org/10.1016/s1470-2045(18)30649-1).
56. Food and Drug Administration. Center for Drug Evaluation and Research. Clinical pharmacology and biopharmaceutics review(s) NDA 202570 Review – Crizotinib. 2011.
57. Food and Drug Administration. Center for Drug Evaluation and Research. Clinical pharmacology and biopharmaceutics review(s) NDA 208434 Review – Alectinib. 2015.
58. Food and Drug Administration. Center for Drug Evaluation and Research. Clinical pharmacology and biopharmaceutics review(s) NDA 205755 Review – Ceritinib. 2014.
59. Food and Drug Administration. Center for Drug Evaluation and Research. Clinical pharmacology and biopharmaceutics review(s) NDA 208772 Review – Brigatinib. 2016.
60. Food and Drug Administration. Center for Drug Evaluation and Research. Clinical pharmacology and biopharmaceutics review(s) NDA 210868 Review – Lorlatinib. 2018.

61. Groenland SL, Geel DR, Janssen JM, de Vries N, Rosing H, Beijnen JH, et al. Exposure-response analyses of anaplastic lymphoma kinase inhibitors crizotinib and alectinib in non-small cell lung cancer patients. *Clin Pharmacol Ther.* 2021;109(2):394-402. <https://doi.org/10.1002/cpt.1989>.
62. Mueller-Schoell A, Groenland SL, Scherf-Clavel O, van Dyk M, Huisinga W, Michelet R, et al. Therapeutic drug monitoring of oral targeted antineoplastic drugs. *Eur J Clin Pharmacol.* 2021;77(4):441-464. <https://doi.org/10.1007/s00228-020-03014-8>.
63. Gupta N, Wang X, Offman E, Rich B, Kerstein D, Hanley M, et al. Brigatinib dose rationale in anaplastic lymphoma kinase-positive non-small cell lung cancer: Exposure-response analyses of pivotal ALTA Study. *CPT Pharmacometrics Syst Pharmacol.* 2020;9(12):718-730. <https://doi.org/10.1002/psp4.12569>.
64. Yamazaki S. Translational modeling and simulation for molecularly targeted small molecule anticancer agents: Case studies of multiple tyrosine kinase inhibitors, crizotinib and lorlatinib. In early drug development, f.G. Giordanetto (ed.). 2018. <https://doi.org/10.1002/9783527801756.ch16>.
65. Planchard D, Smit EF, Groen HJM, Mazieres J, Besse B, Helland Å, et al. Dabrafenib plus trametinib in patients with previously untreated BRAFV600E-mutant metastatic non-small-cell lung cancer: An open-label, phase 2 trial. *Lancet Oncol.* 2017;18(10):1307-1316. [https://doi.org/10.1016/S1470-2045\(17\)30679-4](https://doi.org/10.1016/S1470-2045(17)30679-4).
66. Ouellet D, Kassir N, Chiu J, Mouksassi MS, Leonowens C, Cox D, et al. Population pharmacokinetics and exposure-response of trametinib, a MEK inhibitor, in patients with BRAF V600 mutation-positive melanoma. *Cancer Chemother Pharmacol.* 2016;77(4):807-817. <https://doi.org/10.1007/s00280-016-2993-y>.
67. Groenland SL, Janssen JM, Nijenhuis C, de Vries N, Rosing H, Wilgenhof S, et al. 567P exposure-response analyses of dabrafenib and trametinib in melanoma patients. *Ann Oncol.* 2020;31:S486-487.
68. Corcoran RB, Settleman J, Engelman JA. Potential therapeutic strategies to overcome acquired resistance to BRAF or MEK inhibitors in BRAF mutant cancers. *Oncotarget.* 2011;2(4):336-346. <https://doi.org/10.18632/oncotarget.262>.
69. Ranzani M, Alifrangis C, Perna D, Dutton-Regester K, Pritchard A, Wong K, et al. BRAF/NRAS wild-type melanoma, NF1 status and sensitivity to trametinib. *Pigment Cell Melanoma Res.* 2015;28(1):117-119. <https://doi.org/10.1111/pcmr.12316>.
70. European Medicines Agency. Assessment report 315207, Mekinist and Tafinlar. 2017.
71. Corcoran RB, Atreya CE, Falchook GS, Kwak EL, Ryan DP, Bendell JC, et al. Combined BRAF and MEK inhibition with dabrafenib and trametinib in BRAF V600-mutant colorectal cancer. *J Clin Oncol.* 2015;33(34):4023-4031. <https://doi.org/10.1200/jco.2015.63.2471>.
72. Stones CJ, Kim JE, Joseph WR, Leung E, Marshall ES, Finlay GJ, et al. Comparison of responses of human melanoma cell lines to MEK and BRAF inhibitors. *Front Genet.* 2013;4:66. <https://doi.org/10.3389/fgene.2013.00066>.
73. Liu L, Mayes PA, Eastman S, Shi H, Yadavilli S, Zhang T, et al. The BRAF and MEK inhibitors dabrafenib and trametinib: Effects on immune function and in combination with immunomodulatory antibodies targeting PD-1, PD-L1, and CTLA-4. *Clin Cancer Res.* 2015;21(7):1639-1651. <https://doi.org/10.1158/1078-0432.Ccr-14-2339>.
74. Scatena C, Franceschi S, Franzini M, Sanguinetti C, Romiti N, Caponi L, et al. Dabrafenib and trametinib prolong coagulation through the inhibition of tissue factor in BRAF(v600e) mutated melanoma cells in vitro. *Cancer Cell Int.* 2019;19:223. <https://doi.org/10.1186/s12935-019-0938-3>.
75. Negrao MV, Raymond VM, Lanman RB, Robichaux JP, He J, Nilsson MB, et al. Molecular landscape of BRAF-mutant NSCLC reveals an association between clonality and driver mutations and identifies targetable non-V600 driver mutations. *J Thorac Oncol.* 2020;15(10):1611-1623. <https://doi.org/10.1016/j.jtho.2020.05.021>.
76. Doebele RC, Drilon A, Paz-Ares L, Siena S, Shaw AT, Farago AF, et al. Entrectinib in patients with advanced or metastatic NTRK fusion-positive solid tumours: Integrated analysis of three phase 1-2 trials. *Lancet Oncol.* 2020;21(2):271-282. [https://doi.org/10.1016/s1470-2045\(19\)30691-6](https://doi.org/10.1016/s1470-2045(19)30691-6).
77. Food and Drug Administration. Center for Drug Evaluation and Research. Multi-disciplinary review and evaluation NDA 210861 and NDA 211710 – larotrectinib. 2018.
78. Yu H, Steeghs N, Nijenhuis CM, Schellens JH, Beijnen JH, Huitema AD. Practical guidelines for therapeutic drug monitoring of anticancer tyrosine kinase inhibitors: Focus on the pharmacokinetic targets. *Clin Pharmacokinet.* 2014;53(4):305-325. <https://doi.org/10.1007/s40262-014-0137-2>.
79. Di Maio M, Gridelli C, Gallo C, Shepherd F, Piantedosi FV, Cigolari S, et al. Chemotherapy-induced neutropenia and treatment efficacy in advanced non-small-cell lung cancer: A pooled analysis of three randomised trials. *Lancet Oncol.* 2005;6(9):669-677. [https://doi.org/10.1016/s1470-2045\(05\)70255-2](https://doi.org/10.1016/s1470-2045(05)70255-2).

80. Kishida Y, Kawahara M, Teramukai S, Kubota K, Komuta K, Minato K, et al. Chemotherapy-induced neutropenia as a prognostic factor in advanced non-small-cell lung cancer: Results from Japan Multinational Trial Organization LC00-03. *Br J Cancer*. 2009;101(9):1537-1542. <https://doi.org/10.1038/sj.bjc.6605348>.
81. Centanni M, Krishnan SM, Friberg LE. Model-based dose individualization of sunitinib in gastrointestinal stromal tumors. *Clin Cancer Res*. 2020;26(17):4590-4598. <https://doi.org/10.1158/1078-0432.Ccr-20-0887>.
82. Wallin JE, Friberg LE, Karlsson MO. Model-based neutrophil-guided dose adaptation in chemotherapy: Evaluation of predicted outcome with different types and amounts of information. *Basic Clin Pharmacol Toxicol*. 2010;106(3):234-242. <https://doi.org/10.1111/j.1742-7843.2009.00520.x>.
83. Elferink F, van der Vijgh WJ, Klein I, Vermorken JB, Gall HE, Pinedo HM. Pharmacokinetics of carboplatin after i.v. Administration. *Cancer Treat Rep*. 1987;71(12):1231-1237.
84. Ivanov AI, Christodoulou J, Parkinson JA, Barnham KJ, Tucker A, Woodrow J, et al. Cisplatin binding sites on human albumin. *J Biol Chem*. 1998;273(24):14721-14730. <https://doi.org/10.1074/jbc.273.24.14721>.
85. Schellens JH, Ma J, Planting AS, van der Burg ME, van Meerten E, de Boer-Dennert M, et al. Relationship between the exposure to cisplatin, DNA-adduct formation in leucocytes and tumour response in patients with solid tumours. *Br J Cancer*. 1996;73(12):1569-1575. <https://doi.org/10.1038/bjc.1996.296>.
86. Campbell AB, Kalman SM, Jacobs C. Plasma platinum levels: Relationship to cisplatin dose and nephrotoxicity. *Cancer Treat Rep*. 1983;67(2):169-172.
87. Reece PA, Stafford I, Russell J, Khan M, Gill PG. Creatinine clearance as a predictor of ultrafilterable platinum disposition in cancer patients treated with cisplatin: Relationship between peak ultrafilterable platinum plasma levels and nephrotoxicity. *J Clin Oncol*. 1987;5(2):304-309. <https://doi.org/10.1200/jco.1987.5.2.304>.
88. Ibrahim ME, Chang C, Hu Y, Hogan SL, Mercke N, Gomez M, et al. Pharmacokinetic determinants of cisplatin-induced subclinical kidney injury in oncology patients. *Eur J Clin Pharmacol*. 2019;75(1):51-57. <https://doi.org/10.1007/s00228-018-2552-z>.
89. Mense ES, Smit AAJ, Crul M, Franssen EJF. The effect of rapid infusion of cisplatin on nephrotoxicity in patients with lung carcinoma. *J Clin Pharm Ther*. 2019;44(2):249-257. <https://doi.org/10.1111/jcpt.12781>.
90. Chatelut E, White-Koning ML, Mathijssen RH, Puisset F, Baker SD, Sparreboom A. Dose banding as an alternative to body surface area-based dosing of chemotherapeutic agents. *Br J Cancer*. 2012;107(7):1100-1106. <https://doi.org/10.1038/bjc.2012.357>.
91. Schmitt A, Gladieff L, Laffont CM, Evrard A, Boyer JC, Lansiaux A, et al. Factors for hematopoietic toxicity of carboplatin: Refining the targeting of carboplatin systemic exposure. *J Clin Oncol*. 2010;28(30):4568-4574. <https://doi.org/10.1200/jco.2010.29.3597>.
92. Jodrell DI, Egorin MJ, Canetta RM, Langenberg P, Goldbloom EP, Burroughs JN, et al. Relationships between carboplatin exposure and tumor response and toxicity in patients with ovarian cancer. *J Clin Oncol*. 1992;10(4):520-528. <https://doi.org/10.1200/jco.1992.10.4.520>.
93. Calvert AH, Newell DR, Gumbrell LA, O'Reilly S, Burnell M, Boxall FE, et al. Carboplatin dosage: Prospective evaluation of a simple formula based on renal function. *J Clin Oncol*. 1989;7(11):1748-1756. <https://doi.org/10.1200/jco.1989.7.11.1748>.
94. Delanaye P, Ebert N, Melsom T, Gaspari F, Mariat C, Cavalier E, et al. Iohexol plasma clearance for measuring glomerular filtration rate in clinical practice and research: A review. Part 1: How to measure glomerular filtration rate with iohexol? *Clin Kidney J*. 2016;9(5):682-699. <https://doi.org/10.1093/ckj/sfw070>.
95. Dowling TC, Wang ES, Ferrucci L, Sorkin JD. Glomerular filtration rate equations overestimate creatinine clearance in older individuals enrolled in the Baltimore Longitudinal Study on Aging: Impact on renal drug dosing. *Pharmacotherapy*. 2013;33(9):912-921. <https://doi.org/10.1002/phar.1282>.
96. Ekhart C, de Jonge ME, Huijtema AD, Schellens JH, Rodenhuis S, Beijnen JH. Flat dosing of carboplatin is justified in adult patients with normal renal function. *Clin Cancer Res*. 2006;12(21):6502-6508. <https://doi.org/10.1158/1078-0432.Ccr-05-1076>.
97. Millward MJ, Webster LK, Toner GC, Bishop JF, Rischin D, Stokes KH, et al. Carboplatin dosing based on measurement of renal function--experience at the Peter MacCallum Cancer Institute. *Aust N Z J Med*. 1996;26(3):372-379. <https://doi.org/10.1111/j.1445-5994.1996.tb01925.x>.
98. Schmitt A, Gladieff L, Lansiaux A, Bobin-Dubigeon C, Etienne-Grimaldi MC, Boisdrion-Celle M, et al. A universal formula based on cystatin C to perform individual dosing of carboplatin in normal weight, underweight, and obese patients. *Clin Cancer Res*. 2009;15(10):3633-3639. <https://doi.org/10.1158/1078-0432.Ccr-09-0017>.

99. Beunders R, van Groenendaal R, Leijte GP, Kox M, Pickkers P. Proenkephalin compared to conventional methods to assess kidney function in critically ill sepsis patients. *Shock*. 2020;54(3):308-314. <https://doi.org/10.1097/shk.0000000000001510>.
100. Harris BDW, Phan V, Perera V, Szyca A, Galetti P, Martin JH, et al. Inability of current dosing to achieve carboplatin therapeutic targets in people with advanced non-small cell lung cancer: Impact of systemic inflammation on carboplatin exposure and clinical outcomes. *Clin Pharmacokinet*. 2020;59(8):1013-1026. <https://doi.org/10.1007/s40262-020-00870-6>.
101. Veal GJ, Errington J, Tilby MJ, Pearson ADJ, Foot ABM, McDowell H, et al. Adaptive dosing and platinum-DNA adduct formation in children receiving high-dose carboplatin for the treatment of solid tumours. *Br J Cancer*. 2007;96(5):725-731. <https://doi.org/10.1038/sj.bjc.6603607>.
102. Veal GJ, Errington J, Hayden J, Hobin D, Murphy D, Dommert RM, et al. Carboplatin therapeutic monitoring in preterm and full-term neonates. *Eur J Cancer*. 2015;51(14):2022-2030. <https://doi.org/10.1016/j.ejca.2015.07.011>.
103. Picton SV, Keeble J, Holden V, Errington J, Boddy AV, Veal GJ. Therapeutic monitoring of carboplatin dosing in a premature infant with retinoblastoma. *Cancer Chemother Pharmacol*. 2009;63(4):749-752. <https://doi.org/10.1007/s00280-008-0787-6>.
104. Mendelsohn LG, Shih C, Chen VJ, Habeck LL, Gates SB, Shackelford KA. Enzyme inhibition, polyglutamation, and the effect of LY231514 (MTA) on purine biosynthesis. *Semin Oncol*. 1999;26(2 Suppl 6):42-47.
105. Shih C, Chen VJ, Gossett LS, Gates SB, MacKellar WC, Habeck LL, et al. LY231514, a pyrrolo[2,3-d]pyrimidine-based antifolate that inhibits multiple folate-requiring enzymes. *Cancer Res*. 1997;57(6):1116-1123.
106. Stoop MP, Visser S, van Dijk E, Aerts J, Stricker BH, Luider TM. High and individually variable enzymatic activity precludes accurate determination of pemetrexed, methotrexate and their polyglutamate metabolite concentrations in plasma. *J Pharm Biomed Anal*. 2018;148:89-92. <https://doi.org/10.1016/j.jpba.2017.09.014>.
107. Visser S, Koolen SLW, de Bruijn P, Belderbos HNA, Cornelissen R, Mathijssen RHJ, et al. Pemetrexed exposure predicts toxicity in advanced non-small-cell lung cancer: A prospective cohort study. *Eur J Cancer*. 2019;121:64-73. <https://doi.org/10.1016/j.ejca.2019.08.012>.
108. Latz JE, Karlsson MO, Rusthoven JJ, Ghosh A, Johnson RD. A semimechanistic-physiologic population pharmacokinetic/pharmacodynamic model for neutropenia following pemetrexed therapy. *Cancer Chemother Pharmacol*. 2006;57(4):412-426. <https://doi.org/10.1007/s00280-005-0077-5>.
109. Boosman RJ, Dorlo TPC, de Rouw N, Burgers JA, Dingemans AC, van den Heuvel MM, et al. Toxicity of pemetrexed during renal impairment explained - implications for safe treatment. *Int J Cancer*. 2021;149(8):1576-1584. <https://doi.org/10.1002/ijc.33721>.
110. Dickgreber NJ, Fink TH, Latz JE, Hossain AM, Musib LC, Thomas M. Phase I and pharmacokinetic study of pemetrexed plus cisplatin in chemo-naïve patients with locally advanced or metastatic malignant pleural mesothelioma or non-small cell lung cancer. *Clin Cancer Res*. 2009;15(1):382-389. <https://doi.org/10.1158/1078-0432.Ccr-08-0128>.
111. McDonald AC, Vasey PA, Adams L, Walling J, Woodworth JR, Abrahams T, et al. A phase I and pharmacokinetic study of LY231514, the multitargeted antifolate. *Clin Cancer Res*. 1998;4(3):605-610.
112. Rinaldi DA, Burris HA, Dorr FA, Woodworth JR, Kuhn JG, Eckardt JR, et al. Initial phase I evaluation of the novel thymidylate synthase inhibitor, LY231514, using the modified continual reassessment method for dose escalation. *J Clin Oncol*. 1995;13(11):2842-2850. <https://doi.org/10.1200/jco.1995.13.11.2842>.
113. Rinaldi DA, Kuhn JG, Burris HA, Dorr FA, Rodriguez G, Eckhardt SG, et al. A phase I evaluation of multitargeted antifolate (MTA, LY231514), administered every 21 days, utilizing the modified continual reassessment method for dose escalation. *Cancer Chemother Pharmacol*. 1999;44(5):372-380. <https://doi.org/10.1007/s002800050992>.
114. Joerger M, Huitema AD, Krähenbühl S, Schellens JH, Cerny T, Reni M, et al. Methotrexate area under the curve is an important outcome predictor in patients with primary CNS lymphoma: A pharmacokinetic-pharmacodynamic analysis from the IELSG no. 20 trial. *Br J Cancer*. 2010;102(4):673-677. <https://doi.org/10.1038/sj.bjc.6605559>.
115. Latz JE, Chaudhary A, Ghosh A, Johnson RD. Population pharmacokinetic analysis of ten phase II clinical trials of pemetrexed in cancer patients. *Cancer Chemother Pharmacol*. 2006;57(4):401-411. <https://doi.org/10.1007/s00280-005-0036-1>.
116. de Rouw N, Boosman RJ, Huitema ADR, Hilbrands LB, Svensson EM, Derijks HJ, et al. Rethinking the application of pemetrexed for patients with renal impairment: A pharmacokinetic analysis. *Clin Pharmacokinet*. 2021;60(5):649-654. <https://doi.org/10.1007/s40262-020-00972-1>.



117. Bruno R, Hille D, Riva A, Vivier N, ten Bokkel Huinnink WW, van Oosterom AT, et al. Population pharmacokinetics/pharmacodynamics of docetaxel in phase II studies in patients with cancer. *J Clin Oncol*. 1998;16(1):187-196. <https://doi.org/10.1200/jco.1998.16.1.187>.
118. Chen N, Li Y, Ye Y, Palmisano M, Chopra R, Zhou S. Pharmacokinetics and pharmacodynamics of nab-paclitaxel in patients with solid tumors: Disposition kinetics and pharmacology distinct from solvent-based paclitaxel. *J Clin Pharmacol*. 2014;54(10):1097-1107. <https://doi.org/10.1002/jcph.304>.
119. Smorenburg CH, Sparreboom A, Bontenbal M, Stoter G, Nooter K, Verweij J. Randomized cross-over evaluation of body-surface area-based dosing versus flat-fixed dosing of paclitaxel. *J Clin Oncol*. 2003;21(2):197-202. <https://doi.org/10.1200/jco.2003.01.058>.
120. Charles KA, Rivory LP, Stockler MR, Beale P, Beith J, Boyer M, et al. Predicting the toxicity of weekly docetaxel in advanced cancer. *Clin Pharmacokinet*. 2006;45(6):611-622. <https://doi.org/10.2165/00003088-200645060-00004>.
121. Engels FK, Loos WJ, van der Bol JM, de Bruijn P, Mathijssen RH, Verweij J, et al. Therapeutic drug monitoring for the individualization of docetaxel dosing: A randomized pharmacokinetic study. *Clin Cancer Res*. 2011;17(2):353-362. <https://doi.org/10.1158/1078-0432.Ccr-10-1636>.
122. Bruno R, Olivares R, Berille J, Chaikin P, Vivier N, Hammershaimb L, et al. Alpha-1-acid glycoprotein as an independent predictor for treatment effects and a prognostic factor of survival in patients with non-small cell lung cancer treated with docetaxel. *Clin Cancer Res*. 2003;9(3):1077-1082.
123. Ozawa K, Minami H, Sato H. Logistic regression analysis for febrile neutropenia (FN) induced by docetaxel in Japanese cancer patients. *Cancer Chemother Pharmacol*. 2008;62(3):551-557. <https://doi.org/10.1007/s00280-007-0648-8>.
124. Baker SD, Li J, ten Tije AJ, Figg WD, Graveland W, Verweij J, et al. Relationship of systemic exposure to unbound docetaxel and neutropenia. *Clin Pharmacol Ther*. 2005;77(1):43-53. <https://doi.org/10.1016/j.clpt.2004.09.005>.
125. Pallis AG, Agelaki S, Kakolyris S, Kotsakis A, Kalykaki A, Vardakis N, et al. Chemotherapy-induced neutropenia as a prognostic factor in patients with advanced non-small cell lung cancer treated with front-line docetaxel-gemcitabine chemotherapy. *Lung Cancer*. 2008;62(3):356-363. <https://doi.org/10.1016/j.lungcan.2008.03.030>.
126. Lombard A, Mistry H, Aarons L, Ogungbenro K. Dose individualisation in oncology using chemotherapy-induced neutropenia: Example of docetaxel in non-small cell lung cancer patients. *Br J Clin Pharmacol*. 2021;87(4):2053-2063. <https://doi.org/10.1111/bcp.14614>.
127. Joerger M, Huitema AD, Richel DJ, Dittrich C, Pavlidis N, Briasoulis E, et al. Population pharmacokinetics and pharmacodynamics of paclitaxel and carboplatin in ovarian cancer patients: A study by the European Organization for Research and Treatment of Cancer-Pharmacology and Molecular Mechanisms Group and New Drug Development Group. *Clin Cancer Res*. 2007;13(21):6410-6418. <https://doi.org/10.1158/1078-0432.Ccr-07-0064>.
128. Huizing MT, Giaccone G, van Warmerdam LJ, Rosing H, Bakker PJ, Vermorken JB, et al. Pharmacokinetics of paclitaxel and carboplatin in a dose-escalating and dose-sequencing study in patients with non-small-cell lung cancer. The European Cancer Centre. *J Clin Oncol*. 1997;15(1):317-329. <https://doi.org/10.1200/jco.1997.15.1.317>.
129. Jiko M, Yano I, Sato E, Takahashi K, Motohashi H, Masuda S, et al. Pharmacokinetics and pharmacodynamics of paclitaxel with carboplatin or gemcitabine, and effects of CYP3A5 and MDR1 polymorphisms in patients with urogenital cancers. *Int J Clin Oncol*. 2007;12(4):284-290. <https://doi.org/10.1007/s10147-007-0681-y>.
130. Xin DS, Zhou L, Li CZ, Zhang SQ, Huang HQ, Qiu GD, et al. TC > 0.05 as a pharmacokinetic parameter of paclitaxel for therapeutic efficacy and toxicity in cancer patients. *Recent Pat Anticancer Drug Discov*. 2018;13(3):341-347. <https://doi.org/10.2174/1574892813666180305170439>.
131. Mielke S, Sparreboom A, Steinberg SM, Gelderblom H, Unger C, Behringer D, et al. Association of paclitaxel pharmacokinetics with the development of peripheral neuropathy in patients with advanced cancer. *Clin Cancer Res*. 2005;11(13):4843-4850. <https://doi.org/10.1158/1078-0432.Ccr-05-0298>.
132. Hertz DL, Kidwell KM, Vangipuram K, Li F, Pai MP, Burness M, et al. Paclitaxel plasma concentration after the first infusion predicts treatment-limiting peripheral neuropathy. *Clin Cancer Res*. 2018;24(15):3602-3610. <https://doi.org/10.1158/1078-0432.Ccr-18-0656>.

133. Joerger M, von Pawel J, Kraff S, Fischer JR, Eberhardt W, Gauler TC, et al. Open-label, randomized study of individualized, pharmacokinetically (PK)-guided dosing of paclitaxel combined with carboplatin or cisplatin in patients with advanced non-small-cell lung cancer (NSCLC). *Ann Oncol*. 2016;27(10):1895-1902. <https://doi.org/10.1093/annonc/mdw290>.
134. Zhang J, Zhou F, Qi H, Ni H, Hu Q, Zhou C, et al. Randomized study of individualized pharmacokinetically-guided dosing of paclitaxel compared with body-surface area dosing in chinese patients with advanced non-small cell lung cancer. *Br J Clin Pharmacol*. 2019;85(10):2292-2301. <https://doi.org/10.1111/bcp.13982>.
135. Joerger M, Kraff S, Jaehde U, Hilger RA, Courtney JB, Cline DJ, et al. Validation of a commercial assay and decision support tool for routine paclitaxel therapeutic drug monitoring (TDM). *Ther Drug Monit*. 2017;39(6):617-624. <https://doi.org/10.1097/ftd.0000000000000446>.
136. Socinski MA, Manikhas GM, Stroyakovsky DL, Makhson AN, Cheporov SV, Orlov SV, et al. A dose finding study of weekly and every-3-week nab-paclitaxel followed by carboplatin as first-line therapy in patients with advanced non-small cell lung cancer. *J Thorac Oncol*. 2010;5(6):852-861. <https://doi.org/10.1097/jto.0b013e3181d5e39e>.
137. Mini E, Nobili S, Caciagli B, Landini I, Mazzei T. Cellular pharmacology of gemcitabine. *Ann Oncol*. 2006;17 Suppl 5:v7-12. <https://doi.org/10.1093/annonc/mdj941>.
138. Qiu MT, Ding XX, Hu JW, Tian HY, Yin R, Xu L. Fixed-dose rate infusion and standard rate infusion of gemcitabine in patients with advanced non-small-cell lung cancer: A meta-analysis of six trials. *Cancer Chemother Pharmacol*. 2012;70(6):861-873. <https://doi.org/10.1007/s00280-012-1974-z>.
139. Patil V, Noronha V, Joshi A, Chougule A, Kannan S, Bhattacharjee A, et al. Phase III non-inferiority study evaluating efficacy and safety of low dose gemcitabine compared to standard dose gemcitabine with platinum in advanced squamous lung cancer. *EClinicalMedicine*. 2019;9:19-25. <https://doi.org/10.1016/j.eclinm.2019.03.011>.
140. Zwitter M, Kovac V, Smrdel U, Kocijancic I, Segedin B, Vrankar M. Phase I-II trial of low-dose gemcitabine in prolonged infusion and cisplatin for advanced non-small cell lung cancer. *Anticancer Drugs*. 2005;16(10):1129-1134. <https://doi.org/10.1097/00001813-200511000-00013>.
141. Xiong JP, Feng M, Qiu F, Xu J, Tao QS, Zhang L, et al. Phase II trial of low-dose gemcitabine in prolonged infusion and cisplatin for advanced non-small cell lung cancer. *Lung Cancer*. 2008;60(2):208-214. <https://doi.org/10.1016/j.lungcan.2007.10.004>.
142. Kreidieh FY, Moukadem HA, El Saghir NS. Overview, prevention and management of chemotherapy extravasation. *World J Clin Oncol*. 2016;7(1):87-97. <https://doi.org/10.5306/wjco.v7.i1.87>.
143. Piccirillo MC, Daniele G, Di Maio M, Bryce J, De Feo G, Del Giudice A, et al. Vinorelbine for non-small cell lung cancer. *Expert Opin Drug Saf*. 2010;9(3):493-510. <https://doi.org/10.1517/14740331003774078>.
144. Wong M, Balleine RL, Blair EY, McLachlan AJ, Ackland SP, Garg MB, et al. Predictors of vinorelbine pharmacokinetics and pharmacodynamics in patients with cancer. *J Clin Oncol*. 2006;24(16):2448-2455. <https://doi.org/10.1200/jco.2005.02.1295>.
145. Schott AF, Rae JM, Griffith KA, Hayes DF, Sterns V, Baker LH. Combination vinorelbine and capecitabine for metastatic breast cancer using a non-body surface area dosing scheme. *Cancer Chemother Pharmacol*. 2006;58(1):129-135. <https://doi.org/10.1007/s00280-005-0132-2>.
146. Kan M, Imaoka H, Watanabe K, Sasaki M, Takahashi H, Hashimoto Y, et al. Chemotherapy-induced neutropenia as a prognostic factor in patients with pancreatic cancer treated with gemcitabine plus nab-paclitaxel: A retrospective cohort study. *Cancer Chemother Pharmacol*. 2020;86(2):203-210. <https://doi.org/10.1007/s00280-020-04110-3>.
147. Brahmer JR, Drake CG, Wollner I, Powderly JD, Picus J, Sharfman WH, et al. Phase I study of single-agent anti-programmed death-1 (MDX-1106) in refractory solid tumors: Safety, clinical activity, pharmacodynamics, and immunologic correlates. *J Clin Oncol*. 2010;28(19):3167-3175. <https://doi.org/10.1200/jco.2009.26.7609>.
148. Ellassaiss-Schaap K, Rossenu S, Lindauer A, Kang SP, de Greef R, Sachs JR, et al. Using model-based "learn and confirm" to reveal the pharmacokinetics-pharmacodynamics relationship of pembrolizumab in the KEYNOTE-001 trial. *CPT Pharmacometrics Syst Pharmacol*. 2017;6(1):21-28.
149. Topalian SL, Hodi FS, Brahmer JR, Gettinger SN, Smith DC, McDermott DF, et al. Safety, activity, and immune correlates of anti-PD-1 antibody in cancer. *N Engl J Med*. 2012;366(26):2443-2454. <https://doi.org/10.1056/NEJMoa1200690>.
150. Deng R, Bumbaca D, Pastuskovas CV, Boswell CA, West D, Cowan KJ, et al. Preclinical pharmacokinetics, pharmacodynamics, tissue distribution, and tumor penetration of anti-PD-L1 monoclonal antibody, an immune checkpoint inhibitor. *MAbs*. 2016;8(3):593-603. <https://doi.org/10.1080/19420862.2015.1136043>.

151. Song X, Pak M, Chavez C, Liang M, Lu H, Schwickart M, et al. Pharmacokinetics and pharmacodynamics of MEDI4736, a fully human anti-programmed death ligand 1 (PD-L1) monoclonal antibody, in patients with advanced solid tumors. *J Clin Oncol*. 2015;33(15\_suppl):e14009-e14009. [https://doi.org/10.1200/jco.2015.33.15\\_suppl.e14009](https://doi.org/10.1200/jco.2015.33.15_suppl.e14009).
152. Baverel PG, Dubois VFS, Jin CY, Zheng Y, Song X, Jin X, et al. Population pharmacokinetics of durvalumab in cancer patients and association with longitudinal biomarkers of disease status. *Clin Pharmacol Ther*. 2018;103(4):631-642. <https://doi.org/10.1002/cpt.982>.
153. Dai H, Yugmeyer Y, Mangal N. Characterizing exposure-response relationship for therapeutic monoclonal antibodies in immuno-oncology and beyond: Challenges, perspectives, and prospects. *Clin Pharmacol Ther*. 2020;108(6):1156-1170. <https://doi.org/10.1002/cpt.1953>.
154. Turner DC, Kondic AG, Anderson KM, Robinson AG, Garon EB, Riess JW, et al. Pembrolizumab exposure-response assessments challenged by association of cancer cachexia and catabolic clearance. *Clin Cancer Res*. 2018;24(23):5841-5849. <https://doi.org/10.1158/1078-0432.Ccr-18-0415>.
155. Agrawal S, Feng Y, Roy A, Kollia G, Lestini B. Nivolumab dose selection: Challenges, opportunities, and lessons learned for cancer immunotherapy. *J Immunother Cancer*. 2016;4(72):eCollection 2016. <https://doi.org/10.1186/s40425-016-0177-2>.
156. Bajaj G, Wang X, Agrawal S, Gupta M, Roy A, Feng Y. Model-based population pharmacokinetic analysis of nivolumab in patients with solid tumors. *CPT Pharmacometrics Syst Pharmacol*. 2017;6(1):58-66. <https://doi.org/10.1002/psp4.12143>.
157. Liu C, Yu J, Li H, Liu J, Xu Y, Song P, et al. Association of time-varying clearance of nivolumab with disease dynamics and its implications on exposure response analysis. *Clin Pharmacol Ther*. 2017;101(5):657-666. <https://doi.org/10.1002/cpt.656>.
158. Wang R, Zheng J, Shao X, Ishii Y, Roy A, Bello A, et al. Development of a prognostic composite cytokine signature based on the correlation with nivolumab clearance: Translational PK/PD analysis in patients with renal cell carcinoma. *J Immunother Cancer*. 2019;7(1):348. <https://doi.org/10.1186/s40425-019-0819-2>.
159. Centanni M, Moes D, Trocóniz IF, Ciccolini J, van Hasselt JGC. Clinical pharmacokinetics and pharmacodynamics of immune checkpoint inhibitors. *Clin Pharmacokinet*. 2019;58(7):835-857. <https://doi.org/10.1007/s40262-019-00748-2>.
160. Hendriks J, Haanen J, Voest EE, Schellens JHM, Huitema ADR, Beijnen JH. Fixed dosing of monoclonal antibodies in oncology. *Oncologist*. 2017;22(10):1212-1221. <https://doi.org/10.1634/theoncologist.2017-0167>.
161. Topkan E. Weight gain as a surrogate marker of longer survival in advanced non-small cell lung cancer patients. *Ann Transl Med*. 2016;4(19):381. <https://doi.org/10.21037/atm.2016.09.33>.
162. Del Ferraro C, Grant M, Koczywas M, Dorr-Uyemura LA. Management of anorexia-cachexia in late stage lung cancer patients. *J Hosp Palliat Nurs*. 2012;14(6). <https://doi.org/10.1097/NJH.0b013e31825f3470>.
163. Heinhuis KM, Barkman HJ, Beijnen JH, Hendriks J. A cost analysis study of the implementation of fixed-dosing of monoclonal antibodies in the Netherlands Cancer Institute. *Int J Clin Pharm*. 2021;43(1):181-190. <https://doi.org/10.1007/s11096-020-01131-z>.
164. Yoo SH, Keam B, Kim M, Kim SH, Kim YJ, Kim TM. Low-dose nivolumab can be effective in non-small cell lung cancer: Alternative option for financial toxicity. *ESMO Open*. 2018;3(5):e000332. <https://doi.org/10.1136/esmoopen-2018-000332>.
165. Renner A, Burotto M, Rojas C. Immune checkpoint inhibitor dosing: Can we go lower without compromising clinical efficacy? *J Glob Oncol*. 2019;5:1-5. <https://doi.org/10.1200/JGO.19.00142>.
166. Gray JE, Villegas A, Daniel D, Vicente D, Murakami S, Hui R, et al. Three-year overall survival with durvalumab after chemoradiotherapy in stage III NSCLC-update from PACIFIC. *J Thorac Oncol*. 2020;15(2):288-293. <https://doi.org/10.1016/j.jtho.2019.10.002>.
167. Herbst RS, Garon EB, Kim DW, Cho BC, Perez-Gracia JL, Han JY, et al. Long-term outcomes and retreatment among patients with previously treated, programmed death-ligand 1-positive, advanced non-small-cell lung cancer in the KEYNOTE-010 study. *J Clin Oncol*. 2020;38(14):1580-1590. <https://doi.org/10.1200/jco.19.02446>.
168. Spigel DR, McCleod M, Hussein MN, Waterhouse DM, Einhorn L, Horn L, et al. CheckMate 153: Randomized results of continuous vs 1-year fixed-duration nivolumab in patients with advanced non-small cell lung cancer. *Ann Oncol*. 2017;28:Abstract 1297O.
169. von Pawel J, Bordonni R, Satouchi M, Fehrenbacher L, Cobo M, Han JY, et al. Long-term survival in patients with advanced non-small-cell lung cancer treated with atezolizumab versus docetaxel: Results from the randomised phase III OAK study. *Eur J Cancer*. 2019;107:124-132. <https://doi.org/10.1016/j.ejca.2018.11.020>.

170. Feng Y, Roy A, Masson E, Chen TT, Humphrey R, Weber JS. Exposure-response relationships of the efficacy and safety of ipilimumab in patients with advanced melanoma. *Clin Cancer Res.* 2013;19(14):3977-3986. <https://doi.org/10.1158/1078-0432.Ccr-12-3243>.
171. Sharma P, Siefker-Radtke A, de Braud F, Basso U, Calvo E, Bono P, et al. Nivolumab alone and with ipilimumab in previously treated metastatic urothelial carcinoma: CheckMate 032 nivolumab 1 mg/kg plus ipilimumab 3 mg/kg expansion cohort results. *J Clin Oncol.* 2019;37(19):1608-1616. <https://doi.org/10.1200/jco.19.00538>.
172. Ascierto PA, Del Vecchio M, Robert C, Mackiewicz A, Chiarion-Sileni V, Arance A, et al. Ipilimumab 10 mg/kg versus ipilimumab 3 mg/kg in patients with unresectable or metastatic melanoma: A randomised, double-blind, multicentre, phase 3 trial. *Lancet Oncol.* 2017;18(5):611-622. [https://doi.org/10.1016/s1470-2045\(17\)30231-0](https://doi.org/10.1016/s1470-2045(17)30231-0).
173. Ascierto PA, Del Vecchio M, Mackiewicz A, Robert C, Chiarion-Sileni V, Arance A, et al. Overall survival at 5 years of follow-up in a phase III trial comparing ipilimumab 10 mg/kg with 3 mg/kg in patients with advanced melanoma. *J Immunother Cancer.* 2020;8(1). <https://doi.org/10.1136/jitc-2019-000391>.
174. Hellmann MD, Rizvi NA, Goldman JW, Gettinger SN, Borghaei H, Brahmer JR, et al. Nivolumab plus ipilimumab as first-line treatment for advanced non-small-cell lung cancer (CheckMate 012): Results of an open-label, phase 1, multicohort study. *Lancet Oncol.* 2017;18(1):31-41. [https://doi.org/10.1016/s1470-2045\(16\)30624-6](https://doi.org/10.1016/s1470-2045(16)30624-6).
175. European Medicines Agency. Yervoy: EPAR-Product information. 2021.
176. O'Brien L, Westwood P, Gao L, Heathman M. Population pharmacokinetic meta-analysis of ramucirumab in cancer patients. *Br J Clin Pharmacol.* 2017;83(12):2741-2751. <https://doi.org/10.1111/bcp.13403>.
177. Lu JF, Bruno R, Eppler S, Novotny W, Lum B, Gaudreault J. Clinical pharmacokinetics of bevacizumab in patients with solid tumors. *Cancer Chemother Pharmacol.* 2008;62(5):779-786. <https://doi.org/10.1007/s00280-007-0664-8>.
178. Yang K, Wang YJ, Chen XR, Chen HN. Effectiveness and safety of bevacizumab for unresectable non-small-cell lung cancer: A meta-analysis. *Clin Drug Investig.* 2010;30(4):229-241. <https://doi.org/10.2165/11532260-000000000-00000>.
179. Menz BD, Stocker SL, Verougstraete N, Kocic D, Galetti P, Stove CP, et al. Barriers and opportunities for the clinical implementation of therapeutic drug monitoring in oncology. *Br J Clin Pharmacol.* 2021;87(2):227-236. <https://doi.org/10.1111/bcp.14372>.
180. European Medicines Agency. Xalkori: EPAR-Product information. 2020.
181. European Medicines Agency. Alecensa: EPAR-Product information. 2020.
182. European Medicines Agency. Zykadia: EPAR-Product information. 2020.
183. European Medicines Agency. Alunbrig: EPAR-Product information. 2020.
184. European Medicines Agency. Lorviqua: EPAR-Product information. 2020.
185. European Medicines Agency. Tafinlar: EPAR-Product information. 2020.
186. European Medicines Agency. Mekinist: EPAR-Product information. 2020.
187. European Medicines Agency. Vitkravi: EPAR-Product information. 2020.
188. European Medicines Agency. Rozlytrek: EPAR-Product information. 2020.
189. Scheithauser W, Ramanathan RK, Moore M, Macarulla T, Goldstein D, Hammel P, et al. Dose modification and efficacy of nab-paclitaxel plus gemcitabine vs. Gemcitabine for patients with metastatic pancreatic cancer: phase III MPACT trial. *J Gastrointest Oncol.* 2016;7(3):469-478.
190. Bellesoeur A, Ollier E, Allard M, Hirsch L, Boudou-Rouquette P, Arrondeau J, et al. Is there an exposure-response relationship for nivolumab in real-world NSCLC patients? *Cancers (Basel).* 2019;11(11):1784. <https://doi.org/10.3390/cancers11111784>.
191. Chatterjee MS, Elassaiss-Schaap J, Lindauer A, Turner DC, Sostelly A, Freshwater T, et al. Population pharmacokinetic/pharmacodynamic modeling of tumor size dynamics in pembrolizumab-treated advanced melanoma. *CPT Pharmacometrics Syst Pharmacol.* 2017;6(1):29-39. <https://doi.org/10.1002/psp4.12140>.
192. Zielinski CC. A phase I study of MEDI4736, NNT-PD-L1 antibody in patients with advanced solid tumors. *Transl Lung Cancer Res.* 2014;3(6):406-407. <https://doi.org/10.3978/j.issn.2218-6751.2014.08.07>.
193. Segal NH, Hamid O, Hwu W, Massard C, Butler M, Antonia S, et al. 1058PD - a Phase I multi-arm dose-expansion study of the anti-programmed cell death-ligand-1 (PD-L1) antibody MEDI4736: Preliminary data. *Ann Oncol.* 2014;25:iv365. <https://doi.org/10.1093/annonc/mdu342.11>.

194. Morrissey KM, Marchand M, Patel H, Zhang R, Wu B, Phyllis Chan H, et al. Alternative dosing regimens for atezolizumab: An example of model-informed drug development in the postmarketing setting. *Cancer Chemother Pharmacol.* 2019;84(6):1257-1267. <https://doi.org/10.1007/s00280-019-03954-8>.
195. Smit EF, Garon EB, Reck M, Cappuzzo F, Bidoli P, Cohen RB, et al. Exposure-response relationship for ramucirumab from the randomized, double-blind, phase 3 REVEL trial (docetaxel versus docetaxel plus ramucirumab) in second-line treatment of metastatic non-small cell lung cancer. *Cancer Chemother Pharmacol.* 2018;82(1):77-86. <https://doi.org/10.1007/s00280-018-3560-5>.
196. European Medicines Agency. Cyramza: EPAR-Product information. 2020.
197. European Medicines Agency. Avastin: EPAR-Product information. 2020.



# PART 2



**BOOSTING DRUGS TO  
ENHANCE EXPOSURE OR  
DIMINISH RESISTANCE  
TO THERAPY**



# CHAPTER 2.1

# Cytochrome P<sub>450</sub> 3A<sub>4</sub>, 3A<sub>5</sub> and 2C8 expression in breast, prostate, lung, endometrial and ovarian tumors: relevance for resistance to taxanes

*Cancer Chemother Pharmacol. 2019;84(3):487-499*

René J. Boosman\*  
Maarten van Eijk\*  
Alfred H. Schinkel  
Alwin D.R. Huitema  
Jos H. Beijnen

\*these authors contributed equally and thus share first authorship

Author's contribution: R.J. Boosman and M. van Eijk designed this review, performed the literature search, wrote the first draft of the manuscript and edited the contribution of the co-authors in this manuscript.

## **ABSTRACT**

Enzymes of the cytochrome P450 (CYP) subfamily 3A and 2C play a major role in the metabolism of taxane anticancer agents. While their function in hepatic metabolism of taxanes is well established, expression of these enzymes in solid tumors may play a role in the in situ metabolism of drugs as well, potentially affecting the intrinsic taxane susceptibility of these tumors. This article reviews the available literature on intratumoral expression of docetaxel- and paclitaxel-metabolizing enzymes in mammary, prostate, lung, endometrial, and ovarian tumors. Furthermore, the clinical implications of the intratumoral expression of these enzymes are reviewed and the potential of concomitant treatment with protease inhibitors (PIs) as a method to inhibit CYP3A4-mediated metabolism is discussed.

## INTRODUCTION

Breast, prostate, and lung cancer were among the top five most diagnosed cancers worldwide in 2018, while endometrial and ovarian cancer were the most common and deadly gynecologic malignancies in Europe.<sup>1</sup> Despite the emergence of new targeted therapies such as immunotherapy, hormonal therapies, tyrosine kinase, and poly (ADP-ribose) polymerase (PARP) inhibitors, the taxanes, docetaxel and paclitaxel, are still important drugs used in the treatment of these malignancies both as single agents and as part of combination regimens.<sup>2-4</sup> This applies especially in malignancies with fewer treatment options available, such as triple negative breast cancer (TNBC) and metastatic castration-resistant prostate cancer (mCRPC).<sup>5-7</sup> Moreover, a significant increase in survival has been observed in patients with metastatic and non-metastatic hormone naïve prostate cancer treated with docetaxel in addition to androgen-deprivation therapy (ADT) in the CHAARTED and STAMPEDE trials.<sup>8,9</sup>

The taxanes (see Figure 1) bind to the tubulin  $\beta$  subunit, where they stabilize the microtubules by precluding depolymerization. Thereby, cell arrest in the mitotic G2/M phase is induced, leading to cell death.<sup>10</sup> Although paclitaxel and docetaxel come from a similar class of chemotherapeutic agents, their pharmacological characteristics exhibit several differences. Compared to paclitaxel, docetaxel has a longer half-life, higher cytotoxicity, a lower schedule dependency, a different adverse effect profile, longer retention time, and higher in vivo accumulation in tumors.<sup>11,12</sup> This has led to the more frequent use of docetaxel compared to paclitaxel.<sup>13</sup> Unfortunately, patients treated with docetaxel or paclitaxel will often develop resistance.<sup>14-18</sup> Interestingly, despite the similar structural characteristics of the two drugs, a lack of cross-resistance has been observed. For instance, docetaxel has shown activity in a number of paclitaxel-refractory solid tumors.<sup>19-21</sup>

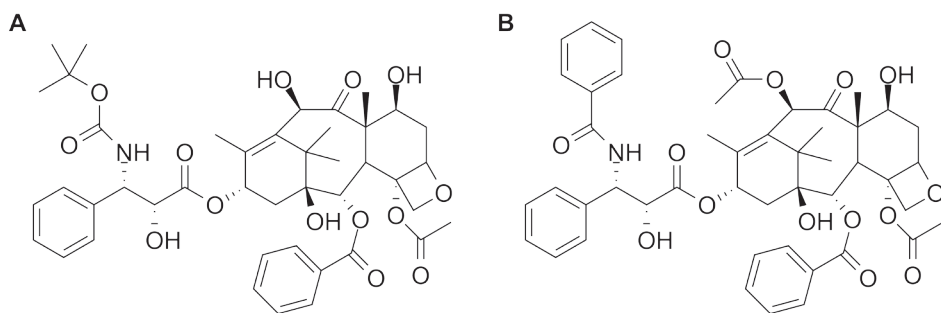


Figure 1. Chemical structures of the taxanes: (A) docetaxel and (B) paclitaxel.

Various mechanisms by which resistance to taxane-based chemotherapy can arise have been proposed. These mechanisms can broadly be classified into the following: (1) pre-target events resulting in reduced intracellular drug concentrations, (2) alterations of the drug-target interaction, or (3) factors influencing the cellular response to damage of the cytoskeleton.<sup>22</sup> Pre-target events could, for example, involve upregulation of the ATP-binding cassette (ABC) drug

efflux transporters such as P-glycoprotein (P-gp, ABCB1) or multidrug resistance protein (MRP1, ABCC1) and breast cancer resistance protein (BCRP, ABCG2).<sup>23</sup> Furthermore, hepatic clearance through metabolizing enzymes from the cytochrome P450 (CYP) superfamily can contribute to decreased plasma exposure. Both paclitaxel and docetaxel are mainly metabolized by CYP3A4. In addition, docetaxel is metabolized by CYP3A5 and paclitaxel by CYP2C8.<sup>24-26</sup>

CYP enzymes are also expressed in a variety of extrahepatic tissues. CYP3A, for example, is markedly expressed in the tissue of the digestive tract.<sup>27</sup> Similarly, it is known that various malignant tissues express CYP enzymes.<sup>28</sup> A variety of studies showed expression of CYP3A4 protein in breast, colorectal, esophageal tumors, and Ewing's sarcoma.<sup>29-33</sup> This expression of CYP enzymes in tumors may limit the intracellular concentrations of docetaxel and paclitaxel, which may cause pre-target resistance. The metabolites of both taxanes show very little if any cytotoxic activity. It has previously been described that the major metabolite of paclitaxel in humans, 6 $\alpha$ -hydroxypaclitaxel, does not induce growth inhibition in tumor cell lines.<sup>34</sup> Likewise, the metabolites of docetaxel show little-to-no antitumor activity.<sup>35</sup> The intratumoral expression of CYP enzymes could, therefore, limit efficacy or even contribute to the development of resistance to taxane therapy. This review will elaborate on the possible role of the CYP enzyme system in tumors of the breast, prostate, lung, ovaries, and endometrium in relation to the clinical pharmacology of docetaxel and paclitaxel. To this end, the expression of CYP enzymes in tumor tissue of different malignancies will be discussed, and possibilities for attenuation of CYP enzymes in tumors will be considered. To our knowledge, Oyama *et al.* were the first to review the intratumoral expression of CYP enzymes in 2004.<sup>28</sup> In this review, we provide updated data on CYP3A4, CYP3A5, and CYP2C8 expression and review the impact of the intratumoral expression on taxane-based therapy.

## DRUG-METABOLIZING CYP ENZYMES

CYP enzymes are found predominantly in the liver and intestines and serve as a clearance mechanism by catalyzing the degradation of exogenous and endogenous substances. Approximately 60 human CYP genes are known, consisting of 18 gene families and 43 subfamilies.<sup>36</sup> CYP enzymes have a broad spectrum of functionalities in relation to cancer. On one hand, these enzymes may protect against carcinogens and even play a role in the activation of anticancer agents. For example, cyclophosphamide, an alkylating prodrug used as immune suppressor and chemotherapeutic for a range of tumors, is metabolized by CYP2A6, CYP2B6, CYP3A4, CYP3A5, CYP2C9, CYP2C18, and CYP2C19 to its active metabolites 4-hydroxy-cyclophosphamide and aldophosphamide.<sup>37</sup> On the other hand, CYP enzymes may play a role in the activation of carcinogens and the metabolism of anticancer drugs. For example, CYP1B1 is overexpressed in many tumor types in comparison to normal tissue and is known for its ability to activate a variety of carcinogens such as polycyclic aromatic hydrocarbons (PAH), heterocyclic amines, aromatic amines, and nitropolycyclic hydrocarbons. Moreover, many anticancer agents are metabolized by the CYP enzyme system into their inactive form.<sup>38-40</sup>

One of the most abundantly expressed CYP enzymes is CYP3A4 which is responsible for the degradation of more than 60% of all marketed drugs.<sup>41</sup> The regulation of its expression has been investigated in a number of studies but has not been fully elucidated. The human pregnane X receptor or steroid xenobiotic receptor (SXR) is the most frequently studied receptor for the control of the CYP3A4 expression.<sup>42-45</sup> Activation of this receptor occurs after binding with CYP inducers, such as rifampicin but also in response to endogenous steroids such as estradiol.<sup>46</sup> <sup>47</sup> Binding of the ligand to the receptor results in the dimerization of the SXR with the 9-*cis*-retinoid X receptor (RXR $\alpha$ ). This heterodimer subsequently binds to its response element on the CYP genes resulting in the transcriptional activation of CYP enzymes.<sup>48</sup> In addition, SXR can enhance drug efflux through the induction of P-gp.<sup>49</sup> It is known that steroid-dependent neoplasms such as breast and endometrial cancer express higher levels of SXR in neoplastic tissues than normal tissues.<sup>50, 51</sup> Paclitaxel, through SXR, markedly induces expression of CYP3A4 and CYP2C8 and P-gp, thereby preventing its own uptake and increasing its own metabolism and excretion when given in a weekly dosing schedule<sup>49, 52, 53</sup> Conversely, docetaxel does not appear to enhance the activity of CYP3A4, although it does activate the transcriptional activation of SXR and CYP3A4 mRNA in human hepatocytes. However, this effect is very weak in comparison to that of paclitaxel.<sup>52, 53</sup> If one of the above-mentioned mechanisms would similarly be present in tumor tissue, this could contribute to the development of resistance or unresponsiveness to chemotherapy in these cells.

## EXPRESSION OF CYP3A4, CYP3A5, AND CYP2C8 IN TUMORS

The expression of drug-metabolizing CYP enzymes in human tumors and other extrahepatic tissues has been a subject of investigation for several years.<sup>54</sup> Due to the metabolism or activation of many anticancer drugs by CYP enzymes, it is of particular interest to investigate whether CYP enzymes are also expressed in tumor tissue.<sup>40, 55</sup> CYP expression in tumor and non-tumor tissues of the breast, colon, and lung has been thoroughly studied. However, tumor tissues such as the endometrium and prostate remain poorly investigated.<sup>28</sup> Methods often used to study the presence of CYP enzymes in tissues include immunohistochemistry (IHC) or western blot.<sup>56, 57</sup> In addition, the presence of mRNA can be measured using reverse transcription polymerase chain reaction (RT-PCR) or northern blotting.<sup>58, 59</sup> Studies investigating the presence of CYP3A4/5 and CYP2C in extrahepatic tissues and tumors are summarized in Table 1.

Table 1. Overview of literature studies reporting the expression of CYP3A and CYP2C protein or mRNA from patient samples.

Study	References	CYP3A		
		Protein	Healthy (n)	mRNA
		Tumor (n)		Tumor (n)
<b>Breast Cancer</b>				
Albin <i>et al.</i> (1993)	68	0% (12)	0% (12)	-
Hellmold <i>et al.</i> (1998)	63	-	0%(15)	75% (4)
Murray <i>et al.</i> (1993)	66	22% (54) <sup>a</sup>	-	-
Huang <i>et al.</i> (1996)	62	-	-	15% (13)
Yokose <i>et al.</i> (1999)	67	0% (6)	-	-
Iskan <i>et al.</i> (2001)	64	-	-	0% (8) <sup>a</sup> 0% (4) <sup>b</sup>
Miyoshi <i>et al.</i> (2002)	101	37% (38) <sup>a,d</sup>	-	-
El-Rayes <i>et al.</i> (2003)	56	+ (29)	+ (29)	-
Kapucuoglu <i>et al.</i> (2003)	29	100% (25) <sup>a</sup>	68% (25) <sup>a</sup>	-
Knüpfer <i>et al.</i> (2004)	72	-	-	-
Schmidt <i>et al.</i> (2004)	71	100% (11) <sup>a</sup> 0% (10) <sup>b</sup>	-	-
Miyoshi <i>et al.</i> (2005)	102	52% (31) <sup>a</sup>	-	-
Haas <i>et al.</i> (2006)	70	25% (393) <sup>a,b</sup>	-	-
Vaclavikova <i>et al.</i> (2007)	65	-	-	BLQ (40) <sup>a</sup>
Murray <i>et al.</i> (2010)	32	52% (170) <sup>a,d,e</sup> 19% (170) <sup>b,d,e</sup>	-	-
Sakurai <i>et al.</i> (2011)	103	55% (42) <sup>a</sup>	-	-
Floriano-Sanchez <i>et al.</i> (2014)	69	+ (48) <sup>a</sup>	+(48) <sup>a</sup>	-
<b>Prostate Cancer</b>				
Murray <i>et al.</i> (1995)	79	61% (51)	-	-
Yokose <i>et al.</i> (1999)	67	0% (6)	-	-
Finnström <i>et al.</i> (2001)	58	-	-	10% (28) <sup>a,f</sup> 86% (28) <sup>b,f</sup>
Koch <i>et al.</i> (2002)	74	-	-	-
Di Paolo <i>et al.</i> (2005)	80	-	58% (24) <sup>a</sup> 54% (24) <sup>b</sup>	-
Moilanen <i>et al.</i> (2007)	77	-	100% (6) <sup>b</sup>	-
Bièche <i>et al.</i> (2007)	54	-	-	-
Leskelä <i>et al.</i> (2007)	76	0% (35) <sup>b</sup>	100% (10) <sup>b</sup>	0% (10) <sup>b</sup>
Fujimura <i>et al.</i> (2009)	81	75% (107) <sup>a</sup>	93% (88) <sup>a</sup>	-

CYP2C				
Protein		mRNA		
Healthy (n)	Tumor (n)	Healthy (n)	Tumor (n)	Healthy (n)
-	0% (12)	0% (12)	-	-
73% (15)	-	0% (14) <sup>c</sup>	100% (4)	100% (15)
-	-	-	-	-
73% (11) <sup>a</sup> 82% (11) <sup>b</sup>	-	-	100% (13)	100% (11)
-	33% (6)	-	-	-
0% (8) <sup>a</sup> 0% (4) <sup>b</sup>	-	-	83% (6)	83% (6)
-	-	-	-	-
-	-	-	-	-
-	-	-	-	-
-	-	-	100% (10) <sup>c</sup>	-
-	-	-	-	-
-	-	-	-	-
BLQ (40) <sup>a</sup>	-	-	-	-
-	30% (170)	-	-	-
-	-	-	-	-
-	-	-	-	-
-	25% (51)	-	-	-
-	83% (6)	-	-	-
11% (28) <sup>a,f</sup> 86% (28) <sup>b,f</sup>	-	-	-	-
0% (47) <sup>a</sup> + (47) <sup>b</sup>	-	-	-	-
-	-	-	-	-
-	-	-	-	-
+ (32) <sup>b</sup>	-	-	-	-
+ (10) <sup>b</sup>	-	-	-	-
-	-	-	-	-



Table 1. Continued.

Study	References	CYP3A		
		Protein		mRNA
		Tumor (n)	Healthy (n)	Tumor (n)
Mitsiades <i>et al.</i> (2012)	75	-	-	+ (146) <sup>a,b</sup>
<b>NSCLC</b>				
Nakajima <i>et al.</i> (1994)	85	-	-	-
Kivistö <i>et al.</i> (1995)	86	25% (32)	34% (32)	-
Kivistö <i>et al.</i> (1996)	87	100% (8)	100% (8)	0% (8) <sup>a</sup> 50% (8) <sup>b</sup>
Anttila <i>et al.</i> (1997)	88	-	18.5% (27) <sup>a</sup>	-
Macé <i>et al.</i> (1998)	84	-	-	-
Yokose <i>et al.</i> (1999)	67	0% (18)		
Fujitaka <i>et al.</i> (2001)	90	-	-	+ (10) <sup>a</sup>
Bièche <i>et al.</i> (2007)	54	-	-	-
Qixing <i>et al.</i> (2017)	89	74% (87) <sup>***.a,d</sup> 49% (87) <sup>b,d</sup>	+(87) <sup>a</sup> +(87) <sup>***.b</sup>	-
<b>Endometrial Cancer</b>				
Hukkanen <i>et al.</i> (1998)	94	-	-	-
Yokose <i>et al.</i> (1999)	67	0% (12)		
Sarkar <i>et al.</i> (2003)	95	-	-	-
Masuyama <i>et al.</i> (2003)	50	-	-	+ (20) <sup>a</sup>
<b>Ovarian Cancer</b>				
Yokose <i>et al.</i> (1999)	67	0% (12)	-	-
Klose <i>et al.</i> (1999)	91	-	-	-
Downie <i>et al.</i> (2005)	98	91% (99)/ 80% (22) <sup>a,g</sup> 66% (99)/ 55% (22) <sup>b,g</sup>	64% (13) <sup>a</sup> 55% (13) <sup>b</sup>	-
Bièche <i>et al.</i> (2007)	54	-	-	-
DeLoia <i>et al.</i> (2008)	97	-	-	9% (47) <sup>a</sup> 89% (47) <sup>b</sup>

The percentages shown indicate the number of samples in which CYP enzymes could be detected, with in parentheses the total amount of samples/patients analyzed. (+) indicates CYP enzymes were expressed, but the exact number of positive samples was not described or presented as immunoreactivity score. (-) indicates not measured. P values indicate higher proportion, immunoreactivity score, or expression level compared to respective tumor/non-tumor sample. \*P < 0.05, \*\*P < 0.01, \*\*\*P < 0.001.

BLQ: below limit of quantification, NSCLC: non-small cell lung cancer

CYP2C				
Protein		mRNA		
Healthy (n)	Tumor (n)	Healthy (n)	Tumor (n)	Healthy (n)
+ (29) <sup>a,b</sup>	-	-	-	-
-	+ (27)	+ (11)	-	-
-	-	-	-	-
0% (8) <sup>a</sup> 100% (8) <sup>b</sup>	-	-	-	-
13% (8) <sup>a</sup> 100% (8) <sup>b</sup>	-	-	-	-
0% (14) <sup>a</sup> 93% (14) <sup>b</sup>	-	-	-	100% (14)
	0% (18)			
+ (10) <sup>a</sup>	-	-	+(10) <sup>c</sup>	+(10)
+ (6) <sup>b</sup>	-	-	-	-
-	-	-	-	-
57% (7) <sup>a</sup> 43% (7) <sup>b</sup>	-	-	-	-
	0% (12)			
57% (23) <sup>a</sup>	-	-	-	-
-	-	-	-	-
-	0% (12)	-	-	-
-	-	-	-	100% (1)
-	17% (99)/ 10% (22) <sup>g</sup>	36% (13)	-	-
+ (15) <sup>b</sup>	-	-	-	+(15)
-	-	-	69% (48) <sup>c</sup>	-

<sup>a</sup> Only CYP3A4.

<sup>b</sup> Only CYP3A5.

<sup>c</sup> Only CYP2C8.

<sup>d</sup> Percentage indicates a fraction of tumors with moderate/high expression.

<sup>e</sup> Original data from publication received from the authors.

<sup>f</sup> No distinction between tumor and non-tumor tissue.

<sup>g</sup> Percentages for primary ovarian cancer and peritoneal metastases, respectively.

### Breast cancer

CYP enzymes are responsible for the phase I metabolism of estrogen and, therefore, have a prominent role in the pathogenesis of breast cancer. In extrahepatic tissues, CYP1B1 is responsible for the conversion of  $17\beta$ -estradiol ( $E_2$ ) into 4-hydroxyestradiol which may act as a carcinogen, while CYP1A1 and CYP3A4, on the other hand, metabolize  $E_2$  into its non-carcinogenic 2-hydroxy metabolite.<sup>60, 61</sup> This extrahepatic expression of enzymes may also have implications for treatment with taxanes. Studies using RT-PCR to detect CYP3A4 mRNA have produced variable results with some studies indeed finding relevant CYP3A4 expression<sup>62, 63</sup>, and some others find no expression of CYP3A at all.<sup>64, 65</sup> Other experiments using IHC or western blot to detect CYP3A protein expression also produced contrasting results.<sup>63, 66-68</sup> When comparing expression levels in malignant versus healthy tissue, results are similarly ambiguous with some studies finding a lower CYP3A4 expression in malignant tissues compared to adjacent morphologically normal tissue<sup>66</sup>, and other studies suggesting increased expression of CYP3A4 in tumors.<sup>29, 69</sup> In one of the larger trials investigating CYP expression in mammary tumors, Haas and colleagues analyzed tissue from 393 breast cancer patients using IHC. Their analysis showed expression in 25% of mammary tumor samples screened for CYP3A4/5. Moreover, this CYP3A4/5 expression showed a significant association with a positive nodal status in patients ( $p = 0.018$ ).<sup>70</sup> In 2010, Murray and colleagues<sup>32</sup> also found an association between CYP3A4 expression and survival. Although the difference was marginal, patients with tumors that showed a low/negative CYP3A4 immunoreactivity had a mean survival of 79 months (95% confidence interval (CI): 77-81 months), while patients with tumors that showed moderate/strong CYP3A4 immunoreactivity had a mean survival period of 86 months (95% CI: 79-93 months).<sup>32</sup> Some studies have investigated the mRNA and protein expression of enzymes of the CYP2C subfamily in breast cancer tumors with similar contradictory results.<sup>62, 63, 65, 67, 68, 71, 72</sup> Schmidt and colleagues, in addition to detecting CYP3A4 and CYP2C9 in breast cancer microsomes, also investigated the ability of these microsomes to metabolize ifosfamide. Using LC/MS, a minimal in vitro ifosfamide N-dechloroethylation ( $0.12 \pm 0.07$  pmol/min/mg<sub>protein</sub>) could be detected in all four measured breast cancer microsomes. In comparison, previous studies in liver samples from female patients had shown activities of  $132 \pm 57$  pmol/min/mg<sub>protein</sub> for ifosfamide N-dechloroethylation.<sup>74-73</sup> Although very minimal, this demonstrates that the mechanism of CYP3A4-mediated ifosfamide metabolism is present in breast cancer microsomes.

Despite the large variability in reported expression frequencies, some larger studies suggest that the CYP3A4 protein is present somewhere between 20 and 55% of breast cancer tissues. For CYP2C enzymes, there also appears to be some expression in mammary tissue, whereas, for CYP3A5, this evidence is very limited. Although, in the majority of studies, the functionality of the enzyme remains to be elucidated, the fundamental conditions for CYP mediated metabolism appear to be present in a subpopulation of breast cancers which may have implications for taxane chemotherapy.

### Prostate cancer

Interestingly, several studies which measured CYP3A mRNA in both normal prostate and cancerous tissue seem to suggest that CYP3A5 is the most abundant CYP in these tissues.<sup>54, 58, 74-77</sup> Even though about 80% of Caucasians are CYP3A5 deficient.<sup>78</sup> While studies investigating CYP3A protein expression in tumor samples have mainly found relatively high expression of both CYP3A4 and

CYP3A5 both in tumor and non-tumor tissue.<sup>79-81</sup> Furthermore, enzymes of the CYP2C family were also detected in tumor samples in some studies.<sup>67, 79</sup> In 2009, Fujimura and colleagues detected CYP3A4 in healthy prostate and prostate cancer tissue and found that prostate cancer cells had a lower CYP3A4 immunoreactivity score (sum of the proportion of positively stained cells and staining intensity;  $3.6 \pm 2.6$ ) compared to the benign epithelium ( $4.5 \pm 2.1$ ;  $p < 0.0001$ ). Moreover, this lower immunoreactivity score showed a significant inverse correlation with a higher Gleason score and a poorer prognosis in patients.<sup>81</sup> This result was supported by the finding of a decreased expression of CYP3A4 and CYP3A5 in CRPC cells compared to benign prostate tissue.<sup>75</sup> Physiologically, this could be explained by a reduced conversion of androgens, such as testosterone into the inactive  $6\beta$ -hydroxytestosterone ( $6\beta$ -OH-T) metabolite, leading to increased androgen-dependent proliferation. A hypothesis is supported by the association between CYP3A4 and CYP3A5 polymorphisms and haplotypes and prostate cancer risk and aggressiveness.<sup>82, 83</sup> In conclusion, heterogeneous CYP3A4, CYP3A5, and CYP2C8 expression in neoplasms of the prostate is observed, possibly contributing to variable treatment response to taxanes, even though the expression may be decreased in malignant tissue in comparison to healthy tissue.

#### Non-small cell lung cancer (NSCLC)

RT-PCR analyses have shown that CYP3A4 and CYP3A5 are present in healthy and malignant lung tissue.<sup>54, 84, 85</sup> Yet, results of IHC analyses are less clear, although the CYP3A4 protein is expressed in about 20% of the observed tissue samples.<sup>86-88</sup> A more recent study showed that CYP3A4 expression was significantly higher in tumor tissue when compared with normal lung tissue.<sup>89</sup> These results, obtained from an online data set on CYP3A4 and CYP3A5 expression, did not contain data whether the patients received prior chemotherapy or not. Therefore, the study also featured an IHC analysis of 92 patients, who were included prior to any chemotherapy treatment. In this subset, a significant higher CYP3A4 expression was observed in comparison with the adjacent healthy tissue. In addition, CYP3A4 expression was significantly correlated with advanced TNM stages ( $p = 0.013$ ) and poor histological differentiation ( $p = 0.017$ ), while CYP3A5 was only significantly associated with histological differentiation. Moreover, an association between high-CYP3A4 or low-CYP3A5 expression and poor survival could be observed.<sup>89</sup> CYP2C gene-expression levels were found to be significantly increased in lung cancer tissue compared to healthy lung tissue.<sup>90</sup> In the study by Klose *et al.*, CYP2C8 mRNA expression was found to be highly variable, although some older studies were able to detect CYP2C8 protein or mRNA.<sup>84, 85, 91</sup> In conclusion, taxane-metabolizing enzymes appear to be present in both healthy and malignant lung tissue, and upregulation of these enzymes may be observed in malignant tissue.

#### Endometrial cancer

Estrogen itself is an important contributor to the growth and development of endometrial tumors. Contrary to the effects of progesterone, estrogen stimulates the endometrium to proliferate. A misbalance in favor of estrogen may, therefore, contribute to the early stages of endometrial cancer formation.<sup>92</sup> The extrahepatic metabolism of estrogen by CYP1B1, 1A1, and CYP3A4 is described above. As in breast cancer, these enzymes may also be present in endometrial tumors and play a role in local estrogen metabolism. The presence of CYP3A4 and CYP3A5 enzymes in endometrial

cells seems variable with some studies finding no CYP3A4 and CYP3A5 mRNA, but high expression of CYP3A7 mRNA in the endometrium and placenta.<sup>93</sup> In contrast to this finding, other studies found expression of CYP2C, CYP3A4, CYP3A5, and CYP3A7 mRNA among other CYP enzymes in normal endometrium tissue.<sup>94-95</sup> Another study found that CYP3A4 and CYP3A7 mRNA expression was low in normal endometrium, but was significantly upregulated in endometrial cancer tissues.<sup>50</sup> Together, this suggests some expression on an mRNA level of taxane-metabolizing enzymes of the CYP3A subfamily in healthy endometrium and endometrial cancer, although the small body of evidence does not allow for any strong conclusions.

### Ovarian cancer

As in breast and endometrial cancer, it is thought that estrogen plays a similar role in tumor initiation and promotion in ovarian cancer.<sup>96</sup> CYP enzymes may, therefore, also play a similar role in ovarian tumors. The presence of CYP2C8 and CYP3A5 mRNA has been reported in ovarian tissue.<sup>54-91</sup> However, mRNA in both studies was collected from the whole gland tissue, whereas ovarian tumors are mainly of epithelial origin.<sup>97</sup> Downie *et al.* found that CYP3A5, among other CYP enzymes, had a significantly greater intensity of IHC staining ( $p < 0.001$ ) in primary ovarian cancer tissue compared with normal ovary.<sup>98</sup> A later study investigated the presence of taxane-metabolizing enzymes in ovarian cancer and found that CYP3A4 is expressed at very low levels in ovarian cancer, while CYP3A5 and CYP2C8 were expressed in the majority of ovarian tumors, regardless of histologic type, stage, or grade.<sup>97</sup> As in endometrium, evidence regarding the expression of taxane-metabolizing CYP enzymes in the ovaries and in ovarian cancer is limited. Although the studies available seem to suggest a relatively high expression compared to other tissues, especially for CYP3A5.

## **TAXANES AND CYP3A EXPRESSION IN TUMOR CELLS**

The hepatic induction of CYP3A enzymes by paclitaxel and to a lesser degree by docetaxel prompts questions whether a similar mechanism could have an effect on the expression of CYP3A enzymes in tumors.<sup>52</sup> This mechanism may be of clinical relevance during the application of taxane chemotherapy as it may impact treatment outcome.<sup>49, 52-53</sup> In vitro studies have shown that human prostate cancer (DU-145) and breast cancer (MCF-7) cells lines indeed express a higher amount of CYP3A4 protein in response to treatment with docetaxel.<sup>99, 100</sup> In addition, Ikezoe and colleagues found a 2.0-fold increase in CYP3A4 expression in DU-145 xenografts in BNX nude mice after treatment with docetaxel.<sup>99</sup> Fujitaka and colleagues observed an increase in CYP3A4 mRNA expression in peripheral mononuclear cells from patients with previously untreated lung cancer after treatment with docetaxel. For CYP2C8, no such increase could be observed.<sup>90</sup> Similarly, DeLoia *et al.* investigated gene expression of CYP2C8, CYP3A4, CYP3A5, and ABCB1 in epithelial ovarian tumors, and exposed these tumor cells to docetaxel and paclitaxel *ex vivo*. There was no apparent correlation between any single gene expressed and taxane disposition, although a strong correlation between the ratio of CYP3A5:ABCB1 and the clearance of docetaxel was observed.<sup>97</sup>

The presence of CYPs in tumors can similarly be linked to clinical outcomes of docetaxel treatment. Miyoshi *et al.* found that CYP3A4 expression in tumors, measured by mRNA and IHC, correlates with clinical outcomes in breast cancer patients treated with docetaxel. Patients with low CYP3A4 mRNA levels ( $n = 14$ ) exhibited a significantly higher response rate to docetaxel treatment than those with high CYP3A4 mRNA levels ( $n = 9$ , 71% vs. 11%,  $p < 0.01$ ).<sup>101</sup> In addition, patients with CYP3A4-negative tumors ( $n = 15$ ), determined by IHC, showed a significantly higher response rate to docetaxel treatment than those with CYP3A4-positive tumors ( $n = 16$ , 67% vs. 19%,  $p < 0.01$ ).<sup>102</sup> Later, breast cancer tissue obtained from a larger trial in 42 patients who underwent docetaxel treatment as adjuvant chemotherapy after surgery was analyzed for CYP3A4 expression using IHC. The 19 patients with CYP3A4-negative tumors showed a significantly higher response rate to docetaxel treatment than the 23 patients with CYP3A4-positive tumors (63.2% vs. 26.1%,  $p < 0.01$ ). Moreover, a higher clinical benefit rate was observed in CYP3A4-negative tumors (73.7% vs. 26.1%,  $p < 0.01$ ) as well as a longer time to progression ( $8.9 \pm 5.8$  months vs.  $5.2 \pm 4.4$  months,  $p < 0.05$ ). These results suggest that assessing CYP3A4 expression in breast cancer may be a relevant tool to predict the response of the tumor to docetaxel treatment.<sup>103</sup> In 16 patients with NSCLC receiving docetaxel or docetaxel and carboplatin for advanced disease, CYP3A4 gene expression in peripheral mononuclear cells was analyzed. After 24 h, the CYP3A4 expression was significantly increased when compared to baseline. Treatment with carboplatin monotherapy did not cause any statistically significant difference in CYP3A4 expression. In the same study, 20 autopsy samples (10 NSCLC + 10 control) from chemotherapy-naïve patients were analyzed on the levels of CYP3A4 gene expression. Although the variability in gene expression was high, there was no significant difference between healthy and cancerous tissue. In the case of CYP2C8, however, increased expression in tumor tissue could be observed.<sup>90</sup>

Despite the small number of patients included in these studies, the evidence presented seems to indicate that an increase in intratumoral CYP3A4 expression can be observed after treatment with taxanes. Increased CYP3A4 expression could be inversely correlated to clinical response rates to these drugs. Together, this suggests that these CYP enzymes are part of a resistance mechanism in which the in situ metabolism of docetaxel is accelerated, thereby diminishing response to docetaxel-containing chemotherapy.

## CONCOMITANT TREATMENT WITH TAXANES AND HIV-PROTEASE INHIBITORS

As a notorious group of CYP3A4 inhibitors, it is of great interest to know whether or not HIV-protease inhibitors (PIs) will have an effect on intratumoral CYP3A4 functionality. Ritonavir, developed as an HIV PI, is one of the most potent inhibitors of CYP3A4 known, although the precise mechanism of inhibition has yet to be clarified.<sup>104, 105</sup> Ritonavir is used in HIV therapy to boost the concentration of other drugs with a known CYP3A4-dependent metabolism.<sup>106</sup> Its effect on CYP3A4 is irreversible, and consequently, the reversal of inhibition is dependent on the degradation half-life of CYP3A4, which is thought to be about 29 h. After cessation of ritonavir treatment, CYP3A4 expression returns

to baseline after approximately six days.<sup>107, 108</sup> Docetaxel is strongly metabolized by CYP3A4, and hence, it is hypothesized that concomitant treatment of docetaxel and ritonavir will increase the antitumor activity of docetaxel.<sup>99</sup> Pharmacokinetic parameters of docetaxel such as clearance and half-life are decreased and increased, respectively, when co-administered with ritonavir.<sup>109-111</sup> Several in vivo studies have shown the effect on the tumor response after co-administration with ritonavir.<sup>99, 112</sup> In one study with an immunocompetent, orthotopic Cyp3a<sup>-/-</sup> mouse model, the effect of intravenous docetaxel and oral ritonavir on Cyp3a expressing K14cre; Brca1<sup>F/F</sup>; p53<sup>F/F</sup> mammary tumors was studied.<sup>112</sup> The co-treatment led to a decrease in tumor volume greater than docetaxel treatment alone (70% vs. 30% shrinkage of the initial tumor volume after 3 weeks of treatment). In addition, the median time in which the tumor reached the critical tumor size (approximately 1500 mm<sup>3</sup>) was significantly increased when docetaxel and ritonavir were given together (65.6 ± 8.6 days vs. 53.6 ± 1.5 days for docetaxel monotherapy). As expected, the plasma concentration of docetaxel did not show significant differences in the ritonavir co-administered group. However, the intratumoral docetaxel concentration was significantly higher after 9 days of treatment with docetaxel and ritonavir in comparison with docetaxel monotherapy. Furthermore, the docetaxel metabolite concentrations were lower in the combination treatment group compared to the group treated with single-agent docetaxel, suggesting that ritonavir specifically inhibited the intratumoral metabolism of docetaxel.<sup>112</sup>

PIs do not only interfere with the metabolism of taxanes by direct inhibition of CYP3A4, but could also amplify their antitumor effects via additional mechanisms. Table 2 summarizes the proposed synergistic effect of the PIs to docetaxel treatment. Using western blot analysis, it was shown that ritonavir could potentiate the effect of docetaxel on the activation of caspase-3 and the cleavage of PARP (which is cleaved as a late event during apoptosis). Ritonavir can inhibit the docetaxel-induced increase in CYP3A4 mRNA completely in the mouse androgen-dependent prostate cancer cells. In vivo docetaxel markedly decreased the growth rate and size of DU145 tumors in male BNX mice. Ritonavir alone showed no statistical significance either in growth or in weight of the tumors. Interestingly, the combination of the taxane and the PI showed an additional statistically significant decrease in both growth and tumor weights in comparison with the monotherapy of docetaxel. Histologically, a site composed of necrotic and fibrotic tissue was observed, but no cells of cancerous origin were detected. Moreover, the organs of the mice were not affected. In addition, ritonavir has shown to block the DNA-binding activity of nuclear factor-κB (NFκB) in the DU145 cells and in vivo.<sup>99</sup>

In various types of cancer including prostate cancer, hyperactivity of the NFκB pathway has been observed.<sup>113</sup> This hyperactivity often results in the development of resistance to several anticancer drugs such as paclitaxel and docetaxel.<sup>99, 112</sup> By decreasing the DNA-binding activity of NFκB, it is possible that ritonavir surpasses this resistance mechanism of docetaxel and will, therefore, increase the effectiveness of the docetaxel treatment. In the lung cancer cell line NCI-H460, a decrease in growth of 39 and 21% was observed when treated with single-agent nelfinavir and docetaxel, respectively. However, when the cell lines were incubated with nelfinavir prior to docetaxel, a growth inhibition of 51% was observed. Similar effects were observed in the NCI-H520 cell line, suggesting that the nelfinavir-induced inhibition of the Akt signaling results in more sensitivity

to docetaxel treatment.<sup>114</sup> The activation of Akt pathway is described in the literature as being responsible for the development of resistance, and as a result, tumors are often overexpressing Akt in these cell populations.<sup>115</sup> Moreover, docetaxel resistance is tackled in some studies by inhibiting the Akt pathway and therefore resensitizing the tumor cells for docetaxel treatment.<sup>116, 117</sup> Whether ritonavir acts the same way as nelfinavir on NSCLC cells is not studied in the earlier mentioned article. Yet, there are reports that ritonavir can block the Akt signaling in ovarian cancer and breast cancer and, thus, can re-sensitize the resistant tumor cells for docetaxel treatment.<sup>118, 119</sup>

In summary, the co-treatment of docetaxel with ritonavir enhances the cytotoxic activity of docetaxel in the tumor and ritonavir could, therefore, potentiate the effect of docetaxel as a chemotherapeutic agent. Currently, the first phase I and II trials using an oral formulation of docetaxel called ModraDoc006 co-administered with ritonavir are underway in mCRPC (NCT03136640) and metastatic breast cancer (NCT03890744). Earlier trials with this formulation in patients with various solid tumors have shown promising antitumor activity and highlight the potential of this innovative way of attenuating CYP activity to boost oral docetaxel bioavailability and to possibly improve clinical efficacy.<sup>120-122</sup>

*Table 2. Proposed synergistic effects of protease inhibitors to docetaxel treatment as examined in in vitro studies.*

Cell line	Protease inhibitor	Proposed effect	References
NCI-H460 & NCI-H520	Nelfinavir	Nelfinavir-induced inhibition of Akt signaling leading to more sensitivity to docetaxel	114
DU145 cell line	Ritonavir	Increased effect of docetaxel on activation of caspase-3 and cleavage of PARP	99
DU145 cell line	Ritonavir	Reduced DNA binding activity of NFκB, surpassing one resistance mechanism of docetaxel	99
DU145 cell line	Ritonavir	Blocked the docetaxel-induced increase in CYP3A4 mRNA, decreasing the metabolism of docetaxel	99

## DISCUSSION

Although evidence remains slightly contradictory and many studies are limited by low sample sizes, there appears to be relevant expression of taxane-metabolizing enzymes CYP3A4, CYP3A5 and CYP2C8, among other CYP enzymes, in some malignant and non-malignant tissues of the breast, prostate, lung, endometrium, and ovaries.<sup>29, 32, 56, 58, 62, 63, 66, 67, 69-72, 76, 77, 79-81, 84, 86-89, 94, 95, 97, 98, 101-103</sup> Individual studies in NSCLC, and breast and ovarian cancer show increased expression in malignant versus non-malignant tissue<sup>69, 89, 98</sup>, whereas, in prostate cancer, this ratio may be decreased<sup>76, 81</sup> What is important to note, however, is that mRNA expression does not necessarily correlate with protein expression, and that protein detection by IHC discloses no information on the functional status of an enzyme. CYP3A4 appears to be upregulated as a response to docetaxel in a preclinical setting.<sup>90, 99</sup> Moreover, CYP3A4 expression can function as a predictor of the efficacy of docetaxel chemotherapy.<sup>101, 102</sup>



Other than the synergistic mechanisms described above, PIs may contribute to inhibition of tumor proliferation through intrinsic antitumor effects.<sup>109</sup> Several mechanisms have been described by which these inhibitors are capable of reducing cancer growth.<sup>123</sup> For example, in breast cancer cells, ritonavir has been shown to inhibit heat shock protein 90 (Hsp90) and Akt, thereby inhibiting the growth of these cells.<sup>118</sup> In the androgen-independent prostate cancer cell lines, DU-145 and PC3, the HIV PIs saquinavir, ritonavir, and indinavir were effective in inhibiting the proliferation of these cells in a dose-dependent manner. Ritonavir was most prone to inhibit the proliferation, showing a 50% decrease in the growth of DU145 (half maximum inhibitory concentration ( $IC_{50}$ ) of  $3 \times 10^{-6}$  mol/L) and PC-3 cells ( $IC_{50}$  of  $8 \times 10^{-6}$  mol/L). However, the studied concentrations are approximately 1,000-fold higher than the concentrations observed after standard dosage regimens of ritonavir in humans, raising the question whether the inhibition of proliferation can be observed in clinical practice.<sup>99, 124</sup>

Although this review focusses specifically on PIs as a boosting strategy, the effect of other CYP3A4 inhibitors on the intratumoral concentrations of docetaxel may be an interesting topic for further study. One such example is cobicistat, specifically developed as a boosting agent, and an equally potent but more specific inhibitor of CYP3A4 than ritonavir, without inducing properties. Consequently, it might have fewer unwanted drug–drug interactions.<sup>125</sup>

Considering the currently available information, in addition to hepatic CYP enzymes, intratumoral enzymes may play a role in the in situ metabolism of taxane chemotherapy and could, therefore, present an important factor influencing the outcomes of treatment. In the future, more systematic analysis of CYP expression in tumors may be a tool by which treatment response may be predicted or function as a criterion by which patients may be selected for treatment. In conclusion, the attenuation of CYP enzymes in tumors appears to be an interesting area of research through which the clinical benefit of anticancer agents may be potentiated.

## REFERENCES

1. World Health Organization International Agency for Research on Cancer (IACR). GLOBOCAN 2018: IARC Global Cancer Observatory. Available from: <http://gco.iarc.fr/today/home>. Accessed on 31 May 2019.
2. Montero A, Fossella F, Hortobagyi G, Valero V. Docetaxel for treatment of solid tumours: a systematic review of clinical data. *Lancet Oncol*. 2005;6(4):229-239. [https://doi.org/10.1016/s1470-2045\(05\)70094-2](https://doi.org/10.1016/s1470-2045(05)70094-2).
3. Crown J, O'Leary M. The taxanes: an update. *Lancet*. 2000;355(9210):1176-1178. [https://doi.org/10.1016/s0140-6736\(00\)02074-2](https://doi.org/10.1016/s0140-6736(00)02074-2).
4. Akram T, Maseelall P, Fanning J. Carboplatin and paclitaxel for the treatment of advanced or recurrent endometrial cancer. *Am J Obstet Gynecol*. 2005;192(5):1365-1367. <https://doi.org/10.1016/j.ajog.2004.12.032>.
5. Tannock IF, de Wit R, Berry WR, Horti J, Pluzanska A, Chi KN, et al. Docetaxel plus prednisone or mitoxantrone plus prednisone for advanced prostate cancer. *N Engl J Med*. 2004;351(15):1502-1512. <https://doi.org/10.1056/NEJMoa040720>.
6. Masoud V, Pagès G. Targeted therapies in breast cancer: New challenges to fight against resistance. *World J Clin Oncol*. 2017;8(2):120-134. <https://doi.org/10.5306/wjco.v8.i2.120>.
7. Serpa Neto A, Tobias-Machado M, Kaliks R, Wroclawski ML, Pompeo AC, Del Giglio A. Ten years of docetaxel-based therapies in prostate adenocarcinoma: a systematic review and meta-analysis of 2244 patients in 12 randomized clinical trials. *Clin Genitourin Cancer*. 2011;9(2):115-123. <https://doi.org/10.1016/j.clgc.2011.05.002>.
8. Sweeney CJ, Chen YH, Carducci M, Liu G, Jarrard DF, Eisenberger M, et al. Chemohormonal therapy in metastatic hormone-sensitive prostate cancer. *N Engl J Med*. 2015;373(8):737-746. <https://doi.org/10.1056/NEJMoa1503747>.
9. James ND, Sydes MR, Clarke NW, Mason MD, Dearnaley DP, Spears MR, et al. Addition of docetaxel, zoledronic acid, or both to first-line long-term hormone therapy in prostate cancer (STAMPEDE): survival results from an adaptive, multiarm, multistage, platform randomised controlled trial. *Lancet*. 2016;387(10024):1163-1177. [https://doi.org/10.1016/s0140-6736\(15\)01037-5](https://doi.org/10.1016/s0140-6736(15)01037-5).
10. Tulsyan S, Chaturvedi P, Singh AK, Agarwal G, Lal P, Agrawal S, et al. Assessment of clinical outcomes in breast cancer patients treated with taxanes: multi-analytical approach. *Gene*. 2014;543(1):69-75. <https://doi.org/10.1016/j.gene.2014.04.004>.
11. Gligorov J, Lotz JP. Preclinical pharmacology of the taxanes: implications of the differences. *Oncologist*. 2004;9 Suppl 2:3-8. [https://doi.org/10.1634/theoncologist.9-suppl\\_2-3](https://doi.org/10.1634/theoncologist.9-suppl_2-3).
12. Lyseng-Williamson KA, Fenton C. Docetaxel: a review of its use in metastatic breast cancer. *Drugs*. 2005;65(17):2513-2531. <https://doi.org/10.2165/00003495-200565170-00007>.
13. Cortes JE, Pazdur R. Docetaxel. *J Clin Oncol*. 1995;13(10):2643-2655. <https://doi.org/10.1200/jco.1995.13.10.2643>.
14. Gan L, Wang J, Xu H, Yang X. Resistance to docetaxel-induced apoptosis in prostate cancer cells by p38/p53/p21 signaling. *Prostate*. 2011;71(11):1158-1166. <https://doi.org/10.1002/pros.21331>.
15. Patterson SG, Wei S, Chen X, Sallman DA, Gilvary DL, Zhong B, et al. Novel role of Stat1 in the development of docetaxel resistance in prostate tumor cells. *Oncogene*. 2006;25(45):6113-6122. <https://doi.org/10.1038/sj.onc.1209632>.
16. Codony-Servat J, Marin-Aguilera M, Visa L, Garcia-Albéniz X, Pineda E, Fernández PL, et al. Nuclear factor-kappa B and interleukin-6 related docetaxel resistance in castration-resistant prostate cancer. *Prostate*. 2013;73(5):512-521. <https://doi.org/10.1002/pros.22591>.
17. Brown I, Shali K, McDonald SL, Moir SE, Hutcheon AW, Heys SD, et al. Reduced expression of p27 is a novel mechanism of docetaxel resistance in breast cancer cells. *Breast Cancer Res*. 2004;6(5):R601-607. <https://doi.org/10.1186/bcr918>.
18. Zhang X, Zhong S, Xu Y, Yu D, Ma T, Chen L, et al. MicroRNA-3646 contributes to docetaxel resistance in human breast cancer cells by GSK-3 $\beta$ / $\beta$ -catenin signaling pathway. *PLoS One*. 2016;11(4):e0153194. <https://doi.org/10.1371/journal.pone.0153194>.
19. Valero V, Jones SE, Von Hoff DD, Booser DJ, Mennel RG, Ravdin PM, et al. A phase II study of docetaxel in patients with paclitaxel-resistant metastatic breast cancer. *J Clin Oncol*. 1998;16(10):3362-3368. <https://doi.org/10.1200/jco.1998.16.10.3362>.
20. Verschraegen CF, Sittisomwong T, Kudelka AP, Guedes E, Steger M, Nelson-Taylor T, et al. Docetaxel for patients with paclitaxel-resistant Müllerian carcinoma. *J Clin Oncol*. 2000;18(14):2733-2739. <https://doi.org/10.1200/jco.2000.18.14.2733>.

21. Kondoh C, Takahari D, Shitara K, Mizota A, Nomura M, Yokota T, et al. Efficacy of docetaxel in patients with paclitaxel-resistant advanced gastric cancer. *Gan To Kagaku Ryoho*. 2012;39(10):1511-1515.
22. Zunino F, Cassinelli G, Polizzi D, Perego P. Molecular mechanisms of resistance to taxanes and therapeutic implications. *Drug Resist Updat*. 1999;2(6):351-357. <https://doi.org/10.1054/drup.1999.0108>.
23. Germano S, O'Driscoll L. Breast cancer: understanding sensitivity and resistance to chemotherapy and targeted therapies to aid in personalised medicine. *Curr Cancer Drug Targets*. 2009;9(3):398-418. <https://doi.org/10.2174/156800909788166529>.
24. Engels FK, Ten Tije AJ, Baker SD, Lee CK, Loos WJ, Vulto AG, et al. Effect of cytochrome P450 3A4 inhibition on the pharmacokinetics of docetaxel. *Clin Pharmacol Ther*. 2004;75(5):448-454. <https://doi.org/10.1016/j.clpt.2004.01.001>.
25. Cresteil T, Monsarrat B, Dubois J, Sonnier M, Alvinerie P, Gueritte F. Regioselective metabolism of taxoids by human CYP3A4 and 2C8: structure-activity relationship. *Drug Metab Dispos*. 2002;30(4):438-445. <https://doi.org/10.1124/dmd.30.4.438>.
26. Shou M, Martinet M, Korzekwa KR, Krausz KW, Gonzalez FJ, Gelboin HV. Role of human cytochrome P450 3A4 and 3A5 in the metabolism of taxotere and its derivatives: enzyme specificity, interindividual distribution and metabolic contribution in human liver. *Pharmacogenetics*. 1998;8(5):391-401. <https://doi.org/10.1097/00008571-199810000-00004>.
27. Thelen K, Dressman JB. Cytochrome P450-mediated metabolism in the human gut wall. *J Pharm Pharmacol*. 2009;61(5):541-558. <https://doi.org/10.1211/jpp/61.05.0002>.
28. Oyama T, Kagawa N, Kunugita N, Kitagawa K, Ogawa M, Yamaguchi T, et al. Expression of cytochrome P450 in tumor tissues and its association with cancer development. *Front Biosci*. 2004;9:1967-1976. <https://doi.org/10.2741/1378>.
29. Kapucuoglu N, Coban T, Raunio H, Pelkonen O, Edwards RJ, Boobis AR, et al. Expression of CYP3A4 in human breast tumour and non-tumour tissues. *Cancer Lett*. 2003;202(1):17-23. <https://doi.org/10.1016/j.canlet.2003.08.015>.
30. Martinez C, Garcia-Martin E, Pizarro RM, Garcia-Gamito FJ, Agúndez JA. Expression of paclitaxel-inactivating CYP3A activity in human colorectal cancer: implications for drug therapy. *Br J Cancer*. 2002;87(6):681-686. <https://doi.org/10.1038/sj.bjc.6600494>.
31. Murray GI, Shaw D, Weaver RJ, McKay JA, Ewen SW, Melvin WT, et al. Cytochrome P450 expression in oesophageal cancer. *Gut*. 1994;35(5):599-603. <https://doi.org/10.1136/gut.35.5.599>.
32. Murray GI, Patimalla S, Stewart KN, Miller ID, Heys SD. Profiling the expression of cytochrome P450 in breast cancer. *Histopathology*. 2010;57(2):202-211. <https://doi.org/10.1111/j.1365-2559.2010.03606.x>.
33. Zia H, Murray GI, Vyhldal CA, Leeder JS, Anwar AE, Bui MM, et al. CYP3A isoforms in Ewing's sarcoma tumours: an immunohistochemical study with clinical correlation. *Int J Exp Pathol*. 2015;96(2):81-86. <https://doi.org/10.1111/iepp.12115>.
34. Sparreboom A, Huizing MT, Boesen JJ, Nooijen WJ, van Tellingen O, Beijnen JH. Isolation, purification, and biological activity of mono- and dihydroxylated paclitaxel metabolites from human feces. *Cancer Chemother Pharmacol*. 1995;36(4):299-304. <https://doi.org/10.1007/bf00689047>.
35. Sparreboom A, Van Tellingen O, Scherrenburg EJ, Boesen JJ, Huizing MT, Nooijen WJ, et al. Isolation, purification and biological activity of major docetaxel metabolites from human feces. *Drug Metab Dispos*. 1996;24(6):655-658.
36. Nelson DR. Cytochrome P450 nomenclature. *Methods Mol Biol*. 1998;107:15-24. <https://doi.org/10.1385/0-89603-519-0.15>.
37. de Jonge ME, Huitema AD, Rodenhuis S, Beijnen JH. Clinical pharmacokinetics of cyclophosphamide. *Clin Pharmacokinet*. 2005;44(11):1135-1164. <https://doi.org/10.2165/00003088-200544110-00003>.
38. Bruno RD, Njar VC. Targeting cytochrome P450 enzymes: a new approach in anti-cancer drug development. *Bioorg Med Chem*. 2007;15(15):5047-5060. <https://doi.org/10.1016/j.bmc.2007.05.046>.
39. Rendic S, Guengerich FP. Contributions of human enzymes in carcinogen metabolism. *Chem Res Toxicol*. 2012;25(7):1316-1383. <https://doi.org/10.1021/tx300132k>.
40. Zanger UM, Schwab M. Cytochrome P450 enzymes in drug metabolism: regulation of gene expression, enzyme activities, and impact of genetic variation. *Pharmacol Ther*. 2013;138(1):103-141. <https://doi.org/10.1016/j.pharmthera.2012.12.007>.
41. Traunecker HC, Stevens MC, Kerr DJ, Ferry DR. The acridonecarboxamide GF120918 potently reverses P-glycoprotein-mediated resistance in human sarcoma MES-Dx5 cells. *Br J Cancer*. 1999;81(6):942-951. <https://doi.org/10.1038/sj.bjc.6690791>.

42. Bertilsson G, Heidrich J, Svensson K, Asman M, Jendeborg L, Sydow-Bäckman M, et al. Identification of a human nuclear receptor defines a new signaling pathway for CYP3A induction. *Proc Natl Acad Sci U S A*. 1998;95(21):12208-12213. <https://doi.org/10.1073/pnas.95.21.12208>.
43. Blumberg B, Sabbagh W, Jr., Jugulion H, Bolado J, Jr., van Meter CM, Ong ES, et al. SXR, a novel steroid and xenobiotic-sensing nuclear receptor. *Genes Dev*. 1998;12(20):3195-3205. <https://doi.org/10.1101/gad.12.20.3195>.
44. Kliewer SA, Moore JT, Wade L, Staudinger JL, Watson MA, Jones SA, et al. An orphan nuclear receptor activated by pregnanes defines a novel steroid signaling pathway. *Cell*. 1998;92(1):73-82. [https://doi.org/10.1016/s0092-8674\(00\)80900-9](https://doi.org/10.1016/s0092-8674(00)80900-9).
45. Lehmann JM, McKee DD, Watson MA, Willson TM, Moore JT, Kliewer SA. The human orphan nuclear receptor PXR is activated by compounds that regulate CYP3A4 gene expression and cause drug interactions. *J Clin Invest*. 1998;102(5):1016-1023. <https://doi.org/10.1172/jci3703>.
46. Banerjee M, Robbins D, Chen T. Modulation of xenobiotic receptors by steroids. *Molecules*. 2013;18(7):7389-7406. <https://doi.org/10.3390/molecules18077389>.
47. Goodwin B, Hodgson E, Liddle C. The orphan human pregnane X receptor mediates the transcriptional activation of CYP3A4 by rifampicin through a distal enhancer module. *Mol Pharmacol*. 1999;56(6):1329-1339. <https://doi.org/10.1124/mol.56.6.1329>.
48. Huss JM, Wang SI, Astrom A, McQuiddy P, Kasper CB. Dexamethasone responsiveness of a major glucocorticoid-inducible CYP3A gene is mediated by elements unrelated to a glucocorticoid receptor binding motif. *Proc Natl Acad Sci U S A*. 1996;93(10):4666-4670. <https://doi.org/10.1073/pnas.93.10.4666>.
49. Synold TW, Dussault I, Forman BM. The orphan nuclear receptor SXR coordinately regulates drug metabolism and efflux. *Nat Med*. 2001;7(5):584-590. <https://doi.org/10.1038/87912>.
50. Masuyama H, Hiramatsu Y, Kodama J, Kudo T. Expression and potential roles of pregnane X receptor in endometrial cancer. *J Clin Endocrinol Metab*. 2003;88(9):4446-4454. <https://doi.org/10.1210/jc.2003-030203>.
51. Miki Y, Suzuki T, Kitada K, Yabuki N, Shibuya R, Moriya T, et al. Expression of the steroid and xenobiotic receptor and its possible target gene, organic anion transporting polypeptide-A, in human breast carcinoma. *Cancer Res*. 2006;66(1):535-542. <https://doi.org/10.1158/0008-5472.Can-05-1070>.
52. Nallani SC, Goodwin B, Buckley AR, Buckley DJ, Desai PB. Differences in the induction of cytochrome P450 3A4 by taxane anticancer drugs, docetaxel and paclitaxel, assessed employing primary human hepatocytes. *Cancer Chemother Pharmacol*. 2004;54(3):219-229. <https://doi.org/10.1007/s00280-004-0799-9>.
53. Harmsen S, Meijerman I, Beijnen JH, Schellens JH. Nuclear receptor mediated induction of cytochrome P450 3A4 by anticancer drugs: a key role for the pregnane X receptor. *Cancer Chemother Pharmacol*. 2009;64(1):35-43. <https://doi.org/10.1007/s00280-008-0842-3>.
54. Bièche I, Narjoz C, Asselah T, Vacher S, Marcellin P, Lidereau R, et al. Reverse transcriptase-PCR quantification of mRNA levels from cytochrome (CYP)1, CYP2 and CYP3 families in 22 different human tissues. *Pharmacogenet Genomics*. 2007;17(9):731-742. <https://doi.org/10.1097/FPC.ob013e32810f2e58>.
55. Patterson LH, Murray GI. Tumour cytochrome P450 and drug activation. *Curr Pharm Des*. 2002;8(15):1335-1347. <https://doi.org/10.2174/1381612023394502>.
56. El-Rayes BF, Ali S, Heilbrun LK, Lababidi S, Bouwman D, Visscher D, et al. Cytochrome p450 and glutathione transferase expression in human breast cancer. *Clin Cancer Res*. 2003;9(5):1705-1709.
57. Murray GI, Taylor MC, McFadyen MC, McKay JA, Greenlee WF, Burke MD, et al. Tumor-specific expression of cytochrome P450 CYP1B1. *Cancer Res*. 1997;57(14):3026-3031.
58. Finnström N, Bjelfman C, Söderström TG, Smith G, Egevad L, Norlén BJ, et al. Detection of cytochrome P450 mRNA transcripts in prostate samples by RT-PCR. *Eur J Clin Invest*. 2001;31(10):880-886. <https://doi.org/10.1046/j.1365-2362.2001.00893.x>.
59. McLemore TL, Adelberg S, Liu MC, McMahon NA, Yu SJ, Hubbard WC, et al. Expression of CYP1A1 gene in patients with lung cancer: evidence for cigarette smoke-induced gene expression in normal lung tissue and for altered gene regulation in primary pulmonary carcinomas. *J Natl Cancer Inst*. 1990;82(16):1333-1339. <https://doi.org/10.1093/jnci/82.16.1333>.
60. Yager JD, Davidson NE. Estrogen carcinogenesis in breast cancer. *N Engl J Med*. 2006;354(3):270-282. <https://doi.org/10.1056/NEJMra050776>.
61. Tsuchiya Y, Nakajima M, Yokoi T. Cytochrome P450-mediated metabolism of estrogens and its regulation in human. *Cancer Lett*. 2005;227(2):115-124. <https://doi.org/10.1016/j.canlet.2004.10.007>.
62. Huang Z, Fasco MJ, Figge HL, Keyomarsi K, Kaminsky LS. Expression of cytochromes P450 in human breast tissue and tumors. *Drug Metab Dispos*. 1996;24(8):899-905.

63. Hellmold H, Rylander T, Magnusson M, Reihner E, Warner M, Gustafsson JA. Characterization of cytochrome P450 enzymes in human breast tissue from reduction mammoplasties. *J Clin Endocrinol Metab.* 1998;83(3):886-895. <https://doi.org/10.1210/jcem.83.3.4647>.
64. Iscan M, Kilaavuniemi T, Coban T, Kapucuoglu N, Pelkonen O, Raunio H. The expression of cytochrome P450 enzymes in human breast tumours and normal breast tissue. *Breast Cancer Res Treat.* 2001;70(1):47-54. <https://doi.org/10.1023/a:1012526406741>.
65. Vaclavikova R, Hubackova M, Stribrna-Sarmanova J, Kodet R, Mrhalova M, Novotny J, et al. RNA expression of cytochrome P450 in breast cancer patients. *Anticancer Res.* 2007;27(6c):4443-4450.
66. Murray GI, Weaver RJ, Paterson PJ, Ewen SW, Melvin WT, Burke MD. Expression of xenobiotic metabolizing enzymes in breast cancer. *J Pathol.* 1993;169(3):347-353. <https://doi.org/10.1002/path.1711690312>.
67. Yokose T, Doy M, Taniguchi T, Shimada T, Kakiki M, Horie T, et al. Immunohistochemical study of cytochrome P450 2C and 3A in human non-neoplastic and neoplastic tissues. *Virchows Arch.* 1999;434(5):401-411. <https://doi.org/10.1007/s004280050359>.
68. Albin N, Massaad L, Toussaint C, Mathieu MC, Morizet J, Parise O, et al. Main drug-metabolizing enzyme systems in human breast tumors and peritumoral tissues. *Cancer Res.* 1993;53(15):3541-3546.
69. Floriano-Sanchez E, Rodriguez NC, Bandala C, Coballase-Urrutia E, Lopez-Cruz J. CYP3A4 expression in breast cancer and its association with risk factors in Mexican women. *Asian Pac J Cancer Prev.* 2014;15(8):3805-3809. <https://doi.org/10.7314/apjcp.2014.15.8.3805>.
70. Haas S, Pierl C, Harth V, Pesch B, Rabstein S, Brüning T, et al. Expression of xenobiotic and steroid hormone metabolizing enzymes in human breast carcinomas. *Int J Cancer.* 2006;119(8):1785-1791. <https://doi.org/10.1002/ijc.21915>.
71. Schmidt R, Baumann F, Knüpfner H, Brauckhoff M, Horn LC, Schönfelder M, et al. CYP3A4, CYP2C9 and CYP2B6 expression and ifosfamide turnover in breast cancer tissue microsomes. *Br J Cancer.* 2004;90(4):911-916. <https://doi.org/10.1038/sj.bjc.6601492>.
72. Knüpfner H, Schmidt R, Stanitz D, Brauckhoff M, Schönfelder M, Preiss R. CYP2C and IL-6 expression in breast cancer. *Breast.* 2004;13(1):28-34. <https://doi.org/10.1016/j.breast.2003.07.002>.
73. Schmidt R, Baumann F, Hanschmann H, Geissler F, Preiss R. Gender difference in ifosfamide metabolism by human liver microsomes. *Eur J Drug Metab Pharmacokinet.* 2001;26(3):193-200. <https://doi.org/10.1007/bf03190396>.
74. Koch I, Weil R, Wolbold R, Brockmüller J, Hustert E, Burk O, et al. Interindividual variability and tissue-specificity in the expression of cytochrome P450 3A mRNA. *Drug Metab Dispos.* 2002;30(10):1108-1114. <https://doi.org/10.1124/dmd.30.10.1108>.
75. Mitsiades N, Sung CC, Schultz N, Danila DC, He B, Eedunuri VK, et al. Distinct patterns of dysregulated expression of enzymes involved in androgen synthesis and metabolism in metastatic prostate cancer tumors. *Cancer Res.* 2012;72(23):6142-6152. <https://doi.org/10.1158/0008-5472.Can-12-1335>.
76. Leskelä S, Honrado E, Montero-Conde C, Landa I, Cascón A, Letón R, et al. Cytochrome P450 3A5 is highly expressed in normal prostate cells but absent in prostate cancer. *Endocr Relat Cancer.* 2007;14(3):645-654. <https://doi.org/10.1677/erc-07-0078>.
77. Moilanen AM, Hakkola J, Vaarala MH, Kauppila S, Hirvikoski P, Vuoristo JT, et al. Characterization of androgen-regulated expression of CYP3A5 in human prostate. *Carcinogenesis.* 2007;28(5):916-921. <https://doi.org/10.1093/carcin/bgl222>.
78. Blanco JG, Edick MJ, Hancock ML, Winick NJ, Dervieux T, Amylon MD, et al. Genetic polymorphisms in CYP3A5, CYP3A4 and NQO1 in children who developed therapy-related myeloid malignancies. *Pharmacogenetics.* 2002;12(8):605-611. <https://doi.org/10.1097/00008571-200211000-00004>.
79. Murray GI, Taylor VE, McKay JA, Weaver RJ, Ewen SW, Melvin WT, et al. The immunohistochemical localization of drug-metabolizing enzymes in prostate cancer. *J Pathol.* 1995;177(2):147-152. <https://doi.org/10.1002/path.1711770208>.
80. Di Paolo OA, Teitel CH, Nowell S, Coles BF, Kadlubar FF. Expression of cytochromes P450 and glutathione S-transferases in human prostate, and the potential for activation of heterocyclic amine carcinogens via acetyl-coA-, PAPS- and ATP-dependent pathways. *Int J Cancer.* 2005;117(1):8-13. <https://doi.org/10.1002/ijc.21152>.
81. Fujimura T, Takahashi S, Urano T, Kumagai J, Murata T, Takayama K, et al. Expression of cytochrome P450 3A4 and its clinical significance in human prostate cancer. *Urology.* 2009;74(2):391-397. <https://doi.org/10.1016/j.urology.2009.02.033>.

82. Loukola A, Chadha M, Penn SG, Rank D, Conti DV, Thompson D, et al. Comprehensive evaluation of the association between prostate cancer and genotypes/haplotypes in CYP17A1, CYP3A4, and SRD5A2. *Eur J Hum Genet.* 2004;12(4):321-332. <https://doi.org/10.1038/sj.ejhg.5201101>.
83. Plummer SJ, Conti DV, Paris PL, Curran AP, Casey G, Witte JS. CYP3A4 and CYP3A5 genotypes, haplotypes, and risk of prostate cancer. *Cancer Epidemiol Biomarkers Prev.* 2003;12(9):928-932.
84. Macé K, Bowman ED, Vautravers P, Shields PG, Harris CC, Pfeifer AM. Characterisation of xenobiotic-metabolising enzyme expression in human bronchial mucosa and peripheral lung tissues. *Eur J Cancer.* 1998;34(6):914-920. [https://doi.org/10.1016/s0959-8049\(98\)00034-3](https://doi.org/10.1016/s0959-8049(98)00034-3).
85. Nakajima T, Elovaara E, Gonzalez FJ, Gelboin HV, Raunio H, Pelkonen O, et al. Styrene metabolism by cDNA-expressed human hepatic and pulmonary cytochromes P450. *Chem Res Toxicol.* 1994;7(6):891-896. <https://doi.org/10.1021/tx00042a026>.
86. Kivistö KT, Fritz P, Linder A, Friedel G, Beaune P, Kroemer HK. Immunohistochemical localization of cytochrome P450 3A in human pulmonary carcinomas and normal bronchial tissue. *Histochem Cell Biol.* 1995;103(1):25-29. <https://doi.org/10.1007/bf01464472>.
87. Kivistö KT, Griese EU, Fritz P, Linder A, Hakkola J, Raunio H, et al. Expression of cytochrome P 450 3A enzymes in human lung: a combined RT-PCR and immunohistochemical analysis of normal tissue and lung tumours. *Naunyn Schmiedebergs Arch Pharmacol.* 1996;353(2):207-212. <https://doi.org/10.1007/bf00168759>.
88. Anttila S, Hukkanen J, Hakkola J, Stjernvall T, Beaune P, Edwards RJ, et al. Expression and localization of CYP3A4 and CYP3A5 in human lung. *Am J Respir Cell Mol Biol.* 1997;16(3):242-249. <https://doi.org/10.1165/ajrcmb.16.3.9070608>.
89. Qixing M, Juqing X, Yajing W, Gaochao D, Wenjie X, Run S, et al. The expression levels of CYP3A4 and CYP3A5 serve as potential prognostic biomarkers in lung adenocarcinoma. *Tumour Biol.* 2017;39(4):1010428317698340. <https://doi.org/10.1177/1010428317698340>.
90. Fujitaka K, Oguri T, Isoe T, Fujiwara Y, Kohno N. Induction of cytochrome P450 3A4 by docetaxel in peripheral mononuclear cells and its expression in lung cancer. *Cancer Chemother Pharmacol.* 2001;48(1):42-46. <https://doi.org/10.1007/s002800100291>.
91. Klose TS, Blaisdell JA, Goldstein JA. Gene structure of CYP2C8 and extrahepatic distribution of the human CYP2Cs. *J Biochem Mol Toxicol.* 1999;13(6):289-295. [https://doi.org/10.1002/\(sici\)1099-0461\(1999\)13:6<289::aid-jbt1>3.0.co;2-n](https://doi.org/10.1002/(sici)1099-0461(1999)13:6<289::aid-jbt1>3.0.co;2-n).
92. Rodriguez AC, Blanchard Z, Maurer KA, Gertz J. Estrogen signaling in endometrial cancer: A key oncogenic pathway with several open questions. *Horm Cancer.* 2019;10(2-3):51-63. <https://doi.org/10.1007/s12672-019-0358-9>.
93. Schuetz JD, Kauma S, Guzelian PS. Identification of the fetal liver cytochrome CYP3A7 in human endometrium and placenta. *J Clin Invest.* 1993;92(2):1018-1024. <https://doi.org/10.1172/jci116607>.
94. Hukkanen J, Mäntylä M, Kangas L, Wirta P, Hakkola J, Paakki P, et al. Expression of cytochrome P450 genes encoding enzymes active in the metabolism of tamoxifen in human uterine endometrium. *Pharmacol Toxicol.* 1998;82(2):93-97. <https://doi.org/10.1111/j.1600-0773.1998.tb01404.x>.
95. Sarkar MA, Vadlamuri V, Ghosh S, Glover DD. Expression and cyclic variability of CYP3A4 and CYP3A7 isoforms in human endometrium and cervix during the menstrual cycle. *Drug Metab Dispos.* 2003;31(1):1-6. <https://doi.org/10.1124/dmd.31.1.1>.
96. Ho SM. Estrogen, progesterone and epithelial ovarian cancer. *Reprod Biol Endocrinol.* 2003;1:73. <https://doi.org/10.1186/1477-7827-1-73>.
97. DeLoia JA, Zamboni WC, Jones JM, Strychor S, Kelley JL, Gallion HH. Expression and activity of taxane-metabolizing enzymes in ovarian tumors. *Gynecol Oncol.* 2008;108(2):355-360. <https://doi.org/10.1016/j.ygyno.2007.10.029>.
98. Downie D, McFadyen MC, Rooney PH, Cruickshank ME, Parkin DE, Miller ID, et al. Profiling cytochrome P450 expression in ovarian cancer: identification of prognostic markers. *Clin Cancer Res.* 2005;11(20):7369-7375. <https://doi.org/10.1158/1078-0432.Ccr-05-0466>.
99. Ikezoe T, Hisatake Y, Takeuchi T, Ohtsuki Y, Yang Y, Said JW, et al. HIV-1 protease inhibitor, ritonavir: a potent inhibitor of CYP3A4, enhanced the anticancer effects of docetaxel in androgen-independent prostate cancer cells in vitro and in vivo. *Cancer Res.* 2004;64(20):7426-7431. <https://doi.org/10.1158/0008-5472.Can-03-2677>.
100. Li WJ, Zhong SL, Wu YJ, Xu WD, Xu JJ, Tang JH, et al. Systematic expression analysis of genes related to multidrug-resistance in isogenic docetaxel- and adriamycin-resistant breast cancer cell lines. *Mol Biol Rep.* 2013;40(11):6143-6150. <https://doi.org/10.1007/s11033-013-2725-x>.

101. Miyoshi Y, Ando A, Takamura Y, Taguchi T, Tamaki Y, Noguchi S. Prediction of response to docetaxel by CYP3A4 mRNA expression in breast cancer tissues. *Int J Cancer*. 2002;97(1):129-132. <https://doi.org/10.1002/ijc.1568>.
102. Miyoshi Y, Taguchi T, Kim SJ, Tamaki Y, Noguchi S. Prediction of response to docetaxel by immunohistochemical analysis of CYP3A4 expression in human breast cancers. *Breast Cancer*. 2005;12(1):11-15. <https://doi.org/10.2325/jbcs.12.11>.
103. Sakurai K, Enomoto K, Matsuo S, Amano S, Shiono M. CYP3A4 expression to predict treatment response to docetaxel for metastasis and recurrence of primary breast cancer. *Surg Today*. 2011;41(5):674-679. <https://doi.org/10.1007/s00595-009-4328-7>.
104. Eagling VA, Back DJ, Barry MG. Differential inhibition of cytochrome P450 isoforms by the protease inhibitors, ritonavir, saquinavir and indinavir. *Br J Clin Pharmacol*. 1997;44(2):190-194. <https://doi.org/10.1046/j.1365-2125.1997.00644.x>.
105. Sevrioukova IF, Poulos TL. Structure and mechanism of the complex between cytochrome P4503A4 and ritonavir. *Proc Natl Acad Sci U S A*. 2010;107(43):18422-18427. <https://doi.org/10.1073/pnas.1010693107>.
106. Hull MW, Montaner JS. Ritonavir-boosted protease inhibitors in HIV therapy. *Ann Med*. 2011;43(5):375-388. <https://doi.org/10.3109/07853890.2011.572905>.
107. Ramsden D, Zhou J, Tweedie DJ. Determination of a degradation constant for CYP3A4 by direct suppression of mRNA in a novel human hepatocyte model, HepatoPac. *Drug Metab Dispos*. 2015;43(9):1307-1315. <https://doi.org/10.1124/dmd.115.065326>.
108. Rock BM, Hengel SM, Rock DA, Wienkers LC, Kunze KL. Characterization of ritonavir-mediated inactivation of cytochrome P450 3A4. *Mol Pharmacol*. 2014;86(6):665-674. <https://doi.org/10.1124/mol.114.094862>.
109. Yu H, Hendrikk JJ, Rottenberg S, Schellens JH, Beijnen JH, Huitema AD. Development of a tumour growth inhibition model to elucidate the effects of ritonavir on intratumoural metabolism and anti-tumour effect of docetaxel in a mouse model for hereditary breast cancer. *Aaps j*. 2016;18(2):362-371. <https://doi.org/10.1208/s12248-015-9838-1>.
110. Rudek MA, Chang CY, Steadman K, Johnson MD, Desai N, Deeken JF. Combination antiretroviral therapy (cART) component ritonavir significantly alters docetaxel exposure. *Cancer Chemother Pharmacol*. 2014;73(4):729-736. <https://doi.org/10.1007/s00280-014-2399-7>.
111. Hendrikk JJ, Lagas JS, Wagenaar E, Rosing H, Schellens JH, Beijnen JH, et al. Oral co-administration of elacridar and ritonavir enhances plasma levels of oral paclitaxel and docetaxel without affecting relative brain accumulation. *Br J Cancer*. 2014;110(11):2669-2676. <https://doi.org/10.1038/bjc.2014.222>.
112. Hendrikk JJ, Lagas JS, Song JY, Rosing H, Schellens JH, Beijnen JH, et al. Ritonavir inhibits intratumoral docetaxel metabolism and enhances docetaxel antitumor activity in an immunocompetent mouse breast cancer model. *Int J Cancer*. 2016;138(3):758-769. <https://doi.org/10.1002/ijc.29812>.
113. Suh J, Payvandi F, Edelstein LC, Amenta PS, Zong WX, Gélinas C, et al. Mechanisms of constitutive NF-kappaB activation in human prostate cancer cells. *Prostate*. 2002;52(3):183-200. <https://doi.org/10.1002/pros.10082>.
114. Yang Y, Ikezoe T, Nishioka C, Bandobashi K, Takeuchi T, Adachi Y, et al. NFV, an HIV-1 protease inhibitor, induces growth arrest, reduced Akt signalling, apoptosis and docetaxel sensitization in NSCLC cell lines. *Br J Cancer*. 2006;95(12):1653-1662. <https://doi.org/10.1038/sj.bjc.6603435>.
115. Wendel HG, De Stanchina E, Fridman JS, Malina A, Ray S, Kogan S, et al. Survival signalling by Akt and eIF4E in oncogenesis and cancer therapy. *Nature*. 2004;428(6980):332-337. <https://doi.org/10.1038/nature02369>.
116. Dey G, Bharti R, Das AK, Sen R, Mandal M. Resensitization of Akt induced docetaxel resistance in breast cancer by 'iturin A' a lipopeptide molecule from marine bacteria *Bacillus megaterium*. *Sci Rep*. 2017;7(1):17324. <https://doi.org/10.1038/s41598-017-17652-z>.
117. Vinod BS, Nair HH, Vijayakurup V, Shabna A, Shah S, Krishna A, et al. Resveratrol chemosensitizes HER-2-overexpressing breast cancer cells to docetaxel chemoresistance by inhibiting docetaxel-mediated activation of HER-2-Akt axis. *Cell Death Discov*. 2015;1:15061. <https://doi.org/10.1038/cddiscovery.2015.61>.
118. Srirangam A, Mitra R, Wang M, Gorski JC, Badve S, Baldrige L, et al. Effects of HIV protease inhibitor ritonavir on Akt-regulated cell proliferation in breast cancer. *Clin Cancer Res*. 2006;12(6):1883-1896. <https://doi.org/10.1158/1078-0432.Ccr-05-1167>.
119. Kumar S, Bryant CS, Chamala S, Qazi A, Seward S, Pal J, et al. Ritonavir blocks AKT signaling, activates apoptosis and inhibits migration and invasion in ovarian cancer cells. *Mol Cancer*. 2009;8:26. <https://doi.org/10.1186/1476-4598-8-26>.

120. de Weger VA, Stuurman FE, Hendriks J, Moes JJ, Sawicki E, Huitema ADR, et al. A dose-escalation study of bi-daily once weekly oral docetaxel either as ModraDoc001 or ModraDoc006 combined with ritonavir. *Eur J Cancer*. 2017;86:217-225. <https://doi.org/10.1016/j.ejca.2017.09.010>.
121. de Weger VA, Stuurman FE, Koolen SLW, Moes JJ, Hendriks J, Sawicki E, et al. A Phase I dose escalation study of once-weekly oral administration of docetaxel as ModraDoc001 capsule or ModraDoc006 tablet in combination with ritonavir. *Clin Cancer Res*. 2019;25(18):5466-5474. <https://doi.org/10.1158/1078-0432.Ccr-17-2299>.
122. de Weger VA, Stuurman FE, Mergui-Roelvink M, Nuijen B, Huitema ADR, Beijnen JH, et al. A phase I dose-escalation trial of bi-daily (BID) weekly oral docetaxel as ModraDoc006 in combination with ritonavir. *Ann Oncol*. 2016;27:vi127. <https://doi.org/10.1093/annonc/mdw368.42>.
123. Gills JJ, Lopiccio J, Tsurutani J, Shoemaker RH, Best CJ, Abu-Asab MS, et al. Nelfinavir, a lead HIV protease inhibitor, is a broad-spectrum, anticancer agent that induces endoplasmic reticulum stress, autophagy, and apoptosis in vitro and in vivo. *Clin Cancer Res*. 2007;13(17):5183-5194. <https://doi.org/10.1158/1078-0432.Ccr-07-0161>.
124. European Medicines Agency. Norvir: Summary of product characteristics.
125. Marzolini C, Gibbons S, Khoo S, Back D. Cobicistat versus ritonavir boosting and differences in the drug-drug interaction profiles with co-medications. *J Antimicrob Chemother*. 2016;71(7):1755-1758. <https://doi.org/10.1093/jac/dkw032>.



# CHAPTER 2.2

# Ritonavir-boosted exposure of kinase inhibitors: an open label, single-arm pharmacokinetic proof-of- concept trial with erlotinib

*Pharm Res. 2022 [Epub ahead of print]*

René J. Boosman  
Cornedine J. de Gooijer  
Stefanie L. Groenland  
Jacobus A. Burgers  
Paul Baas  
Vincent van der Noort  
Jos H. Beijnen  
Alwin D.R. Huitema  
Neeltje Steeghs

Author's contribution: R.J. Boosman contributed to the design of this study, performed the data management, conducted the data analysis, wrote the first draft of the manuscript and edited the contribution of the co-authors on this manuscript.

# ABSTRACT

## Background

Although kinase inhibitors (KIs) are generally effective, their use has a large impact on the current health care budget. Dosing strategies to reduce treatment costs are warranted. Boosting pharmacokinetic exposure of KIs metabolized by cytochrome P450 (CYP)3A4 with ritonavir might result in lower doses needed and subsequently reduces treatment costs. This study is a proof-of-concept study to evaluate if the dose of erlotinib can be reduced by co-administration with ritonavir.

## Methods

In this open-label, single-arm study, we compared the pharmacokinetics of monotherapy erlotinib 150 mg once daily (QD) (control arm) with erlotinib 75 mg QD plus ritonavir 200 mg QD (intervention arm). Complete pharmacokinetic profiles at steady-state were taken up to 24 h after erlotinib intake for both dosing strategies.

## Results

Nine patients were evaluable in this study. For the control arm, the systemic exposure over 24 h, maximum plasma concentration and minimal plasma concentration of erlotinib were 29.3  $\mu\text{g}\cdot\text{h}/\text{mL}$  (coefficient of variation (CV) 58%), 1.84  $\mu\text{g}/\text{mL}$  (CV 60%) and 1.00  $\mu\text{g}/\text{mL}$  (CV 62%), respectively, compared with 28.9  $\mu\text{g}\cdot\text{h}/\text{mL}$  (CV 116%,  $p = 0.545$ ), 1.68  $\mu\text{g}/\text{mL}$  (CV 68%,  $p = 0.500$ ) and 1.06  $\mu\text{g}/\text{mL}$  (CV 165%,  $p = 0.150$ ) for the intervention arm. Exposure to the metabolites of erlotinib (OSI-413 and OSI-420) was statistically significant lower following erlotinib plus ritonavir dosing. Similar results regarding safety in both dosing strategies were observed, no grade 3 or higher adverse event was reported.

## Conclusions

Pharmacokinetic exposure at a dose of 75 mg erlotinib when combined with the strong CYP3A4 inhibitor ritonavir is similar to 150 mg erlotinib. Ritonavir-boosting is a promising strategy to reduce erlotinib treatment costs and provides a rationale for other expensive therapies metabolized by CYP3A4.

## INTRODUCTION

Identification of oncogenic driver mutations has shifted the treatment paradigm in cancer towards the use of oral kinase inhibitors (KIs).<sup>1</sup> The last decades, many KIs have been developed for these driver mutations and certainly more will follow. Since the costs of these drugs have a large impact on the healthcare budget,<sup>2</sup> new and efficient dosing strategies are warranted to use KIs as effectively as possible.

For many KIs, pharmacokinetic exposure at the approved dosing regimen is related to efficacy and/or toxicity and thus plays an important role in treatment outcome.<sup>3</sup> Most of the KIs are metabolized via the cytochrome P450 (CYP)3A4 enzyme system.<sup>4</sup> Inhibition of this enzyme system can thus result in higher exposure of the drug and might allow for lower dosages to reduce health care costs. Erlotinib is a KI which inhibits the epidermal growth factor receptor (EGFR) and has several indications in e.g. non-small cell lung cancer (NSCLC) and in pancreatic cancer in a dosing regimen of 150 mg once daily (QD).<sup>5</sup> In other tumor types bearing EGFR driver mutations, erlotinib treatment has been shown to be potentially therapeutic.<sup>6, 7</sup> Erlotinib is for approximately 70% metabolized by CYP3A4 and for the remaining part by CYP1A2. OSI-413 and OSI-420 are the O-desmethylated products of this metabolic route and although these metabolites exhibit some antitumor activity, in comparison with erlotinib this effect seems limited.<sup>5</sup>

In a previous study, it has been found that ketoconazole, a potent CYP3A4 inhibitor, is able to increase the area under the plasma concentration-time curve from zero to infinity ( $AUC_{0-\infty}$ ) and maximum concentration ( $C_{max}$ ) of erlotinib by approximately a twofold in healthy volunteers.<sup>8</sup> A drug, more commonly used to boost the pharmacokinetics of other drugs is ritonavir.<sup>9-11</sup> Similar to ketoconazole, it is a potent CYP3A4 inhibitor associated with relatively low treatment costs, but has marginal side effects. The aim of this study was to investigate whether it is possible to decrease the dose of erlotinib when it is co-administered with ritonavir.

## METHODS

### *Study design and patients*

This single-arm, phase I, open-label, pharmacokinetic trial was designed to compare the pharmacokinetics of erlotinib 150 mg monotherapy to the pharmacokinetics of erlotinib 75 mg in combination with ritonavir 200 mg. This study was approved by the medical ethical committee (the Netherlands Cancer Institute, Amsterdam) and performed in accordance with the Declaration of Helsinki. Written informed consent was obtained from all participating patients. This trial was registered in the Netherlands Trial Register (identifier: NL7542).

All patients  $\geq 18$  years old were eligible for study participation, provided that they were currently treated with or planned for treatment with erlotinib in a dosing schedule of 150 mg QD. Patients treated simultaneously with co-medication, which could influence the pharmacokinetics of

erlotinib, were excluded. Additional exclusion criteria were: active uncontrolled infections, severe cardiac dysfunction in the past six months prior to treatment, impairment of the hepatic function and pregnancy or breast feeding women. Smoking has been attributed to an increased activity of CYP1A isoforms and thus might have an effect on part of the metabolism of erlotinib.<sup>12</sup> Therefore, current smokers (within one week from start) were also excluded from this study.

In Figure 1 the schematic overview of the trial is provided. Since the elimination half-life of erlotinib is approximately 36 hours<sup>5</sup>, steady-state erlotinib concentrations were assumed to be reached after 7.5 days. Therefore, all patients were treated with single agent erlotinib 150 mg QD for at least eight days, after which pharmacokinetic exposure was determined (day 1). Subsequently, patients were treated for one week with single agent erlotinib 75 mg QD, followed by the concomitant treatment of erlotinib 75 mg QD with ritonavir 200 mg QD for one additional week. Afterwards, pharmacokinetic exposure was once again determined (day 15). After trial termination, patients continued with erlotinib 150 mg QD monotherapy.

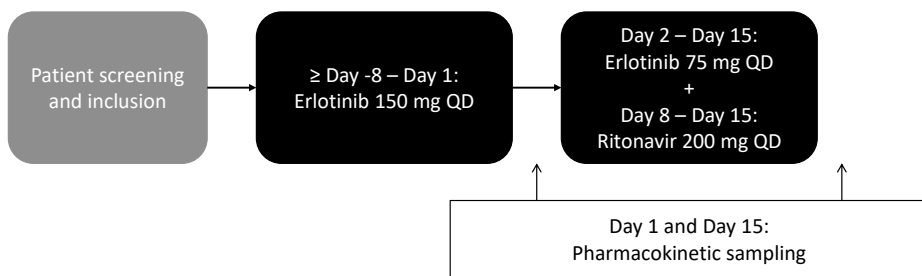


Figure 1. Schematic overview of the trial design. QD: once daily.

#### Pharmacokinetic sampling and bioanalysis

Pharmacokinetic samples were drawn on day 1 (steady-state of single agent erlotinib 150 mg QD) and day 15 (steady-state erlotinib 75 mg QD plus ritonavir 200 mg QD). During these days, patients were admitted to the hospital and blood samples were drawn. Blood samples were collected on the following time points respective to the erlotinib intake: Pre-dose and 30 min and 1, 2, 3, 4, 5, 6, 8 and 24 h after intake. Blood samples were drawn in K2-EDTA tubes, centrifuged for 1500 x g for 10 minutes at 4 °C. Subsequently, plasma was collected and stored at -20 °C until bioanalysis. Erlotinib and ritonavir concentrations were determined using a previously validated bioanalytical method with a detection range of 20-10,000 ng/mL for erlotinib and 2.0-2,000 ng/mL for ritonavir.<sup>13-14</sup> The metabolites of erlotinib, OSI-413 and OSI-420, were separated and measured as described previously, with a lower limit of quantification of 2.0 ng/mL and 0.465 ng/mL, respectively.<sup>15</sup>

### Objectives

The primary aim of this study was to investigate the effect of ritonavir on the pharmacokinetics of erlotinib, measured as AUC over 24 hours ( $AUC_{0-24h}$ ),  $C_{max}$  and trough concentration ( $C_{min}$ ). Secondary objectives included the incidence and severity of adverse events in therapy with and without ritonavir and the effect of ritonavir on the pharmacokinetics of OSI-413 and OSI-420.

### Safety

All adverse events were recorded from start of the study until 21 days after the first pharmacokinetic assessment. The incidence, severity and start of the adverse events were collected and graded according to CTCAE version 5.0. Changes in co-medication were recorded during the study.

### Sample size calculation and statistical analysis

The current study was declared successful when the lower boundary of the one-side 95% confidence interval (CI) of the ratio between the geometric mean in  $AUC_{0-24h}$  of erlotinib with and without ritonavir exceeded 0.5, where 0.5 indicates no effect of ritonavir on the pharmacokinetics of erlotinib given that the dose in combination with ritonavir was reduced to 50%. For the calculation of the sample size, we assumed that the concomitant intake with ritonavir would result in 64% increase in erlotinib exposure, similar to the results of ketoconazole on the erlotinib exposure.<sup>8</sup> In that same study, an intraindividual variability between two erlotinib administrations was found to be approximately 57%. Using these factors, a simulation involving 20,000 trials, showed that 10 patients had to be included in order to obtain a power of 89.5% (with a one-sided  $\alpha$  of 0.05). Overall, slow inclusion of patients was encountered, partly due to a halted accrual during the COVID-19 pandemic. Therefore, an interim analysis was performed in October 2021 after inclusion of nine evaluable patients. Assessment of a worst-case scenario for a potentially tenth patient was assessed on the primary endpoint. In this worst-case scenario, it was assumed that in this patient, ritonavir did not affect the pharmacokinetics of erlotinib and thus the ratio between the exposure of erlotinib with and without ritonavir would be equal to 0.5.

Pharmacokinetic parameters were calculated using a non-compartmental analysis. The linear-log trapezoidal method was used to calculate the  $AUC_{0-24h}$ .  $C_{max}$  was defined as the highest measured concentration over 24 h and  $C_{min}$  was calculated as the average concentration of pre-dose and 24 h after erlotinib intake. The statistical analyses and power calculation were performed using R version 4.1.1 (R-project, Vienna, Austria). When appropriate, paired t-tests or Wilcoxon signed rank tests were used to determine p-values, a p-value < 0.05 was considered to be statistical significant.

## RESULTS

Between August 2019 and September 2021, a total of 13 patients were included in this study. In four of the participants the second pharmacokinetic sampling was not performed due to disease progression (n = 2), need for interacting co-medication during the study (n = 1) or discontinuation due to adverse events (grade 2 rash, n = 1), resulting in a total of nine evaluable patients. In Table 1 the demographic characteristics at baseline of these patients are depicted.

Table 1. Demographic characteristics of the evaluable patients. Values are presented as number (percentage) or as median [range] as appropriate.

	n = 9
<b>Age</b> , years	59 [52-73]
<b>Gender</b> , male	5 (56%)
<b>Weight</b> (kg)	77.8 [54.8 - 117.5]
<b>Height</b> (m)	1.75 [1.63-1.92]
<b>BSA</b> (m <sup>2</sup> )	1.98 [1.65-2.41]
<b>WHO PS</b>	
0	6 (67%)
1	3 (33%)
<b>Tumor type</b>	
Pancreatic cancer	3 (33%)
NSCLC	2 (22%)
Bile duct cancer	2 (22%)
Bladder cancer	1 (11%)
Urethral cancer	1 (11%)

BSA: Body surface area, NSCLC: Non-small cell lung cancer, WHO PS: World Health Organization Performance Status

### Pharmacokinetics

The pharmacokinetic exposure of erlotinib, OSI-413, OSI-420 and ritonavir during erlotinib monotherapy and during erlotinib in combination with ritonavir, are depicted in Table 2 and Figure 2. Exposure to erlotinib in terms of  $AUC_{0-24h}$ ,  $C_{max}$  and  $C_{min}$  was not statistically significant different between both groups with ratios of the geometric mean of 0.99 (95% CI: 0.58-1.69,  $p = 0.545$ ), 0.91 (95% CI: 0.55-1.49,  $p = 0.500$ ) and 1.06 (95% CI: 0.59-1.93,  $p = 0.150$ ), respectively. The interim analysis after inclusion of nine patients, showed that in a worst-case scenario the ratio of the geometric mean of erlotinib exposure would be 0.92 (0.56-1.51,  $p = 0.420$ ) still meeting the objective of this study. Therefore, the study was closed after inclusion of nine patients.

Following the combination of erlotinib and ritonavir, a statistically significant decrease in  $AUC_{0-24h}$  and  $C_{max}$  of OSI-413 and OSI-420 and a statistically significant decrease in  $C_{min}$  of OSI-420 was observed. Coefficients of variability (CV%) of the exposure parameters for erlotinib, its metabolites and ritonavir ranged between 58%-162% for erlotinib alone and 86-443% for erlotinib plus ritonavir.

**Safety**

In Table 3, the number of patients experiencing adverse events during treatment with erlotinib alone or during treatment with erlotinib and ritonavir are shown. Overall, only grade 1 or 2 diarrhea, skin rash and/or nausea were noticed, none of the patients experienced a grade 3 or higher adverse event. In four patients (44%), monotherapy erlotinib resulted in a treatment-related adverse event. In two of these patients, their skin rash resolved following the combination of erlotinib with ritonavir. However, three other patients developed adverse events during combination therapy, resulting in five patients (56%) experiencing treatment-related adverse events.

*Table 2. Geometric means of the pharmacokinetic parameters of erlotinib administered with and without ritonavir. The ratio of this geometric mean (including their 95% CI) and corresponding p-values. Geometric means are reported as geometric mean (CV%).*

	<b>Erlotinib monotherapy 150 mg QD</b>	<b>Erlotinib 75 mg QD + ritonavir 200 mg QD</b>	<b>Ratio of geometric mean [95% CI]</b>	<b>p-value</b>
<b>Erlotinib</b>				
AUC <sub>0-24h</sub> (µg·h/mL)	29.3 (58%)	28.9 (116%)	0.99 [0.58-1.69]	0.545
C <sub>max</sub> (µg/mL)	1.84 (60%)	1.68 (86%)	0.91 [0.55-1.49]	0.500
C <sub>min</sub> (µg/mL)	1.00 (62%)	1.06 (165%)	1.06 [0.59-1.93]	0.150
<b>OSI-413</b>				
AUC <sub>0-24h</sub> (µg·h/mL)	1.55 (120%)	0.823 (174%)	0.53 [0.34-0.83]	0.020
C <sub>max</sub> (ng/mL)	90.0 (107%)	43.7 (134%)	0.48 [0.31-0.76]	0.004
C <sub>min</sub> (ng/mL)	49.5 (152%)	29.4 (263%)	0.59 [0.37-0.94]	0.064
<b>OSI-420</b>				
AUC <sub>0-24h</sub> (ng·h/mL)	380 (144%)	118 (351%)	0.31 [0.15-0.62]	0.027
C <sub>max</sub> (ng/mL)	26.1 (141%)	7.24 (230%)	0.28 [0.13-0.57]	0.002
C <sub>min</sub> (ng/mL)	10.5 (162%)	4.34 (443%)	0.41 [0.22-0.76]	0.049
<b>Ritonavir</b>				
AUC <sub>0-24h</sub> (µg·h/mL)	0	26.4 (96%)	-	-
C <sub>max</sub> (µg/mL)	0	3.18 (89%)	-	-
C <sub>min</sub> (µg/mL)	0	0.243 (129%)	-	-

95% CI: 95% confidence interval, AUC<sub>0-24h</sub>: area under the concentration-time curve 24 h after erlotinib intake, C<sub>max</sub>: maximal concentration C<sub>min</sub>: trough concentration



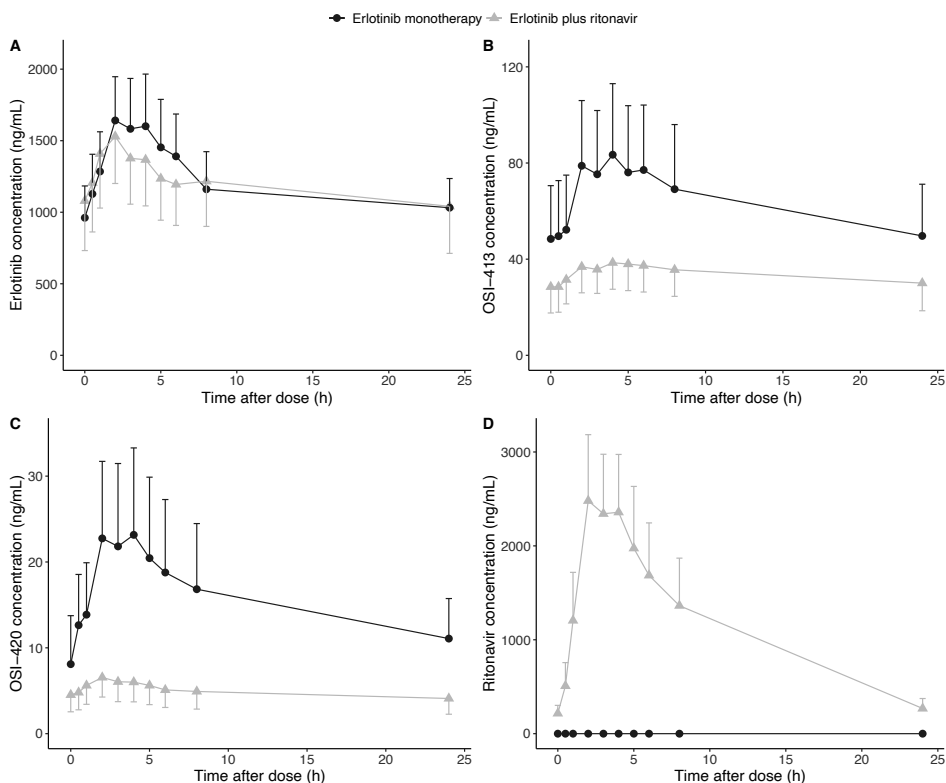


Figure 2. Concentration-time curves of monotherapy erlotinib (in black) and of the combination therapy of erlotinib and ritonavir (in gray) of A) erlotinib, B) the metabolite OSI-413, C) the metabolite OSI-420 and D) ritonavir. The error bars depict the standard error of the geometric mean in one direction.

Table 3. Reported treatment-related adverse events following erlotinib alone and following the combination of erlotinib and ritonavir, according to CTCAE version 5.0.

	Erlotinib monotherapy 150 mg QD	Erlotinib 75 mg QD + ritonavir 200 mg QD
<b>Diarrhea</b>		
Grade 1 or 2	2	2
≥ grade 3	0	0
<b>Skin rash</b>		
Grade 1 or 2	3	1
≥ grade 3	0	0
<b>Nausea</b>		
Grade 1 or 2	0	2
≥ grade 3	0	0
<b>Number of patients experiencing any AE</b>	4	5

AE: adverse events

## DISCUSSION

In this proof-of-concept study, we investigated if lower doses of erlotinib could be administered when combined with the potent CYP3A4 inhibitor ritonavir. We found that concomitant intake of 75 mg of erlotinib with 200 mg ritonavir resulted in similar steady-state erlotinib exposure in terms of  $AUC_{0-24h}$ ,  $C_{max}$  and  $C_{min}$  as with monotherapy of 150 mg of erlotinib, supporting the concept of halving the dose of erlotinib when concomitantly administered with a strong CYP3A4 inhibitor. In the treatment of human immunodeficiency virus, pharmacokinetic-boosting with ritonavir has already been shown safe and effective.<sup>11, 16</sup> In this study, we showed that ritonavir boosting is also feasible during erlotinib therapy and, therefore, might be implemented for other KIs as well.

KIs are notorious for their high pharmacokinetic inter- and inpatient variability, often showing values up to 80%.<sup>17</sup> Since ritonavir is expected to increase the bioavailability of erlotinib by decreasing the first pass effect due to inhibition of intestinal and liver CYP3A4 activity, the variability on the pharmacokinetic exposure of erlotinib was expected to decrease following the erlotinib plus ritonavir treatment. Nonetheless, in this study high CV% were observed for erlotinib, its metabolites and ritonavir for both dosing strategies. Moreover, there seemed to be a trend in which higher CV% were found in the exposure parameters after the combination therapy when compared to erlotinib alone. However, since we included a limited number of patients, conclusions regarding the origin of this variability cannot be drawn.

Regarding the metabolites of erlotinib, the  $AUC_{0-24h}$  of OSI-413 and OSI-420 were both statistically significant decreased following the combination therapy with ritonavir. Since these metabolites are the main product of the enzymatic conversion of erlotinib via CYP3A4, it was to be expected that the exposure to these metabolites was lowered. However, one needs to assure that lower exposure to these metabolites does not influence the efficacy of therapy. Due to the low abundance of OSI-413 and OSI-420, it has been reported that their contribution to the antitumor activity is very limited in comparison with parent erlotinib.<sup>5, 18</sup> Therefore, the decreased exposure of these metabolites following the combination therapy with ritonavir is most likely not clinically relevant.

The majority of the currently approved KIs are metabolized via CYP3A4.<sup>19</sup> The exposure of many of these drugs has been shown to be substantially influenced by concomitant intake with highly potent CYP3A4 inhibitors.<sup>4</sup> Consequently, the concomitant intake with ritonavir is often advised to be avoided. However, the increase in drug exposure can also be used in favor of precision dosing. While target therapies are becoming more expensive and already cover large parts of health care budgets<sup>2</sup>, strategies to reduce these costs need to be implemented to ensure affordable health care systems. Decreasing the dose or dose frequencies might be one way for cost saving. The concomitant intake of KIs with ritonavir can therefore be helpful to decrease the costs in healthcare but maintain the therapeutic exposure of these drugs. The therapeutic potential of ritonavir might not only be limited to pharmacokinetic boosting of the systemic exposure of drugs. It has been reported that enhanced intratumoral drug metabolism by an increased expression of CYP3A4 could play an important role in the development of drug resistance.<sup>20</sup> Administration

of CYP3A4 inhibitors have been found to decrease the intratumoral metabolism of drugs with a CYP3A4-dependent metabolism.<sup>21, 22</sup> Additional research should investigate this promising strategy to overcome resistance mechanisms or inadequate intratumoral drug exposure.

In conclusion, this study shows that the pharmacokinetic exposure at a dose of 75 mg QD erlotinib, when combined with 200 mg QD ritonavir, is similar to 150 mg QD erlotinib. A substantial decrease in the costs of therapy is expected with this ritonavir-boosting strategy. Based on these results, boosting with strong CYP3A4 inhibitor like ritonavir seems a promising dosing strategy for other CYP3A4 metabolically-dependent KIs to reduce their financial footprint on the health care budget.

## REFERENCES

1. Faehling M, Schwenk B, Kramberg S, Eckert R, Volckmar A-L, Stenzinger A, et al. Oncogenic driver mutations, treatment, and EGFR-TKI resistance in a Caucasian population with non-small cell lung cancer: survival in clinical practice. *Oncotarget*. 2017;8(44):77897-77914. <https://doi.org/10.18632/oncotarget.20857>.
2. Shih YC, Smieliauskas F, Geynisman DM, Kelly RJ, Smith TJ. Trends in the cost and use of targeted cancer therapies for the privately insured nonelderly: 2001 to 2011. *J Clin Oncol*. 2015;33(19):2190-2196. <https://doi.org/10.1200/jco.2014.58.2320>.
3. Verheijen RB, Yu H, Schellens JHM, Beijnen JH, Steeghs N, Huitema ADR. Practical recommendations for therapeutic drug monitoring of kinase inhibitors in oncology. *Clin Pharmacol Ther*. 2017;102(5):765-776. <https://doi.org/10.1002/cpt.787>.
4. Teo YL, Ho HK, Chan A. Metabolism-related pharmacokinetic drug-drug interactions with tyrosine kinase inhibitors: current understanding, challenges and recommendations. *Br J Clin Pharmacol*. 2015;79(2):241-253. <https://doi.org/10.1111/bcp.12496>.
5. European Medicines Agency. Tarceva: EPAR-Product information. 2019.
6. Townsley CA, Major P, Siu LL, Dancey J, Chen E, Pond GR, et al. Phase II study of erlotinib (OSI-774) in patients with metastatic colorectal cancer. *Br J Cancer*. 2006;94(8):1136-1143. <https://doi.org/10.1038/sj.bjc.6603055>.
7. Philip PA, Mahoney MR, Allmer C, Thomas J, Pitot HC, Kim G, et al. Phase II study of erlotinib in patients with advanced biliary cancer. *J Clin Oncol*. 2006;24(19):3069-3074. <https://doi.org/10.1200/jco.2005.05.3579>.
8. Rakhit A, Pantze MP, Fettner S, Jones HM, Charoin J-E, Riek M, et al. The effects of CYP3A4 inhibition on erlotinib pharmacokinetics: computer-based simulation (SimCYP™) predicts in vivo metabolic inhibition. *Eur J Clin Pharmacol*. 2008;64(1):31-41. <https://doi.org/10.1007/s00228-007-0396-z>.
9. Vermunt M, Marchetti S, Beijnen J. Pharmacokinetics and toxicities of oral docetaxel formulations co-administered with ritonavir in phase I trials. *Clin Pharmacol*. 2021;13:21-32. <https://doi.org/10.2147/cpaa.S292746>.
10. López-Cortés LF, Castaño MA, López-Ruz MA, Rios-Villegas MJ, Hernández-Quero J, Merino D, et al. Effectiveness of ritonavir-boosted protease inhibitor monotherapy in clinical practice even with previous virological failures to protease inhibitor-based regimens. *PLoS One*. 2016;11(2):e0148924. <https://doi.org/10.1371/journal.pone.0148924>.
11. Hull MW, Montaner JS. Ritonavir-boosted protease inhibitors in HIV therapy. *Ann Med*. 2011;43(5):375-388. <https://doi.org/10.3109/07853890.2011.572905>.
12. Hamilton M, Wolf JL, Rusk J, Beard SE, Clark GM, Witt K, et al. Effects of smoking on the pharmacokinetics of erlotinib. *Clin Cancer Res*. 2006;12(7):2166-2171. <https://doi.org/10.1158/1078-0432.Ccr-05-2235>.
13. Lankheet NA, Hillebrand MJ, Rosing H, Schellens JH, Beijnen JH, Huitema AD. Method development and validation for the quantification of dasatinib, erlotinib, gefitinib, imatinib, lapatinib, nilotinib, sorafenib and sunitinib in human plasma by liquid chromatography coupled with tandem mass spectrometry. *Biomed Chromatogr*. 2013;27(4):466-476. <https://doi.org/10.1002/bmc.2814>.
14. Hendrikx JJ, Hillebrand MJ, Thijssen B, Rosing H, Schinkel AH, Schellens JH, et al. A sensitive combined assay for the quantification of paclitaxel, docetaxel and ritonavir in human plasma using liquid chromatography coupled with tandem mass spectrometry. *J Chromatogr B Analyt Technol Biomed Life Sci*. 2011;879(28):2984-2990. <https://doi.org/10.1016/j.jchromb.2011.08.034>.
15. Rood JJM, Toraño JS, Somovilla VJ, Beijnen JH, Sparidans RW. Bioanalysis of erlotinib, its O-demethylated metabolites OSI-413 and OSI-420, and other metabolites by liquid chromatography-tandem mass spectrometry with additional ion mobility identification. *J Chromatogr B*. 2021;1166:122554. <https://doi.org/10.1016/j.jchromb.2021.122554>.
16. Horberg M, Klein D, Hurlley L, Silverberg M, Towner W, Antoniskis D, et al. Efficacy and safety of ritonavir-boosted and unboosted atazanavir among antiretroviral-naïve patients. *HIV Clin Trials*. 2008;9(6):367-374. <https://doi.org/10.1310/hct0906-367>.
17. Groenland SL, Mathijssen RHJ, Beijnen JH, Huitema ADR, Steeghs N. Individualized dosing of oral targeted therapies in oncology is crucial in the era of precision medicine. *Eur J Clin Pharmacol*. 2019;75(9):1309-1318. <https://doi.org/10.1007/s00228-019-02704-2>.
18. European Medicines Agency. Tarceva: EPAR-Scientific discussion. 2005.
19. Jackson KD, Durandis R, Vergne MJ. Role of cytochrome P450 enzymes in the metabolic activation of tyrosine kinase inhibitors. *Int J Mol Sci*. 2018;19(8):2367. <https://doi.org/10.3390/ijms19082367>.

20. van Eijk M, Boosman RJ, Schinkel AH, Huitema ADR, Beijnen JH. Cytochrome P450 3A4, 3A5, and 2C8 expression in breast, prostate, lung, endometrial, and ovarian tumors: relevance for resistance to taxanes. *Cancer Chemother Pharmacol*. 2019;84(3):487-499. <https://doi.org/10.1007/s00280-019-03905-3>.
21. Hendriks JJMA, Lagas JS, Song J-Y, Rosing H, Schellens JHM, Beijnen JH, et al. Ritonavir inhibits intratumoral docetaxel metabolism and enhances docetaxel antitumor activity in an immunocompetent mouse breast cancer model. *Int J Cancer*. 2016;138(3):758-769. <https://doi.org/10.1002/ijc.29812>.
22. Lubberman FJE, van Erp NP, Ter Heine R, van Herpen CML. Boosting axitinib exposure with a CYP3A4 inhibitor, making axitinib treatment personal. *Acta Oncol*. 2017;56(9):1238-1240. <https://doi.org/10.1080/0284186x.2017.1311024>.



# PART 3



# PREDICTION OF PHARMACOKINETICS



# CHAPTER 3.1

# Optimization of chemotherapy in the era of immunotherapy

*Eur Respir J. 2018;52(4):1801698*

René J. Boosman  
Jacobus A. Burgers

Author's contribution: R.J. Boosman contributed to the concept of this editorial, performed the literature search, wrote the first draft of the manuscript and edited the contribution of the co-author in this manuscript.

## **ABSTRACT**

Even in the era of immuno- and personalized therapy, optimal use of old-fashioned chemotherapy is of utmost importance, also for patients with renal insufficiency or declining renal function.

## OPTIMIZATION OF CHEMOTHERAPY IN THE ERA OF IMMUNOTHERAPY

Even in the era of immunotherapy and personalized medicine, chemotherapy remains a cornerstone in the treatment of non-small cell lung cancer (NSCLC).<sup>1</sup> Chemotherapy improves the length and quality of life of patients with metastatic disease for tumors both with and without oncogenic drivers. Chemotherapy in combination with checkpoint inhibitors is about to become the most effective first-line therapy for NSCLC.<sup>2</sup> Also in the adjuvant setting, *i.e.* adding chemotherapy after surgery, chemotherapy improves survival with an absolute increase of 4% at 5 years.<sup>3</sup>

The optimal use of chemotherapy is an important factor in optimizing the prognosis for patients. The fear of, or actual occurrence of, side-effects might interfere with its optimal use. A common complication of chemotherapy is the development of renal failure. The decline in renal function can occur as a direct toxic effect of the chemotherapeutic agent, but also patient-related and other drug-related factors play pivotal roles.<sup>4</sup> Nephrotoxicity often is a reason of treatment discontinuation or dose reduction resulting in a suboptimal treatment schedule.<sup>5</sup> The fact that about 60% of the people with cancer have underlying compromised renal function stresses the importance of this topic.<sup>6</sup>

In this issue of the *European Respiratory Journal*, Visser *et al.*<sup>7</sup> describe the impact of pemetrexed on the renal function of patients with NSCLC. Pemetrexed is a therapeutic option for many patients. It is currently approved for treatment of nonsquamous NSCLC and mesothelioma. The approval for nonsquamous NSCLC involves first-line therapy in combination with cisplatin, and more recently in combination with carboplatin and pembrolizumab, as continuation and switch maintenance treatment and second-line therapy. In mesothelioma, the pemetrexed–cisplatin combination is the only approved regimen.<sup>8</sup>

In the currently approved dose of 500 mg/m<sup>2</sup>, pemetrexed pharmacokinetics are linear. It is eliminated via the kidneys, with 70%–90% of the administered drug recovered in the urine within 24 h<sup>9</sup>, it shows a biphasic elimination, and pemetrexed clearance linearly correlates with creatinine clearance.<sup>10, 11</sup> Systemic exposure is importantly correlated with toxicity and efficacy<sup>12, 13</sup>, with a higher exposure leading to a higher incidence of dose-limiting hematological toxicity.<sup>10</sup> Renal function and dose of pemetrexed are the sole determinants for total systemic exposure.<sup>10.</sup>

<sup>14, 15</sup>

Although nephrotoxicity is not amongst the list of dose-limiting toxicities of pemetrexed<sup>16</sup>, it is commonly encountered. Pemetrexed enters the proximal tubule cells both via the basolateral and the apical side. Inside the cells pemetrexed is polyglutamylated, which impairs transport of pemetrexed out of the cell and results in raised intracellular concentrations. The inhibition of enzymes involved in the folate pathway by pemetrexed, impairing DNA and RNA synthesis of the tubule cells, further adds to the nephrotoxic effect of pemetrexed.<sup>4</sup>

Presently Visser *et al.*<sup>7</sup> showed in their prospective study, which was performed in a standard hospital setting, that patients with an estimated glomerular filtration rate (eGFR) of < 90 mL/min prior to the treatment with pemetrexed were at increased risk to develop acute kidney disease. The authors were able to confirm this observation in an independent retrospective cohort of NSCLC patients. Both cohorts also showed that a decrease in renal function during first-line pemetrexed–platinum treatment predicted for the development of renal disease during maintenance pemetrexed. During the maintenance treatment, almost 30% of the patients developed a decline in renal function, of whom 60% had to stop chemotherapy. The authors also noticed a statistically non-significant relationship between the cumulative dose of pemetrexed and nephrotoxicity.

It is obvious that renal toxicity has more impact on patients with a pre-existing impaired renal function. Whether this patient population also were more likely to develop significant nephrotoxicity has already been suggested in other studies. The paper by Visser *et al.*<sup>7</sup>, however, is the first to show the predictive properties of baseline reduced eGFR and reduced renal function during therapy for a (further) reduction in renal function due to pemetrexed. This is in line with a similar French study which had shown that renal toxicity was the main reason for interruption of treatment with pemetrexed and bevacizumab.<sup>17</sup>

The study by Visser *et al.*<sup>7</sup> has limitations, related to its partially retrospective design, the fact that the effect of pemetrexed was studied when given in combination with the nephrotoxic agents carboplatin and cisplatin, the lack of data on concomitant medication, and the relatively small number of patients. Nonetheless, the study paves the way for new strategies and research ideas and once again underlines the importance of optimal treatment for all patients, including those with a renal impairment.

A way to improve care for this friable population might be a change of our standard dosing practice. The current, standard practice of pemetrexed dosing on body surface area, by which the renal function is not taken into account, confronts the clinicians with two major problems: 1) a potentially effective treatment is withheld from patients with an eGFR < 45 mL/min<sup>11</sup>; and 2) deterioration of renal function as a result of pemetrexed treatment, leading to adverse effects and cessation of the treatment<sup>11, 18</sup>, might prevent optimal anti-tumor therapy, as is also shown by Visser *et al.*<sup>7</sup> This applies both to those patients with normal renal function and to those patients with a diminished renal function at the start of therapy.<sup>4, 9</sup>

New studies on individualized pemetrexed dosing in patients with NSCLC and mesothelioma based on their renal function are, therefore, being eagerly awaited, also in the new immunotherapy era, in which triple combinations of chemotherapy and immunotherapy are about to become standard of NSCLC care.

## REFERENCES

1. Hellmann MD, Li BT, Chaft JE, Kris MG. Chemotherapy remains an essential element of personalized care for persons with lung cancers. *Ann Oncol*. 2016;27(10):1829-1835. <https://doi.org/10.1093/annonc/mdw271>.
2. Gandhi L, Rodriguez-Abreu D, Gadgeel S, Esteban E, Felip E, De Angelis F, et al. Pembrolizumab plus chemotherapy in metastatic non-small-cell lung cancer. *N Engl J Med*. 2018;378(22):2078-2092. <https://doi.org/10.1056/NEJMoa1801005>.
3. Burdett S, Pignon JP, Tierney J, Tribodet H, Stewart L, Le Pechoux C, et al. Adjuvant chemotherapy for resected early-stage non-small cell lung cancer. *Cochrane Database Syst Rev*. 2015(3):Cd011430. <https://doi.org/10.1002/14651858.Cd011430>.
4. Perazella MA. Onco-nephrology: renal toxicities of chemotherapeutic agents. *Clin J Am Soc Nephrol*. 2012;7(10):1713-1721. <https://doi.org/10.2215/cjn.02780312>.
5. Sbitti Y, Chahdi H, Slimani K, Debbagh A, Mokhlis A, Albouzidi A, et al. Renal damage induced by pemetrexed causing drug discontinuation: a case report and review of the literature. *J Med Case Rep*. 2017;11(1):182. <https://doi.org/10.1186/s13256-017-1348-6>.
6. Sahni V, Choudhury D, Ahmed Z. Chemotherapy-associated renal dysfunction. *Nat Rev Nephrol*. 2009;5(8):450-462. <https://doi.org/10.1038/nrneph.2009.97>.
7. Visser S, Huisbrink J, van 't Veer NE, van Toor JJ, van Boxem AJM, van Walree NC, et al. Renal impairment during pemetrexed maintenance in patients with advanced nonsmall cell lung cancer: a cohort study. *Eur Respir J*. 2018;52(4). <https://doi.org/10.1183/13993003.00884-2018>.
8. Vogelzang NJ, Rusthoven JJ, Symanowski J, Denham C, Kaukel E, Ruffie P, et al. Phase III study of pemetrexed in combination with cisplatin versus cisplatin alone in patients with malignant pleural mesothelioma. *J Clin Oncol*. 2003;21(14):2636-2644. <https://doi.org/10.1200/jco.2003.11.136>.
9. Physicians' Desk Reference. Alimta, Pemetrexed for injection. Thomson PDR, Montvale. 2006:1722.
10. Latz JE, Chaudhary A, Ghosh A, Johnson RD. Population pharmacokinetic analysis of ten phase II clinical trials of pemetrexed in cancer patients. *Cancer Chemother Pharmacol*. 2006;57(4):401-411. <https://doi.org/10.1007/s00280-005-0036-1>.
11. European Medicines Agency. Alimta: EPAR-Product information. 2017.
12. Ikesue H, Watanabe H, Hirano M, Chikamori A, Suetsugu K, Ryokai Y, et al. Risk factors for predicting severe neutropenia induced by pemetrexed plus carboplatin therapy in patients with advanced non-small cell lung cancer. *Biol Pharm Bull*. 2015;38(8):1192-1198. <https://doi.org/10.1248/bpb.b15-00162>.
13. Latz JE, Rusthoven JJ, Karlsson MO, Ghosh A, Johnson RD. Clinical application of a semimechanistic-physiologic population PK/PD model for neutropenia following pemetrexed therapy. *Cancer Chemother Pharmacol*. 2006;57(4):427-435. <https://doi.org/10.1007/s00280-005-0035-2>.
14. Ouellet D, Periclou AP, Johnson RD, Woodworth JR, Lalonde RL. Population pharmacokinetics of pemetrexed disodium (ALIMTA) in patients with cancer. *Cancer Chemother Pharmacol*. 2000;46(3):227-234. <https://doi.org/10.1007/s002800000144>.
15. Chen CY, Lin JW, Huang JW, Chen KY, Shih JY, Yu CJ, et al. Estimated creatinine clearance rate is associated with the treatment effectiveness and toxicity of pemetrexed as continuation maintenance therapy for advanced nonsquamous non-small-cell lung cancer. *Clin Lung Cancer*. 2015;16(6):e131-140. <https://doi.org/10.1016/j.clcc.2015.01.001>.
16. Takimoto CH, Hammond-Thelin LA, Latz JE, Forero L, Beeram M, Forouzes B, et al. Phase I and pharmacokinetic study of pemetrexed with high-dose folic acid supplementation or multivitamin supplementation in patients with locally advanced or metastatic cancer. *Clin Cancer Res*. 2007;13(9):2675-2683. <https://doi.org/10.1158/1078-0432.Ccr-06-2393>.
17. Sassié M, Dugué AE, Clarisse B, Lesueur P, Avrillon V, Bizieux-Thaminy A, et al. Renal insufficiency is the leading cause of double maintenance (bevacizumab and pemetrexed) discontinuation for toxicity to advanced non-small cell lung cancer in real world setting. *Lung Cancer*. 2015;89(2):161-166. <https://doi.org/10.1016/j.lungcan.2015.05.005>.
18. Middleton G, Gridelli C, De Marinis F, Pujol JL, Reck M, Ramlau R, et al. Evaluation of changes in renal function in PARAMOUNT: a phase III study of maintenance pemetrexed plus best supportive care versus placebo plus best supportive care after induction treatment with pemetrexed plus cisplatin for advanced nonsquamous non-small-cell lung cancer. *Curr Med Res Opin*. 2018;34(5):865-871. <https://doi.org/10.1080/03007995.2018.1439462>.

# CHAPTER 3.2

# Rethinking the application of pemetrexed for patients with renal impairment: a pharmacokinetic analysis

*Clin Pharmacokinet.* 2021;60(5):649-654

Nikki de Rouw  
René J. Boosman  
Alwin D.R. Huitema  
Luuk B. Hilbrands  
Elin M. Svensson  
Hieronymus J. Derijks  
Michel M. van den Heuvel  
David M. Burger  
Rob ter Heine

Author's contribution: R.J. Boosman contributed to the concept of this manuscript, performed the data management and provided comments on the first draft of the manuscript.



# ABSTRACT

## Background

Pemetrexed is used for the treatment for non-small cell lung cancer and mesothelioma. Patients with renal impairment are withheld treatment with this drug as it is unknown what dose is well tolerated in this population.

## Objective

The purpose of our study was to investigate the pharmacokinetics (PK) of pemetrexed in patients with renal impairment.

## Methods

A population PK analysis of pemetrexed was performed using non-linear mixed-effects modelling with phase I data obtained from the manufacturer. Additionally, the impact of renal function on pemetrexed PK was assessed with a simulation study using the developed PK model and a previously developed PK model lacking the phase I data.

## Results

The dataset included 548 paired observations of 47 patients, with a wide range of estimated glomerular filtration rates (eGFR; 14.4–145.6 mL/min). Pemetrexed PK were best described by a three-compartment model with eGFR (calculated using the Chronic Kidney Disease Epidemiology Collaboration (CKD-EPI) formula) as a linear covariate on renal pemetrexed clearance. Using the developed model, we found that renal clearance accounts for up to 84% (95% confidence interval 69–98%) of total pemetrexed clearance, whereas the manufacturer previously reported a 50% contribution of renal clearance.

## Conclusion

Renal function is more important for the clearance of pemetrexed than previously thought and this should be taken into account in patients with renal impairment. Furthermore, a third compartment may contribute to prolonged exposure to pemetrexed during drug washout.

## INTRODUCTION

Pemetrexed is an antifolate drug used for the chemotherapeutic treatment of non-small cell lung cancer (NSCLC), mesothelioma and thymoma.<sup>1-3</sup> A single intravenous dose of 500 mg/m<sup>2</sup> is administered every 21 days. Although pemetrexed is excreted in the urine<sup>4</sup>, dosing recommendations do not include adjustment for renal function. Due to fatal toxicities in a study of pemetrexed in patients with renal impairment, pemetrexed is currently contraindicated when the estimated creatinine clearance (CR<sub>CL</sub>) is < 45 mL/min.<sup>5</sup>

Approximately 25% of the lung cancer population has a CR<sub>CL</sub> < 60 mL/min.<sup>6</sup> Since it is unclear what the well tolerated pemetrexed dose is for patients with impaired renal function, a large group is withheld effective treatment. Understanding the relationship between dose, renal function, pharmacokinetics (PK), toxicity and treatment outcome is essential to enable treatment in patients with impaired renal function and to prevent toxicity in patients who are already treated with pemetrexed.

Existing data on the effect of renal dysfunction on pemetrexed PK are conflicting. In phase I studies, the manufacturer showed that 70–90% of the pemetrexed dose is excreted in the urine as unchanged drug within 24 h after administration, through both tubular secretion and glomerular filtration.<sup>4,5</sup> However, a large population PK study by the manufacturer, published by Latz *et al.* in 2006, in which the PK data of 10 phase II trials were pooled for analysis, showed that renal elimination contributed only approximately 50% to the clearance of pemetrexed.<sup>7</sup> Notably, this study and other more recent pemetrexed PK studies excluded patients with moderate to severe renal dysfunction (CR<sub>CL</sub> < 45 mL/min).<sup>8,9</sup> Thus, extrapolation of these studies to patients with impaired renal function can be questioned. Therefore, the purpose of our study was to investigate the PK of pemetrexed in patients with renal impairment.

## METHODS

### *Data*

Rich anonymised PK data collected during the renal impairment study by the manufacturer and as described by Mita *et al.*<sup>5</sup>, were obtained from the manufacturer through the Clinical Study Data Request (CSDR) platform.<sup>10</sup> The following patient demographics were collected for each individual: sex, age, ethnicity, weight, height and serum creatinine. Furthermore, data on pemetrexed dose, infusion rate, sampling times and pemetrexed plasma concentrations were extracted from the dataset. Patients included in the study were not allowed to use aspirin or other non-steroidal anti-inflammatory agents from 2 days before (5 days for longer-acting agents) until 2 days after pemetrexed treatment due to a possible PK interaction.

### *Population pharmacokinetic modelling*

A population PK analysis was performed using the non-linear mixed-effect modelling software package NONMEM V7.4 (Icon plc, Dublin, Ireland). The following proxies for renal function were tested as continuous covariates for pemetrexed clearance: estimated CR<sub>CL</sub> (calculated using

the Cockcroft–Gault formula<sup>11</sup>) and estimated glomerular filtration rates (eGFR; calculated using the Modification of Diet in Renal Disease (MDRD)<sup>12</sup> and Chronic Kidney Disease–Epidemiology Collaboration (CKD-EPI)<sup>13</sup> formulae). MDRD and CKD-EPI were used as absolute values, and thus uncorrected for body surface area (BSA). When including renal function as a covariate for clearance, we estimated both the non-renal contribution to clearance ( $CL_{NR}$ ) and the renal clearance ( $CL_R$ ). The renal function estimate ( $CR_{CL}$  or eGFR) that resulted in the best model fit (decrease in objective function value [OFV]) and largest decrease in interindividual variability (IIV) was retained in the final model. Model selection and diagnostics were performed in line with best practice.<sup>14</sup> A detailed description of the PK analysis can be found in the electronic supplementary material.

#### Assessment of the impact of renal function on pemetrexed pharmacokinetics

After model development, we compared the manufacturer's model (published by Latz *et al.*<sup>7</sup>) and the model developed herein, on several aspects. First, we assessed the difference in exposure, using the target area under the concentration-time curve from the start of infusion until infinity (AUC). In a virtual study, a cohort of 1,000 patients was simulated with NONMEM V7.4 using Monte Carlo simulations. Age, sex, height and weight were extracted from the National Health and Nutrition Examination Survey (NHANES) database<sup>15</sup>, and serum creatinine was randomly drawn from a normal distribution based on a median (male 110  $\mu\text{mol/L}$ , female 95  $\mu\text{mol/L}$ ) with 25% variability (based on clinical data). These variables were used to calculate  $CR_{CL}$ . Dosing was based on BSA according to the drug label (500 mg/m<sup>2</sup>). Subsequently, pemetrexed exposure (AUC) was simulated for these individuals using the manufacturer's PK model and the model developed herein. This was performed for a population with a  $CR_{CL} \geq 45$  mL/min and a population with a  $CR_{CL} < 45$  mL/min. To compare exposure between these groups, the geometric means of the AUCs with the coefficient of variation were calculated.

Second, the disposition of pemetrexed was investigated visually. We simulated one PK curve up to 96 h after administration, with both models using a systemic pemetrexed clearance of 3 L/h for a typical individual with impaired renal function (age 40 years, height 180 cm, weight 70 kg, BSA 1.85 m<sup>2</sup>). A 3 L/h clearance was chosen as it represents a typical individual with decreased pemetrexed clearance, for example due to renal impairment.

## RESULTS

#### Dataset characteristics

The final dataset consisted of 47 patients with a total of 548 paired observations of time and plasma concentrations over a time window of 0–72 h after administration. Table 1 shows the baseline characteristics of the population. Approximately three-quarters of the population were male and the median age was 62 years (range 25–79), with a wide range in eGFR (14.4–145.6 mL/min, calculated using the CKD-EPI).

Table 1. Baseline characteristics of the population. Values are presented as numbers (percentages) or medians [ranges], as appropriate.

Total	n = 47
Sex, male	36 (77%)
Age (years)	62 [25-79]
Weight (kg)	79.3 [48.1-124.3]
BSA (m <sup>2</sup> )	1.95 [1.44-2.47]
CrCl (mL/min)	69.4 [16.8-202.4]
CKD-EPI (mL/min)	73.4 [14.4-145.6]
CKD-EPI ≥ 45 mL/min	42 (89%)
CKD-EPI < 45 mL/min	5 (11%)
Pemetrexed dose (mg/m <sup>2</sup> )	500 [150-600]

BSA: body surface area, CKD-EPI: Chronic Kidney Disease-Epidemiology Collaboration formula, CrCl: creatinine clearance

#### Population pharmacokinetic model

The PK data were best described by a three-compartment model. Inclusion of renal function as a covariate for clearance of pemetrexed resulted in significant improvement of the model ( $p < 0.0001$ ). Inclusion of the eGFR calculated using the CKD-EPI formula<sup>43</sup> explained approximately 45% of the IIV in clearance (reduction from 38.7 to 21.0% IIV in clearance). Of the three tested renal function formulae, CKD-EPI best explained the observed IIV in clearance. Typical population values for  $CL_R$  and  $CL_{NR}$  (with 95% confidence intervals) were 3.42 L/h (2.80–3.99) and 0.66 L/h (0.24–1.13). For central volume of distribution ( $V_1$ ) and peripheral volume of distribution ( $V_2$  and  $V_3$ ), typical values were 6.70 L (5.93–7.53), 8.01 L (7.20–8.95) and 1.23 L (1.02–1.55), respectively. The detailed results of the base model and covariate models are described in the electronic supplementary material.

#### Effect of renal function on pemetrexed pharmacokinetics

The box and whiskers plot in Figure 1 depicts the predicted exposure according to both models (manufacturer's model and the present model), for two separate groups:  $CR_{CL} < 45$  mL/min and  $CR_{CL} \geq 45$  mL/min. In their study, Latz *et al.* concluded that renal elimination contributed to the clearance of pemetrexed by approximately 50%. This is reflected in Figure 1, where it can be observed that exposure seems to be in the same order of magnitude regardless of renal function, with moderate variability (white bars). With our model, developed using the data of patients with a wide range of renal function, a major impact of renal function on pemetrexed exposure can be observed from both the increased variability in AUC as well as the increased exposure in the renal impairment group. We predict that pemetrexed exposure in patients with renal impairment is approximately 1.7-fold higher than previously postulated by the manufacturer (see Table 2).

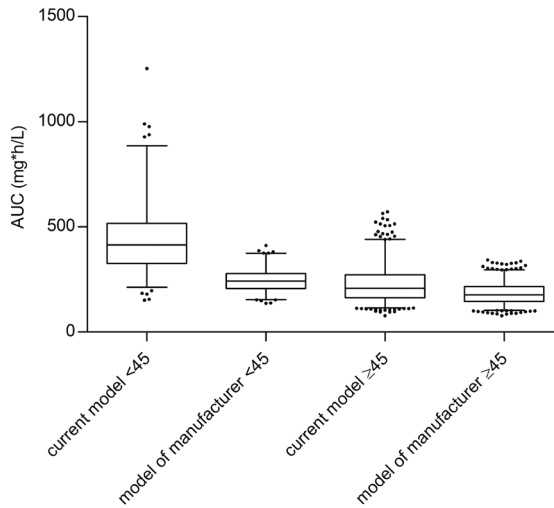


Figure 1. Box and whiskers plot for simulation exposure using both the present model and the manufacturer's model, separated for two categories of renal function (CrCl of < 45 and  $\geq$  45 mL/min, respectively). The box represents the 25th–75th percentiles with geometric mean, and the whiskers indicate the 2.5th–97.5th percentile. The dots represent the outliers. CrCl: creatinine clearance.

Table 2. Comparison of geometric mean AUCs of the simulated population with both the current model and the model of the manufacturer, divided in impaired and adequate renal function (CrCl of < 45 and  $\geq$  45 mL/min respectively).

Group (model/CrCl)	Geometric mean AUC (CV%)	Ratio
Current < 45 mL/min	415 (38.9)	1.7
Manufacturer < 45 mL/min	240 (21.9)	
Current $\geq$ 45 mL/min	208 (41.4)	1.2
Manufacturer $\geq$ 45 mL/min	172 (29.5)	

AUC: area under the concentration-time curve, CrCl: creatinine clearance, CV: coefficient of variation

Figure 2 shows two simulated PK curves, one for each model, using the same systemic clearance of pemetrexed of 3 L/h. For the present model, the impact of the presence of a third compartment on the concentration-time curve can be observed, resulting in prolonged higher exposure at approximately 48 h after drug administration and onwards.

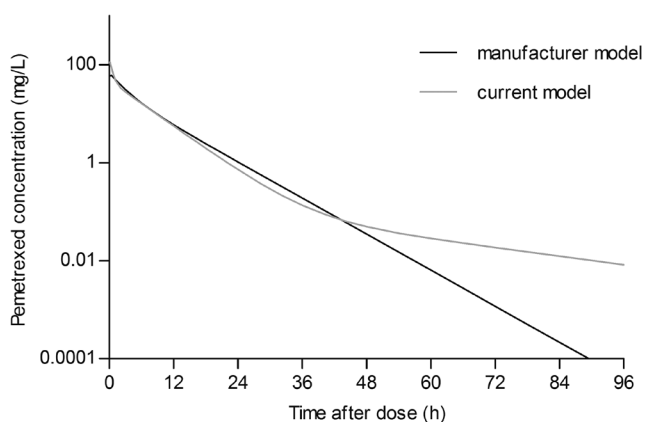


Figure 2. Two concentration-time curves of pemetrexed using both models with the same systemic pemetrexed clearance of 3 L/h, to demonstrate the difference in distribution compartments. The black line represents the curve of the typical individual simulated using the manufacturer's model, and shows two compartments, while the light-gray line represents the present model, identifying the third compartment > 24 h. AUC area under the concentration-time curve.

## DISCUSSION

This thorough PK analysis of pemetrexed in a population that included patients with impaired renal function, led to two major findings. First, we found that renal function is more important for pemetrexed clearance than the 50% contribution previously described by the manufacturer.<sup>16</sup> The manufacturer's analysis did not include patients with impaired renal function ( $CR_{CL} < 45$  mL/min). We showed, in a representative population, that  $CL_R$  accounts for up to 84% of total pemetrexed clearance, which is in line with the manufacturer's early mass balance studies showing that 70–90% of the administered dose could be recovered in urine.<sup>4</sup> Thus, impaired renal function has a more pronounced impact on pemetrexed exposure than previously thought. Our second important finding relates to the disposition of pemetrexed. To date, it has been found that pemetrexed distributes over two compartments.<sup>7–9</sup> The data used in this analysis included sampling up to 72 h after administration and this revealed the presence of a third compartment. A third compartment can suggest the presence of extravascular fluid or a difference in redistributing tissues. It is unknown what holds true for pemetrexed, but as this is a hydrophilic drug, extravascular distribution is plausible. However, Dickgreber *et al.* showed no effect of third space fluid on the PK and toxicity of pemetrexed.<sup>17</sup> This implicates that during drug washout, there can be prolonged exposure to higher concentrations of pemetrexed than previously thought. The driving mechanism for pemetrexed toxicity is the subject of discussion. Mita *et al.* showed no correlation between renal function (and thus exposure) and non-hematological toxicities.<sup>5</sup> With regard to hematotoxicity, it is hypothesized that neutropenia is associated with the total exposure (AUC).<sup>18,19</sup> Based on this, it has been suggested that the dose should be adjusted to reach a target based on renal function, instead of BSA.<sup>7,9,20</sup> AUC-based dosing in a 21-day cycle is also routinely applied for carboplatin,

where  $CR_{cl}$  and the desired AUC are used to calculate the patient's individual dose.<sup>21</sup> It is unknown whether this hypothesis holds true for pemetrexed, as it is known that for other antifolate drugs, such as methotrexate, hematological toxicity is threshold-driven.<sup>22</sup> For example, in an early phase I trial, it was shown that prolonged exposure to low concentrations of pemetrexed from daily administration resulted in severe neutropenia as a dose-limiting toxicity, with a maximum tolerated dose of only 4 mg/m<sup>2</sup> for 5 consecutive days without supplementation of vitamin B12 or folic acid.<sup>23</sup> The predominant role of time above the threshold concentration in determining toxicity is supported by the observation that the maximum tolerated dose of pemetrexed administered in a 21-day cycle, also without vitamin supplementation, was markedly higher (600 mg/m<sup>2</sup>).<sup>4</sup> Threshold-driven toxicity will be an issue, particularly in renal impairment, as clearance becomes so low that the pemetrexed plasma concentration exceeds the toxicity threshold for a prolonged period. This would explain why previous studies with pemetrexed in patients with renal impairment were not successful.<sup>5</sup> Currently, the PK determinant for the efficacy of pemetrexed is a topic of discussion. Dose adjustment to reach an AUC target will probably entail toxicity concerns when there is low systemic clearance, for example due to renal dysfunction. To allow safe and effective treatment in renal impairment, innovative interventions are needed to overcome toxicity. For example, rescue therapy with folinic acid, as widely applied with pemetrexed's structural analogue methotrexate<sup>24</sup>, may be a feasible option.

A limitation of this study is that the number of patients with severe renal impairment (eGFR < 30 mL/min) was limited due to the toxicity concerns that arose during the conduction of the phase I study. Nonetheless, as it stands, these data are the only currently available data to elucidate the clinical PK of pemetrexed in patients with impaired renal function.

## CONCLUSION

Overall, we found that the contribution of renal function was greater than previously thought and that a third compartment may contribute to prolonged exposure during drug washout. Since both factors may contribute to pemetrexed toxicity, they should be accounted for when developing dosing strategies for pemetrexed in patients with renal impairment. The present PK model can be used to further unravel the PK–toxicity relationship of pemetrexed. In parallel, we must think of innovative strategies to overcome the hematological toxicity of pemetrexed in patients with impaired renal function, such as rescue therapy with folinic acid.

## REFERENCES

1. Planchard D, Popat S, Kerr K, Novello S, Smit EF, Faivre-Finn C, et al. Metastatic non-small cell lung cancer: ESMO Clinical Practice Guidelines for diagnosis, treatment and follow-up. *Ann Oncol*. 2018;29(Suppl 4):iv192-iv237. <https://doi.org/10.1093/annonc/mdy275>.
2. Baas P, Fennell D, Kerr KM, Van Schil PE, Haas RL, Peters S. Malignant pleural mesothelioma: ESMO Clinical Practice Guidelines for diagnosis, treatment and follow-up. *Ann Oncol*. 2015;26 Suppl 5:v31-39. <https://doi.org/10.1093/annonc/mdv199>.
3. Girard N, Ruffini E, Marx A, Faivre-Finn C, Peters S. Thymic epithelial tumours: ESMO Clinical Practice Guidelines for diagnosis, treatment and follow-up. *Ann Oncol*. 2015;26 Suppl 5:v40-55. <https://doi.org/10.1093/annonc/mdv277>.
4. Rinaldi DA, Kuhn JG, Burris HA, Dorr FA, Rodriguez G, Eckhardt SG, et al. A phase I evaluation of multitargeted antifolate (MTA, LY231514), administered every 21 days, utilizing the modified continual reassessment method for dose escalation. *Cancer Chemother Pharmacol*. 1999;44(5):372-380. <https://doi.org/10.1007/s002800050992>.
5. Mita AC, Sweeney CJ, Baker SD, Goetz A, Hammond LA, Patnaik A, et al. Phase I and pharmacokinetic study of pemetrexed administered every 3 weeks to advanced cancer patients with normal and impaired renal function. *J Clin Oncol*. 2006;24(4):552-562. <https://doi.org/10.1200/jco.2004.00.9720>.
6. Launay-Vacher V, Etesami R, Janus N, Spano JP, Ray-Coquard I, Oudard S, et al. Lung cancer and renal insufficiency: prevalence and anticancer drug issues. *Lung*. 2009;187(1):69-74. <https://doi.org/10.1007/s00408-008-9123-5>.
7. Latz JE, Chaudhary A, Ghosh A, Johnson RD. Population pharmacokinetic analysis of ten phase II clinical trials of pemetrexed in cancer patients. *Cancer Chemother Pharmacol*. 2006;57(4):401-411. <https://doi.org/10.1007/s00280-005-0036-1>.
8. Visser S, Koolen SLW, de Bruijn P, Belderbos HNA, Cornelissen R, Mathijssen RHJ, et al. Pemetrexed exposure predicts toxicity in advanced non-small-cell lung cancer: A prospective cohort study. *Eur J Cancer*. 2019;121:64-73. <https://doi.org/10.1016/j.ejca.2019.08.012>.
9. Srinivasan M, Chaturvedula A, Fossler MJ, Patil A, Gota V, Prabhash K. Population pharmacokinetics of pemetrexed in adult non-small cell lung cancer in Indian patients. *J Clin Pharmacol*. 2019;59(9):1216-1224. <https://doi.org/10.1002/jcph.1417>.
10. CSDR. Available from: <https://www.clinicalstudydatarequest.com/Posting.aspx?ID=19619&GroupID=SUMMARIES>. Accessed on 20 Nov 2019.
11. Cockcroft DW, Gault MH. Prediction of creatinine clearance from serum creatinine. *Nephron*. 1976;16(1):31-41. <https://doi.org/10.1159/000180580>.
12. Levey AS, Coresh J, Greene T, Marsh J, Stevens LA, Kusek JW, et al. Expressing the Modification of Diet in Renal Disease Study equation for estimating glomerular filtration rate with standardized serum creatinine values. *Clin Chem*. 2007;53(4):766-772. <https://doi.org/10.1373/clinchem.2006.077180>.
13. Levey AS, Stevens LA, Schmid CH, Zhang YL, Castro AF, 3rd, Feldman HI, et al. A new equation to estimate glomerular filtration rate. *Ann Intern Med*. 2009;150(9):604-612. <https://doi.org/10.7326/0003-4819-150-9-200905050-00006>.
14. Byon W, Smith MK, Chan P, Tortorici MA, Riley S, Dai H, et al. Establishing best practices and guidance in population modeling: an experience with an internal population pharmacokinetic analysis guidance. *CPT Pharmacometrics Syst Pharmacol*. 2013;2(7):e51. <https://doi.org/10.1038/psp.2013.26>.
15. National Health and Nutrition Examination Survey. Available from: <https://www.cdc.gov/nchs/nhanes/index.htm>. Accessed on 20 Nov 2019.
16. Latz JE, Schneck KL, Nakagawa K, Miller MA, Takimoto CH. Population pharmacokinetic/pharmacodynamic analyses of pemetrexed and neutropenia: effect of vitamin supplementation and differences between Japanese and Western patients. *Clin Cancer Res*. 2009;15(1):346-354. <https://doi.org/10.1158/1078-0432.Ccr-08-0791>.
17. Dickgreber NJ, Sorensen JB, Paz-Ares LG, Schytte TK, Latz JE, Schneck KB, et al. Pemetrexed safety and pharmacokinetics in patients with third-space fluid. *Clin Cancer Res*. 2010;16(10):2872-2880. <https://doi.org/10.1158/1078-0432.Ccr-09-3324>.



18. Latz JE, Karlsson MO, Rusthoven JJ, Ghosh A, Johnson RD. A semimechanistic-physiologic population pharmacokinetic/pharmacodynamic model for neutropenia following pemetrexed therapy. *Cancer Chemother Pharmacol*. 2006;57(4):412-426. <https://doi.org/10.1007/s00280-005-0077-5>.
19. Latz JE, Rusthoven JJ, Karlsson MO, Ghosh A, Johnson RD. Clinical application of a semimechanistic-physiologic population PK/PD model for neutropenia following pemetrexed therapy. *Cancer Chemother Pharmacol*. 2006;57(4):427-435. <https://doi.org/10.1007/s00280-005-0035-2>.
20. de Rouw N, Croes S, Posthuma R, Agterhuis DE, Schoenmaekers J, Derijks HJ, et al. Pharmacokinetically-guided dosing of pemetrexed in a patient with renal impairment and a patient requiring hemodialysis. *Lung Cancer*. 2019;130:156-158. <https://doi.org/10.1016/j.lungcan.2019.01.018>.
21. Calvert AH, Newell DR, Gumbrell LA, O'Reilly S, Burnell M, Boxall FE, et al. Carboplatin dosage: prospective evaluation of a simple formula based on renal function. *J Clin Oncol*. 1989;7(11):1748-1756. <https://doi.org/10.1200/jco.1989.7.11.1748>.
22. Chabner BA, Young RC. Threshold methotrexate concentration for in vivo inhibition of DNA synthesis in normal and tumorous target tissues. *J Clin Invest*. 1973;52(8):1804-1811. <https://doi.org/10.1172/jci107362>.
23. McDonald AC, Vasey PA, Adams L, Walling J, Woodworth JR, Abrahams T, et al. A phase I and pharmacokinetic study of LY231514, the multitargeted antifolate. *Clin Cancer Res*. 1998;4(3):605-610.
24. Bleyer WA. The clinical pharmacology of methotrexate: new applications of an old drug. *Cancer*. 1978;41(1):36-51. [https://doi.org/10.1002/1097-0142\(197801\)41:1<36::aid-cnrcr2820410108>3.0.co;2-i](https://doi.org/10.1002/1097-0142(197801)41:1<36::aid-cnrcr2820410108>3.0.co;2-i).

## SUPPLEMENTAL MATERIAL

### *Pharmacokinetic analysis detailed methods and results*

#### *Base model*

Based on previous research and upon visual inspection of the data, two- and three compartment models were considered to describe the data. Volumes of distribution and base- and intercompartmental clearances were allometrically scaled to a total body weight of 70 kg, with an allometric exponent of 1 for all volume parameters and an exponent of 0.75 for flow parameters. Proportional, additive and combined error models were evaluated to describe residual variability. The structural model with the lowest objective function value (OFV) and best goodness-of-fit (GOF) was selected for further covariate analysis. For the residual error, we tested proportional, additive and combined proportional and additive error models. The final structural model was a three-compartment linear model with a proportional residual error. Interindividual variability in clearance and volume of distribution was assumed to be log-normally distributed.

#### *Covariate model*

The following measures for renal function were tested as covariates for pemetrexed clearance: creatinine clearance (CrCl) according the Cockcroft-Gault formula (CG), and eGFR according the MDRD and CKD-EPI formulae. The eGFR normalizes to a body surface area (BSA) of 1.73 m<sup>2</sup> to allow for interindividual comparison. As clearance depends on the absolute eGFR, we calculated the individual eGFR for each individual by multiplying the calculated normalized eGFR by (BSA/1.73), where BSA is the calculated body surface area of the respective individual using the DuBois & DuBois formula.<sup>1</sup> Based on the empirical Bayesian estimates for pemetrexed clearance obtained from the base model and renal function (CKD-EPI) a linear covariate relationship seemed plausible (see Figure S1).

Thus, the covariate effect was linearly modelled and normalized to the population median, assuming the following relationship:

$$CL = CL_{NR} + (CL_R \cdot (\text{renal function} / \text{median renal function of the population}))$$

where CL is the total systemic pemetrexed clearance,  $CL_{NR}$  is non-renal clearance and  $CL_R$  is renal clearance. In this equation the non-renal clearance ( $CL_{NR}$ ) was allometrically scaled. Renal clearance was not allometrically scaled, as the calculated eGFR or CrCl from serum creatinine already depend on body surface area or total body weight. The renal function measure that resulted in the largest decrease in objective function value (OFV) together with the largest decrease in interindividual variability (IIV) on clearance when tested as covariate in the base model was retained in the final model. Adding CKD-EPI to the model resulted in the best fit, resulting in the following final model for clearance:

$$CL = CL_{NR} + (CL_R \cdot (\text{CKD-EPI} / 75))$$

In this formula, 75 is the median CKD-EPI in mL/min of our dataset. Inclusion of CKD-EPI reduced the IIV on clearance from 38.7 to 21.0% and resulted in a  $\Delta$ OFV of -54.27. As parameters were allometrically scaled, no other size descriptors were tested as possible covariates. The NONMEM code of the final model can be found at the end of this document.

#### Model evaluation

During model development, models were assessed using standard goodness-of-fit (GOF) plots. To support the appropriateness of the final model, a visual predictive check (VPC) was performed. For the VPC, prediction correction was applied and 500 replicates were simulated to obtain 95% confidence prediction intervals of the 5<sup>th</sup>, 50<sup>th</sup> and 95<sup>th</sup> percentiles, respectively.<sup>2</sup> Parameter uncertainty was estimated by means of sampling importance resampling (SIR).<sup>3</sup>

Table S1 describes the population estimates of the base model and the tested covariate models. Figure S2 and S3 show the goodness-of-fit and the VPC for the final model (with CKD-EPI as a covariate).

To check if the model could adequately assess pemetrexed pharmacokinetics over the range of eGFR the conditional weighted residuals (CWRES) versus CKD-EPI were assessed. Figure S4 shows homogenous distribution of the CWRES around 0, indicating no systematic bias.

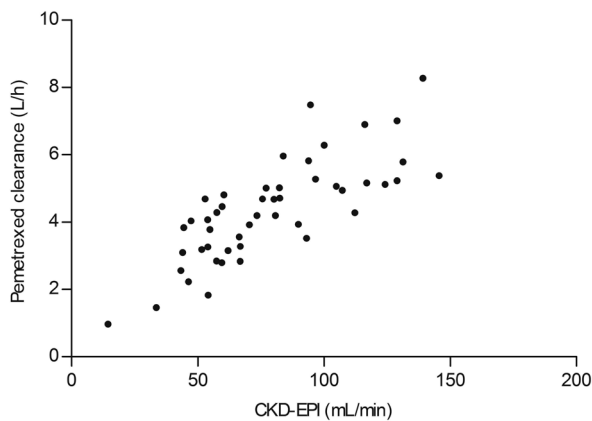


Figure S1. eGFR as CKD-EPI versus estimated individual pemetrexed clearances as obtained with the base model.

Table S1. Population estimates for the base model and the covariate models.

	Population estimates [SIR-derived 95% confidence intervals]			
	Base	Cockcroft-Gault	MDRD	CKD-EPI (final model)
<b>CL</b> (L/h)	3.77 [3.38-4.20]	-	-	-
<b>CL<sub>non-renal</sub></b> (L/h)	-	0.59 [0.09-1.22]	0.75 [0.24-1.31]	0.66 [0.24-1.13]
<b>CL<sub>renal</sub></b> (L/h)	-	3.42 [2.67-4.09]	3.41 [2.71-4.10]	3.42 [2.80-3.99]
<b>IIV<sub>CL</sub></b> (%)	38.7 [31.8-46.5]	23.3 [19.2-28.5]	22.6 [18.2-28.1]	21.0 [17.3-25.0]
<b>V<sub>1</sub></b> (L)	6.70 [5.97-7.57]	6.71 [5.95-7.50]	6.70 [5.84-7.56]	6.70 [5.93-7.53]
<b>IIV<sub>V1</sub></b> (CV%)	33.6 [25.1-42.5]	32.6 [25.1-40.9]	33.2 [25.6-41.6]	33.2 [26.0-41.4]
<b>Q<sub>1</sub></b> (mL/min)	6.56 [5.45-7.90]	6.53 [5.42-7.83]	6.56 [5.38-7.80]	6.56 [5.50-7.69]
<b>V<sub>2</sub></b> (L)	8.01 [7.09-8.92]	8.02 [7.17-8.94]	8.02 [7.07-9.01]	8.01 [7.20-8.95]
<b>IIV<sub>V2</sub></b> (CV%)	31.2 [24.9-39.8]	31.4 [24.9-39.7]	31.8 [25.3-38.6]	31.9 [25.8-40.5]
<b>Q<sub>2</sub></b> (mL/min)	0.04 [0.04-0.05]	0.04 [0.04-0.05]	0.04 [0.04-0.05]	0.04 [0.04-0.05]
<b>V<sub>3</sub></b> (L)	1.25 [1.05-1.51]	1.26 [1.05-1.56]	1.24 [1.03-1.55]	1.23 [1.02-1.55]
<b>IIV<sub>V3</sub></b> (CV%)	48.1 [30.0-70.3]	49.7 [31.5-75.4]	48.1 [30.2-70.4]	46.8 [30.3-72.0]
<b>Correlation (%)</b>				
<b>IIV<sub>V1,V2</sub></b>	32.5	31.7	33.2	33.2
<b>IIV<sub>V1,V3</sub></b>	63.1	63.0	63.9	62.6
<b>IIV<sub>V2,V3</sub></b>	61.9	65.4	63.1	63.4
<b>Residual prop. error (%)</b>	23.5 [21.9-25.4]	23.6 [22.1-25.1]	23.5 [21.9-25.4]	23.5 [22.0-25.3]
<b>Objective function value (OFV)</b>	1402.57	1356.98	1354.43	1348.3

CKD-EPI: Chronic Kidney Disease Epidemiology Collaboration, CL: clearance, IIV: intraindividual variability, MDRD: Modification of Diet in Renal Disease, Q: intercompartmental clearance, SIR: sampling-importance resampling, V: volume of distribution

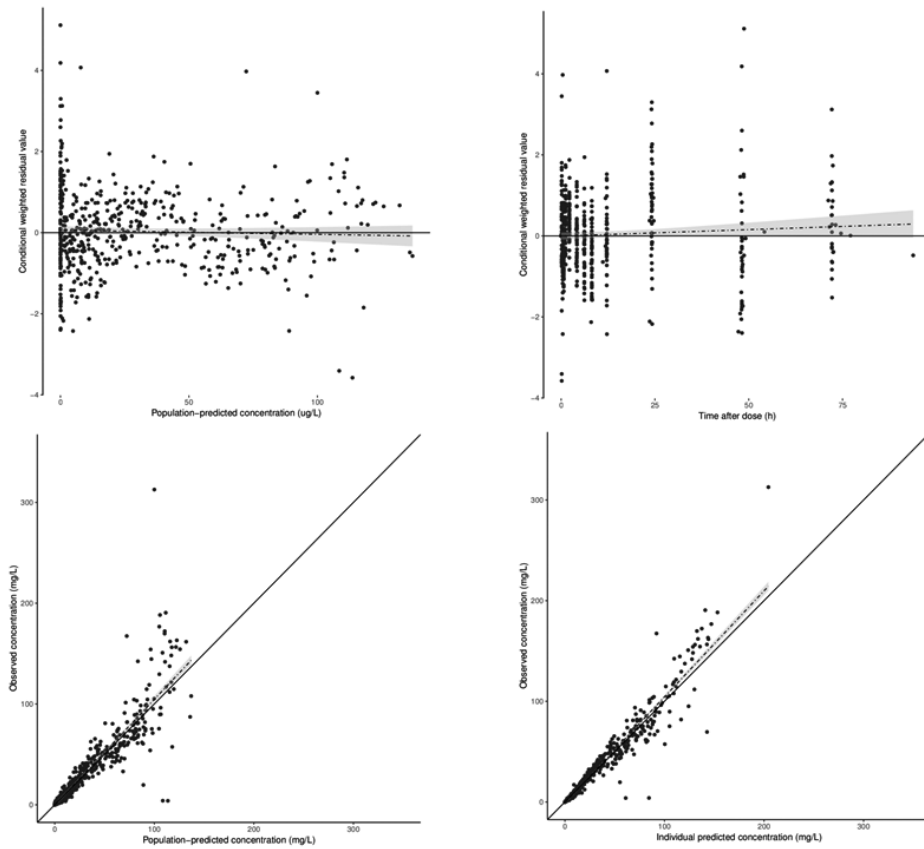


Figure S2. Standard goodness-of-fit plots for the final model of pemetrexed. The upper panels show the population predicted concentration (PRED) versus conditional weighted residuals (CWRES) and the time after dose (TAD) versus CWRES, respectively. The CWRES do not indicate model misspecification, as the data is homogenous distributed with the trendline approximating zero and most of the data lying within a -3 to +3 interval. The bottom panels visualized the good correlation for the individual predicted and population predicted pemetrexed concentrations versus the observed concentrations.

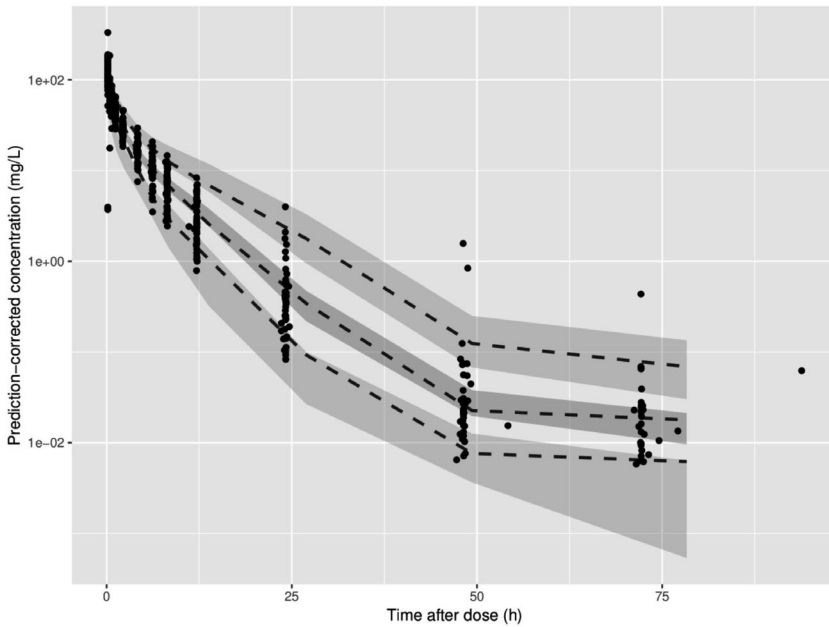


Figure S3. Visual predictive check (VPC) for the final model. The black dots represent the observed concentrations. The dashed lines represent the 95th – median – 5th percentile of the predictions. The shaded gray areas represent the corresponding 95% confidence intervals. The majority of the predicted concentrations are in line with the observed concentrations, indicating sufficient validity of the model.

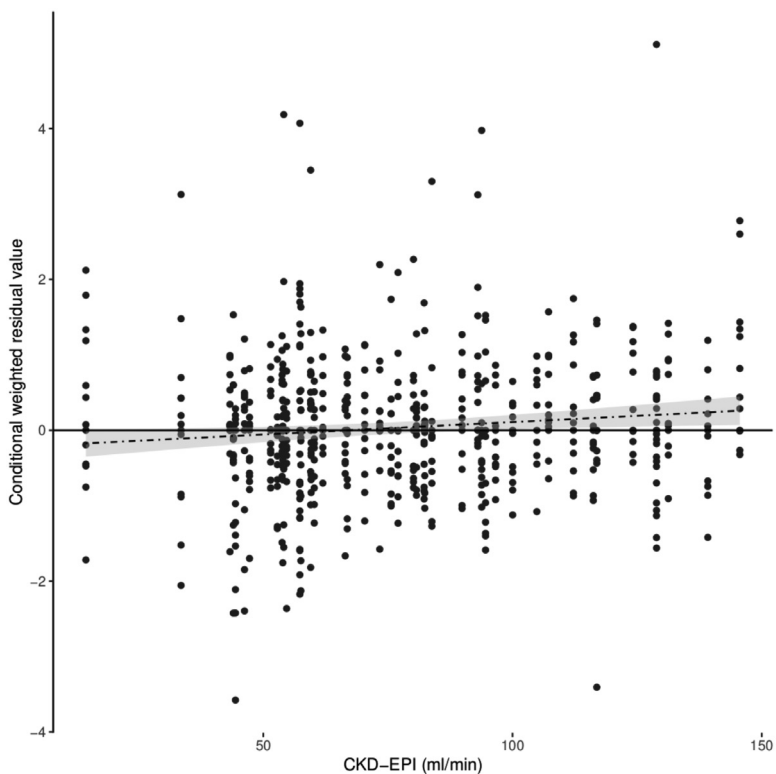


Figure S4. The conditional weighted residuals (CWRES) versus CKD-EPI shows homogenous distribution of the CWRES, with the trendline approximating zero.

#### NONMEM code final model

```

$PROB PEMETREXED PK
$INPUT XX
$DATA XX IGNORE=@
$SUBROUTINE ADVAN5
$MODEL COMP=(CENTRAL) COMP=(PERI) COMP=(PERI2)

$PK
ALLOCL=(WT/70)**0.75      ;SCALING FOR BASE CL AND Q
ALLOV=(WT/70)            ;SCALING FOR V

CLBASE = THETA(1)*ALLOCL
CLRENAL = THETA(2)
TVCL = CLBASE + (CLRENAL * (CKDEPI/75))
CL = TVCL * EXP(ETA(1))

```

V1 = THETA(3)\*ALLOV\*EXP(ETA(2))  
Q = THETA(4)\*ALLOCL  
V2 = THETA(5)\*ALLOV\*EXP(ETA(3))  
Q2 = THETA(6)\*ALLOCL  
V3 = THETA(7)\*ALLOV\*EXP(ETA(4))

D1=0.16667  
S1=V1  
S2=V2  
S3=V3

K10=CL/V1  
K12=Q/V1  
K21=Q/V2  
K13=Q2/V1  
K31=Q2/V3

\$ERROR  
IPRED = F  
Y=F+F\*ERR(1)

\$THETA  
(0, 0.664) ; CL BASE  
(0, 3.42) ; CL RENAL  
(0, 6.7) ; V1  
(0, 6.56) ; Q  
(0, 8.01) ; V2  
(0, 0.0415) ; Q2  
(0, 1.23) ; V3

\$OMEGA  
0.0442; IIV CL  
\$OMEGA BLOCK(3)  
0.110 ; IIV V1  
0.035 0.102; IIV V2  
0.097 0.095 0.219; IIV V3

\$SIGMA  
0.0553



## REFERENCES

1. Du Bois D, Du Bois EF. A formula to estimate the approximate surface area if height and weight be known. 1916. *Nutrition*. 1989;5(5):303-311.
2. Bergstrand M, Hooker AC, Wallin JE, Karlsson MO. Prediction-corrected visual predictive checks for diagnosing nonlinear mixed-effects models. *AAPS J*. 2011;13(2):143-151. <https://doi.org/10.1208/s12248-011-9255-z>.
3. Dosne AG, Bergstrand M, Karlsson MO. An automated sampling importance resampling procedure for estimating parameter uncertainty. *J Pharmacokinet Pharmacodyn*. 2017;44(6):509-520. <https://doi.org/10.1007/s10928-017-9542-0>.



# CHAPTER 3.3

# Optimized versus standard dosing of pemetrexed – a randomized controlled trial

*Submitted*

René J. Boosman\*

Nikki de Rouw\*

Jacobus A. Burgers

Alwin D.R. Huitema

Anne-Marie C. Dingemans

Hieronymus J. Derijks

David M. Burger

Berber Piet

Lizza E.L. Hendriks

Bonne Biesma

Melinda A. Pruis

Daphne W. Dumoulin

Sander Croes

Ron H.J. Mathijssen

Michel M. van den Heuvel

Rob ter Heine

\*these authors contributed equally and thus share first authorship

Author's contribution: R.J. Boosman and N. de Rouw contributed to the design of this study, performed the data management, conducted the data analysis, wrote the first draft of the manuscript and edited the contribution of the co-authors on this manuscript.

# ABSTRACT

## Objectives

Pemetrexed is a chemotherapeutic drug in the treatment of non-small cell lung cancer and mesothelioma. Optimized dosing of pemetrexed based on renal function instead of body surface area (BSA) is hypothesized to reduce pharmacokinetic variability in systemic exposure and could therefore improve treatment outcomes. In this study, optimized dosing was compared to standard BSA-based dosing.

## Materials and Methods

A multicenter randomized (1:1) controlled trial was performed to assess superiority of optimized dosing versus BSA-based dosing in patients who were eligible for pemetrexed-based chemotherapy. The individual exposure to pemetrexed in terms of area under the concentration-time curve (AUC) was determined during the first cycle of treatment. The fraction of patients attaining to a predefined typical target-AUC ( $164 \text{ mg}\cdot\text{h}/\text{L} \pm 25\%$ ) was calculated. Safety was monitored during therapy, and quality of life (QoL) questionnaires were collected at baseline and after 12 weeks of treatment.

## Results

A total of 81 patients were included, with relatively low variability in estimated creatinine clearance (median (interquartile range)  $95.2$  ( $83.6$ - $111.7$ )  $\text{mL}/\text{min}$ ). Target attainment was not statistically significant different between both arms ( $89\%$  vs  $84\%$  ( $p = 0.505$ )). The AUC of pemetrexed was similar between the optimized dosing arm ( $n = 37$ ) and the standard of care arm ( $n = 44$ ) ( $155 \text{ mg}\cdot\text{h}/\text{L}$  vs  $160 \text{ mg}\cdot\text{h}/\text{L}$  ( $p = 0.436$ )). Moreover, no statistically significant differences were observed in hematological toxicity and QoL.

## Conclusion

We found that optimized dosing of pemetrexed in patients with an adequate renal function does not show added value on the attainment of a pharmacokinetic endpoint, safety, nor QoL compared to standard of care dosing.

## INTRODUCTION

The multitargeted antifolate pemetrexed is a cytostatic agent and frequently used in the treatment of non-small cell lung cancer (NSCLC), mesothelioma and thymoma. Pemetrexed is administered in a dosing regimen of 500 mg/m<sup>2</sup> every three weeks (Q3W), either alone or in combination with a platinum agent and/or pembrolizumab.<sup>1-3</sup> The kidneys mainly facilitate the elimination of pemetrexed; it was found that renal function has a pivotal contribution to the total clearance and thus systemic exposure (in terms of the area under the concentration-time curve (AUC)).<sup>4,5</sup> Both the efficacy and toxicity of treatment with pemetrexed have been related to the systemic exposure.<sup>5-7</sup> As the risk of severe hematological toxicities increases with renal impairment, treatment with pemetrexed is contra-indicated in patients with a creatinine clearance < 45 mL/min.<sup>5-8</sup> Since the conventional body surface area (BSA)-based dosing does not take into account renal function, patients are potentially at increased risk for toxic or sub-therapeutic exposure when applied at the same dose over the full range of creatinine clearances of > 45 mL/min. In the approved dose of 500 mg/m<sup>2</sup>, unwanted high systemic exposure due to pharmacokinetic variability has been linked to an increase in hematological toxicities.<sup>6</sup> Furthermore, it has been proven that impaired renal function is a risk factor for pemetrexed-induced pancytopenia.<sup>9</sup> In terms of efficacy, it was shown that administration of pemetrexed in patients with creatinine clearance > 60 mL/min resulted in poorer efficacy outcomes than in patients with creatinine clearance between 45 and 60 mL/min.<sup>10</sup> To overcome this high variability in exposure to pemetrexed, a dosing strategy based on renal function has been proposed repeatedly.<sup>5,7</sup> Thus far, this strategy has never been evaluated in a randomized clinical trial. Therefore, the aim of this study was to prospectively investigate dosing of pemetrexed based on renal function.

## METHODS

### *Study design and patients*

The IMPROVE-II study was a multicenter, open label, randomized (1:1) phase II trial designed to compare optimized renal function-based dosing versus standard of care (BSA-based) dosing of pemetrexed on therapeutic pharmacokinetic target attainment.

The study was approved by the medical ethics committee (Commissie Mensgebonden Onderzoek Regio Arnhem Nijmegen, Nijmegen, The Netherlands, (Clinicaltrials.gov identifier: NCT03655821)) and written informed consent was obtained for all study participants. All patients with an indication for pemetrexed-based treatment and a predicted creatinine clearance > 45 mL/min (as assessed with the Cockcroft-Gault equation<sup>11</sup>) were eligible to participate in the study. Exclusion criteria were: creatinine-influencing factors (such as obesity (defined as a body mass index (BMI) > 40 kg/m<sup>2</sup>), limb amputation or use of cimetidine or trimethoprim) and hemostatic problems complicating blood sampling procedures. At baseline, the following patient demographics and characteristics were collected: age, sex, ethnicity (to calculate estimated glomerular filtration rate (eGFR)), weight, height, treatment indication, disease stage, combination therapy and serum creatinine. The total study period was 12 weeks or four treatment cycles.

### Study objectives and endpoints

The primary objective of this study was to assess whether the optimized dosing of pemetrexed in patients based on renal function led to a higher proportion of patients attaining to a pharmacokinetic target than when patients were dosed on BSA. For exploratory purposes, we performed a post-hoc subgroup analysis, dividing the patients in each treatment group into two groups based on the median value of creatinine clearance in the study population.

Secondary objectives included the incidence of hematological adverse events, the incidence of toxicity-related dose reductions, treatment delays (defined as > 3 days delay) and treatment discontinuation, and the patients' quality of life during study participation.

### Justification of the pharmacokinetic target

A pharmacokinetic target was chosen based on several considerations. Firstly, pemetrexed can be administered in different treatment modalities. Besides monotherapy, doublet or triple therapy with platinum agents and/or programmed death protein 1 (PD-1) immunotherapy are all applied. This not only leads to a wide variety of possible treatment schedules, but possibly also to a partial overlap in efficacy and toxicity, complicating the identification of individual effects of pemetrexed. Secondly, the patient group receiving pemetrexed is heterogeneous. Treatment indication, disease stage and treatment line are all highly variable within the treated population. As large numbers of patients would be required, a study based on response measures was not considered feasible. Since pemetrexed exposure has been shown to be a good predictor for efficacy and safety<sup>6</sup>, a pharmacokinetic endpoint is the most sensitive and unbiased endpoint for a dose individualization study.

An AUC of 164 mg·h/L was previously shown to be a safe and effective target.<sup>6</sup> In addition, it was shown that a large proportion of patients (> 90%) receiving pemetrexed in a dose based on their estimated renal function would reach within 75-125% of this target, while less than three-quarter of patients receiving a dose based on BSA would fall within this target AUC range.<sup>5, 6</sup>

### Safety

The occurrence of grade II and grade III/IV anemia, leukopenia, neutropenia, and thrombocytopenia (Common Terminology Criteria for Adverse Events (CTCAE v5.0)) were investigated.

### Quality of life

The incidence of dose delays and dose reductions was assessed, as these relate directly to toxicity. Moreover, two validated quality of life questionnaires (the general EORTC QLQ-C30 and the lung cancer specific EORTC LC13) were taken and scored at baseline and 12 weeks after study treatment initiation.<sup>12</sup>

### Treatment

In line with the product label, pemetrexed and concomitant chemo- and/or immunotherapy were administered in a 21-day treatment cycle. Patients in the standard of care arm received pemetrexed in the approved dose of 500 mg/m<sup>2</sup>. The optimized renal function-based dose was derived from

the previously established and validated relationship between creatinine clearance (assessed with the Cockcroft-Gault equation) and pemetrexed clearance.<sup>13</sup> Since,  $\text{dose} = \text{AUC} \cdot \text{clearance}$ , the dose was calculated with the following equation:

$$\text{Dose (mg)} = 423 + 464 \cdot (\text{Creatinine clearance (mL/min)} / 92.6)$$

Every cycle, the optimized dose was recalculated based on the most recent creatinine clearance. Concomitant (chemo)immunotherapy and co-medications were administered following standard local treatment protocols.

#### Randomization

Patients were randomly assigned to either the optimized dosing arm or standard of care arm in a 1:1 ratio using an automated system with variable block randomization (block sizes: 4, 6, 8) (Castor EDC v.14.81).

#### Pharmacokinetic sampling and bioanalysis

One pharmacokinetic curve was obtained for each patient, and individual exposure was determined using a previously validated limited sampling schedule (four samples taken at 0.5-1, 1-2, 4-5 and 6-8 hours after the start of pemetrexed infusion).<sup>14</sup> Samples were analyzed using a validated bioanalytical assay, as published previously.<sup>15</sup>

#### Statistical analysis

Based on Monte Carlo simulations on a validated pharmacokinetic model<sup>13</sup>, we expected that approximately 60% of the patients would reach therapeutic exposure when pemetrexed was dosed on BSA compared to 85% of the patients when pemetrexed was dosed based on renal function. To show the superiority of renal function-based dosing compared to standard of care dosing, assuming an improvement of attainment of therapeutic exposure from 60% to 85%, a total of 94 patients (47 per treatment arm) were needed to be included to reach a power of 80% with a significance level of 5% (two-sided). Due to the halted accrual of patients during the COVID-19 pandemic, an unplanned interim analysis was performed in April 2021 after the inclusion of 81 out of 94 patients. Worst- and best-case scenarios for the primary outcome were tested to justify pre-term analysis. The best-case scenario was defined as the scenario in which all future patients randomized in the optimized dosing arm would attain the target AUC, while all patients in the standard-of-care-dosing arm would fall outside this target. Conversely, the worst-case scenario would represent all upcoming patients in the standard-of-care-dosed arm to reach target AUC, while optimized dosing would not yield in target attainment.

As pharmacokinetic parameters often follow a log-normal distribution, AUCs per group are presented as geometric mean. A chi-squared test was performed to test for statistically significant difference ( $p$ -value  $< 0.05$ ) in the fraction of patients attaining to target between both treatment arms. Regarding the subgroup analysis, statistically significant differences ( $p$ -value  $< 0.05$ ) in AUC were assessed using a Mann Whitney U test. A chi-square test was performed to test for statistically



significant difference ( $p$ -value  $< 0.05$ ) in the fraction of patients that experienced  $\geq 1$  hematological toxicity event between groups. Each subcategory of the quality-of-life questionnaire resulted in a score between 0-100 per patient. Median scores are presented as median (+ standard deviation (SD)). Change in quality of life was calculated (end of study versus baseline). Results of patients who were not able to complete both questionnaires were excluded from the dataset. Statistically significant differences ( $p$ -value  $< 0.05$ ) between the two treatment groups were calculated using a Mann-Whitney U test. All statistical analyses were performed using the R software package V4.1.0.<sup>16</sup>

## RESULTS

### *Patient characteristics and pharmacokinetic analysis*

Between March 2019 and April 2021 a total of 81 patients were included in the study, 44 in the standard-of-care arm and 37 in the optimized dosing arm. The difference in group size was mostly due to a combination of the block randomization and dropout shortly after randomization (before start of cycle treatment 1). Moreover, one patient was accidentally treated with a BSA-based dose while randomized in the optimized dosing arm. The baseline characteristics were comparable between groups (Table 1). The majority of patients was diagnosed with NSCLC and received pemetrexed as a part of the first line treatment. Presented in Table 2 is the target attainment for both groups. The geometric mean AUC's were 159.9 and 154.7 mg·h/L for the BSA and the optimized dosing group, respectively. Target attainment was not statistically significant different between both groups ( $p = 0.505$ ).

The median creatinine clearance in the study population was 95 mL/min, therefore, the subgroup analysis was based on a creatinine clearance  $< 95$  mL/min and  $> 95$  mL/min. Figure 1 visualizes the AUC of pemetrexed in both randomization groups when subdivided. As expected, for the standard of care arm, a statistically significant difference in pemetrexed AUC was observed between the creatinine clearance subgroups ( $p = 0.003$ ), whereas this was not observed for the optimized dosing arm ( $p = 0.34$ ). Overall a higher percentage of patients in the optimized dosing arm attained to the target AUC when compared to patient in the standard-of-care dosing arm based on the creatinine clearance group, albeit not statistically significant. As shown in Table 2, for patients with creatinine clearance  $< 95$  mL/min dosed on BSA a higher median AUC and greater variability in exposure was observed compared to patients receiving optimized dose ( $p = 0.07$ ). This trend was not observed for patients with creatinine clearance  $> 95$  mL/min.

To justify the pre-term analysis of 81 patients, we calculated the outcomes of a best-case and worst-case scenario. In case of both scenarios (all remaining patients in the individualized group ( $n = 10$ ) on target and all remaining patients in the BSA group off target ( $n = 3$ ) or vice versa), no significant difference was observed ( $p = 0.082$  and  $p = 0.083$ ).

Table 1. Baseline characteristics and primary outcome measures for the BSA group, optimized dosing group and the total patient group. Values are presented as numbers (percentages) or medians [interquartile ranges], as appropriate.

	BSA (n = 44)	Optimized (n = 37)	Total (n = 81)
<b>Diagnosis, n (%)</b>			
NSCLC	35 (80%)	27 (73%)	62 (77%)
Mesothelioma	7 (16%)	9 (24%)	16 (20%)
Thymoma	2 (5%)	1 (3%)	3 (4%)
<b>First-line treatment, n (%)</b>			
Age (years)	63 [57-69]	67 [59-72]	65 [58-71]
Gender, male (%)	16 (36%)	22 (59%)	38 (47%)
BSA (m <sup>2</sup> )	1.87 [1.71-2.00]	1.95 [1.78-2.00]	1.91 [1.75-2.00]
eGFR (mL/min)	99.3 [84.0-118.4]	93.8 [78.7-101.4]	95.2 [83.6-111.7]
CKD-EPI (mL/min/1.73m <sup>2</sup> )	94.6 [81.9-100.5]	85.1 [80.1-93.5]	90.1 [80.9-98.9]
Treatment cycles	4 [4-4]	4 [4-4]	4 [4-4]
Pemetrexed dose per cycle (mg)	950 [850-1,000]	850 [818-885]	885 [825-975]
<b>Concomitant oncological therapy</b>			
None	8 (18%)	7 (19%)	15 (19%)
Carboplatin	11 (25%)	12 (32%)	23 (28%)
Carboplatin + pembrolizumab	18 (41%)	11 (30%)	29 (36%)
Cisplatin	4 (9%)	5 (14%)	9 (11%)
Cisplatin + pembrolizumab	3 (7%)	2 (5%)	7 (9%)

BSA: body surface area, CKD-EPI: Chronic Kidney Disease Epidemiology Collaboration, eGFR: estimated glomerular filtration rate, NSCLC: non-small cell lung cancer

Table 2. Target attainment and geometric mean AUC for the BSA group and the optimized dosing group in total and in the subgroup analysis. AUCs are presented median [interquartile ranges].

	BSA (n = 44)	Optimized (n = 37)	p-value
<b>AUC (mg·h/L)</b>			
Total	159.9 [145.0-176.0]	154.7 [137.6-171.5]	0.436
> 95 mL/min	154.2 [141.5-163.9]	151.0 [136.8-160.1]	0.908
< 95 mL/min	176.3 [156.0-196.7]	163.3 [143.6-172.3]	0.073
<b>Target attainment, n (%)</b>			
Total	37 (84.1)	33 (89.1)	0.505
> 95 mL/min	23 (88.5%)	15 (93.8%)	0.571
< 95 mL/min	14 (77.8%)	18 (85.7%)	0.520

AUC: area under the concentration-time curve, BSA: body surface area

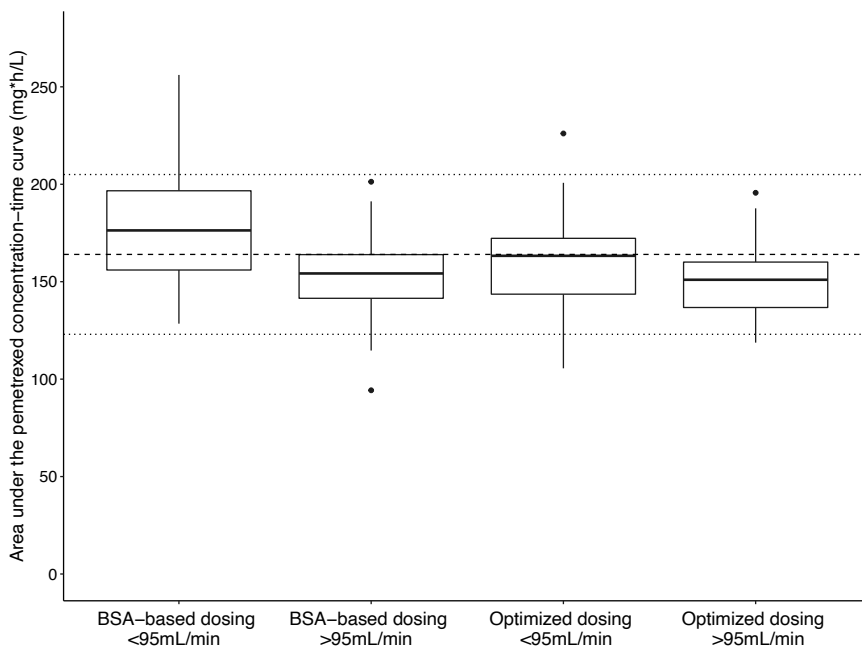


Figure 1. Boxplots for the AUC per subgroup. The box represents the 25th–75th percentiles with geometric mean, the whiskers indicate the 2.5th–97.5th percentile and the dots visualize the outlying observation. The target AUC  $\pm$  its 25% range are depicted by the horizontal dashed lines.

### Safety

Table 3 shows the number of patients that experienced  $\geq 1$  hematological toxicity event. One patient in the optimized dosing arm was excluded from this analysis due to incorrect (BSA-based) dosing from cycle 2 onward. Overall, there were no statistically significant differences between groups. Grade II anemia occurred in approximately 40–50% of patients. The incidence of grade III/IV hematological events were relatively low, ranging from 0% to 15.9%. Treatment delays and dose reductions due to toxicity occurred equally in both groups. Reported reasons other than hematological toxicity included hypokalemia, diarrhea, vomiting, kidney injury, pericarditis, fatigue, pneumonia, diverticulitis, and autoimmune reaction.

### Quality of life

In total, 58 patients completed the QLQ-C13 questionnaire both at baseline and after 12 weeks of pemtrexed therapy. The lung cancer specific LC13 questionnaire was filled in by 54 patients. Within-patient baseline and end of treatment scores were not statistically significant different in any of the four categories as indicated by the EORTC (functional scale, quality of life, symptom scale and the specific lung cancer scale). A wide range in change between  $t = 12$  weeks and baseline questionnaire was observed with the median around zero in both groups. Median changes and ranges are presented in Table 4. The change in end of treatment versus baseline score was not statistically significant different between groups.

Table 3. Fraction of patients experiencing at least ( $\geq 1$ ) toxicity event in both groups. Results are presented as numbers (percentages).

	BSA-based (n = 44)	Optimized (n = 36)	p-value
<b>Anemia</b>			
Grade 2	22 (50.0%)	14 (38.9%)	0.32
$\geq$ Grade 3	1 (2.2%)	4 (11.1%)	0.10
<b>Leukopenia</b>			
Grade 2	3 (6.8%)	2 (5.5%)	0.82
$\geq$ Grade 3	0	0	-
<b>Neutropenia</b>			
Grade 2	15 (34.1%)	9 (25.0%)	0.38
$\geq$ Grade 3	7 (15.9%)	4 (11.1%)	0.54
<b>Thrombocytopenia</b>			
Grade 2	3 (6.8%)	0	-
$\geq$ Grade 3	1 (2.2%)	1 (2.8%)	0.89
<b>Cycle delay</b>	13 (29.5%)	9 (25.0%)	0.65
<b>Dose reductions</b>	5 (11.4%)	3 (8.3%)	0.65

BSA: body surface area

Table 4. The difference [ranges] in end of treatment versus baseline score per subgroup of the EORTC-C13 and LC13 questionnaires.

	Standard of care arm (n = 33)	Individualized-dosing arm (n = 25)	p-value
<b>Functional scale</b>	-2.2 [-44-44]	-2.2 [-27-33]	1.0
<b>Quality of life</b>	0 [-50-67]	-8.8 [-58-50]	0.37
<b>Symptom scale</b>	0 [-39-47]	-1.4 [-17-22]	0.55
<b>Specific lung cancer scale</b>	-1.4 [-44-22]	-2.8 [-19-19]	0.82

## DISCUSSION

In the era of precision medicine, one should also aim to implement precision dosing. In this study we hypothesized that patients would benefit from optimized dosing of pemetrexed. We found that an optimized renal function-based pemetrexed dosing did not result in higher pharmacokinetic target attainment compared to standard of care BSA dosing. Moreover, no significant differences were observed with regards to safety events and quality of life. With this randomized study, we were the first to prospectively evaluate a renal function dosing regimen of pemetrexed.

The target attainment in the optimized dosing group (89.1%) was as expected, while in the BSA-based dosing group the target attainment (84.1%) was much higher than expected. This is possibly due to the limited number of patients in the extremes of the renal function range (creatinine clearance 45-60 mL/min or > 125 mL/min), thus resulting in a limited variation in exposure. This could also explain why we did not find a statistically significant difference in target attainment between both groups and only a small variation in administered dose within the optimized dosing arm. Interestingly, there was a significant difference in AUC in the subgroup analysis within the BSA-based dosing group when stratified on renal function ( $p = 0.003$ ). This confirms the strong influence of renal function on exposure if not taken into account with dosing. Especially in patients with a mild renal impairment (creatinine clearance: 45-60 mL/min), dosing based on renal function could serve a pivotal role in attaining a target systemic exposure. This is reflected in the observed exposure within the standard dosing group. Patients with a creatinine clearance < 95 mL/min show higher exposure and greater variability compared to patients with a creatinine clearance > 95 mL/min ( $p = 0.07$ ). Although this finding was not statistically significant this trend clearly indicates that patients with decreased renal function could benefit from this strategy. The limited number of patients in the extremes of the renal function range also reflects in the low variation in the administered pemetrexed dose in the optimized dosing group. Moreover, the median administered pemetrexed dose is lower in the optimized dosing group (850 mg) compared to the BSA-based group (950 mg). The median dose in the optimized dosing group corresponds with the calculated doses based on creatinine clearance. Although the median dose is lower, target exposure is attained (164 mg·h/L  $\pm$  25%) and efficacy is thus not compromised.

The large population pharmacokinetic analysis by Latz *et al.* was used as a premise for the individualized dosing strategy in this clinical study. In their analysis, they present creatinine clearance as a covariate for systemic pemetrexed clearance.<sup>13</sup> Nowadays, creatinine clearance is being widely substituted by the estimated glomerular filtration rate (calculated with the Chronic Kidney Disease Epidemiology Collaboration (CKD-EPI) equation), as this gives a more accurate prediction of renal function.<sup>17</sup> In our recent pharmacokinetic analysis, we found CKD-EPI eGFR to be a better predictor of pemetrexed pharmacokinetics than creatinine clearance calculated/estimated by Cockcroft-Gault equation. In addition, in the same analysis we found that renal function has an even larger impact on the systemic pemetrexed clearance than previously thought.<sup>4, 5</sup> Nonetheless, we expect this would not affect the non-significant outcome difference in this analysis in patients with adequate renal function. Regarding renal function measures, it could be argued that creatinine-based equations (thus muscle mass-dependent) are not ideal in patients with cancer. Cachexia is often observed in patients with lung cancer<sup>18, 19</sup>, resulting in seemingly low serum creatinine concentrations and thus overestimation of renal function. When deploying a renal function-based dosing strategy, this could theoretically lead to overdosing and thus increased exposure and higher risk for toxicity.

Recently, we found that the hematological toxicity of pemetrexed, in particular neutropenia, is more likely to be time-above-threshold driven instead of total exposure.<sup>20</sup> However, this is particularly relevant in patients with renal impairment. In patients with adequate renal function, AUC and time

above threshold are closely related, in contrast to patients with renal impairment.<sup>20</sup> Our results indeed show no statistical significant differences in hematological toxicities between both dosing arms, underlining this hypothesis.

From a patients perspective, quality of life is a valuable study endpoint. It is rather difficult to assess quality of life in relatively small patient groups (n = 44 and 37, respectively in our study). For pemetrexed as a single agent, two studies reported that quality of life during pemetrexed maintenance therapy was similar to placebo.<sup>21,22</sup> The scores at baseline and 12 weeks are comparable to our findings. Quality of life can be negatively influenced by factors such as progression of disease (non-responders) or severe treatment toxicity. However, in case of partial or complete response to treatment without toxicity, quality of life can improve. Moreover, our relatively small patient groups are heterogeneous in terms of diagnosis, disease stage, treatment modality and treatment line. This is reflected in the wide range in differences between baseline and end of treatment for both groups we observed.

In conclusion, our study did not support the superiority of renal function-based dosing of pemetrexed in patients with adequate renal function in terms of pharmacokinetic outcomes.

## REFERENCES

1. Planchard D, Popat S, Kerr K, Novello S, Smit EF, Faivre-Finn C, et al. Metastatic non-small cell lung cancer: ESMO Clinical Practice Guidelines for diagnosis, treatment and follow-up. *Ann Oncol*. 2018;29(Suppl 4):iv192-iv237. <https://doi.org/10.1093/annonc/mdy275>.
2. Baas P, Fennell D, Kerr KM, Van Schil PE, Haas RL, Peters S, et al. Malignant pleural mesothelioma: ESMO Clinical Practice Guidelines for diagnosis, treatment and follow-up. *Ann Oncol*. 2015;26 Suppl 5:v31-39. <https://doi.org/10.1093/annonc/mdv199>.
3. Girard N, Ruffini E, Marx A, Faivre-Finn C, Peters S, Committee EG. Thymic epithelial tumours: ESMO Clinical Practice Guidelines for diagnosis, treatment and follow-up. *Ann Oncol*. 2015;26 Suppl 5:v40-55. <https://doi.org/10.1093/annonc/mdv277>.
4. de Rouw N, Boosman RJ, Huitema ADR, Hilbrands LB, Svensson EM, Derijks HJ, et al. Rethinking the application of pemetrexed for patients with renal impairment: A pharmacokinetic analysis. *Clin Pharmacokinet*. 2021. <https://doi.org/10.1007/s40262-020-00972-1>.
5. Mita AC, Sweeney CJ, Baker SD, Goetz A, Hammond LA, Patnaik A, et al. Phase I and pharmacokinetic study of pemetrexed administered every 3 weeks to advanced cancer patients with normal and impaired renal function. *J Clin Oncol*. 2006;24(4):552-562. <https://doi.org/10.1200/JCO.2004.00.9720>.
6. Latz JE, Rusthoven JJ, Karlsson MO, Ghosh A, Johnson RD. Clinical application of a semimechanistic-physiologic population PK/PD model for neutropenia following pemetrexed therapy. *Cancer Chemother Pharmacol*. 2006;57(4):427-435. <https://doi.org/10.1007/s00280-005-0035-2>.
7. Visser S, Koolen SLW, de Bruijn P, Belderbos HNA, Cornelissen R, Mathijssen RHJ, et al. Pemetrexed exposure predicts toxicity in advanced non-small-cell lung cancer: A prospective cohort study. *Eur J Cancer*. 2019;121:64-73. <https://doi.org/10.1016/j.ejca.2019.08.012>.
8. European Medicine Agency (EMA). Alimta: EPAR-Product Information. 2017.
9. Ando Y, Hayashi T, Ujita M, Murai S, Ohta H, Ito K, et al. Effect of renal function on pemetrexed-induced haematotoxicity. *Cancer Chemother Pharmacol*. 2016;78(1):183-189. <https://doi.org/10.1007/s00280-016-3078-7>.
10. Chen CY, Lin JW, Huang JW, Chen KY, Shih JY, Yu CJ, et al. Estimated creatinine clearance rate is associated with the treatment effectiveness and toxicity of pemetrexed as continuation maintenance therapy for advanced nonsquamous non-small-cell lung cancer. *Clin Lung Cancer*. 2015;16(6):e131-140. <https://doi.org/10.1016/j.clcc.2015.01.001>.
11. Cockcroft DW, Gault MH. Prediction of creatinine clearance from serum creatinine. *Nephron*. 1976;16(1):31-41. <https://doi.org/10.1159/000180580>.
12. Aaronson NK, Ahmedzai S, Bergman B, Bullinger M, Cull A, Duez NJ, et al. The European Organization for Research and Treatment of Cancer QLQ-C30: a quality-of-life instrument for use in international clinical trials in oncology. *J Natl Cancer Inst*. 1993;85(5):365-376. <https://doi.org/10.1093/jnci/85.5.365>.
13. Latz JE, Chaudhary A, Ghosh A, Johnson RD. Population pharmacokinetic analysis of ten phase II clinical trials of pemetrexed in cancer patients. *Cancer Chemother Pharmacol*. 2006;57(4):401-411. <https://doi.org/10.1007/s00280-005-0036-1>.
14. de Rouw N, Visser S, Koolen SLW, Aerts JGJV, Burger DM, ter Heine R. Development and validation of a limited sampling strategy for pemetrexed therapeutic drug monitoring and research purposes. 3rd International Workshop on Clinical Pharmacology of Anticancer Drugs (ICPAD); Amsterdam 2018.
15. van den Hombergh E, de Rouw N, van den Heuvel M, Croes S, Burger DM, Derijks J, et al. Simple and rapid quantification of the multi-enzyme targeting antifolate pemetrexed in human plasma. *Ther Drug Monit*. 2020;42(1):146-150. <https://doi.org/10.1097/FTD.0000000000000672>.
16. R Core Team (2020). R: A language and environment for statistical computing. R Foundation for Statistical Computing, Vienna, Austria. URL <https://www.R-project.org/>.
17. Levey AS, Stevens LA, Schmid CH, Zhang YL, Castro AF, Feldman HI, et al. A new equation to estimate glomerular filtration rate. *Ann Intern Med*. 2009;150(9):604-612. <https://doi.org/10.7326/0003-4819-150-9-200905050-00006>.
18. Kimura M, Naito T, Kenmotsu H, Taira T, Wakuda K, Oyakawa T, et al. Prognostic impact of cancer cachexia in patients with advanced non-small cell lung cancer. *Support Care Cancer*. 2015;23(6):1699-1708. <https://doi.org/10.1007/s00520-014-2534-3>.

19. Zhu R, Liu Z, Jiao R, Zhang C, Yu Q, Han S, et al. Updates on the pathogenesis of advanced lung cancer-induced cachexia. *Thorac Cancer*. 2019;10(1):8-16. <https://doi.org/10.1111/1759-7714.12910>.
20. Boosman RJ, Dorlo TPC, de Rouw N, Burgers JA, Dingemans AC, van den Heuvel MM, et al. Toxicity of pemetrexed during renal impairment explained - implications for safe treatment. *Int J Cancer*. 2021;149(8):1576-1584. <https://doi.org/10.1002/ijc.33721>.
21. Belani CP, Brodowicz T, Ciuleanu TE, Krzakowski M, Yang SH, Franke F, et al. Quality of life in patients with advanced non-small-cell lung cancer given maintenance treatment with pemetrexed versus placebo (H3E-MC-JMEN): results from a randomised, double-blind, phase 3 study. *Lancet Oncol*. 2012;13(3):292-299. [https://doi.org/10.1016/S1470-2045\(11\)70339-4](https://doi.org/10.1016/S1470-2045(11)70339-4).
22. Gridelli C, de Marinis F, Pujol JL, Reck M, Ramlau R, Parente B, et al. Safety, resource use, and quality of life in paramount: a phase III study of maintenance pemetrexed versus placebo after induction pemetrexed plus cisplatin for advanced nonsquamous non-small-cell lung cancer. *J Thorac Oncol*. 2012;7(11):1713-1721. <https://doi.org/10.1097/JTO.0b013e318267cf84>.



# CHAPTER 3.4

Prediction of the  
pharmacokinetics of  
pemetrexed with  
a low test dose:  
a proof-of-concept study

*Submitted*

René J. Boosman  
Nikki de Rouw  
Alwin D.R. Huitema  
Jacobus A. Burgers  
Rob ter Heine

Author's contribution: R.J. Boosman contributed to the design of this study, performed the data management, conducted the data analysis, wrote the first draft of the manuscript and edited the contribution of the co-authors on this manuscript.

# ABSTRACT

## Purpose

Pemetrexed is a cytotoxic drug used for treatment of lung cancer and mesothelioma. The use of a low test dosing of cytotoxic drugs may aid in dose individualization without causing harm. The aim of this proof-of-concept study was to assess if the pharmacokinetics (PK) of a test dose could predict the pharmacokinetics of a therapeutic pemetrexed dose.

## Methods

Ten patients received both a low test dose (100 µg) and a therapeutic dose of pemetrexed after which plasma concentrations pemetrexed were measured. Pharmacokinetic analysis was performed by means of non-linear mixed effects modelling. The predictive performances of test dose clearance and renal function towards a therapeutic dose were assessed.

## Results

PK of a pemetrexed test dose was best described by a one-compartment model with linear elimination. A high variability in the administered dose was observed for the test dose, but not for the therapeutic dose. A statistically significant correlation between test dose clearance and therapeutic dose clearance was observed (Spearman's rho: 0.758,  $p = 0.02$ ). The predictive performance of test dose clearance was worse than renal function (mean predictive error (+95% confidence interval (CI)): 53.9% (50.1-57.6%) vs 19.4% (12.4-26.4%) and normalized root-mean square error (+95% CI): 57.8% (30.5-85.1%) vs 25.7% (20.3-31.0%).

## Conclusion

We show that test dosing of pemetrexed is feasible, however, there seems no added value for a low test dosing in dose individualization of pemetrexed.

## INTRODUCTION

Pemetrexed is a drug from the class of antifolates, used as first-line treatment option for patients with non-small cell lung cancer (NSCLC) and mesothelioma in a dose of 500 mg/m<sup>2</sup> every three weeks.<sup>1,2</sup> As with many cytotoxic drugs, dose individualization should be performed to balance the narrow line between subtherapeutic and toxic exposure.<sup>3,4</sup> With these type of drugs, it is desirable to administer the right dose from the first dose onwards. The use of body surface area (BSA) to individualize dosing of anticancer drugs is a matter of frequent debate.<sup>5,6</sup> Alternatives for BSA-based dosing regimens should thus be explored, especially for drugs that are renally cleared, like pemetrexed.<sup>7-10</sup> Moreover, a relationship between the pharmacokinetics (PK) of pemetrexed and toxicity and response has been described previously<sup>10,11</sup>, further underlining the importance of a PK-guided precision dosing strategy.

One way to investigate the PK of cytotoxic drugs, may be by means of a test dose.<sup>12,13</sup> Provided that extrapolation is possible, a low test dose may be used to safely predict the PK of cytotoxic drugs at a full dose. To the extent of our knowledge, no test dosing studies have thus far been performed with pemetrexed. Therefore, we performed a test dosing proof-of-concept study with pemetrexed and explored the performance of test dosing to predict PK of therapeutic dose pemetrexed.

## METHODS

### *Study design & patients*

Patients were included in two sequential prospective open-label studies. In the first study a low test dose of 100 µg pemetrexed was administered. Within seven days, patients were enrolled in the second study. In this study, the PK of pemetrexed of a therapeutic dose of pemetrexed was studied. Both studies were approved by a Medical Ethical Committee, conducted in accordance with the declaration of Helsinki, and publicly registered (clinicaltrials.gov identifiers NCT03655834 & NCT03655821).

Patients (≥ 18 years old) who were eligible for pemetrexed-based chemotherapy were included. Individual data on age, gender, ethnicity, body weight, height, and serum creatinine were available. After pemetrexed administration, PK blood samples were collected at pre-dose and 0.5-1 h, 1-2 h, 4-5 h and 6-8 h after administration, based on a previously established limited sampling strategy.<sup>14</sup> Plasma was isolated and stored at -20 °C until further analysis.

### *Bioanalysis*

Pemetrexed concentrations after the test dose were determined using a reversed phase ultra-high performance liquid chromatography (UPLC) with tandem mass spectrometry detection. This method was validated to measure pemetrexed concentrations in the range of 0.06-25.0 µg/L. Quantification of the pemetrexed plasma concentrations after the therapeutic dose was performed by means of UPLC coupled with ultraviolet detection validated in the range of 0.25-500 mg/L.<sup>15</sup>

### Pharmacokinetic analysis

We performed a parametric compartmental PK analysis for pemetrexed after administration of the low test dose and therapeutic dose, by means of non-linear mixed effects modelling using the software package NONMEM 7.4.3 (Icon, Ireland). For both PK datasets (test dose and therapeutic dose) one and two-compartment linear pharmacokinetic models were evaluated. Interindividual variability (IIV) was assumed to be log-normally distributed. For the residual error, additive, proportional and combined additive and proportional error models were evaluated.

### Extrapolation from test dose to a therapeutic dose

Individual clearance, besides dose, is the main parameter driving the area under the pemetrexed concentration time curve (AUC).<sup>8, 16</sup> Therefore, the individual prediction for clearance was used to assess the predictive performance from test dose to therapeutic dose, as a surrogate for AUC. The clearance estimated from the therapeutic dose data, was considered the true clearance. In a previous PK model, it was shown that estimated glomerular filtration rate (eGFR; assessed by the Chronic Kidney Disease Epidemiology Collaboration (CKD-EPI)<sup>17</sup>) is a strong predictor for the clearance of a therapeutic dose of pemetrexed.<sup>7</sup> The predicted pemetrexed clearance (in L/h) derived from this model is defined in equation 1:

$$\text{Predicted pemetrexed clearance} = 0.66 + 3.42 * (\text{eGFR}/75) \quad (1)$$

The individual predicted test dose clearance and the individual clearance as predicted with equation 1 were compared with the true pemetrexed clearance. The correlation between predicted clearances and true clearance was calculated with the Spearman's rank correlation coefficient (Spearman's rho).<sup>18</sup> Predictive performance in terms of bias and precision was evaluated based on the mean predictive error (MPE) and normalized root-mean-square error (NRMSE), with the observed therapeutic clearance as true. The corresponding 95% confidence intervals (CI) of MPE and NRMSE were calculated as described by Sheiner *et al.*<sup>19</sup> and Faber<sup>20</sup>, respectively.

### Model evaluation

Models were assessed by means of inspection of goodness-of-fit plots, physiological plausibility, stability of parameter estimates and change in the objective function (OFV) of the models. A  $p < 0.05$  corresponding to a decrease of  $\geq 3.84$  in OFV was considered a statistically significant model improvement in case of nested models (with one degree of freedom). Parameter precision was determined by a sampling importance resampling (SIR) procedure.<sup>21</sup>

## **RESULTS**

Ten patients were enrolled in the study and a total of 40 pemetrexed plasma concentrations after the test dose were available. During the therapeutic dose administration, in one patient an extra sample directly after the therapeutic pemetrexed administration was accidentally drawn.

Therefore, a total of 41 pemetrexed plasma concentrations after a therapeutic dose were available for analysis. In Table 1, the patient characteristics are presented. The individual eGFR was similar prior to both doses, with a relative difference ranging from -6.7% to +11.3%.

Table 1. Patient demographics of included patients, values are presented as numbers (percentages) or medians [ranges], as appropriate.

<b>Total number of patients</b>	10
<b>Gender</b>	
Male	2 (20%)
Female	8 (80%)
<b>Age, years</b>	64 [51-72]
<b>Tumor type</b>	
NSCLC	5 (50%)
Mesothelioma	4 (40%)
Thymoma	1 (10%)
<b>Renal function</b>	
Prior to test dose	
eGFR (assessed with CKD-EPI) (mL/min)	97 [76-121]
Prior to therapeutic dose	
eGFR (assessed with CKD-EPI) (mL/min)	101 [74-127]
<b>Body surface area (m<sup>2</sup>)<sup>a</sup></b>	1.83 [1.36-2.29]
<b>Pemetrexed dose</b>	
Test dose (µg)	100 [100-100]
Therapeutic dose (mg)	899 [805-1143]

<sup>a</sup> BSA was assessed with the Dubois method.<sup>25</sup>

CKD-EPI: Chronic Kidney Disease Epidemiology Collaboration, eGFR: estimated glomerular filtration rate

### *Pharmacokinetic analysis*

In Table 2, the parameter estimates and their (SIR-derived) 95% confidence intervals for the models of both the test dose and the therapeutic dose are presented.

#### *Test dose model*

The test dose data were best described by a one-compartment model with linear elimination and a proportional error model. Extremely high interpatient variability was observed in the test dose data. Upon inspection of the empirical Bayes estimates for volume of distribution and clearance, a very high correlation was observed. This was highly indicative for variability in the administered dose as a consequence of variability in preparation and/or administration of the very low dose. Therefore, IIV was added on the administered dose which showed a statistically significant improvement of the model ( $p \ll 0.01$ ) as indicated by a drop in OFV of 88.1 points.

### Therapeutic dose model

A two-compartment model with linear elimination and a proportional error model, described the therapeutic data best.

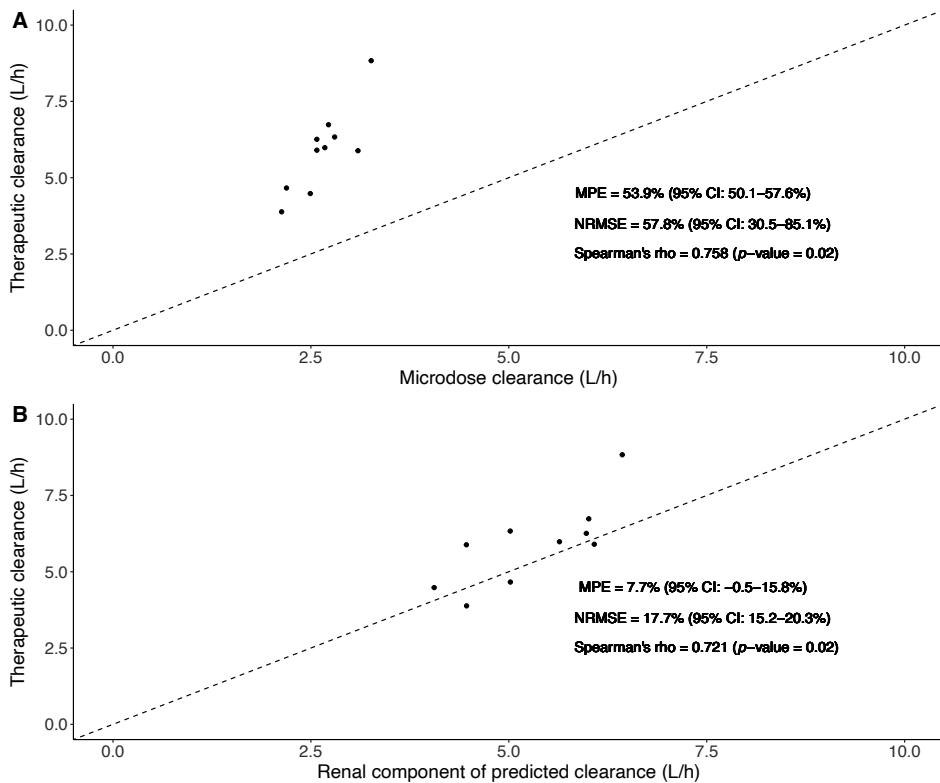


Figure 1. Predictive performance of A) test dose clearance on the true therapeutic clearance and B) renal component of the predicted clearance (according to the model of de Rouw *et al.*?) on the true therapeutic clearance. MPE; mean predictive error, NRMSE: normalized root-mean square error. The line of unity is represented by the dashed line.

### Extrapolation from test dose to a therapeutic dose

Figure 1 depicts the predictive performance of the test dose model and the earlier described renal function-based PK model. For both the test dose and the eGFR a statistically significant correlation between the predicted clearance and the true clearance is observed (Spearman's rho: 0.758 ( $p$  = 0.02) and 0.721 ( $p$  = 0.02), respectively). The MPE and NRMSE of the predicted test dose clearance over the true clearance are higher than the predicted renal component of clearance by the model of de Rouw *et al.* over the true clearance. Values (including their 95% CI) for the MPE are 53.9% (50.1-57.6%) versus 7.7% (-0.5-15.8%) and for the NRMSE 57.8% (30.5-85.1%) versus 17.7% (15.2-20.3%). This indicates that prediction of a therapeutic clearance is better performed by means of measurement of eGFR compared to the assessment of a test dose clearance.

Table 2. Parameter estimates and their (SIR-derived) 95% confidence intervals of the base model for test dose and the base and final model for therapeutic dose.

	Test dose base model (n = 10)	Therapeutic dose model (n = 10)
CL (L/h)	2.32 [1.35-3.36]	5.73 [4.81-6.86]
IIV CL (%)	11.3 [5.76-17.0]	23.9 [15.1-35.3]
Scaling factor for test dose CL	-	-
<b>Volume of distribution</b>		
Central compartment (L)	4.07 [2.44-6.29]	7.28 [4.06-10.1]
Peripheral compartment (L)	-	5.39 [3.50-7.14]
Q (L/h)	-	4.53 [1.99-11.4]
F	1 <sup>a</sup>	-
IIV F (%)	139 [98.6-176]	
<b>Proportional error (%)</b>	<b>24.7 [18.8-32.4]</b>	<b>26.7 [22.1-34.8]</b>

<sup>a</sup> fixed value.

CL: clearance, F: dose effect, IIV: interindividual variability, Q: intercompartmental clearance

## DISCUSSION

In this proof-of-concept study we show that pemetrexed PK can be assessed after administration of a test dose. Furthermore, a significant relationship between the predicted test dose clearance and the true clearance was found. However, from our analysis it appears that the use of a low test dose does not outperform renal function to predict pemetrexed clearance.

If complete linearity between PK of a test dose and therapeutic dose exists, one would expect a 1:1 ratio between PK parameters. For clearance and volume of distribution, these ratios both exceed more than a twofold. This might hint to non-linear scalability of PK parameters of test dose to the PK parameters at a therapeutic dose, potentially due to non-linear PK.

Non-linearity of the PK may be attributed to saturation of the organic anion transporter 3 (OAT3), reduced folate carrier (RFC) and proton-coupled folate transporter (PCFT) at the therapeutic dose. Both RFC and PCFT are important transporters for rapid cellular uptake of pemetrexed<sup>22</sup>, while OAT3 is extensively expressed in the kidneys and plays a major role in the active secretion of pemetrexed.<sup>23</sup> For all these transporters, concentrations at which half of the transporters are bound (Km values) are reported to lie above the measured pemetrexed concentrations after a test dose administration.<sup>24</sup> However, for a therapeutic dose, > 50% of these transporters are expected to be saturated the first six hours after pemetrexed administration. Thus, at therapeutic doses the saturation would result in a decreased cellular uptake as well as less active secretion. In our study, we found elimination rate constants of test dose and therapeutic dose to be 0.57 h<sup>-1</sup> and 0.45 h<sup>-1</sup> respectively. This indicates that a lower percentage of pemetrexed is excreted per time unit after a therapeutic dose when compared to a test dose. Saturation of the above-mentioned transporters might thus be a valid explanation for the differences in PK parameters between test dose and therapeutic dose.



We hypothesize that the high apparent variability on the administered test dose illustrates specific challenges for the reproducibility of the preparation, or administration, of a test dose. For the robustness and reliability of a PK study, it is important to accurately know the administered dose. Although the cause is currently unknown, we hypothesize that small preparation errors, such as insufficient homogenization of the (stock) solution, may result in variability in the administered dose. It is important to consider this specific obstacle when starting a test dose study.

We assessed the feasibility of pemetrexed test dosing and to predict its PK at a therapeutic dose. We found that the PK of a test dose pemetrexed can be assessed and that the predicted clearance has a correlation with the therapeutic clearance. Although the feasibility of a test dosing was shown, our findings do not support the use of low test dosing to individualize dosing of pemetrexed.

## REFERENCES

1. Planchard D, Popat S, Kerr K, Novello S, Smit EF, Faivre-Finn C, et al. Metastatic non-small cell lung cancer: ESMO Clinical Practice Guidelines for diagnosis, treatment and follow-up. *Ann Oncol*. 2018;29(Suppl 4):iv192-iv237. <https://doi.org/10.1093/annonc/mdy275>.
2. Baas P, Fennell D, Kerr KM, Van Schil PE, Haas RL, Peters S. Malignant pleural mesothelioma: ESMO Clinical Practice Guidelines for diagnosis, treatment and follow-up. *Ann Oncol*. 2015;26 Suppl 5:v31-39. <https://doi.org/10.1093/annonc/mdv199>.
3. Visser S, Koolen SLW, de Bruijn P, Belderbos HNA, Cornelissen R, Mathijssen RHJ, et al. Pemetrexed exposure predicts toxicity in advanced non-small-cell lung cancer: A prospective cohort study. *Eur J Cancer*. 2019;121:64-73. <https://doi.org/10.1016/j.ejca.2019.08.012>.
4. Dickgreber NJ, Sorensen JB, Paz-Ares LG, Schytte TK, Latz JE, Schneck KB, et al. Pemetrexed safety and pharmacokinetics in patients with third-space fluid. *Clin Cancer Res*. 2010;16(10):2872-2880. <https://doi.org/10.1158/1078-0432.Ccr-09-3324>.
5. Felici A, Verweij J, Sparreboom A. Dosing strategies for anticancer drugs: the good, the bad and body-surface area. *Eur J Cancer*. 2002;38(13):1677-1684. [https://doi.org/10.1016/S0959-8049\(02\)00151-X](https://doi.org/10.1016/S0959-8049(02)00151-X).
6. Mathijssen RHJ, de Jong FA, Loos WJ, van der Bol JM, Verweij J, Sparreboom A. Flat-fixed dosing versus body surface area-based dosing of anticancer drugs in adults: Does it make a difference? *The Oncologist*. 2007;12(8):913-923. <https://doi.org/10.1634/theoncologist.12-8-913>.
7. de Rouw N, Boosman RJ, Huitema ADR, Hilbrands LB, Svensson EM, Derijks HJ, et al. Rethinking the application of pemetrexed for patients with renal impairment: a pharmacokinetic analysis. *Clin Pharmacokinet*. 2021;60(5):649-654. <https://doi.org/10.1007/s40262-020-00972-1>.
8. Latz JE, Chaudhary A, Ghosh A, Johnson RD. Population pharmacokinetic analysis of ten phase II clinical trials of pemetrexed in cancer patients. *Cancer Chemother Pharmacol*. 2006;57(4):401-411. <https://doi.org/10.1007/s00280-005-0036-1>.
9. Chen CY, Lin JW, Huang JW, Chen KY, Shih JY, Yu CJ, et al. Estimated creatinine clearance rate is associated with the treatment effectiveness and toxicity of pemetrexed as continuation maintenance therapy for advanced nonsquamous non-small-cell lung cancer. *Clin Lung Cancer*. 2015;16(6):e131-140. <https://doi.org/10.1016/j.clcc.2015.01.001>.
10. Latz JE, Rusthoven JJ, Karlsson MO, Ghosh A, Johnson RD. Clinical application of a semimechanistic-physiologic population PK/PD model for neutropenia following pemetrexed therapy. *Cancer Chemother Pharmacol*. 2006;57(4):427-435. <https://doi.org/10.1007/s00280-005-0035-2>.
11. Boosman RJ, Dorlo TPC, de Rouw N, Burgers JA, Dingemans A-MC, van den Heuvel MM, et al. Toxicity of pemetrexed during renal impairment explained—Implications for safe treatment. *Int J Cancer*. 2021;149(8):1576-1584. <https://doi.org/10.1002/ijc.33721>.
12. Kangaroo SB, Naveed F, Ng ESM, Chaudhry MA, Wu J, Bahlis NJ, et al. Development and Validation of a Test Dose Strategy for Once-Daily i.v. Busulfan: Importance of Fixed Infusion Rate Dosing. *Biol Blood Marrow Transplant*. 2012;18(2):295-301. <https://doi.org/10.1016/j.bbmt.2011.07.015>.
13. Cano JP, Bruno R, Lena N, Favre R, Iliadis A, Imbert AM. Dosage predictions in high-dose methotrexate infusions. Part 1: Evaluation of the classic test-dose protocol. *Cancer Drug Deliv*. 1985;2(4):271-276. <https://doi.org/10.1089/cdd.1985.2.271>.
14. de Rouw N, Visser S, Koolen SLW, Aerts J, van den Heuvel MM, Derijks HJ, et al. A limited sampling schedule to estimate individual pharmacokinetics of pemetrexed in patients with varying renal functions. *Cancer Chemother Pharmacol*. 2020;85(1):231-235. <https://doi.org/10.1007/s00280-019-04006-x>.
15. van den Hombergh E, de Rouw N, van den Heuvel M, Croes S, Burger DM, Derijks J, et al. Simple and Rapid Quantification of the Multi-Enzyme Targeting Antifolate Pemetrexed in Human Plasma. *Ther Drug Monit*. 2020;42(1).
16. Ouellet D, Periclou AP, Johnson RD, Woodworth JR, Lalonde RL. Population pharmacokinetics of pemetrexed disodium (ALIMTA) in patients with cancer. *Cancer Chemother Pharmacol*. 2000;46(3):227-234. <https://doi.org/10.1007/s002800000144>.
17. Levey AS, Stevens LA, Schmid CH, Zhang YL, Castro AF, Feldman HI, et al. A new equation to estimate glomerular filtration rate. *Ann Intern Med*. 2009;150(9):604-612. <https://doi.org/10.7326/0003-4819-150-9-200905050-00006>.

18. Spearman C. The proof and measurement of association between two things. *Am J Psychol.* 1904;15(1):72-101.
19. Sheiner LB, Beal SL. Some suggestions for measuring predictive performance. *J Pharmacokinetic Biopharm.* 1981;9(4):503-512. <https://doi.org/10.1007/BF01060893>.
20. Faber NM. Estimating the uncertainty in estimates of root mean square error of prediction: application to determining the size of an adequate test set in multivariate calibration. *Chemometrics and Intelligent Laboratory Systems.* 1999;49(1):79-89. [https://doi.org/10.1016/S0169-7439\(99\)00027-1](https://doi.org/10.1016/S0169-7439(99)00027-1).
21. Dosne AG, Bergstrand M, Karlsson MO. An automated sampling importance resampling procedure for estimating parameter uncertainty. *J Pharmacokinetic Pharmacodyn.* 2017;44(6):509-520. <https://doi.org/10.1007/s10928-017-9542-0>.
22. Zhao R, Qiu A, Tsai E, Jansen M, Akabas MH, Goldman ID. The Proton-Coupled Folate Transporter: Impact on Pemetrexed Transport and on Antifolates Activities Compared with the Reduced Folate Carrier. *Mol Pharmacol.* 2008;74(3):854-862. <https://doi.org/10.1124/mol.108.045443>.
23. Kurata T, Iwamoto T, Kawahara Y, Okuda M. Characteristics of Pemetrexed Transport by Renal Basolateral Organic Anion Transporter hOAT3. *Drug Metab Pharmacokinetic.* 2014;29(2):148-153. <https://doi.org/10.2133/dmpk.DMPK-13-RG-042>.
24. European Medicine Agency (EMA). Assessment Report of Pemetrexed Actavis. 2015. Accessed on 16 Mar 2021.
25. Du Bois D, Du Bois EF. A formula to estimate the approximate surface area if height and weight be known. 1916. *Nutrition.* 1989;5(5):303-311.



# CHAPTER 3.5

# Is age just a number? A population pharmacokinetic study of gemcitabine

*Cancer Chemother Pharmacol. 2022 [Epub ahead of print]*

René J. Boosman  
Marie-Rose B.S. Crombag  
Nielka P. van Erp  
Jos H. Beijnen  
Neeltje Steeghs  
Alwin D.R. Huitema

Author's contribution: R.J. Boosman contributed to the design of this study, performed the data management, conducted the data analysis, wrote the first draft of the manuscript and edited the contribution of the co-authors on this manuscript.

# ABSTRACT

## Purpose

Pharmacokinetic exposure to gemcitabine and its metabolite, 2',2'-difluorodeoxyuridine (dFdU), might be altered in elderly compared to their younger counterparts. It is unknown if age-based dose adjustments are necessary to reduce the development of treatment-induced adverse events. The aim of this study was to assess the impact of age on the pharmacokinetics of gemcitabine and dFdU.

## Methods

Pharmacokinetic sampling following a flexible limited-sampling strategy was performed in patients  $\geq 70$  years after gemcitabine infusion. The data was supplemented with pharmacokinetic data in patients included in four previously conducted clinical trials. Nonlinear mixed-effects modelling was performed on the pooled dataset to assess the impact of age on the pharmacokinetics of gemcitabine and dFdU.

## Results

In total, pharmacokinetic data was available of 197 patients, of whom 83 patients were aged  $\geq 70$  years (42%). A two-compartment model for both gemcitabine and dFdU with linear clearances from the central compartments described the data best. Age, tested as continuous and categorical ( $< 70$  years versus  $\geq 70$  years) covariate, did not statistically affect the pharmacokinetics of gemcitabine and dFdU.

## Conclusion

Age was not of influence on the pharmacokinetics of gemcitabine or its metabolite, dFdU. Age-related dose adjustments for gemcitabine based on pharmacokinetic considerations are not recommended.

## INTRODUCTION

Age is an important, yet unchangeable risk factor for the development of many cancer types. Currently, the median age at diagnosis of cancer is 66 years old.<sup>1</sup> Nonetheless, elderly have been notoriously underrepresented in clinical trials.<sup>2,3</sup> Pharmacokinetics in this subgroup might be different due to the gradual, age-related decrease in organ function or enzyme system activity, altered body composition, and/or the presence of comorbidities.<sup>4</sup> For many cytostatic agents there is a thin line between efficacy and toxicity and these parameters are often related to pharmacokinetic exposure. Thus, in case of alterations in pharmacokinetic exposure, treatment outcomes might be influenced.

Gemcitabine is a cytostatic agent used in the treatment of non-small cell lung cancer (NSCLC), bladder cancer, pancreatic cancer, breast cancer and ovarian cancer as monotherapy or in combination with a platinum-based agent or paclitaxel.<sup>5</sup> After administration, active transport by the human equilibrative nucleoside transporters (hENTs) into the cell and subsequent phosphorylation mediates the antitumor activity of gemcitabine. Moreover, both intracellular and extracellular gemcitabine is metabolized by cytidine deaminase (CDA) into 2',2'-difluorodeoxyuridine (dFdU).<sup>6</sup> It is thought that dFdU also plays a role in both the activity and the toxicity of treatment.<sup>7</sup> Currently, gemcitabine is administered in a dosing regimen of 1,000-1,250 mg/m<sup>2</sup>, with dose reductions only performed in case of toxicity.<sup>5</sup> However, since it is a hydrophilic drug and elderly patients often have a decreased total body water, plasma volume and intra- and extracellular body fluid<sup>8</sup>, it is to be expected that the volume of distribution of gemcitabine decreases with age, which might result in higher concentrations of gemcitabine. In addition, the expression of enzymes (such as hENT and CDA) might be altered in the elderly. The efficacy (and toxicity) of gemcitabine is dependent on the (de)activation of gemcitabine and it has been shown that changes in pharmacokinetics of gemcitabine, e.g. in case of prolonged infusion times, can yield severe toxicities.<sup>9</sup> Although contradictory results exist, it has been reported that elderly patients experience more grade 3/4 adverse events after gemcitabine administration.<sup>10</sup> Therefore, it appeared pivotal to elucidate if the gemcitabine and/or dFdU exposure in elderly is increased. Hence, the aim of this study was to determine the impact of age on the exposure of gemcitabine and its metabolite dFdU.

## METHODS

### *Study and patients*

A dataset was composed from both prospectively as retrospectively collected data. In the prospective observational study, elderly patients ( $\geq 70$  years old) who were eligible and planned for treatment with gemcitabine, willing and able to undergo blood sampling, and willing and able to give informed consent for study participation were included. This study was open between September 2012 and September 2021 in the Antoni van Leeuwenhoek hospital (Amsterdam, The Netherlands), the Slotervaart hospital (Amsterdam, The Netherlands) and the Radboudumc (Nijmegen, The Netherlands). This study was performed in accordance with the Declaration of Helsinki and was approved by the Medical Ethical Committee of the Slotervaart hospital, The Netherlands (file identifier: NL39647.048.12).



### Data and pharmacokinetic sampling

During this study, blood samples were taken in a flexible sampling scheme, with the first sample taken at the end of the gemcitabine infusion. Additional blood samples were allowed, based on the willingness and venous access of the study participants. A minimum of one sample and a maximum of ten blood samples were required. Tetrahydrouridine was added to gemcitabine samples within five minutes after sampling to stop cytidine deaminase dependent metabolism of gemcitabine into dFdU.<sup>11</sup> Samples were centrifuged immediately at 1,500 x g for five minute at 4 °C, plasma was collected and stored at -20 °C until bioanalysis. Both gemcitabine and dFdU concentrations were determined with a previously validated bioanalytical assay using high-performance liquid chromatography with tandem mass spectrometry.<sup>12</sup> The lower limits of quantification (LLOQ) for gemcitabine and dFdU in this analysis were 0.5 ng/mL and 5.0 ng/mL, respectively.<sup>12</sup> This data was enriched with retrospective data from previous clinical trials studying the pharmacokinetics of gemcitabine and dFdU that were conducted at the Antoni van Leeuwenhoek hospital.<sup>9, 13-15</sup> Baseline characteristics such as age, body weight, height, ethnicity and serum creatinine concentration on the day of gemcitabine administration were collected. In addition, data regarding the gemcitabine infusion such as dose, infusion duration and pharmacokinetic sampling times were available. It has been reported that an extended infusion time of gemcitabine has a substantial influence on pharmacokinetics of gemcitabine.<sup>16</sup> Therefore, samples drawn after a gemcitabine infusion extending more than one hour were excluded in this analysis.

### Population pharmacokinetic model

#### *Structural model*

Nonlinear mixed effect modelling was used to perform the population pharmacokinetic analysis. One-, two- and three-compartment models for gemcitabine and dFdU with linear clearance from the central compartment of dFdU were considered to describe the structural model. The fraction (fm) of gemcitabine converted to dFdU is unknown and, therefore, pharmacokinetic parameters for dFdU were estimated relative to the fm converted.

#### *Statistical model*

Interindividual variability (IIV) was modelled by an exponential model as expressed in equation 1.

$$P_i = P_{pop} * e^{\eta_i} \quad (1)$$

Where  $P_i$  is the individual parameter estimate,  $P_{pop}$  is the population parameter estimate, and  $\eta_i$  is the IIV with a mean of zero and a variance of  $\omega^2$ .

The unexplained, residual variability of gemcitabine and dFdU was modelled using equation 2:

$$C_{obs,ij} = C_{pred,ij} * (1 + \varepsilon_{p,ij}) + \varepsilon_{a,ij} \quad (2)$$

Where  $C_{obs,ij}$  is the observed concentration,  $C_{pred,ij}$  is the predicted concentration,  $\epsilon_{p,ij}$  is the proportional error and  $\epsilon_{a,ij}$  is the additive error. Both proportional and additive errors have a mean of zero and a variance of  $\sigma^2$ . Concentrations of gemcitabine or dFdU below the LLOQ, were discarded from the analysis.

### Covariate analysis

In previous analyses, body composition was identified as a significant covariate for the pharmacokinetic of gemcitabine and dFdU.<sup>17,18</sup> In the same studies, creatinine clearance (assessed with the Cockcroft-Gault equation<sup>19</sup>) and gender have been reported to influence the clearance of dFdU ( $Cl_{dFdU}$ ).<sup>17,18</sup> In addition, treatment indication (NSCLC) and gender were identified as significant covariates for the volume of distribution of the central compartment of dFdU ( $Vc_{dFdU}$ ).<sup>17,18</sup> To assess if a potential impact of age on the model can be ascribed to the influence of these covariates, they were introduced to the base model. Allometric scaling was performed for volume of distribution and (intercompartmental) clearances in relation to a total body weight of 70 kg. The allometric exponents for volume of distribution (of both the central (Vc) and peripheral compartments (Vp)) were set to 1.0 and for intercompartmental clearances (Q) and clearances (Cl) a value of 0.75 was implemented. For creatinine clearance as covariate on gemcitabine and dFdU clearance, renal and non-renal clearance were estimated separately. Creatinine clearance was tested as standardized creatinine clearance (based on a median weight of 70 kg and corresponding median creatinine clearance of 100 mL/min) on the renal contribution of the total clearance.

To study the effect of age on the exposure of gemcitabine and its metabolite, age was evaluated as covariate in both the base and covariate pharmacokinetic model. Age was tested as continuous covariate and as categorical covariate, with the population divided in two subgroups: patients < 70 years old (0) and patients  $\geq$  70 years old (1). Age as continuous covariate was standardized on the median value of the study population, following equation 3:

$$P_i = P_{pop} * \frac{covariate}{median(covariate)} \theta_{cov} \quad (3)$$

In which 'covariate' is the individual covariate value, 'median(covariate)' is the (median) typical population value for this covariate and  $\theta_{cov}$  is the relative change in population parameter.

Treatment indication, gender and age as categorical variables were tested following equation 4:

$$P_i = P_{pop} * \theta_{cov}^{covariate} \quad (4)$$

In case of missing data, the median value of the study population was imputed. Uncertainty in these imputations were accounted for by the addition of IIV following the exponential model (as in equation 1).

The impact of age on the concentration-time curves of both gemcitabine and dFdU was assessed by means of simulation from the final covariate model. For this purpose, typical patients (male, 70 kg) aged < 70 years and ≥ 70 years, receiving a 30 minute gemcitabine infusion of 1,250 mg/m<sup>2</sup> were simulated. Typical concentrations of gemcitabine and dFdU were assessed up to five hours after the start of the gemcitabine infusion.

#### Model evaluation

Goodness-of-fit (GOF) plots and a visual predictive check (VPC) with n = 1,000 were used to assess model fit. In addition, models were evaluated on their physiological plausibility, stability of parameter estimate and the change in objective function value (OFV). Statistical significance was defined as a p-value < 0.01, which corresponds to a decrease in OFV of 6.63 points (in case of nested models). Sampling importance resampling (SIR) calculation was performed to determine the uncertainty in parameter precision.<sup>20</sup>

#### Software

Data handling and graphical evaluations of the data were performed using R (version 4.1.0). Nonlinear mixed effect modelling was performed by means of NONMEM (version 7.5, ICON Development Solutions, LLC, Ellicott City, MD, USA). Pirana (version 3.0.0) provided the interface for the modelling output.

## **RESULTS**

The dataset contained a total of 789 gemcitabine concentrations and 789 dFdU concentrations from a total of 197 patients treated with gemcitabine. For gemcitabine, there were 41 samples which yielded concentrations below the LLOQ. These concentrations were discarded from the analysis, resulting in a total of 748 gemcitabine concentrations used for this analysis. For dFdU, none of the measured samples were below the LLOQ. The baseline and treatment characteristics of the included patients are depicted in Table 1. Overall, 83 patients aged ≥ 70 years (42%) were included, of whom 80 patients were prospectively included. The elderly subgroup consisted of more male patients, generally had a higher body weight and lower creatinine clearance, and received gemcitabine for other tumor types than their younger counterparts. Moreover, all patient < 70 years were included in clinical trials studying combination therapies, therefore, these patients received lower doses of gemcitabine in comparison with the patients ≥ 70 years. In Figure 1, the concentration-time curves of gemcitabine and dFdU for both age groups are illustrated. Information regarding weight and/or height was not available for 16 patients (8.1%) and serum creatinine concentrations were not taken prior to the gemcitabine administration in seven patients (3.5%). As a result, for 16 patients BSA and for 16 patients creatinine clearance could not be calculated, in total 15 patients missed information regarding both BSA and creatinine clearance. The majority of patients with missing data were aged < 70 years (94% for BSA and 88% for creatinine clearance). For none of the patients, age and gender were missing.

Table 1. Baseline characteristics and pharmacokinetic information of the included patients. Values are represented as median [range] or numbers (percentage) as appropriate.

	< 70 years	≥ 70 years	p-value	Total
<b>No. of patients</b>	114	83		197
<b>Age</b> [range] (years)	55 [27-69]	74 [70-85]		66 [27-85]
<b>Gender, male</b> (%)	44 (38.6%)	57 (68.7%)	<< 0.01	101 (51.3%)
<b>Body weight</b> [range] (kg)	72 [46-121]	77 [52-104]	0.02	74 [46-121]
<b>BSA</b> [range] (m <sup>2</sup> )	1.81 [1.47-2.44]	1.92 [1.54-2.27]	0.001	1.87 [1.47-2.44]
<b>Creatinine clearance</b> [range] (mL/min)	92.8 [43.3-205.4]	64.8 [32.3-130.9]	<< 0.01	76.7 [32.3-205.4]
<b>Gemcitabine dose</b> [range] (mg/m <sup>2</sup> )	735 [297-1318]	1,000 [481-1269]	<< 0.01	974 [297-1318]
<b>No. of samples</b>				
Gemcitabine				
Total	612	136		748
Per patient [range]	5 [2-7]	1 [1-6]	<< 0.01	5 [1-7]
dFdU				
Total	652	137		789
Per patient [range]	6 [4-7]	1 [1-6]	<< 0.01	5 [1-7]
<b>Tumor type</b>				
NSCLC (%)	43 (37.8%)	16 (19.3%)		59 (29.9%)
Bladder cancer (%)	1 (0.9%)	36 (43.4%)	<< 0.01	37 (18.8%)
Mamma cancer (%)	30 (26.3%)	3 (3.6%)		33 (16.8%)
Ovarian cancer (%)	17 (14.9%)	8 (9.6%)		25 (12.7%)
Other (%)	16 (14.0%)	20 (24.1%)		36 (18.3%)
Unknown (%)	7 (6.1%)	0		7 (3.6%)

BSA: body surface area, dFdU: 2',2'-difluorodeoxyuridine, NSCLC: non-small cell lung cancer

### Population pharmacokinetic modelling

The pharmacokinetics of both gemcitabine and dFdU was best described by a two-compartment model with linear clearance from the central compartment. The parameter estimates of the base model of parent and metabolite are reported in Table 2.

### Impact of age

As shown in Figure 1, for patients ≥ 70 years old, limited samples were drawn at the end of the distribution phase. Therefore, the effect of age on  $V_{p_{dFdU}}/fm$  and  $Q_{dFdU}/fm$  could not be identified. The evaluation of age as a continuous covariate on the base model did not yield any statistically significant effects on the parameters. However, as shown in Table 2, inclusion of age as categorical covariate resulted in a statistically significant increase in  $Vc_{gemcitabine}$  of 42% (95% confidence interval (CI)): 16-73%,  $p = 0.001$ ) for patients ≥ 70 years when compared to their younger counterparts. A decrease in IIV of this parameter of approximately 2% was found.

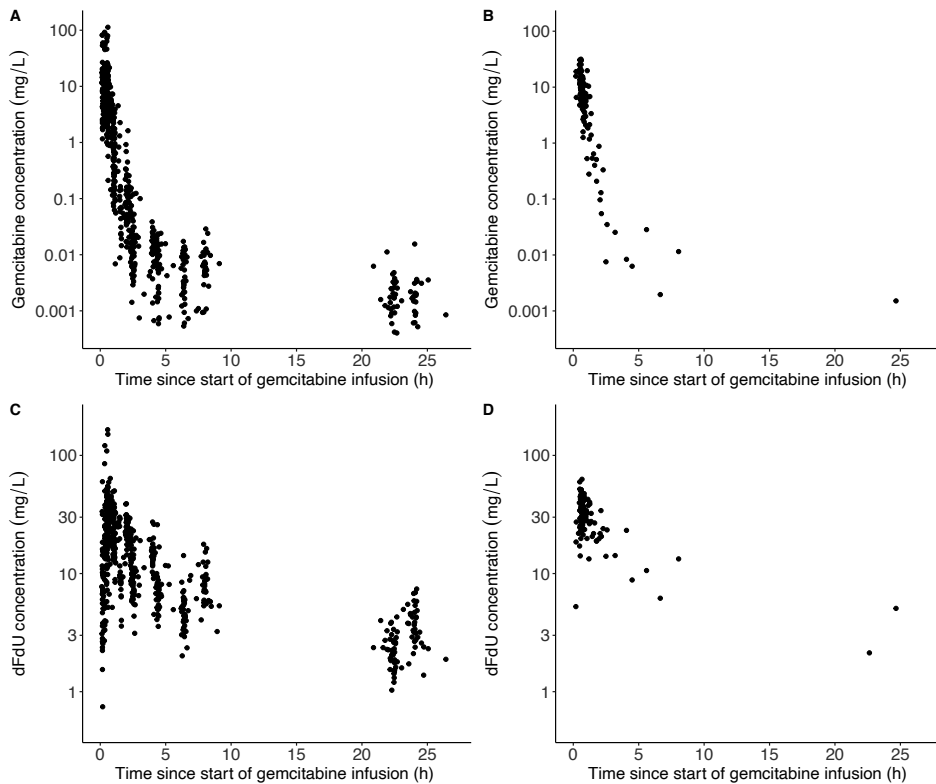


Figure 1. Concentration-time curves of A) gemcitabine in patients < 70 years old, B) gemcitabine in patients  $\geq$  70 years old, C) dFdU in patients < 70 years old and D) dFdU in patients  $\geq$  70 years old. Concentrations of gemcitabine and dFdU are presented on a logarithmic scale.

As indicated, allometric scaling, creatinine clearance, tumor type and gender were all introduced as covariates and again, the effect of age on the model was assessed. Patients  $\geq$  70 years were found to have a non-statistically significant increase of  $V_{c_{\text{gemcitabine}}}$  of 20% (95% CI: -3.5-46%,  $p = 0.117$ ), and a drop in  $ILV$  on this parameter of 1.0% was observed. This indicates that the difference in  $V_{c_{\text{gemcitabine}}}$  between elderly and non-elderly can at least be partly ascribed to previously identified factors other than age. In Figure 2, the VPCs for both gemcitabine and dFdU in this final covariate model are shown. Overall, the observed concentrations of gemcitabine and dFdU are in line with the predicted concentrations, indicating sufficient validity for both the parent and the metabolite. In Figure 3, the results of the simulations are depicted. In general, similar concentration-time curves of both gemcitabine and dFdU in patients < 70 years and  $\geq$  70 years can be observed.

Table 2. Population pharmacokinetic parameter estimates for gemcitabine of the base model (with and without age as covariate) and of the covariate model (with and without age as covariate). Values are presented as: parameter estimate [sampling-importance-resampling (SIR)-derived 95% confidence interval].

	Base model	Base model + age	Covariate model	Covariate model + age
$CL_{\text{gemcitabine}}$ (L/h)	224 [211-242]	224 [210-239]	219 [206-235]	220 [207-235]
$Vc_{\text{gemcitabine}}$ (L)	47.9 [42.9-53.0]	43.4 [39.6-47.8]	46.2 [41.9-50.6]	43.9 [39.5-49.4]
Effect of age <sup>a</sup>		1.42 [1.16-1.73]		1.20 [0.965-1.46]
$Vp_{\text{gemcitabine}}$ (L)	76.3 [62.6-90.7]	73.1 [58.8-89.6]	76.4 [63.9-91.4]	75.1 [64.7-90.7]
$Q_{\text{gemcitabine}}$ (L/h)	7.28 [6.44-8.19]	7.09 [6.01-8.16]	7.25 [6.33-8.20]	7.14 [6.40-8.06]
$CL_{\text{dFdU}}/fm$ (L/h)	6.20 [5.83-6.62]	6.20 [5.79-6.66]		
$CL_{\text{dFdU,non-renal}}/fm$ (L/h)			7.03 [6.36-7.72]	7.02 [6.26-7.90]
$CL_{\text{dFdU,renal}}/fm$ (mL/h)			0.09 [0.07-0.11]	0.09 [0.07-0.11]
Effect of gender			0.809 [0.722-0.909]	0.810 [0.705-0.932]
$Vc_{\text{dFdU}}/fm$ (L)	27.1 [25.0-29.4]	26.6 [24.2-28.8]	28.7 [26.0-31.5]	28.2 [25.7-30.7]
Effect of NSCLC			1.01 [0.889-1.14]	1.02 [0.917-1.13]
Effect of gender			0.813 [0.722-0.901]	0.821 [0.730-0.916]
$Vp_{\text{dFdU}}/fm$ (L)	59.7 [55.4-64.0]	59.7 [56.1-64.4]	58.5 [54.7-62.8]	58.4 [54.3-62.9]
$Q_{\text{dFdU}}/fm$ (L/h)	27.5 [23.6-32.0]	27.3 [23.5-32.1]	26.6 [23.0-31.3]	26.7 [23.1-31.4]
<b>Interindividual variability</b>				
$CL_{\text{gemcitabine}}$	37.4 [32.1-41.3]	36.8 [31.4-40.2]	36.8 [31.3-39.7]	36.3 [30.9-39.9]
$Vc_{\text{gemcitabine}}$	62.0 [50.5-64.0]	59.6 [49.4-62.7]	63.3 [51.8-65.8]	62.3 [50.9-65.0]
$Vp_{\text{gemcitabine}}$	27.5 [4.88-49.7]	29.2 [9.81-52.0]	24.8 [11.2-34.6]	24.8 [10.4-36.6]
$Q_{\text{gemcitabine}}$	32.3 [22.2-40.5]	33.8 [23.3-41.1]	32.1 [21.0-39.6]	32.0 [21.5-40.2]
$CL_{\text{dFdU}}/fm$	33.1 [27.3-37.8]	33.1 [27.6-37.4]	30.3 [25.7-33.6]	30.3 [25.6-33.3]
$Vc_{\text{dFdU}}/fm$	41.4 [34.6-45.5]	41.1 [34.4-45.3]	35.7 [30.1-40.1]	36.2 [30.6-40.2]
$Vp_{\text{dFdU}}/fm$	32.4 [25.3-38.5]	32.4 [25.4-39.1]	26.2 [20.5-21.1]	26.1 [19.8-32.3]
Imputed weight <sup>b</sup>			23.1 [13.8-30.0]	23.1 [13.2-32.3]
Imputed CrCl <sup>b</sup>			32.4 [10.5-49.7]	32.4 [10.6-44.1]
<b>Residual variability</b>				
Prop. error gemcitabine	43.5 [38.3-45.3]	43.6 [38.5-45.1]	43.2 [38.8-44.1]	43.3 [39.4-43.9]
Prop. error dFdU	20.4 [18.8-21.5]	20.3 [18.8-21.6]	20.3 [19.0-21.1]	20.3 [19.0-21.2]

<sup>a</sup> as categorical covariate. <sup>b</sup> in case of missing data (n = 15).

$CL_{\text{gemcitabine}}$ : clearance of gemcitabine,  $Vc_{\text{gemcitabine}}$ : volume of distribution of the central compartment of gemcitabine,  $Vp_{\text{gemcitabine}}$ : volume of distribution of the peripheral compartment of gemcitabine,  $Q_{\text{gemcitabine}}$ : intercompartmental clearance of gemcitabine,  $CL_{\text{dFdU}}/fm$ : apparent clearance of dFdU,  $Vc_{\text{dFdU}}/fm$ : apparent volume of distribution of the central compartment of dFdU, NSCLC: non-small cell lung cancer,  $Vp_{\text{dFdU}}/fm$ : apparent volume of distribution of the peripheral compartment of dFdU,  $Q_{\text{dFdU}}/fm$ : apparent intercompartmental clearance of dFdU, CrCl: creatinine clearance, Prop. error: proportional residual error

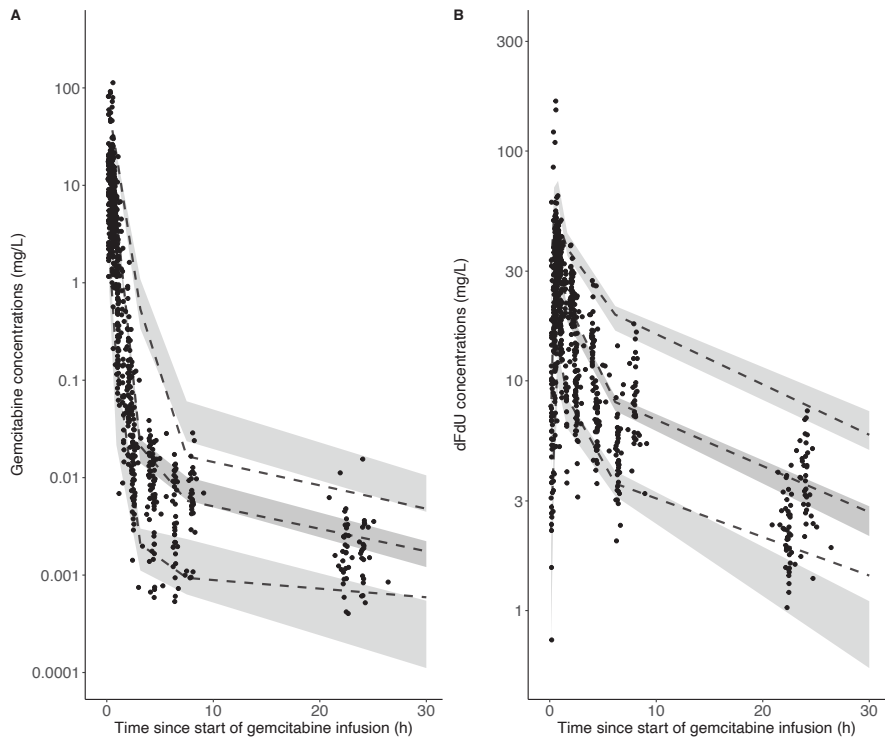


Figure 2. Visual predictive check of the covariate model (with age) with  $n = 1,000$ . A) for gemcitabine and B) for dFdU. Concentrations of gemcitabine and dFdU are presented on a logarithmic scale. The dashed black lines represent the 5<sup>th</sup>, 50<sup>th</sup> and 95<sup>th</sup> percentile of the observed concentrations. The 95% confidence intervals of these percentiles are presented by the gray areas.

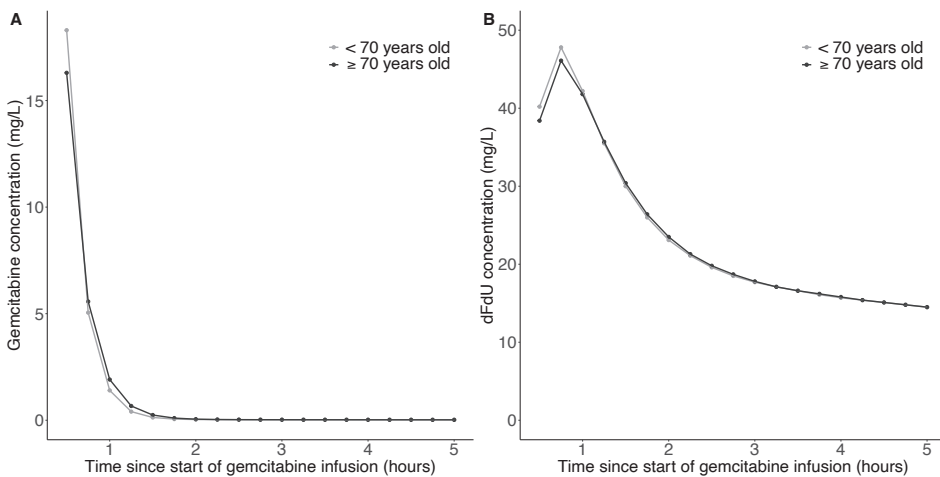


Figure 3. Simulated concentration-time curves of the covariate model including age, for gemcitabine (A) and dFdU (B). The typical curve for patients < 70 years (gray line) and  $\geq 70$  years (black line) are depicted.

## DISCUSSION

In this population pharmacokinetic analysis of gemcitabine and dFdU, a non-significant 20% higher  $V_{c_{\text{gemcitabine}}}$  in patients  $\geq 70$  years old was found. The resulting concentration-time curves of the typical patient only differ marginally and indicate a similar exposure of gemcitabine and dFdU in both age groups. Altogether, the effect of age is considered to have no clinical relevance on the pharmacokinetic exposure of gemcitabine.

Gemcitabine is a hydrophilic drug, indicating that its  $V_c$  is limited to the total body water of the patient. Indeed, our observed values for  $V_{c_{\text{gemcitabine}}}$  correspond to reported values for total body water.<sup>21, 22</sup> In elderly, a decrease in total body water has been observed, hence, we expected a decrease in  $V_{c_{\text{gemcitabine}}}$  with increasing age.<sup>8</sup> Surprisingly, in the base model, we found that patients  $\geq 70$  years had an increase in  $V_{c_{\text{gemcitabine}}}$ . This statistically significant effect vanished with the introduction of known covariates (such as allometric scaling) on the pharmacokinetics of gemcitabine and dFdU. In the cohort with patients  $\geq 70$  years, a statistically significant higher body weight was observed when compared to patients  $< 70$  years. Since total body water is closely related to the total body weight of a person, this might indicate that the initial observed effect of age on  $V_{c_{\text{gemcitabine}}}$  was confounded by this covariate.<sup>21, 22</sup>

Although solid knowledge is lacking, it has been postulated that the expression of hENT is a predictor for efficacy of gemcitabine.<sup>23, 24</sup> Moreover, altered pharmacokinetics of gemcitabine have been associated with the safety of therapy.<sup>9</sup> Since age-related degradation of enzyme complexes have been described, hENT might be less functional in the elderly population, potentially jeopardizing the safety and efficacy of gemcitabine therapy.<sup>25, 26</sup> Activity of hENT might be reflected in the  $Q$  of both gemcitabine and dFdU as this may be the rate limiting step in the distribution between the central and peripheral compartment.<sup>27</sup> Therefore, we assessed the impact of age on  $Q$  of both gemcitabine and dFdU.  $V_p$  and  $Q$  are parameters which can only be derived from pharmacokinetic curves including the terminal distribution phase and can, therefore, be difficult to assess using a limited sampling strategy. Gemcitabine is a drug with a rapid distribution and elimination, and therefore, samples drawn even shortly after infusion are informative for this distribution part. In this study, we found that age had no statistically significant effect on  $V_p$  and  $Q$  of gemcitabine. Since both dFdU and gemcitabine are transported by hENT<sup>27</sup>, we expect that the absent effect of age on  $V_p$  and  $Q$  of gemcitabine can be extrapolated to dFdU.

To our knowledge, this is the first study to prospectively evaluate the impact of age on the parent-metabolite pharmacokinetics of gemcitabine. Nonetheless, the effect of age on the pharmacodynamics of this chemotherapeutic agent has been previously described. In pancreatic cancer patients, it has been shown that therapy with gemcitabine and nanoparticle albumin-bound paclitaxel in elderly patients ( $\geq 70$  years old) has no influence on the efficacy when compared to non-elderly patients ( $< 70$  years), while it has been reported that elderly patients experienced a statistically significant increase in grade 3 or 4 neutropenia.<sup>10</sup> Other studies confirmed the increase in hematological toxicity in elderly<sup>28</sup>, although contradicting studies also have been reported.<sup>29-31</sup>



Our study revealed that implementation of age-based dosing based on pharmacokinetic considerations is not rational. It is likely, that the reported increase in hematological toxicities can be ascribed to exposure-unrelated sensitivity which may come from a lower recovery capacity for hematological parameters or the age-related diminishing of the bone marrow reserve.<sup>32</sup>

In our study we used a threshold of 70 years to classify patients in the non-elderly and elderly study cohort based on earlier literature stating that patients  $\geq 70$  years have an increased risk of chemotherapeutic-induced hematological toxicities.<sup>32</sup> However, it has been reported that frailty is a better predictor for the development of toxicities and age is merely a surrogate marker for frailty.<sup>33</sup> In our study, we did not classify patients based on their frailty score, however, to include frail patients, we kept the inclusion criteria as broad as possible. Obviously, still a selection bias will be introduced, since, only patients who were considered fit for therapy were included in the analysis. However, since our goal was to assess if the current dosing in gemcitabine-receiving elderly population needs to be adjusted, we feel that the use of age to divide the population is justified.

In summary, this study shows no age-related effects on the pharmacokinetics of gemcitabine and does not justify the need for dose adjustments based on pharmacokinetic considerations in elderly. Therefore, dosing according to the drug label is recommended for the current elderly population, qualified for gemcitabine therapy.

## REFERENCES

1. National Cancer Institute. Age and cancer risk. Available via <http://www.cancer.gov>. Accessed on 20 Oct 2021.
2. van Marum RJ. Underrepresentation of the elderly in clinical trials, time for action. *Br J Clin Pharmacol*. 2020;86(10):2014-2016. <https://doi.org/10.1111/bcp.14539>.
3. Ruiters R, Burggraaf J, Rissmann R. Under-representation of elderly in clinical trials: An analysis of the initial approval documents in the Food and Drug Administration database. *Br J Clin Pharmacol*. 2019;85(4):838-844. <https://doi.org/10.1111/bcp.13876>.
4. Lucas C, Byles J, Martin JH. Medicines optimisation in older people: Taking age and sex into account. *Maturitas*. 2016;93:114-120. <https://doi.org/10.1016/j.maturitas.2016.06.021>.
5. European Medicines Agency. Gemzar: Summary of product characteristics.
6. Mini E, Nobili S, Caciagli B, Landini I, Mazzei T. Cellular pharmacology of gemcitabine. *Ann Oncol*. 2006;17 Suppl 5:v7-12. <https://doi.org/10.1093/annonc/mdj941>.
7. Veltkamp SA, Pluim D, van Eindhoven MAJ, Bolijn MJ, Ong FHG, Govindarajan R, et al. New insights into the pharmacology and cytotoxicity of gemcitabine and 2',2'-difluorodeoxyuridine. *Mol Cancer Ther*. 2008;7(8):2415-2425. <https://doi.org/10.1158/1535-7163.Mct-08-0137>.
8. Klotz U. Pharmacokinetics and drug metabolism in the elderly. *Drug Metab Rev*. 2009;41(2):67-76. <https://doi.org/10.1080/03602530902722679>.
9. Leijen S, Veltkamp SA, Huitema AD, van Werkhoven E, Beijnen JH, Schellens JH. Phase I dose-escalation study and population pharmacokinetic analysis of fixed dose rate gemcitabine plus carboplatin as second-line therapy in patients with ovarian cancer. *Gynecol Oncol*. 2013;130(3):511-517. <https://doi.org/10.1016/j.ygyno.2013.05.001>.
10. Li X, Huang DB, Zhang Q, Guo CX, Fu QH, Zhang XC, et al. The efficacy and toxicity of chemotherapy in the elderly with advanced pancreatic cancer. *Pancreatol*. 2020;20(1):95-100. <https://doi.org/10.1016/j.pan.2019.11.012>.
11. Kirstein MN, Hassan I, Guire DE, Weller DR, Dagit JW, Fisher JE, et al. High-performance liquid chromatographic method for the determination of gemcitabine and 2',2'-difluorodeoxyuridine in plasma and tissue culture media. *Journal of Chromatography B*. 2006;835(1):136-142. <https://doi.org/10.1016/j.jchromb.2006.03.023>.
12. Vainchtein LD, Rosing H, Thijssen B, Schellens JH, Beijnen JH. Validated assay for the simultaneous determination of the anti-cancer agent gemcitabine and its metabolite 2',2'-difluorodeoxyuridine in human plasma by high-performance liquid chromatography with tandem mass spectrometry. *Rapid Commun Mass Spectrom*. 2007;21(14):2312-2322. <https://doi.org/10.1002/rcm.3096>.
13. van der Noll R, Smit WM, Wymenga AN, Boss DS, Grob M, Huitema AD, et al. Phase I and pharmacological trial of lapatinib in combination with gemcitabine in patients with advanced breast cancer. *Invest New Drugs*. 2015;33(6):1197-1205. <https://doi.org/10.1007/s10637-015-0281-z>.
14. Joerger M, Burgers JA, Baas P, Doodeman VD, Smits PH, Jansen RS, et al. Gene polymorphisms, pharmacokinetics, and hematological toxicity in advanced non-small-cell lung cancer patients receiving cisplatin/gemcitabine. *Cancer Chemother Pharmacol*. 2012;69(1):25-33. <https://doi.org/10.1007/s00280-011-1670-4>.
15. Van der Noll R, Schellens JHM, Beijnen JH. Safety, pharmacokinetics and preliminary anti-tumor activity of novel (combinations of) targeted anti-cancer drugs. The Netherlands: Utrecht University; 2014.
16. Caffo O, Fallani S, Marangon E, Nobili S, Cassetta MI, Murgia V, et al. Pharmacokinetic study of gemcitabine, given as prolonged infusion at fixed dose rate, in combination with cisplatin in patients with advanced non-small-cell lung cancer. *Cancer Chemother Pharmacol*. 2010;65(6):1197-1202. <https://doi.org/10.1007/s00280-010-1255-7>.
17. Sugiyama E, Kaniwa N, Kim S-R, Hasegawa R, Saito Y, Ueno H, et al. Population pharmacokinetics of gemcitabine and its metabolite in Japanese cancer patients. *Clin Pharmacokinet*. 2010;49(8):549-558. <https://doi.org/10.2165/11532970-000000000-00000>.
18. Jiang X, Galetti P, Links M, Mitchell PL, McLachlan AJ. Population pharmacokinetics of gemcitabine and its metabolite in patients with cancer: effect of oxaliplatin and infusion rate. *Br J Clin Pharmacol*. 2008;65(3):326-333. <https://doi.org/10.1111/j.1365-2125.2007.03040.x>.
19. Cockcroft DW, Gault MH. Prediction of creatinine clearance from serum creatinine. *Nephron*. 1976;16(1):31-41. <https://doi.org/10.1159/000180580>.

20. Dosne AG, Bergstrand M, Harling K, Karlsson MO. Improving the estimation of parameter uncertainty distributions in nonlinear mixed effects models using sampling importance resampling. *J Pharmacokinet Pharmacodyn*. 2016;43(6):583-596. <https://doi.org/10.1007/s10928-016-9487-8>.
21. Serra-Prat M, Lorenzo I, Palomera E, Ramirez S, Yébenes JC. Total body water and intracellular water relationships with muscle strength, frailty and functional performance in an elderly population. A cross-sectional study. *J Nutr Health Aging*. 2019;23(1):96-101. <https://doi.org/10.1007/s12603-018-1129-y>.
22. Steele JM, Berger EY, Dunning MF, Brodie BB. Total body water in man. *American Journal of Physiology-Legacy Content*. 1950;162(2):313-317. <https://doi.org/10.1152/ajplegacy.1950.162.2.313>.
23. Nordh S, Ansari D, Andersson R. hENT1 expression is predictive of gemcitabine outcome in pancreatic cancer: a systematic review. *World J Gastroenterol*. 2014;20(26):8482-8490. <https://doi.org/10.3748/wjg.v20.i26.8482>.
24. Santini D, Perrone G, Vincenzi B, Lai R, Cass C, Alloni R, et al. Human equilibrative nucleoside transporter 1 (hENT1) protein is associated with short survival in resected ampullary cancer. *Ann Oncol*. 2008;19(4):724-728. <https://doi.org/10.1093/annonc/mdm576>.
25. Shi S, Klotz U. Age-related changes in pharmacokinetics. *Curr Drug Metab*. 2011;12(7):601-610. <https://doi.org/10.2174/138920011796504527>.
26. Rattanacheworn P, Kerr SJ, Kittanamongkolchai W, Townamchai N, Udomkarnjananun S, Praditpornsilpa K, et al. Quantification of CYP3A and drug transporters activity in healthy young, healthy elderly and chronic kidney disease elderly patients by a microdose cocktail approach. *Front Pharmacol*. 2021;12(2501). <https://doi.org/10.3389/fphar.2021.726669>.
27. Hodge LS, Taub ME, Tracy TS. The deaminated metabolite of gemcitabine, 2',2'-difluorodeoxyuridine, modulates the rate of gemcitabine transport and intracellular phosphorylation via deoxycytidine kinase. *Drug Metab Dispos*. 2011;39(11):2013-2016. <https://doi.org/10.1124/dmd.111.040790>.
28. Secen N, Sazdanic-Velikić D, Bursac D, Mendebaba B, Tepavac A, Popovic G, et al. Hematological toxicity associated with gemcitabine/cisplatin in elderly non-small cell lung cancer patients. *Eur Respir J*. 2011;38(Suppl 55):p2773.
29. Ishimoto U, Kinoshita A, Hirose Y, Shibata K, Ishii A, Shoji R, et al. The efficacy and safety of nab paclitaxel plus gemcitabine in elderly patients over 75 years with unresectable pancreatic cancer compared with younger patients. *Cancer Chemother Pharmacol*. 2019;84(3):647-654. <https://doi.org/10.1007/s00280-019-03895-2>.
30. Ventriglia J, Laterza MM, Savastano B, Petrillo A, Tirino G, Pompella L, et al. Safety and efficacy of gemcitabine/nabpaclitaxel in elderly patients with metastatic or locally advanced pancreatic adenocarcinoma: a retrospective analysis. *Ann Oncol*. 2017;28:v259. <https://doi.org/10.1093/annonc/mdx369.139>.
31. Crombag MBS, de Vries Schultink AHM, Schellens JHM, Beijnen JH, Huitema ADR. Incidence of hematologic toxicity in older adults treated with gemcitabine or a gemcitabine-containing regimen in routine clinical practice: A multicenter retrospective cohort study. *Drugs Aging*. 2014;31(10):737-747. <https://doi.org/10.1007/s40266-014-0207-z>.
32. Sehl M, Sawhney R, Naeim A. Physiologic aspects of aging: impact on cancer management and decision making, part II. *Cancer J*. 2005;11(6):461-473. <https://doi.org/10.1097/00130404-200511000-00005>.
33. Runzer-Colmenares FM, Urrunaga-Pastor D, Roca-Moscoso MA, De Noriega J, Rosas-Carrasco O, Parodi JF. Frailty and vulnerability as predictors of chemotherapy toxicity in older adults: A longitudinal study in Peru. *J Nutr Health Aging*. 2020;24(9):966-972. <https://doi.org/10.1007/s12603-020-1404-6>.



# PART 4



# EXPOSURE-RESPONSE RELATIONSHIPS

# CHAPTER 4.1

# Exposure-response analysis of osimertinib in EGFR mutation positive non-small cell lung cancer patients in a real-life setting

*Submitted*

René J. Boosman\*  
Merel Jebbink\*  
Wouter B. Veldhuis  
Stefanie L. Groenland  
Bianca A.M.H. van Veggel  
Pim Moeskops  
Adrianus J. de Langen  
Jos H. Beijnen  
Egbert F. Smit  
Alwin D.R. Huitema  
Neeltje Steeghs

\*these authors contributed equally and thus share first authorship

Author's contribution: R.J. Boosman and M. Jebbink contributed to the design of this study performed the data management. R.J. Boosman conducted the data analysis, wrote the first draft of the manuscript and edited the contribution of the co-authors on this manuscript.



# ABSTRACT

## Introduction

Osimertinib, an irreversible inhibitor of the epidermal growth factor receptor (EGFR) is an important drug in the treatment of EGFR-mutation positive non-small cell lung cancer (NSCLC). Clinical trials with osimertinib could not demonstrate an exposure-efficacy relationship, while a relationship between exposure and toxicity has been found. In this study, we report the exposure-response relationships of osimertinib in a real-life setting.

## Methods

A retrospective observational cohort study was performed, including all patients receiving 40-80 mg osimertinib as second-line therapy and from whom pharmacokinetic samples were collected during routine care. Trough plasma concentrations ( $C_{\min, \text{pred}}$ ) were estimated and used as a measure of osimertinib exposure. A previously defined exploratory pharmacokinetic threshold of 166  $\mu\text{g/L}$  was taken to explore the exposure-efficacy relationship.

## Results

A total of 145 NSCLC patients and 513 osimertinib plasma concentration samples were included. Median progression free survival (PFS) was 13.3 (95% confidence interval (CI): 10.3-19.1) months and 9.3 (95% CI: 7.2-11.1) months for patients with  $C_{\min, \text{pred}} < 166 \mu\text{g/L}$  and  $C_{\min, \text{pred}} \geq 166 \mu\text{g/L}$ , respectively ( $p = 0.03$ ). In the multivariate analysis, a  $C_{\min, \text{pred}} < 166 \mu\text{g/L}$  resulted in a non-statistically significant hazard ratio of 0.65 (95% CI: 0.42-1.02;  $p = 0.06$ ). Presence of a EGFR driver-mutation other than the exon 19 del or L858R mutations, led to a shorter PFS with a hazard ratio of 2.46 (95% CI: 1.20-5.03;  $p = 0.01$ ). No relationship between exposure and toxicity was observed ( $p = 0.91$ ).

## Conclusion

In our real-life cohort, no exposure-response relationship was observed for osimertinib in the current dosing scheme. The feasibility of a standard lower fixed dosing of osimertinib in clinical practice should be studied prospectively.

## INTRODUCTION

Mutations in the epidermal growth factor receptor (EGFR) are frequently observed to be an oncogenic driver for the development of non-small cell lung cancer (NSCLC).<sup>1, 2</sup> Several tyrosine kinase inhibitors targeting the intracellular domain of the receptor have shown to result in a significant improvement in progression free survival (PFS) and overall survival (OS).<sup>2-4</sup> The development of secondary driver mutations, most commonly the T790M mutation, drove the development of the third generation EGFR TKI of which osimertinib is currently approved by the EMA.<sup>5</sup> Osimertinib is mutant-selective TKI, having higher affinity for EGFR-mutant tyrosine kinase and less affinity for the wild type variant. Presently, based on the FLAURA trial, osimertinib is the preferred first line treatment option in patients with EGFR mutation positive (EGFRm+) NSCLC.<sup>6</sup>

Osimertinib is dosed in a fixed oral dose of 80 mg once daily (QD).<sup>5, 7</sup> It is reported that the between-subject variability in pharmacokinetic (PK) exposure of osimertinib is high, ranging from 20-78% in a clinical trial population.<sup>7</sup> Furthermore, the exposure of osimertinib was not associated with efficacy, nevertheless a relationship between exposure and the development of toxicity was observed.<sup>8</sup> In addition, it is becoming increasingly evident that sarcopenia is an important predictor for both drug exposure and treatment outcome.<sup>9, 10</sup> In general, patients in clinical practice tend to be more heterogeneous when compared to a standardized clinical trial population.<sup>11</sup> This urges confirmation of the observed treatment outcomes in a real-world setting, which has not yet been performed. Therefore, we set out to investigate the exposure-efficacy, exposure-toxicity and muscle mass-response relationships for patients receiving osimertinib in a real-life setting.

## METHODS

### Patients

A retrospective observational study was performed. Between January 2016 and November 2019 patients receiving osimertinib treatment starting at 40-80 mg QD in the Antoni van Leeuwenhoek Hospital (Amsterdam, The Netherlands) and of whom osimertinib plasma samples were drawn for routine care were included. Data on patient characteristics, including demographic characteristics, prior treatment lines, tumor characteristics, osimertinib dose, treatment toxicity and PFS were retrospectively collected from patient records. At treatment initiation, radiological imaging was performed twice every six weeks, followed by every 12 weeks.

### Objectives

The primary objective of the study was to investigate whether the exposure to osimertinib in patients with NSCLC is related to efficacy. The secondary objectives were to study the relationship between osimertinib exposure and toxicity and the influence of (baseline) covariates on the efficacy of osimertinib. Covariates tested included gender, age, body mass index (BMI), World Health Organization Performance Status (WHO PS), primary EGFR driver mutation, smoking status (never (0-100 cigarettes)/ever (stopped > 100 cigarettes)/current (> 100 cigarettes)<sup>12</sup>), the number

of previous lines of treatment, and sarcopenia. The endpoint for efficacy was defined as the PFS for osimertinib-treated patients. A predefined, exploratory pharmacokinetic threshold (based on the geometric mean reported by the Food and Drug Administration (FDA)) of 166 µg/L was used for the exposure-efficacy analyses.<sup>7,13</sup>

#### Calculation of osimertinib trough concentrations

As routine measurement, osimertinib plasma samples were collected during patient visits to the outpatient clinic of the Antoni van Leeuwenhoek hospital. To calculate the time after osimertinib dose (TAD), the date and time of both the previous osimertinib intake and the blood sampling were recorded. Osimertinib plasma concentrations were determined using a validated liquid chromatography-tandem mass spectrometry assay.<sup>14</sup> Predicted trough concentrations ( $C_{min,pred}$ ) of osimertinib were approximated using the log-linear calculation using an earlier proposed algorithm<sup>15</sup>:

$$C_{min,pred} = C_{measured} * 0.5^{\frac{24-TAD}{t_{1/2}}}$$

Where  $C_{measured}$  is the measured plasma concentration of osimertinib and  $t_{1/2}$  is the average elimination half-life of osimertinib (48 hours<sup>7</sup>). Samples were excluded from the analysis if they were drawn: 1) before steady-state concentration of osimertinib was reached (240 hours after start of osimertinib therapy), 2) with a TAD exceeding the half-life of osimertinib or 3) during osimertinib therapy beyond disease progression.

#### Exposure-efficacy and -toxicity analysis

Efficacy of treatment in patients with a median  $C_{min,pred} < 166$  µg/L was compared to efficacy in patients with a median  $C_{min,pred}$  above this threshold. Patients who did not show progression prior to the final pharmacodynamic cut-off date, were censored. Covariates were included based upon univariable Cox regression analyses. Toxicity analysis was performed by comparing the median  $C_{min,pred}$  between patients with and without clinically relevant toxicities. These toxicities were defined as toxicities, which led to dose reductions, treatment interruptions or treatment discontinuations (at the discretion of the treating physician).

#### Measurement of sarcopenia

Indices for skeletal muscle mass and sarcopenia were calculated based on computed tomography (CT)-scans of the third lumbar vertebrae (L3). Slice selection, segmentation and quantification of the adipose and muscle tissue was performed using Quantib Body Composition version 0.2.1 (Quantib BV, Rotterdam, The Netherlands).<sup>16</sup> A threshold of  $> -15$  Hounsfield units (HU) was set to exclude for intramuscular fat. Individual scans at baseline of therapy were reviewed on completeness and if necessary manually corrected. For diagnosing sarcopenia, the skeletal muscle mass index (SMI) was calculated as the sum of the delineated areas of the abdominal, psoas and erector spinae muscles divided by the squared height of the individual patient. Based on the findings of Martin *et al.* in patients with cancer, the following cut-off values for sarcopenia were used<sup>17</sup>:

- Males and BMI  $\geq 25$  kg/m<sup>2</sup>: SMI  $< 53.0$  cm<sup>2</sup>/m<sup>2</sup>
- Males and BMI  $< 25$  kg/m<sup>2</sup>: SMI  $< 43.0$  cm<sup>2</sup>/m<sup>2</sup>
- Females: SMI  $< 41.0$  cm<sup>2</sup>/m<sup>2</sup>

The influence of sarcopenia on the efficacy, toxicity and pharmacokinetics of osimertinib was examined.

### Statistical analysis

Statistical significant differences between the patient characteristics in both groups were assessed with a Chi-squared test, Fisher exact test or t-test when appropriate, a  $p$ -value  $< 0.05$  was considered to be statistical significant. Statistical analyses were performed using R version 3.4.3 (R-project, Vienna, Austria).

### Ethics

The institutional review board authorized this study on July 19, 2019. The need for a written informed consent was waived as all data were collected as part of routine clinical care.

## RESULTS

A total of 145 patients treated with osimertinib between 2016 and 2019 were included. Table 1 provides an overview of the baseline characteristics. A total of 513 osimertinib plasma concentrations were available, with a median of three samples per patient (range: 1-18 samples). The median trough concentration in the total patient population was 211  $\mu\text{g/L}$  (range: 74.5-826  $\mu\text{g/L}$ ). Overall, 34 patients (23.4%) had a median  $C_{\text{min,pred}} < 166$   $\mu\text{g/L}$ . These patients were found to have a better performance status than patients with  $C_{\text{min,pred}} \geq 166$   $\mu\text{g/L}$  ( $p = 0.034$ ). No other statistically significant differences were observed in the baseline characteristics of the included patients. An inpatient pharmacokinetic variability of 20.8% and an interpatient variability of 37.5% were calculated for the standard dose of 80 mg osimertinib QD.

### Exposure-efficacy analysis

On the final pharmacodynamic data cut-off date (September 1<sup>st</sup>, 2021) 21 patients were still on treatment with osimertinib, of which 14 patients were treated beyond progression. The median follow-up time was 21 months (range: 2.3-80 months), with a median treatment time of 16 months (range 1.4-80 months). Progression occurred in 135 (93.1%) patients with a median PFS of 10.2 months (range: 1.3 -64.6 months). In total, 31 patients (91.2%) in the cohort with a  $C_{\text{min,pred}} < 166$   $\mu\text{g/L}$  and 104 patients (93.7%) in the cohort with a median  $C_{\text{min,pred}} \geq 166$   $\mu\text{g/L}$  were found to have progressed during osimertinib therapy. The Kaplan-Meier curve for the PFS is depicted in Figure 1. The median PFS in the  $C_{\text{min,pred}} < 166$   $\mu\text{g/L}$  was 13.3 months (95% CI: 10.3-19.1 months), while a median PFS of 9.3 months (95% CI: 7.2-11.1 months) was observed for the  $C_{\text{min,pred}} \geq 166$   $\mu\text{g/L}$  ( $p = 0.03$ ). Table 2 and 3 show the univariable and multivariable Cox regression analysis on the PFS, respectively. The presence of brain metastases prior to osimertinib therapy, the primary EGFR

mutation and the number of previous lines of treatment were found to result in a statistically significant higher hazard ratio. In the multivariable analysis, a  $C_{\min, \text{pred}} \geq 166 \mu\text{g/L}$  was not statistically significant associated with a lower PFS and only a driver mutation other than the exon 19del and exon 21L858R is found to be of statistically significant influence on the PFS with a hazard ratio of 2.458 (95% CI: 1.202-5.028).

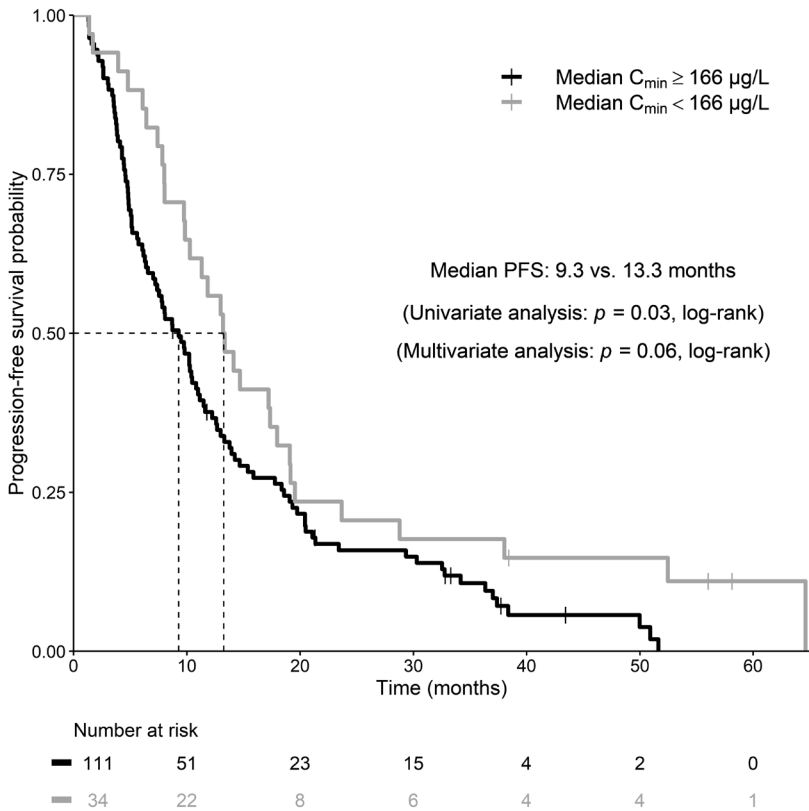


Figure 1. Kaplan-Meier curve of PFS in patients treated with osimertinib in patients with median  $C_{\min, \text{pred}}$  below the population median of  $166 \mu\text{g/L}$  (gray line) and in patients with a median osimertinib  $C_{\min, \text{pred}} \geq 166 \mu\text{g/L}$  (black line). The dotted line represents the median PFS (in months).  $C_{\min}$ : trough plasma concentration; PFS: progression free survival.

Table 1. Baseline characteristics of the study population. Values are presented as numbers (percentages) or medians [ranges], as appropriate.

	Median C <sub>min,pred</sub> < 166ng/mL (n = 34)	Median C <sub>min,pred</sub> ≥ 166ng/mL (n = 111)	p-value	Total (n = 145)
<b>Gender, male</b>	11 (32.4%)	26 (23.4%)	0.412	37 (25.5%)
<b>Age at treatment initiation (years)</b>	61 [31-88]	66 [42-86]	0.082	64 [31-88]
<b>Primary EGFR mutation</b>				
Exon 19 del	21 (61.8%)	61 (55.0%)	0.075	82 (56.6%)
Exon 19 del + other	0	2 (1.8%)		2 (1.4%)
Exon 21 L858R	11 (32.4%)	37 (33.3%)		48 (33.1%)
Exon 21 L858R + other	0	1 (0.9%)		1 (0.7%)
Other	0	10 (9.0%)		10 (6.9%)
Unknown	2 (5.9%)	0		2 (1.4%)
<b>Smoking status</b>				
Never smoked	17 (50.0%)	77 (69.4%)	0.066	94 (64.8%)
Current or former smoker	17 (50.0%)	33 (29.7%)		50 (34.5%)
Unknown		1 (0.9%)		1 (0.7%)
<b>BMI (kg/m<sup>2</sup>)</b>	24.2 [19.8-40.5]	24.2 [17.9-37.3]	0.519	24.2 [17.9-40.5]
<b>Tumor stage</b>				
IIIa	3 (8.8%)	5 (4.5%)	0.595	8 (5.5%)
IIIb	1 (2.9%)	5 (4.5%)		6 (4.1%)
IV	30 (88.2%)	101 (91.0%)		131 (90.3%)
<b>Central nervous system metastasis at osimertinib treatment initiation, yes</b>				
	7 (20.6%)	38 (34.2%)	0.242	45 (31.0%)
<b>Previous lines of therapy</b>				
1	18 (52.9%)	55 (49.5%)	0.706	73 (50.3%)
> 1	16 (47.1%)	56 (50.5%)		72 (49.7%)
<b>Osimertinib dose</b>				
40 mg QD	0	1 (0.9%)	0.766	1 (0.7%)
80 mg QD	34 (100%)	110 (99.1%)		144 (99.3%)
<b>WHO performance status</b>				
0	20 (58.8%)	45 (40.5%)	0.034	65 (44.8%)
1	14 (41.2%)	48 (43.2%)		62 (42.8%)
2	0	16 (14.4%)		16 (11.0%)
3	0	2 (1.8%)		2 (1.4%)

BMI: body-mass index, C<sub>min,pred</sub>: predicted osimertinib trough concentration, EGFR: epidermal growth factor receptor, QD: once daily, WHO: World Health Organization

Table 2. Univariable Cox regression analysis on PFS.

Variable	Hazard ratio	95% confidence interval	p-value
<b>Gender</b> , female	0.709	0.478-1.051	0.087
<b>Age</b>	0.995	0.981-1.010	0.501
<b>Smoking status</b> , never	0.854	0.598-1.221	0.387
<b>BMI</b>	0.984	0.939-1.032	0.508
<b>Stage</b> , IV	1.023	0.563-1.859	0.941
<b>Brain metastases</b> , yes	1.474	1.019-2.132	0.039
<b>Primary EGFR mutation (relative to exon 19 del)</b>			
Exon 21L858R	1.292	0.892-1.870	0.176
Other	4.129	2.072-8.227	0.00005
Exon 19 del + other	0.682	0.164-2.837	0.599
Exon 21 L858R + other	4.189	0.569-30.83	0.160
Unknown	0.281	0.039-2.057	0.212
<b>WHO performance status</b>	1.185	0.937-1.501	0.157
<b>No. of previous lines of treatment</b>	1.180	1.025-1.358	0.021
<b>Median osimertinib C<sub>min,pred</sub> &lt; 166 µg/L</b>	0.629	0.414-0.955	0.030

BMI: body-mass index, C<sub>min,pred</sub>: predicted osimertinib trough concentration, EGFR: epidermal growth factor receptor, QD: once daily, WHO: World Health Organization

Table 3. Multivariable Cox regression analysis on PFS.

Variable	Hazard ratio	95% confidence interval	p-value
<b>Gender</b> , female	0.713	0.458-1.109	0.133
<b>Mutation</b> , other	2.458	1.202-5.028	0.014
<b>Brain metastasis</b>	1.417	0.960-2.093	0.079
<b>No. of previous lines</b>	1.162	0.998-1.353	0.053
<b>Median osimertinib C<sub>min,pred</sub> &lt; 166 µg/L</b>	0.652	0.417-1.019	0.060

C<sub>min,pred</sub>: predicted osimertinib trough concentration

### Exposure-toxicity analysis

In total, 33 patients experienced a clinically relevant toxicity during osimertinib treatment. The development of these toxicities led to dose reductions (n = 25), treatment interruptions (n = 13) and/or treatment discontinuation (n = 4). Toxicities included gastrointestinal disorders (n = 12), skin disorders (n = 9), fatigue (n = 3), decrease in renal function (n = 4), muscle pain/weakness (n = 3), ocular toxicities (n = 3), pneumonitis (n = 2), increase in liver enzymes (ALAT/ASAT) (n = 2), cardiac toxicity (n = 2) and paronychia (n = 1). In 24 patients, these toxicities were observed after the collection of ≥ 1 PK sample. The median osimertinib C<sub>min,pred</sub> of these patients before the observation of these toxicities was 207 µg/L (range: 121-433 µg/L) compared to 213 µg/L (range: 96.9-826 µg/L) in patients who did not experience any clinically relevant toxicity (p = 0.909).

Measurement of sarcopenia

Complete CT-scans including the L3 area were available for 122 (84.1%) patients. The median time between CT-scan and start of osimertinib therapy was 29.0 (± 42.3) days. Sarcopenia was present in 93 patients (76.2%). In Figure 2, the Kaplan-Meier curve in relation to the PFS in these patients is depicted. No statistically significant difference in PFS between patients with and without sarcopenia was observed (median PFS: 10.3 (95% CI: 8.7-13.0) months vs 7.8 (95% CI: 4.9-14.2) months, respectively,  $p = 0.129$ ). Moreover, no relationship between the pharmacokinetics of osimertinib and the sarcopenia status ( $p = 0.868$ ) was found. Regarding toxicity, patients who were rendered to have sarcopenia, were not prone to more clinically relevant toxicity compared to patients without sarcopenia ( $p = 0.720$ ).

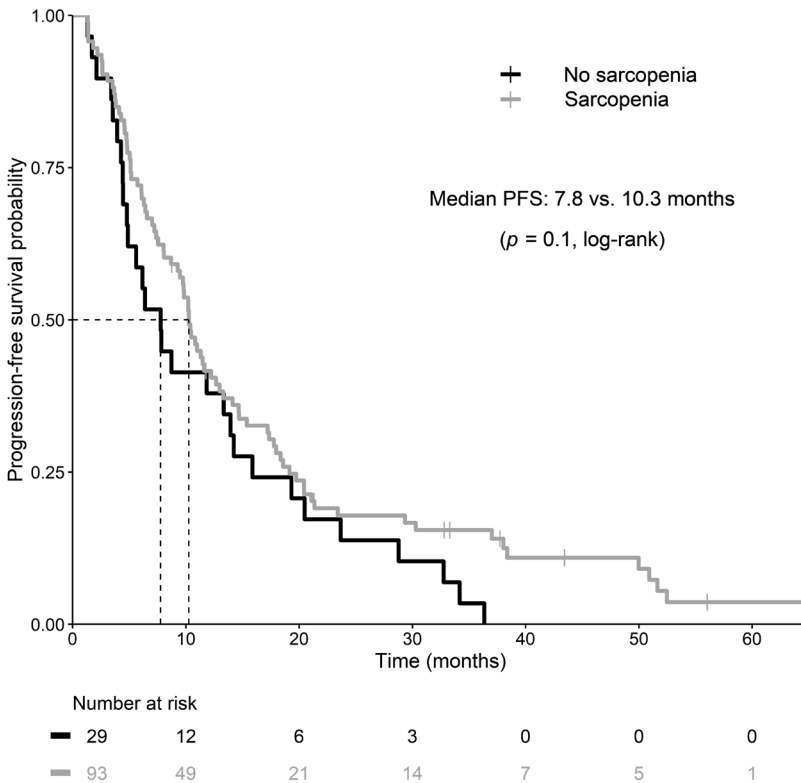


Figure 2. Kaplan-Meier curve of PFS in patients with (gray line) and without sarcopenia (black line). The dotted line represents the median PFS (in months). PFS: progression free survival.



## DISCUSSION

In this retrospective cohort, we studied the influence of pharmacokinetic exposure of osimertinib on the response and toxicity in daily clinical practice. We found that patients with a median osimertinib plasma  $C_{\min, \text{pred}} < 166 \mu\text{g/L}$  had a numerically longer median PFS compared to patients with a  $C_{\min, \text{pred}} \geq 166 \mu\text{g/L}$  (13.3 vs 9.3 months, respectively). In the multivariate analysis, this trend was not observed to be statistically significant indicating that other well-known prognostic factors contribute to this difference. Moreover, exposure to osimertinib was not statistically significantly related to the development of clinically relevant toxicities. In addition, no statistically significant relationships between sarcopenia index and exposure or toxicities were observed. Overall, this implies that osimertinib is a drug with a broad therapeutic range.

The absence of a positive exposure-efficacy relationship in the current dosing regimen is in line with the pharmacological characteristics found for the irreversible EGFR TKIs. *In vitro* data showed that the turnover time for complete renewal of the EGFR protein is approximately 25-140 hours.<sup>18</sup> Moreover, only low (*in vitro*) half maximal inhibitory concentrations of approximately 1.5-6.5  $\mu\text{g/L}$  have been found for binding of osimertinib to mutated EGFR and osimertinib has a long elimination half-life of 48 hours.<sup>7, 19</sup> All these factors taken together suggest that antitumor activity might continue even after the drug is totally cleared from the systemic circulation. Therefore, plasma concentrations would be less informative for efficacy of therapy. Moreover, if no exposure-efficacy relationship is observed in the approved dosing regimen, this might indicate that the current dose of osimertinib can be reduced. Indeed, in the phase I dose-escalation study of osimertinib and in a small retrospective study, it has been found that treatment with 40 mg QD results in a similar antitumor efficacy as for 80 mg of osimertinib.<sup>20-22</sup>

In our study, a trend was observed where patients with low exposure to osimertinib have a higher PFS. This non-statistically significant effect between exposure and efficacy might be due to a confounding effect. It has been described that the apparent (CYP-mediated) clearance of drugs can be reduced in case of cancer-induced inflammation.<sup>23</sup> This inflammation may thus independently be related to both lower osimertinib clearance and a poor treatment outcome. In accordance with this, we found that patients with low exposure had more favorable prognostic markers (e.g. better WHO PS and driver mutations more sensitive to osimertinib) than patients with higher osimertinib exposure.

To our knowledge, this is the first study to assess the relationship between osimertinib exposure and efficacy in a real-life cohort. We found that patients harboring primary EGFR mutations other than exon 19 del and exon 21 L858R have an increased hazard ratio for progression on osimertinib therapy. This observation is in line with study results, reporting lower antitumor activity for osimertinib (and other EGFR TKIs) in other primary EGFR mutations.<sup>24-26</sup> Although the observational group with other primary EGFR mutations is small ( $n = 10$ ), we found a statistically significant shorter PFS, indicating that osimertinib indeed is less effective for these driver mutations.

Approximately 22.8% of patients developed a clinically relevant toxicity. Patients who experienced these toxicities were exposed to similar osimertinib plasma concentrations and a statistically significant relationship could not be distinguished. In a previous analysis, a trend was found in which higher systemic exposure to osimertinib (in terms of the area under the concentration-effect curve (AUC)) was associated with an increase in the development of rash and diarrhea (*p*-value not reported).<sup>9</sup> Moreover, a statistically significant relationship between osimertinib exposure and QTc prolongation was found by these authors. Unfortunately, we could not confirm these results since electrocardiogram assessments were not routinely made for all patients during osimertinib therapy.

In earlier studies, it was found that sarcopenia in NSCLC patients is associated with poorer treatment outcome.<sup>10</sup> This effect was not found in our study, as we did not find a statistically significant effect of the presence of sarcopenia on the PFS in our study population.

Although log-linear extrapolation is an easy-to-implement method to calculate drug  $C_{\min, \text{pred}}$ , it assumes that the measured concentrations come from blood samples drawn after peak plasma concentrations are reached. Since the  $t_{\max}$  of osimertinib is six hours, this method might underpredict the plasma  $C_{\min, \text{pred}}$  for samples drawn within the absorption phase of osimertinib. However, since the ratio between peak and  $C_{\min, \text{pred}}$  for osimertinib is reported to be only 1.6-fold<sup>7</sup>, we assume that log-linear extrapolation is appropriate for this drug even for samples taken before the  $t_{\max}$ .<sup>27</sup> Another limitation of this study is that a maximum of one sample per dosing interval was drawn. Therefore, the effect of other pharmacokinetic parameters, such as AUC, on efficacy and toxicity could not be investigated. Last, in this study we did not take into account the effect of the metabolite concentrations of osimertinib. AZ7550 and AZ5104 are both potent inhibitors of EGFR and their pharmacokinetic exposure could thus influence efficacy and safety outcomes.<sup>28</sup> Nonetheless, it has been reported that plasma levels of these drugs are less than 10% of the total drug exposure in the systemic circulation and it may be assumed that their role is limited.<sup>7</sup>

In conclusion, this study demonstrates that osimertinib has a wide therapeutic window and that the pharmacokinetic exposure of this drug is not related to efficacy or toxicity. Therefore, therapeutic drug monitoring based on plasma concentrations of osimertinib is not recommended. Prospective studies should explore if lower doses of osimertinib (e.g. 40 mg QD) are sufficient to maintain efficacy.

## REFERENCES

1. Rosell R, Moran T, Queralt C, Porta R, Cardenal F, Camps C, et al. Screening for epidermal growth factor receptor mutations in lung cancer. *N Engl J Med*. 2009;361(10):958-967. <https://doi.org/10.1056/NEJMoa0904554>.
2. Douillard JY, Ostoros G, Cobo M, Ciuleanu T, McCormack R, Webster A, et al. First-line gefitinib in Caucasian EGFR mutation-positive NSCLC patients: a phase-IV, open-label, single-arm study. *Br J Cancer*. 2014;110(1):55-62. <https://doi.org/10.1038/bjc.2013.721>.
3. Urata Y, Katakami N, Morita S, Kaji R, Yoshioka H, Seto T, et al. Randomized Phase III Study Comparing Gefitinib With Erlotinib in Patients With Previously Treated Advanced Lung Adenocarcinoma: WJOG 5108L. *J Clin Oncol*. 2016;34(27):3248-3257. <https://doi.org/10.1200/jco.2015.63.4154>.
4. Park K, Tan EH, O'Byrne K, Zhang L, Boyer M, Mok T, et al. Afatinib versus gefitinib as first-line treatment of patients with EGFR mutation-positive non-small-cell lung cancer (LUX-Lung 7): a phase 2B, open-label, randomised controlled trial. *Lancet Oncol*. 2016;17(5):577-589. [https://doi.org/10.1016/s1470-2045\(16\)30033-x](https://doi.org/10.1016/s1470-2045(16)30033-x).
5. European Medicine Agency. Tagrisso: EPAR-Product information. 2021.
6. Soria JC, Ohe Y, Vansteenkiste J, Reungwetwattana T, Chewaskulyong B, Lee KH, et al. Osimertinib in untreated EGFR-mutated advanced non-small-cell lung cancer. *N Engl J Med*. 2018;378(2):113-125. <https://doi.org/10.1056/NEJMoa1713137>.
7. Food and Drug Administration. Center for Drug Evaluation and Research. Clinical pharmacology and biopharmaceutics review(s) NDA 208065 Review – Osimertinib. 2015.
8. Brown K, Comisar C, Witjes H, Maringwa J, de Greef R, Vishwanathan K, et al. Population pharmacokinetics and exposure-response of osimertinib in patients with non-small cell lung cancer. *Br J Clin Pharmacol*. 2017;83(6):1216-1226. <https://doi.org/10.1111/bcp.13223>.
9. Narjoz C, Cessot A, Thomas-Schoemann A, Golmard JL, Huillard O, Boudou-Rouquette P, et al. Role of the lean body mass and of pharmacogenetic variants on the pharmacokinetics and pharmacodynamics of sunitinib in cancer patients. *Invest New Drugs*. 2015;33(1):257-268. <https://doi.org/10.1007/s10637-014-0178-2>.
10. Shiroyama T, Nagatomo I, Koyama S, Hirata H, Nishida S, Miyake K, et al. Impact of sarcopenia in patients with advanced non-small cell lung cancer treated with PD-1 inhibitors: A preliminary retrospective study. *Sci Rep*. 2019;9(1):2447. <https://doi.org/10.1038/s41598-019-39120-6>.
11. Mitchell AP, Harrison MR, Walker MS, George DJ, Abernethy AP, Hirsch BR. Clinical trial participants with metastatic renal cell carcinoma differ from patients treated in real-world practice. *J Oncol Pract*. 2015;11(6):491-497. <https://doi.org/10.1200/jop.2015.004929>.
12. National Center for Health Statistics (NHIS). NHIS - Adult Tobacco Use - Glossary. Available via: <https://www.cdc.gov/nchs>. Accessed on 15 Oct 2021.
13. Verheijen RB, Yu H, Schellens JHM, Beijnen JH, Steeghs N, Huitema ADR. Practical recommendations for therapeutic drug monitoring of kinase inhibitors in oncology. *Clin Pharmacol Ther*. 2017;102(5):765-776. <https://doi.org/10.1002/cpt.787>.
14. Janssen JM, de Vries N, Venekamp N, Rosing H, Huitema ADR, Beijnen JH. Development and validation of a liquid chromatography-tandem mass spectrometry assay for nine oral anticancer drugs in human plasma. *J Pharm Biomed Anal*. 2019;174:561-566. <https://doi.org/10.1016/j.jpba.2019.06.034>.
15. Wang Y, Chia YL, Nedelman J, Schran H, Mahon FX, Molimard M. A therapeutic drug monitoring algorithm for refining the imatinib trough level obtained at different sampling times. *Ther Drug Monit*. 2009;31(5):579-584. <https://doi.org/10.1097/FTD.0b013e3181b2c8cf>.
16. Moeskops P, de Vos B, Veldhuis WB, May AM, Kurk S, Koopman M, et al. Automatic quantification of 3D body composition from abdominal CT with an ensemble of convolutional neural networks. *European Congress of Radiology-ECR 2020*. 2020. <https://doi.org/10.26044/ecr2020/C-09334>.
17. Martin L, Birdsell L, MacDonald N, Reiman T, Clandinin MT, McCargar LJ, et al. Cancer cachexia in the age of obesity: skeletal muscle depletion is a powerful prognostic factor, independent of body mass index. *J Clin Oncol*. 2013;31(12):1539-1547. <https://doi.org/10.1200/jco.2012.45.2722>.
18. Greig MJ, Niessen S, Weinrich SL, Feng JL, Shi M, Johnson TO. Effects of activating mutations on EGFR cellular protein turnover and amino acid recycling determined using SILAC mass spectrometry. *Int J Cell Biol*. 2015;2015:798936. <https://doi.org/10.1155/2015/798936>.

19. Hirano T, Yasuda H, Tani T, Hamamoto J, Oashi A, Ishioka K, et al. In vitro modeling to determine mutation specificity of EGFR tyrosine kinase inhibitors against clinically relevant EGFR mutants in non-small-cell lung cancer. *Oncotarget*. 2015;6(36):38789-38803. <https://doi.org/10.18632/oncotarget.5887>.
20. Jänne PA, Yang JC, Kim DW, Planchard D, Ohe Y, Ramalingam SS, et al. AZD9291 in EGFR inhibitor-resistant non-small-cell lung cancer. *N Engl J Med*. 2015;372(18):1689-1699. <https://doi.org/10.1056/NEJMoa1411817>.
21. European Medicine Agency. Tagrisso: Assessment report. 2016.
22. Sonobe S, Taniguchi Y, Saijo N, Naoki Y, Tamiya A, Omachi N, et al. The efficacy of a reduced dose (40mg) of osimertinib with T790M-positive advanced non-small-cell lung cancer. *Ann Oncol*. 2017;28:130. <https://doi.org/10.1093/annonc/mdx671.016>.
23. Coutant DE, Kulanthaivel P, Turner PK, Bell RL, Baldwin J, Wijayawardana SR, et al. Understanding disease-drug interactions in cancer patients: implications for dosing within the therapeutic window. *Clin Pharmacol Ther*. 2015;98(1):76-86. <https://doi.org/10.1002/cpt.128>.
24. van Veggel B, Madeira RSJFV, Hashemi SMS, Paats MS, Monkhorst K, Heideman DAM, et al. Osimertinib treatment for patients with EGFR exon 20 mutation positive non-small cell lung cancer. *Lung Cancer*. 2020;141:9-13. <https://doi.org/10.1016/j.lungcan.2019.12.013>.
25. Floc'h N, Martin MJ, Riess JW, Orme JP, Staniszewska AD, Ménard L, et al. Antitumor activity of osimertinib, an irreversible mutant-selective EGFR tyrosine kinase inhibitor, in NSCLC harboring EGFR exon 20 insertions. *Mol Cancer Ther*. 2018;17(5):885-896. <https://doi.org/10.1158/1535-7163.Mct-17-0758>.
26. Harrison PT, Vyse S, Huang PH. Rare epidermal growth factor receptor (EGFR) mutations in non-small cell lung cancer. *Semin Cancer Biol*. 2020;61:167-179. <https://doi.org/10.1016/j.semcancer.2019.09.015>.
27. Janssen JM, Dorlo TPC, Beijnen JH, Huitema ADR. Evaluation of extrapolation methods to predict trough concentrations to guide therapeutic drug monitoring of oral anticancer drugs. *Ther Drug Monit*. 2020;42(4):532-539. <https://doi.org/10.1097/ftd.0000000000000767>.
28. Cross DA, Ashton SE, Ghiorghiu S, Eberlein C, Nebhan CA, Spitzler PJ, et al. AZD9291, an irreversible EGFR TKI, overcomes T790M-mediated resistance to EGFR inhibitors in lung cancer. *Cancer Discov*. 2014;4(9):1046-1061. <https://doi.org/10.1158/2159-8290.Cd-14-0337>.

# CHAPTER 4.2

# Toxicity of pemetrexed during renal impairment explained – implications for safe treatment

*Int J Cancer. 2021;149(8):1576-1584*

René J. Boosman  
Thomas P.C. Dorlo  
Nikki de Rouw  
Jacobus A. Burgers  
Anne-Marie C. Dingemans  
Michel M. van den Heuvel  
Lizza E.L. Hendriks  
Bonne Biesma  
Joachim G.J.V. Aerts  
Sander Croes  
Ron H.J. Mathijssen  
Alwin D.R. Huitema  
Rob ter Heine

\*these authors contributed equally and thus share first authorship

Author's contribution: R.J. Boosman contributed to the design of this study, performed the data management, conducted the data analysis, wrote the first draft of the manuscript and edited the contribution of the co-authors on this manuscript.

## ABSTRACT

Pemetrexed is an important component of first line treatment in patients with non-squamous non-small cell lung cancer. However, a limitation is the contraindication in patients with renal impairment due to hematological toxicity. Currently, it is unknown how to safely dose pemetrexed in these patients. The aim of our study was to elucidate the relationship between pemetrexed exposure and toxicity to support the development of a safe dosing regimen in patients with renal impairment. A population pharmacokinetic/pharmacodynamic analysis was performed based on phase II study results in three patients with renal dysfunction, supplemented with data from 106 patients in early clinical studies. Findings were externally validated with data of different pemetrexed dosing regimens. Alternative dosing regimens were evaluated using the developed model. We found that pemetrexed toxicity was driven by the time above a toxicity threshold concentration. The threshold for vitamin-supplemented patients was 0.110 mg/mL (95% CI: 0.092-0.146 mg/mL). It was observed that in patients with renal impairment (estimated glomerular filtration rate (eGFR): < 45 mL/min) the approved dose of 500 mg/m<sup>2</sup> would yield a high probability of severe neutropenia in the range of 51.0% to 92.6%. A pemetrexed dose of 20 mg for patients (eGFR: 20 mL/min) is shown to be neutropenic-equivalent to the approved dose in patients with adequate renal function (eGFR: 90 mL/min), but would result in an approximately 13-fold lower area under the concentration-time curve. The pemetrexed exposure-toxicity relationship is explained by a toxicity threshold and substantially different from previously thought. Without prophylaxis for toxicity, it is unlikely that a therapeutic dose can be safely administered to patients with renal impairment.

## INTRODUCTION

Pemetrexed is a folate analogue and a cornerstone in the treatment of non-squamous non-small cell lung cancer (NSCLC), mesothelioma and thymoma.<sup>1-3</sup> Despite renal function being the main determinant of systemic exposure of pemetrexed, the approved dose is based on body surface area (BSA; 500 mg/m<sup>2</sup> every 21 days). Although pemetrexed treatment is generally well tolerated in patients with adequate renal function, the principle toxicity related to its exposure is myelosuppression, which predominantly presents as neutropenia.<sup>4-5</sup> Since the introduction of vitamin B11 and B12 supplementation during the treatment of pemetrexed, the incidence of severe hematological toxicities decreased, although neutropenia remains frequently observed during treatment.<sup>6</sup> In an early phase I study, BSA-based dosing (150 mg/m<sup>2</sup> Q3W) in a non-vitamin supplemented patient with renal impairment led to severe toxicities, including grade 4 neutropenia and, subsequently, pemetrexed toxicity-related death.<sup>7</sup> Consequently, a creatinine clearance (CrCl) < 45 mL/min became a contraindication in the pemetrexed label. Since lung cancer and mesothelioma are often diagnosed in elderly patients and age is correlated with a decline in renal function, a considerable proportion of patients is likely withheld effective treatment with pemetrexed.<sup>8,9</sup>

The quest to optimize pemetrexed treatment continued and Latz *et al.* suggested a linear relationship between pemetrexed plasma concentration and inhibition of the proliferation rate of neutrophils at the approved 500 mg/m<sup>2</sup> dose level.<sup>10</sup> It was postulated that a dose adjusted to renal function to target a predefined pharmacokinetic (PK)-based cumulative area under the concentration-time curve (AUC) of 164 mg·h/L would prevent toxicity while maintaining efficacy.<sup>11</sup> Additionally, their results indicated that the efficacy and toxicity of pemetrexed are considered to be linearly related to its systemic exposure.<sup>5,10</sup> Therefore, we recently studied this hypothesis in patients with renal impairment aimed at attaining a similar AUC as in patients with adequate renal function in a phase II study. However, our study was halted prematurely as patients unexpectedly developed severe myelotoxicity, despite a presumably nontoxic systemic exposure. This indicated that the exposure-toxicity relationship in patients with impaired renal function was different from previously suggested. To allow safe dosing of pemetrexed in patients with impaired renal function, it is pivotal to unravel this relationship. The aim of our study was to elucidate the relationship between pemetrexed exposure and toxicity to support the development of a safe dosing regimen in patients with renal impairment.

## METHODS

### Data

For the primary analysis of the pemetrexed exposure-neutropenia relationship, a dataset was composed from two sources. Pemetrexed PK and absolute neutrophil count (ANC) pharmacodynamic (PD) data of a phase I dose-finding study (ClinicalTrials.gov NCT0003706) were kindly provided by Eli Lilly.<sup>7,12</sup> In this study, patients with varying renal functions were dose-escalated from a starting dose of pemetrexed of 150 to 500 mg/m<sup>2</sup> every 21 days depending



on their renal function to a maximum of 600 mg/m<sup>2</sup>. Individual data on age, gender, ethnicity, body weight, vitamin B11 and B12 supplementation, serum creatinine and ANCs were available, as well as pemetrexed-dosing related information such as dose, infusion rates, sampling times and plasma concentrations. These data were extended with the results of our single-arm phase II pharmacokinetic and safety study (NCT03656549). In our study, patients with a creatinine clearance < 45 mL/min were dosed based on creatinine clearance to attain a similar cumulative AUC as in patients with adequate renal function (164 mg·h/L ± 25%).<sup>11-13</sup> ANCs were collected just before administration of pemetrexed at each 21-day cycle and at day 14. The estimated glomerular filtration rate (eGFR) based on the Chronic Kidney Disease Epidemiology Collaboration (CKD-EPI<sup>14</sup>) and the CrCl based on the Cockcroft-Gault equation<sup>15</sup> were calculated for the individual patients. None of the patients in the dataset received other anticancer drugs, like cisplatin or carboplatin. A detailed description of the methods and results of this phase II study is included as supplementary data.

For the external validation of the hypothesized relationship, data of patients treated with pemetrexed at the maximum tolerated dose (MTD) in the early phase I studies by McDonald *et al.* and Rinaldi *et al.* were used.<sup>16-18</sup> The demographic and pharmacokinetic data of the study by McDonald *et al.* were provided by Eli Lilly, including age, gender, body weight and serum creatinine, as well as pemetrexed dose, infusion rates, sampling times and plasma concentrations. For the studies by Rinaldi *et al.*, the methods are described in the supplementary material.

#### Pharmacokinetic-pharmacodynamic analysis

The population PK/PD analysis of pemetrexed was performed by means of nonlinear mixed effects modeling. The pharmacokinetics were described using a previously developed model, based on the available pemetrexed pharmacokinetic data of the same dataset in patients with varying renal function.<sup>19</sup> A well-established semimechanistic model describing the interplay between circulating neutrophils and plasma concentrations of pemetrexed served as the basis for the analysis.<sup>5, 10, 20</sup> For the analysis the drug effect of pemetrexed on the proliferation of the neutrophils was modeled either as a linear relationship between drug concentration and neutrophil proliferation rate or as a time-above-threshold relationship. The development and evaluation of this analysis is described in detail in the supplementary material.

#### External validation

To externally evaluate our final model, we performed clinical trial simulations. We compared the predicted frequencies of neutropenia for various dosing regimens. Monte Carlo simulations (n = 1,000 trials) were performed of the trials with the established MTD in the early phase I studies<sup>16-18</sup> for the following dosing regimens: 4 mg/m<sup>2</sup>/day for five consecutive days every three weeks, 40 mg/m<sup>2</sup>/week for four consecutive weeks, every six weeks and 600 mg/m<sup>2</sup> ever three weeks, that were performed without prophylactic vitamin supplementation. The ANCs were simulated on day 8 and day 15, as reported for these dosing regimens. Neutropenia was graded according to the National Cancer Institute Common Terminology Criteria (CTCAE) version 4.03 (with a lower limit of normal ANC of 2.0·10<sup>9</sup>/L).<sup>21</sup> The relative frequency of model-predicted neutropenia per patient was calculated over the total of these 1,000 trial simulations. The distribution of the predicted

number of neutropenic patients per trial associated to this relative frequency was visualized for both relationships and compared with the actual observed frequencies for each dosing regimen. Further details of this external validation are described in the supplementary material.

#### *Evaluation of the relationship between renal function and development of neutropenia*

We assessed the probability for the development of  $\geq$  grade 3 neutropenia after pemetrexed administration in the approved dose across different renal function groups. For this purpose, patients with varying renal functions (eGFR of 5, 10, 15, 20, 25, 30, 35, 40, 45, 60, 75 and 90 mL/min) were simulated ( $n = 1,000$ ) after receiving a single 500 mg/m<sup>2</sup> pemetrexed dose for each eGFR. The probability to develop a  $\geq$ grade 3 neutropenia was calculated for patients with and without vitamin supplementation. The details of the simulations are described in the supplementary material.

In addition, we assessed the typical ANC curves for vitamin-supplemented patients. Typical patients with adequate renal function (eGFR: 90 mL/min) and decreased renal function (eGFR: 20 mL/min) after a pemetrexed dose of 500 mg/m<sup>2</sup> were simulated. Next, we calculated the pemetrexed dose to be administered to a patient with an impaired renal function (eGFR: 20 mL/min) to harbor a similar neutropenic response as a patient dosed with 500 mg/m<sup>2</sup> pemetrexed with an eGFR of 90 mL/min. The corresponding AUC for this dose was calculated.

## RESULTS

### *Data*

In addition to the three patients from our own phase II study, data of 106 patients were obtained. The final dataset thus consisted of 109 patients with known demographic characteristics, vitamin supplementation status and pemetrexed-dose related information. The baseline characteristics of the population are summarized in Table 1. A total of 566 pemetrexed plasma concentrations and 1,513 ANCs at different time points were available for analysis. A wide range in eGFR (calculated using the CKD-EPI equation) of 8.4-154.9 mL/min was observed. Overall, eight patients had a renal function for which pemetrexed is currently contraindicated. In addition, about three-quarters of the patients received vitamin B11 and B12 supplementation.

### *Pharmacokinetic-pharmacodynamic analysis*

The model of Latz *et al.* describing a linear exposure-toxicity relationship<sup>19</sup> was used as a starting point of our analysis. As an alternative model we hypothesized a relationship in which the development of neutropenia after pemetrexed administration is driven by the time above a threshold concentration of pemetrexed. This threshold model was based on the analogy between pemetrexed and methotrexate that also exhibits threshold-driven toxicity.<sup>22</sup> This hypothesis was also driven by the fact that early clinical studies suggested the presence of a threshold-driven toxicity, revealing an MTD for a daily pemetrexed dose of 4 mg/m<sup>2</sup>, compared to a much higher MTD of 600 mg/m<sup>2</sup> when pemetrexed was administered in a 21-day cycle.<sup>16-18</sup> The threshold model characterized the pooled ANC dataset better than the linear exposure-response relationship as observed by a decrease in

Akaike Information Criterion of 33.6 points between both models. However, the goodness-of-fit plots (supplementary data Figures S2 and S3) did not show any relevant improvement between both models. Therefore, external validation was performed for both models (see paragraph "External validation"). Typical values for maximum inhibitory effect ( $E_{max}$ ) and the threshold concentration were 1.16 (95% confidence interval (CI): 0.96-1.37) and 0.030 mg/L (95% CI: 0.017-0.047 mg/L). Vitamin supplementation increased the threshold concentration to 0.110 mg/L (95% CI: 0.092-0.146 mg/L). A detailed description of both models can be found in the supplemental material.

*Table 1. Baseline characteristics of the population used for the PK/PD modelling. Values are presented as numbers (percentages) or medians [ranges], as appropriate.*

	Value
<b>Number of patients</b>	109
<b>Gender, male</b>	75 (68.8%)
<b>Age (years)</b>	62 [25-80]
<b>Weight (kg)</b>	74.4 [47.5-127.2]
<b>BSA (m<sup>2</sup>)</b>	1.90 [1.44-2.60]
<b>eGFR (calculated with CKD-EPI; mL/min)</b>	97.2 [8.4-154.9]
<b>Received vitamin supplementation</b>	78 (71.6%)
<b>Pemetrexed dose (mg/m<sup>2</sup>)</b>	500 [129.5-613.4]

BSA: body surface area, CKD-EPI: Chronic Kidney Disease Epidemiology Collaboration, eGFR: estimated glomerular filtration rate

### External validation

The predictive performance of both the linear and threshold-driven neutropenia relationship for the outcomes of the phase I studies in pemetrexed is depicted in Figure 1. The observed frequency of any grade of neutropenia as found in the phase I pemetrexed studies is marked by a dashed vertical gray line in the panels. For the 600 mg/m<sup>2</sup> every 21 days both relationships predicted similar frequencies of neutropenic events. However, for low dose pemetrexed (4 mg/m<sup>2</sup>/day and 40 mg/m<sup>2</sup>/week), the linear exposure-toxicity relationship underpredicted frequencies of any grade of neutropenia to occur, with a maximum of two out of six patients. In contrast, the threshold relationship predicts higher frequencies in these dosing regimens, which is in line in what has been observed in the clinical studies. The predicted frequencies per grade of neutropenia can be found in the supplemental materials (Figure S5-S7). Thus, a linear relationship between neutrophil proliferation and plasma concentrations as previously suggested by Latz *et al.* seemed incapable of predicting neutropenia in patients with prolonged exposure to low plasma concentrations of pemetrexed, as is the case in patients with daily dosing or patients with renal impairment.

### Evaluation of the relationship between renal function and development of neutropenia

Figure 2 illustrates the probability to develop ≥ grade 3 neutropenia after a single BSA-based pemetrexed dose of 500 mg/m<sup>2</sup> in patients with varying renal function. In patients with adequate renal function (eGFR: 45-90 mL/min) the probabilities range from 18.7% to 45.9% in the vitamin-

supplemented group and between 34.3% and 69.9% in the non-supplemented group. As observed, in vitamin-supplemented patients with impaired renal function, it is predicted that more than half of the patients develop  $\geq$  grade 3 neutropenia, probabilities range from 51.0% for an eGFR of 40 mL/min to 92.6% in patients with an eGFR of 5 mL/min.

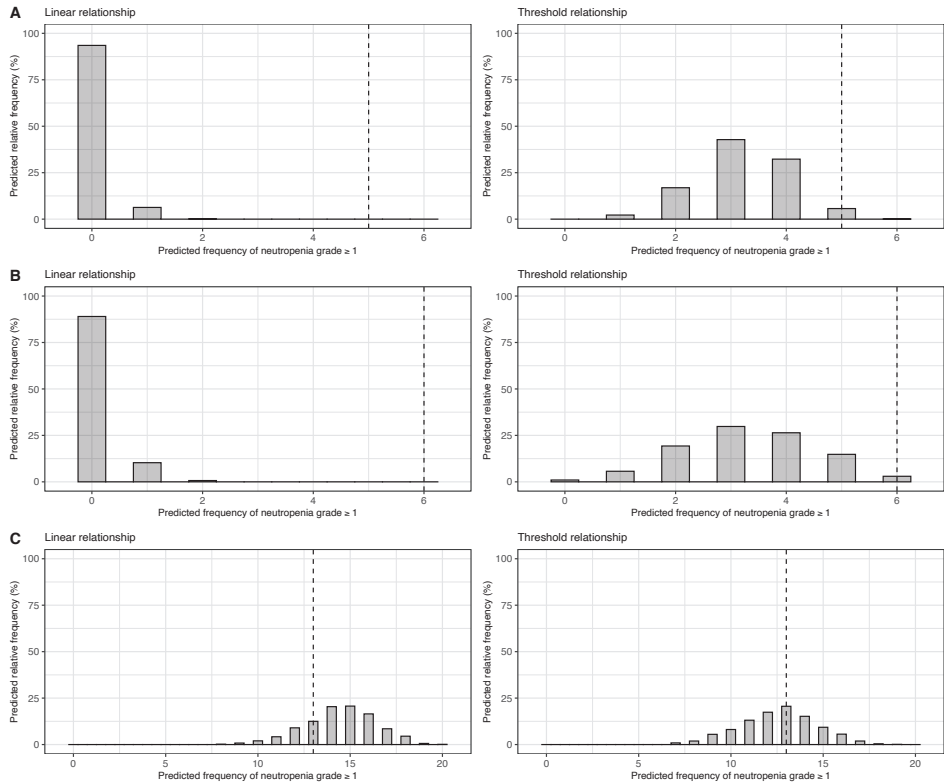


Figure 1. Model-predicted frequencies of  $\geq$  grade 1 of neutropenia observed in the simulations of the phase I studies according to the linear exposure-toxicity relationship (left panel) or the threshold relationship (right panel). A, after pemetrexed 4 mg/m<sup>2</sup>/day for five consecutive days every 21 days. B, after pemetrexed 40 mg/m<sup>2</sup>/week for four consecutive weeks every six weeks. C, after pemetrexed 600 mg/m<sup>2</sup> every 21 days. The y-axis represents the relative frequency of trials in which the predicted frequency of neutropenia was found. The dashed line represents the actual observed frequency.

In Figure 3A-C, the predicted neutropenic responses after pemetrexed treatment in a typical vitamin-supplemented patient are depicted for a threshold-driven relationship. For patients with an adequate renal function (eGFR: 90 mL/min), the approved dose of pemetrexed will result in a predicted ANC nadir of  $2.2 \cdot 10^9$ /L (see Figure 3A). Moreover, in a typical patient with a decreased renal function (eGFR 20 mL/min) the approved dose will result in grade 4 neutropenia (Figure 3B). Figure 3C illustrates the typical ANC values predicted based upon the threshold relationship for a patient with eGFR 90 mL/min dosed with 1,000 mg (corresponding to 500 mg/m<sup>2</sup>) pemetrexed

and a patient with eGFR 20 mL/min dosed with 20 mg of pemetrexed. Note that the curves overlap and therefore, a dose of 20 mg in a patient with impaired renal function is likely as safe as the approved dose in patient with adequate renal function. The calculated pemetrexed AUC of this 20 mg dose with an eGFR of 20 mL/min was 12.7 mg·h/L. This indicates that the dose has to be reduced almost a 50-fold for a neutropenia-equivalent dose, resulting in an approximately 13-fold lower AUC in patients with renal impairment compared to patients with adequate renal function.

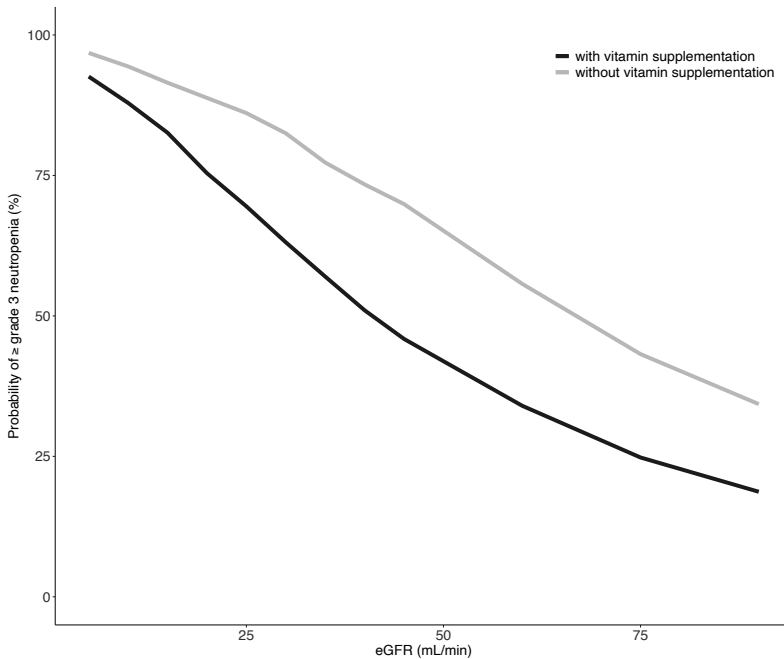


Figure 2. Probability to develop ≥ grade 3 neutropenia in patients with varying renal functions dosed with 500 mg/m<sup>2</sup> pemetrexed, with vitamin supplementation (black line) or without vitamin supplementation (gray line).

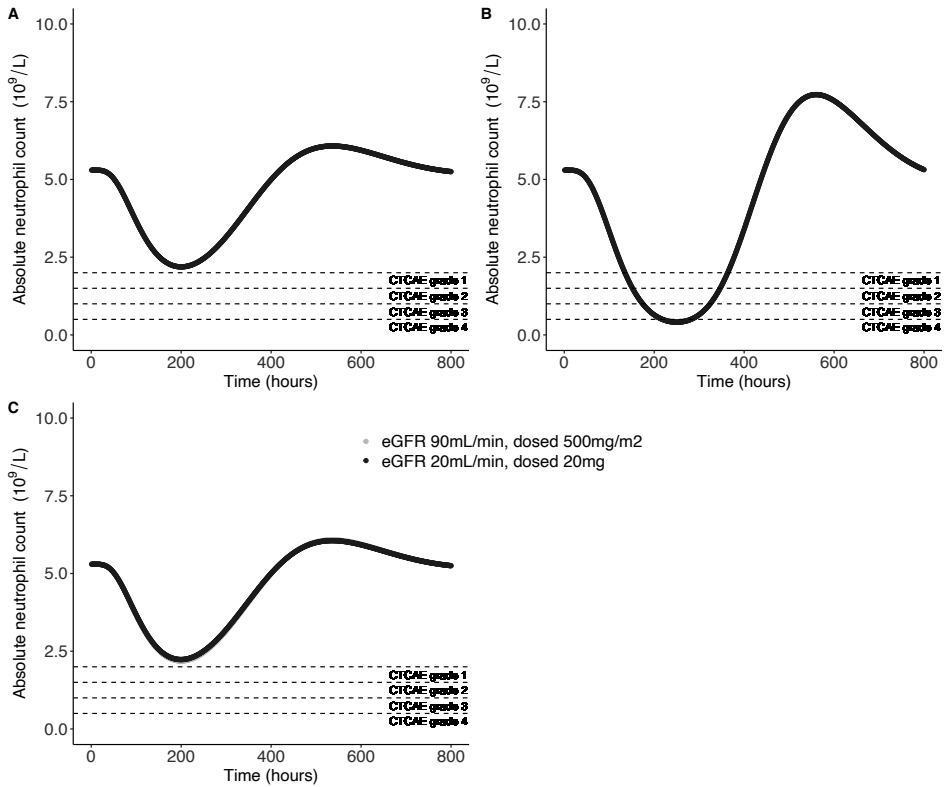


Figure 3. Typical absolute neutrophil count curves for vitamin-supplemented patients according to the model with a threshold-driven exposure-toxicity relationship. A, in a patient with an eGFR of 90 mL/min after a pemetrexed dose of 500 mg/m<sup>2</sup>. B, In a patient with an eGFR of 20 mL/min after a 500 mg/m<sup>2</sup>. C, in a patient with an eGFR of 90 mL/min after a pemetrexed dose of 500 mg/m<sup>2</sup> (gray line) and in a patient with an eGFR of 20 mL/min after a pemetrexed dose of 20 mg (black line), note that the curves overlap substantially. The dashed horizontal lines represent the windows for the CTCAE grade 1-grade 4 neutropenia.

## DISCUSSION

We performed an in-depth analysis of the exposure-toxicity relation of pemetrexed based on pharmacokinetic and ANC data collected from early clinical studies and from our failed renal impairment study. We showed that a threshold-driven toxicity predicts the development of neutropenia and that the previously suggested linear exposure-toxicity relationship is an inappropriate predictor for pemetrexed toxicity in case of long-term exposure to low pemetrexed plasma concentrations, for example, in daily dosing or in case of renal impairment. The clinical implication of our findings is that the therapeutic efficacy of a safe dose in patients with impaired renal can be questioned.

Initially, in an early phase I study, a reduced BSA-based pemetrexed dosing in a vitamin unsupplemented patient with renal impairment led to a systemic exposure of 360 mg<sup>h</sup>/L and fatal toxicities.<sup>7</sup> This is an exposure twice as high as in patients with adequate renal function dosed with the approved dose of pemetrexed. This underlines that dosing in patients with renal impairment is not as straightforward as initially thought.

Other early phase I studies of pemetrexed already showed that prolonged yet low exposure to pemetrexed resulted in severe neutropenia.<sup>16-18</sup> To elaborate, the MTDs in the daily and weekly dose schedule in non-vitamin-supplemented patients with adequate renal function were 4 mg/m<sup>2</sup> and 40 mg/m<sup>2</sup> respectively and, thus, markedly lower than the MTD of 600 mg/m<sup>2</sup> found for pemetrexed in a 21-day cycle. The external validation showed that both the linear and the threshold-driven exposure-toxicity relationship are capable to predict neutropenia in the standard three-weekly dosing schedule. However, only the threshold relationship can accurately predict the development of neutropenia after a prolonged low pemetrexed exposure. Pemetrexed is predominantly cleared by the kidneys, thus patients with renal dysfunction are also exposed to pemetrexed for a prolonged period of time. This suggests that a threshold relationship is capable to predict neutropenic responses in patients with impaired renal function, while a linear exposure-toxicity relationship is not able to capture these responses accurately in this patient group. For methotrexate, another antifolate, structurally similar to pemetrexed, a toxicity threshold was previously identified in patients receiving high-dose treatment<sup>22</sup>, further supporting the plausibility that pemetrexed-induced neutropenia is also dependent on such a threshold-driven relationship. This finding may explain recent findings by Kwok and colleagues<sup>23</sup>, who found that presence of third space fluid during treatment with pemetrexed is a significant risk factor for this toxicity. Presence of third space fluid may result in an increase of a peripheral compartment volume, resulting in a prolonged terminal elimination half-life and, thus, a risk factor for development of toxicity.

The typical pemetrexed threshold concentration identified in our study was 0.030 mg/L for vitamin-unsupplemented patients and 0.110 mg/L for vitamin-supplemented patients. In antiproliferative assays in CCRF-CEM cell lines, Taylor *et al.* and Shih *et al.* showed 0.007 mg/L and 0.011 mg/L pemetrexed respectively to be the concentration in which half of the maximum inhibitory effect

occurred.<sup>24, 25</sup> When corrected for the approximately 81% plasma protein binding of pemetrexed<sup>26</sup> this would translate to values of 0.036 mg/L and 0.057 mg/L respectively, which is in the same order of magnitude as found in our study.

Vogelzang *et al.* showed that 26.3% of patients supplemented with vitamin B11 and B12 during pemetrexed treatment developed grade 3/4 neutropenia versus 37.5% in the unsupplemented group of patients with adequate renal function.<sup>6</sup> This is in line with the results of our model-based predicted frequency for a typical patient with adequate renal function (Figure 2). Moreover, we show that vitamin-supplementation increases the threshold concentration. This is also suggested by an early study in mice showing that lethality as a consequence of toxicity occurs at lower concentrations in the folate-deficient species.<sup>27</sup> Although nowadays vitamin supplementation is standard of care during treatment, does not alter the efficacy of pemetrexed<sup>6</sup> and reduces the occurrence of severe side effects, there remains a high incidence of neutropenia during pemetrexed treatment, especially in the renally impaired patients<sup>4</sup>, underlining the unmet need of a safe and effective dosing regimen for this patient group.

A limitation of our study is that, although based on a large database, only data from a limited number of patients with renal impairment were available. Nonetheless, the external validation confirmed its predictive capability across different dosing regimens and renal functions and this is the largest study thus far with an integrated analysis of the data from two prospective renal impairment studies with pemetrexed. Another limitation may be that none of the patients in our analysis concomitantly used other anticancer drugs, like carboplatin or cisplatin. Although this enabled an unclouded assessment of the neutropenic effects of pemetrexed, it should be noted that pemetrexed is often combined with these drugs. As these platinum-based anticancer agents may also cause myelotoxicity it is likely that the probability of toxicity in combination with these drugs is even higher.<sup>28</sup>

Since we now know that potentially subtherapeutic pemetrexed doses in patients with renal impairment can still result in severe neutropenia, we strongly recommend against administration of pemetrexed in this patient group. A pemetrexed dose leading to an equivalent neutropenic response in patients with renal dysfunction is considerably lower and leads to a substantial (13-fold) lower AUC than after a pemetrexed dose of 500 mg/m<sup>2</sup> for a patient with adequate renal function. Whether the AUC of a pemetrexed dose is the determinant for antitumor efficacy, is currently unknown. The early phase I studies showed that administration of 600 mg/m<sup>2</sup> Q3W superior efficacy of pemetrexed, but similar neutropenic response compared to the 4 mg/m<sup>2</sup>/day for five consecutive days Q3W and the 40 mg/m<sup>2</sup>/week for four consecutive weeks every six weeks dosing regimens.<sup>16-18</sup> This suggests that exposure-response and exposure-toxicity relationships for pemetrexed have different pharmacokinetic drivers. Moreover, for the structural analogue methotrexate a relationship between AUC and efficacy in the treatment of primary central nervous system lymphoma has been observed, while toxicity is explained by a time-above-threshold concentration.<sup>29, 30</sup> We currently assume that AUC is a better predictor for efficacy than the time-above-threshold concentration, and we hypothesize that the efficacy of treatment



with pemetrexed at a substantial lower exposure than found for the approved dose might be compromised. For methotrexate, administration of folinic acid 24-36 hours after start is used to "rescue" nonmalignant cells.<sup>31</sup> Folinic acid, not to be confused with folic acid (vitamin B11), has been shown to be capable to completely reverse pemetrexed-induced cytotoxicity in human tumor cell lines.<sup>27</sup> Moreover, folinic acid has been shown to be able to revert the clinical signs of toxicity and hematological alterations induced by a potentially lethal pemetrexed dose in dogs.<sup>32</sup> Currently, in the drug label of pemetrexed, use of high dose folinic acid rescue for management of pemetrexed overdose is proposed.<sup>33</sup> It may be argued that standard folinic acid rescue (e.g. 30 mg three time daily routinely started 24 hours after administration of pemetrexed, with sufficient wash-out before administration of the next pemetrexed dose) may have the potential to allow safe dosing of pemetrexed in renally impaired patients. Other prophylactic strategies worth studying include the use of prophylactic granulocyte colony-stimulating factor (G-CSF), which is already used as standard of care to reduce the severity of chemotherapy-induced neutropenia<sup>34, 35</sup> or glucarpidase, an enzyme that can inactivate methotrexate and, based on *in vitro* experiments, shows similar activity for pemetrexed.<sup>36, 37</sup> The efficacy and safety of all these strategies should be evaluated in a prospective study to enable pemetrexed treatment at a therapeutic dose in patients with impaired renal function.

In summary, we show that pemetrexed-induced neutropenia is likely driven by the time above a threshold pemetrexed concentration and this has caused previous studies of pemetrexed in patients with impaired renal function to fail. To enable therapeutic dosing of pemetrexed in patients with impaired renal function without toxicity, further investigations on prophylactic treatments are essential.

## REFERENCES

1. Planchard D, Popat S, Kerr K, Novello S, Smit EF, Faivre-Finn C, et al. Metastatic non-small cell lung cancer: ESMO Clinical Practice Guidelines for diagnosis, treatment and follow-up. *Ann Oncol*. 2018;29:iv192-iv237. <https://doi.org/10.1093/annonc/mdy275>.
2. Baas P, Fennell D, Kerr KM, Van Schil PE, Haas RL, Peters S. Malignant pleural mesothelioma: ESMO Clinical Practice Guidelines for diagnosis, treatment and follow-up. *Ann Oncol*. 2015;26:v31-v39. <https://doi.org/10.1093/annonc/mdv199>.
3. Gbolahan OB, Porter RF, Salter JT, Yiannoutsos C, Burns M, Chiorean EG, et al. A phase II study of pemetrexed in patients with recurrent thymoma and thymic carcinoma. *J Thorac Oncol*. 2018;13(12):1940-1948. <https://doi.org/10.1016/j.jtho.2018.07.094>.
4. Ando Y, Hayashi T, Ujita M, Murai S, Ohta H, Ito K, et al. Effect of renal function on pemetrexed-induced haematotoxicity. *Cancer Chemother Pharmacol*. 2016;78(1):183-189. <https://doi.org/10.1007/s00280-016-3078-7>.
5. Latz JE, Karlsson MO, Rusthoven JJ, Ghosh A, Johnson RD. A semimechanistic-physiologic population pharmacokinetic/pharmacodynamic model for neutropenia following pemetrexed therapy. *Cancer Chemother Pharmacol*. 2006;57(4):412-426. <https://doi.org/10.1007/s00280-005-0077-5>.
6. Vogelzang NJ, Rusthoven JJ, Symanowski J, Denham C, Kaukel E, Ruffie P, et al. Phase III study of pemetrexed in combination with cisplatin versus cisplatin alone in patients with malignant pleural mesothelioma. *J Clin Oncol*. 2003;21(14):2636-2644. <https://doi.org/10.1200/jco.2003.11.136>.
7. Mita AC, Sweeney CJ, Baker SD, Goetz A, Hammond LA, Patnaik A, et al. Phase I and pharmacokinetic study of pemetrexed administered every 3 weeks to advanced cancer patients with normal and impaired renal function. *J Clin Oncol*. 2006;24(4):552-562. <https://doi.org/10.1200/JCO.2004.00.9720>.
8. Launay-Vacher V, Etesami R, Janus N, Spano J-P, Ray-Coquard I, Oudard S, et al. Lung cancer and renal insufficiency: prevalence and anticancer drug issues. *Lung*. 2009;187(1):69-74. <https://doi.org/10.1007/s00408-008-9123-5>.
9. Ohara G, Kurishima K, Nakazawa K, Kawaguchi M, Kagohashi K, Ishikawa H, et al. Age-dependent decline in renal function in patients with lung cancer. *Oncol Lett*. 2012;4(1):38-42. <https://doi.org/10.3892/ol.2012.672>.
10. Latz JE, Schneck KL, Nakagawa K, Miller MA, Takimoto CH. Population pharmacokinetic/pharmacodynamic analyses of pemetrexed and neutropenia: effect of vitamin supplementation and differences between Japanese and Western patients. *Clin Cancer Res*. 2009;15(1):346-354. <https://doi.org/10.1158/1078-0432.Ccr-08-0791>.
11. Latz JE, Rusthoven JJ, Karlsson MO, Ghosh A, Johnson RD. Clinical application of a semimechanistic-physiologic population PK/PD model for neutropenia following pemetrexed therapy. *Cancer Chemother Pharmacol*. 2006;57(4):427-435. <https://doi.org/10.1007/s00280-005-0035-2>.
12. CSDR. Available from: <https://www.clinicalstudydatarequest.com/Posting.aspx?ID=19619&GroupID=SUMMARIES>. Accessed on 20 Nov 2019.
13. Latz JE, Chaudhary A, Ghosh A, Johnson RD. Population pharmacokinetic analysis of ten phase II clinical trials of pemetrexed in cancer patients. *Cancer Chemother Pharmacol*. 2006;57(4):401-411. <https://doi.org/10.1007/s00280-005-0036-1>.
14. Levey AS, Stevens LA, Schmid CH, Zhang YL, Castro AF, Feldman HI, et al. A new equation to estimate glomerular filtration rate. *Ann Intern Med*. 2009;150(9):604-612. <https://doi.org/10.7326/0003-4819-150-9-200905050-00006>.
15. Cockcroft DW, Gault MH. Prediction of creatinine clearance from serum creatinine. *Nephron*. 1976;16(1):31-41. <https://doi.org/10.1159/000180580>.
16. McDonald AC, Vasey PA, Adams L, Walling J, Woodworth JR, Abrahams T, et al. A phase I and pharmacokinetic study of LY231514, the multitargeted antifolate. *Clin Cancer Res*. 1998;4(3):605-610.
17. Rinaldi DA, Burris HA, Dorr FA, Woodworth JR, Kuhn JG, Eckardt JR, et al. Initial phase I evaluation of the novel thymidylate synthase inhibitor, LY231514, using the modified continual reassessment method for dose escalation. *J Clin Oncol*. 1995;13(11):2842-2850. <https://doi.org/10.1200/jco.1995.13.11.2842>.
18. Rinaldi DA, Kuhn JG, Burris HA, Dorr FA, Rodriguez G, Eckhardt SG, et al. A phase I evaluation of multitargeted antifolate (MTA, LY231514), administered every 21 days, utilizing the modified continual reassessment method for dose escalation. *Cancer Chemother Pharmacol*. 1999;44(5):372-380. <https://doi.org/10.1007/s002800050992>.

19. de Rouw N, Boosman RJ, Huitema ADR, Hilbrands LB, Svensson EM, Derijks HJ, et al. Rethinking the application of pemetrexed for patients with renal impairment: a pharmacokinetic analysis. *Clin Pharmacokinet.* 2021;60(5):649-654. <https://doi.org/10.1007/s40262-020-00972-1>.
20. Friberg LE, Henningsson A, Maas H, Nguyen L, Karlsson MO. Model of chemotherapy-induced myelosuppression with parameter consistency across drugs. *J Clin Oncol.* 2002;20(24):4713-4721. <https://doi.org/10.1200/jco.2002.02.140>.
21. National Cancer Institute Cancer Therapy Evaluation Program. Common Toxicity Criteria for Adverse Events v4.03 (CTCAE) 2009.
22. Stoller RG, Hande KR, Jacobs SA, Rosenberg SA, Chabner BA. Use of plasma pharmacokinetics to predict and prevent methotrexate toxicity. *N Engl J Med.* 1977;297(12):630-634. <https://doi.org/10.1056/nejm197709222971203>.
23. Kwok WC, Cheong TF, Chiang KY, Ho JCM, Lam DCL, Ip MSM, et al. Haematological toxicity of pemetrexed in patients with metastatic non-squamous non-small cell carcinoma of lung with third-space fluid. *Lung Cancer.* 2021;152:15-20. <https://doi.org/10.1016/j.lungcan.2020.11.028>.
24. Shih C, Chen VJ, Gossett LS, Gates SB, MacKellar WC, Habeck LL, et al. LY231514, a pyrrolo[2,3-d]pyrimidine-based antifolate that inhibits multiple folate-requiring enzymes. *Cancer Res.* 1997;57(6):1116-1123.
25. Taylor EC, Kuhnt D, Shih C, Rinzel SM, Grindey GB, Barredo J, et al. A dideazatetrahydrofolate analogue lacking a chiral center at C-6, N-[4-l2-(2-amino-3,4-dihydro-4-oxo-7H-pyrrolo[2,3-d]pyrimidin-5-yl)ethyl] benzoyl-L-glutamic acid, is an inhibitor of thymidylate synthase. *J Med Chem.* 1992;35(23):4450-4454. <https://doi.org/10.1021/jm00101a023>.
26. Hazarika M, White RM, Johnson JR, Pazdur R. FDA drug approval summaries: pemetrexed (Alimta). *Oncologist.* 2004;9(5):482-488. <https://doi.org/10.1634/theoncologist.9-5-482>.
27. Worzalla JF, Shih C, Schultz RM. Role of folic acid in modulating the toxicity and efficacy of the multitargeted antifolate, LY231514. *Anticancer Res.* 1998;18(5a):3235-3239.
28. Zazuli Z, Kos R, Veltman JD, Uyterlinde W, Longo C, Baas P, et al. Comparison of Myelotoxicity and Nephrotoxicity Between Daily Low-Dose Cisplatin With Concurrent Radiation and Cyclic High-Dose Cisplatin in Non-Small Cell Lung Cancer Patients. *Front Pharmacol.* 2020;11:975. <https://doi.org/10.3389/fphar.2020.00975>.
29. Joerger M, Huitema AD, Krähenbühl S, Schellens JH, Cerny T, Reni M, et al. Methotrexate area under the curve is an important outcome predictor in patients with primary CNS lymphoma: A pharmacokinetic-pharmacodynamic analysis from the IELSG no. 20 trial. *Br J Cancer.* 2010;102(4):673-677. <https://doi.org/10.1038/sj.bjc.6605559>.
30. Chabner BA, Young RC. Threshold methotrexate concentration for in vivo inhibition of DNA synthesis in normal and tumorous target tissues. *J Clin Invest.* 1973;52(8):1804-1811. <https://doi.org/10.1172/jci107362>.
31. Howard SC, McCormick J, Pui CH, Buddington RK, Harvey RD. Preventing and managing toxicities of high-dose methotrexate. *Oncologist.* 2016;21(12):1471-1482. <https://doi.org/10.1634/theoncologist.2015-0164>.
32. European Medicines Agency. Alimta: EPAR-Scientific discussion. 2006.
33. European Medicines Agency. Alimta: EPAR-Product information. 2017.
34. European Medicines Agency. Filgrastim hexal: EPAR-Product information. 2019.
35. Ellman MH, Telfer MC, Turner AF. Benefit of G-CSF for methotrexate-induced neutropenia in rheumatoid arthritis. *Am J Med.* 1992;92(3):337-338. [https://doi.org/10.1016/0002-9343\(92\)90088-s](https://doi.org/10.1016/0002-9343(92)90088-s).
36. Rattu MA, Shah N, Lee JM, Pham AQ, Marzella N. Glucarpidase (voraxaze), a carboxypeptidase enzyme for methotrexate toxicity. *P t.* 2013;38(12):732-744.
37. Auton T, Glover J, Melton R, Bastian G, Lovell E. In vitro demonstration that pemetrexed is a good substrate for glucarpidase. *Cancer Res.* 2007;67(4773).

## SUPPLEMENTAL MATERIAL

### *Current phase II study*

#### *Study methods*

Based on the findings of Latz *et al.*<sup>1</sup> we initiated a single arm phase II pharmacokinetic and safety study using a Simon two-stage design<sup>2</sup> in patients with a creatinine clearance < 45 mL/min (NCT03656549). Dosing of pemetrexed was based on creatinine clearance to attain a similar cumulative AUC as in patients with adequate renal function (164 mg·h/L ± 25%), since it was postulated that dosing to this target would result in a safe and effective treatment based on the previously established linear relationship between pemetrexed exposure and inhibition of neutrophil proliferation.<sup>3,4</sup> The dose in the first cycle was based on measured creatinine clearance and, as a safety measure, administered as 50% of the calculated dose. If this dose was deemed tolerable (< 3 grade neurotoxicity and based on the discretion and professional judgement of the treating physician) an intra-patient dose escalation was performed from the second dose onward. The dose in cycle 2 was based on the individual observed pemetrexed pharmacokinetics in the first cycle<sup>5</sup> and a recent (< 1 week pre-dose) estimation of creatinine clearance. Dosing in every subsequent cycle was adjusted in case of changing renal function and based on tolerability to pemetrexed in prior cycles. The main study endpoint was the fraction of patients who attained therapeutic exposure, defined as the target AUC of 164 mg·h/L ± 25%. Patients with a creatinine clearance < 45 mL/min who were eligible for treatment with pemetrexed and had Eastern Cooperative Oncology Group (ECOG) score of 0-2 were allowed to be included in the study. Patients with contra-indications for pemetrexed (except impaired renal function), co-medication with an influence on the pharmacokinetics of pemetrexed or patient related factors which can lead to inaccurate predications of renal function (e.g. obesity or limb amputation) were excluded. A total of 23 patients were planned to be included, with the first stage interim analysis after the first nine patients, this would yield a type I error of 0.05 and a power of 0.8.

#### *Study results*

In April and May of 2019, three patients with renal dysfunction were included in our phase II study. Table S1 shows the patient characteristics of these patients, the measured ANC nadir after the pemetrexed dose and the calculated area under the concentration-time curve. Although patient 1 (eGFR: 35.8 mL/min) developed a grade 3 neutropenia and a grade 1 papulopustular rash after the cycle 1 dose (302.5 mg), treatment was tolerated well and the adverse events were resolved before the next cycle. Patient 1 subsequently received 100% of the calculated dose (610 mg) in cycle 2 according to the study protocol. The patient again developed a grade 3 neutropenia and pemetrexed treatment was discontinued. Patient 2 and 3 (eGFR 34.6 and 8.4 mL/min, respectively) started pemetrexed treatment simultaneously and both developed general malaise and skin rash. The study was immediately put on hold due to the development of a severe pancytopenia including a grade 4 neutropenia in patient 3 after a 250 mg dose.

## Pharmacokinetic-pharmacodynamic analysis

### *General*

The pharmacokinetic-pharmacodynamic analysis was performed by means of non-linear mixed effects modelling with the software package NONMEM 7.4.3 (Icon, Ireland).

### *Structural model*

The base model for the development of the pemetrexed-induced neutropenic response was based on the model by Friberg *et al.*<sup>6</sup> and consisted of one progenitor compartment, three transit compartment and one observation compartment of circulating neutrophils with feedback to the progenitor compartment. The effect of pemetrexed on neutrophils was modelled as the function  $E_{drug}$  on the progenitor compartment. Equation 1 and 2 represent the function  $E_{drug}$  as a linear function (for the model with the linear exposure-toxicity relationship) or as an  $E_{max}$  model (for the threshold model) respectively.

$$E_{drug} = 1 - DS * C_{pmx} \quad (1)$$

$$E_{drug} = 1 - \frac{Emax * C_{pmx}^{\gamma}}{IC_{50}^{\gamma} + C_{pmx}^{\gamma}} \quad (2)$$

In these equations, DS is the dose stimulus of pemetrexed (in L/mg) and  $C_{pmx}$  is the concentration of pemetrexed (in mg/L).  $E_{max}$  is the maximal inhibitory effect of pemetrexed on the neutrophils.  $\gamma$  is the hill coefficient and  $IC_{50}$  is the pemetrexed concentration at which half of the maximum inhibitory effect on the neutrophils occurs and further called the threshold concentration. Since for methotrexate, a structural analogue of pemetrexed, it is known that concentrations around the threshold concentration greatly change the observed toxicity, we fixed the value for  $\gamma$  on a high value of 20.<sup>7</sup>

Pharmacokinetic (PK) parameters were fixed accordingly to values previously reported.<sup>8</sup> Next to DS,  $E_{max}$  and  $IC_{50}$ , parameters evaluated in the pharmacodynamic (PD) model were baseline absolute neutrophil count (baseline ANC), mean transit time (MTT; time from progenitor compartment to circulation compartment) and the feedback parameter. For MTT, our model did not identify a physiological plausible value, therefore this parameter was fixed to the value observed in the model with the linear exposure-toxicity relationship. The NONMEM code for the final threshold-driven model can be found at the end of this document. A schematic representation of the pharmacokinetic-pharmacodynamic model is shown in Figure S1, including the differential equations describing pemetrexed pharmacodynamic effects on the ANC.

### *Covariate model*

The effect of vitamin supplementation on the neutropenic response was the only covariate tested for the models. Based on the results of Worzalla *et al.*, showing vitamin supplementation results in similar toxicity at higher pemetrexed concentrations rather than decreasing the effect of pemetrexed's toxicity-related deaths, our model featured vitamin supplementation as binary covariate on the threshold concentration ( $IC_{50}$ ).<sup>9</sup>

*Statistical model*

Interindividual variability (IIV) was evaluated for the pharmacodynamic parameters with the use of the exponential model, as shown in equation 3.

$$P_i = P_p * \exp(\eta_i) \quad (3)$$

Where  $P_i$  is the individual estimated parameter,  $P_p$  is the typical or population estimated parameter and  $\eta_i$  is individual estimated value for the IIV.  $\eta$  follows a normal distribution with a mean value of zero and a variance of  $\omega^2$ . The covariance-variance matrix was used to identify covariance and subsequently correlations between individual random effects were derived.  $E_{max}$  and  $IC_{50}$  are correlated parameters, therefore IIV is only estimated on the  $E_{max}$ . Since, the initial estimate for MTT is fixed to the value found in the model with a linear exposure-toxicity relationship, the initial estimate for the IIV on this parameter is also fixed to the value found in the model with a linear exposure-toxicity relationship.

Initially, the difference between observed ANC<sub>s</sub> and the model-predicted ANC<sub>s</sub> was accounted for with a combined proportional and additive error model as shown in equation 4.

$$C_{obs,ij} = C_{pred,ij} * (1 + \epsilon_{p,ij}) + \epsilon_{a,ij} \quad (4)$$

Where  $C_{obs,ij}$  is the observed ANC,  $C_{pred,ij}$  is the predicted ANC,  $\epsilon_{p,ij}$  is the proportional error and  $\epsilon_{a,ij}$  is the additive error. Both proportional and additive errors have a mean of zero and a variance of  $\sigma^2$ .

Based on the estimates of this error model, it was observed that the use of only a proportional error model would be sufficient to describe the pharmacodynamic model.

*Model evaluation*

Models were assessed on several goodness of fit (GOF) plots such as predicted population ANC and predicted individual ANC versus observed ANC, conditional weighted residuals (CWRES) versus predicted population ANC and time after dose of pemetrexed. Furthermore, the models were assessed on physiological plausibility, stability of parameter estimates and change in objective function (OFV). A  $p < 0.05$  corresponding to a decrease of 3.84 in OFV was considered significant model improvement in case of nested models (degree of freedom = 1). Since the model with a linear exposure-toxicity relationship and the threshold model are not hierarchical models, the Akaike information criterion (AIC) was used to compare both models.<sup>10</sup> The uncertainty in parameter precision of the final models were determined by a sampling importance resampling (SIR) procedure.<sup>11</sup>

Table S2 describes the population estimates of the model with a linear exposure-toxicity relationship and the model with a threshold-driven exposure-toxicity relationship. The threshold model shows physiological plausible parameter estimates. When compared with the model with a linear exposure-toxicity relationship a drop in AIC of 33.6 points is observed. Figure S2 and S3

show the goodness-of-fit plots for the model with a linear exposure-toxicity relationship and the threshold model, respectively. Since, for both models, only a small proportion of the datapoints are lying outside the -3 and +3 interval for the CWRES and the data is homogeneously distributed around the unity line, little model misspecification is observed. The visual predictive check for the threshold model is illustrated in Figure S4. The predicted ANC<sub>s</sub> are overall in line with the observed ANC<sub>s</sub>, especially at the nadirs of the ANC<sub>s</sub>, indicating sufficient validity for both models.

#### External validation

For the external validation data from the early phase I studies by McDonald *et al.* and Rinaldi *et al.*<sup>12-14</sup> were used. The number of patients included on the dose level deemed the maximum tolerated dose (MTD) in these studies were six patients at 4 mg/m<sup>2</sup>/day for 5 days every 21 days<sup>12</sup>, six patients at 40 mg/m<sup>2</sup>/week for 4 weeks every 6 weeks<sup>13</sup> and 20 patients at 600 mg/m<sup>2</sup> every 21 days.<sup>14</sup> For the study by McDonald *et al.* we obtained demographic and pharmacokinetic data from the pemetrexed dosing in four out of six patients. For the studies by Rinaldi *et al.*, all of the study participants were assumed to be male of Caucasian origin with a weight of 70 kg and a BSA of 1.73 m<sup>2</sup>. In the absence of reported serum creatinine values, we assumed the eGFR based on the CKD-EPI to be 80 mL/min. We performed a posthoc analysis on these four patients in our previous developed PK model for pemetrexed<sup>8</sup> to obtain PK parameters most fitting to the individual data. The PK parameters for the remaining two patients as well as the patients in the studies by Rinaldi *et al.* were randomly drawn from a normal distribution based on the found parameters (typical values and interindividual variation) in the PK model. The number of patients on the dose levels were simulated a 1,000 times in the model with a linear exposure-toxicity relationship and the threshold-driven model. Neutropenia in the phase I studies was graded based on the ANC<sub>s</sub> on day 8 and day 15 of the study, therefore we simulated the ANC<sub>s</sub> of the patients on these time points. The lowest predicted ANC was used to determine the predicted grade of neutropenia. Figure S5-S7 illustrate the histograms per predicted grade of neutropenia of the simulations.

#### Evaluation of the relationship between renal function and development of neutropenia

For the simulations in which we assessed the typical ANC curves in patients and for the simulation illustrating the frequency of neutropenia across different renal functions, we assumed patients with a weight of 75 kg and a BSA of 2.0 m<sup>2</sup>. For the typical curves, the population predicted ANC was estimated every hour for 800 hours. For the assessment of  $\geq 3$  neutropenia across different renal functions after a 500 mg/m<sup>2</sup> pemetrexed dose, a total of 12 patients with different eGFR were simulated with a value of 5, 10, 15, 20, 25, 30, 35, 40, 45, 60, 75 and 90 mL/min. These patients were simulated a 1,000 times with and without vitamin supplementation. ANC<sub>s</sub> were followed every hour for 800 hours after the pemetrexed dose, the lowest found ANC was translated to the predicted grade of neutropenia.

Table S1. Patient characteristics and neutropenic response of the individual patients in our phase II study with inadequate renal function and a pemetrexed dose based on their renal function.

Patient	Age (years)	Gender	Dose (mg)	eGFR (calculated with CKD-EPI; mL/min)	Cumulative AUC (mg·h/L) (% of target AUC)	Absolute neutrophil count nadir ( $\cdot 10^9/L$ )
1	79	V	Cycle 1: 302.5	35.8 (both cycles)	79.0 (48.2)	0.5 (after cycle 1)
			Cycle 2: 610		171.8 (104.8)	0.6 (after cycle 2)
2	77	M	300	34.6	108.3 (66.0)	1.9
3	69	V	250	8.4	93.8 (57.2)	0.1

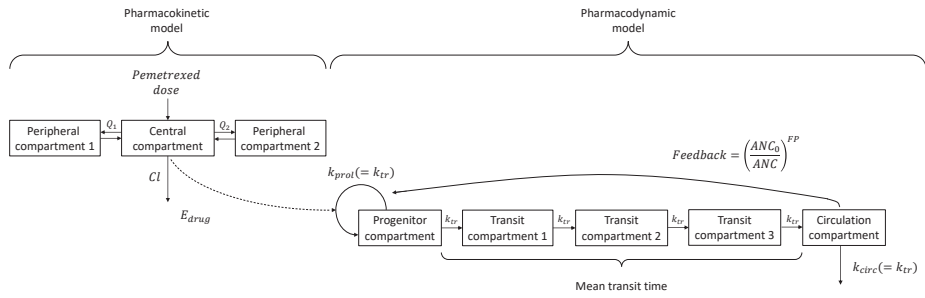
AUC: area under the concentration-time curve, CKD-EPI: Chronic Kidney Disease Epidemiology Collaboration, eGFR: estimated glomerular filtration rate

Table S2. Population estimates for the parameters in the model with a linear exposure-toxicity relationship and a threshold-driven relationship.

Parameter	Population estimate [SIR-derived 95% confidence interval]	
	Linear relationship	Threshold relationship
<b>Baseline ANC</b> ( $10^9/L$ )	5.43 [4.97-5.83]	5.30 [4.92-5.75]
IIV (%)	37.5 [31.6-44.1]	37.1 [31.9-43.3]
<b>MTT</b> (h)	103 [95.5-109.8]	103 FIX
VS on MTT	0.96 [0.906-1.028]	
IIV (%)	19.0 [15.4-23.7]	19.0 FIX
<b>Dose stimulus</b> (L/mg)	0.225 [0.189-0.268]	
VS on dose stimulus	0.691 [0.583-0.813]	
IIV (%)	54.7 [44.9-65.2]	
<b>E<sub>max</sub></b>		1.16 [0.96-1.37]
IIV (%)		54.3 [44.9-66.2]
<b>IC<sub>50</sub></b> (mg/L)		0.03 [0.017-0.047]
VS on IC <sub>50</sub>		3.66 [2.74-4.31]
<b>Gamma</b>		20 FIX
<b>Feedback parameter</b>	0.166 [0.149-0.183]	0.171 [0.155-0.186]
IIV (%)	27.2 [20.8-32.7]	29.0 [21.3-34.9]
<b>Proportional residual error</b>	0.127 [0.118-0.136]	0.124 [0.114-0.136]
<b>Objective function</b>	4670.8	4641.1
<b>AIC</b>	4690.8	4657.2

ANC: absolute neutrophil count, AIC: Akaike Information Criteria, FIX: value is fixed, IIV: intraindividual variability, VS: vitamin B11 and B12 supplementation, MTT: mean transit time





**Equations for  $E_{drug}$**   
 Linear model:  $1 - DS * C_{pmx}$

Threshold model:  $1 - \frac{E_{max} * C_{pmx}^\gamma}{IC_{50} + C_{pmx}^\gamma}$

**Differential equations**

$$\frac{\partial Prog}{\partial t} = -k_{tr} * Prog + k_{prol} * Prog * E_{drug} * Feedback$$

$$\frac{\partial T1}{\partial t} = -k_{tr} * T1 + k_{tr} * Prog$$

$$\frac{\partial T2}{\partial t} = -k_{tr} * T2 + k_{tr} * T1$$

$$\frac{\partial T3}{\partial t} = -k_{tr} * T3 + k_{tr} * T2$$

$$\frac{\partial obs}{\partial t} = -k_{circ} * Circ + k_{tr} * T3$$

Figure S1. Schematic representation of the pharmacokinetic-pharmacodynamic model including the differential equations describing pemetrexed pharmacodynamic effects on the ANC. Cl, total clearance; Q1 and Q2, intercompartmental clearances; ANC, absolute neutrophil count;  $ANC_0$ , ANC at baseline; FP, feedback parameter;  $k_{prol}$ , first-order rate constant of proliferation;  $k_{tr}$ , first-order rate constant of transit compartments;  $k_{circ}$ , first-order rate constant of circulating neutrophils;  $E_{drug}$ , inhibitory effect of pemetrexed on the neutrophils; DS, dose stimulus;  $C_{pmx}$ , pemetrexed plasma concentration;  $E_{max}$ , maximal inhibitory effect of pemetrexed on neutrophils;  $\gamma$ , hill coefficient;  $IC_{50}$ , pemetrexed threshold concentration; Prog, T1, T2, T3, Circ, ANC in progenitor compartment, transit compartment 1-3 and circulation compartment, respectively.

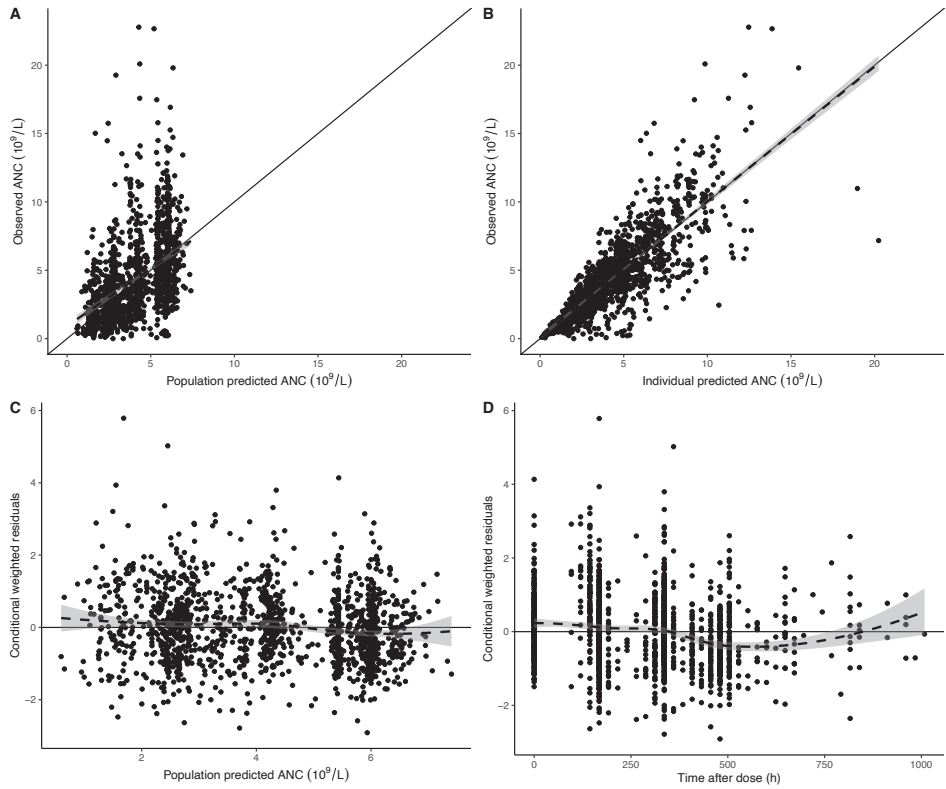


Figure S2. Standard goodness-of-fit plots for the model with a linear exposure-toxicity relationship. A) Population predicted ANC versus observed ANC. B) Individual predicted ANC versus observed ANC. C) Population predicted ANC versus conditional weighted residuals. D) Time after pemetrexed dose versus conditional weighted residuals. The solid black line represents the unity line, the loess line is represented by the dashed black line with a 95% CI illustrated in gray. Figure S2A and 2B show the acceptable correlation between the observed ANCs and the population and individual predicted ANCs. Since the data in Figure S2C and S2D is homogenous distributed with the unity line and lies mostly within the -3 and +3 interval, model misspecification is not indicated.

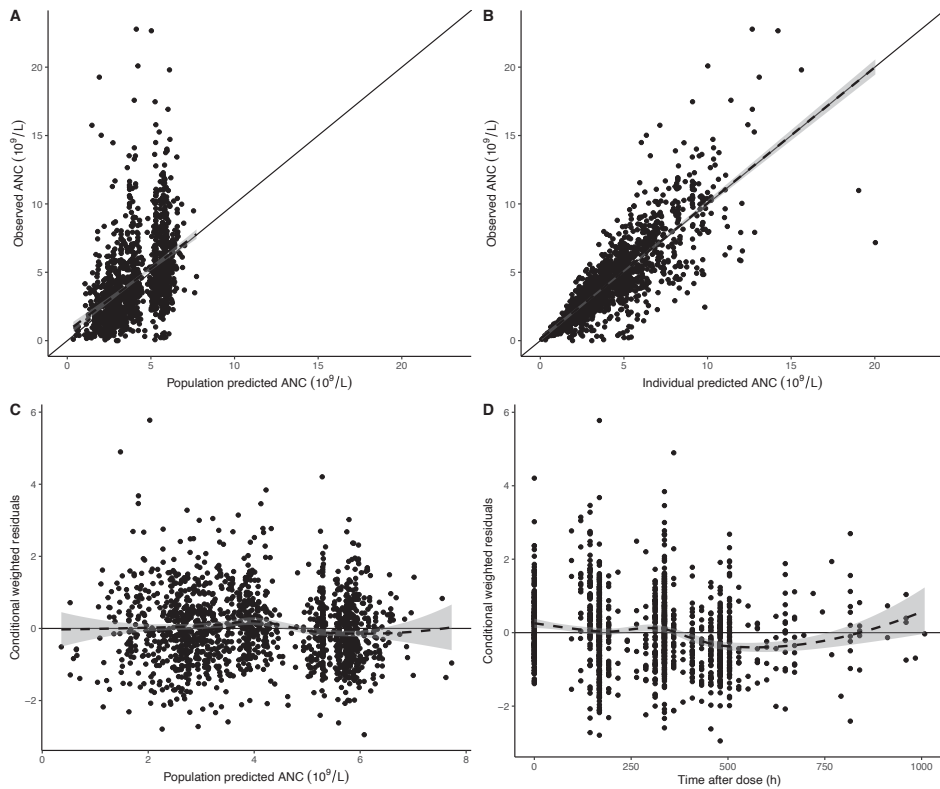


Figure S3. Standard goodness-of-fit plots for the threshold-driven model presented here. A) Population predicted ANC versus observed ANC. B) Individual predicted ANC versus observed ANC. C) Population predicted ANC versus conditional weighted residuals. D) Time after pemetrexed dose versus conditional weighted residuals. The solid black line represents the unity line, the loess line is represented by the dashed black line with a 95% CI illustrated in gray. Figure S3A and 3B show the acceptable correlation between the observed ANCs and the population and individual predicted ANCs. Since the data in Figure S3C and S3D is homogenous distributed with the unity line and lies mostly within the  $-3$  and  $+3$  interval, model misspecification is not indicated.

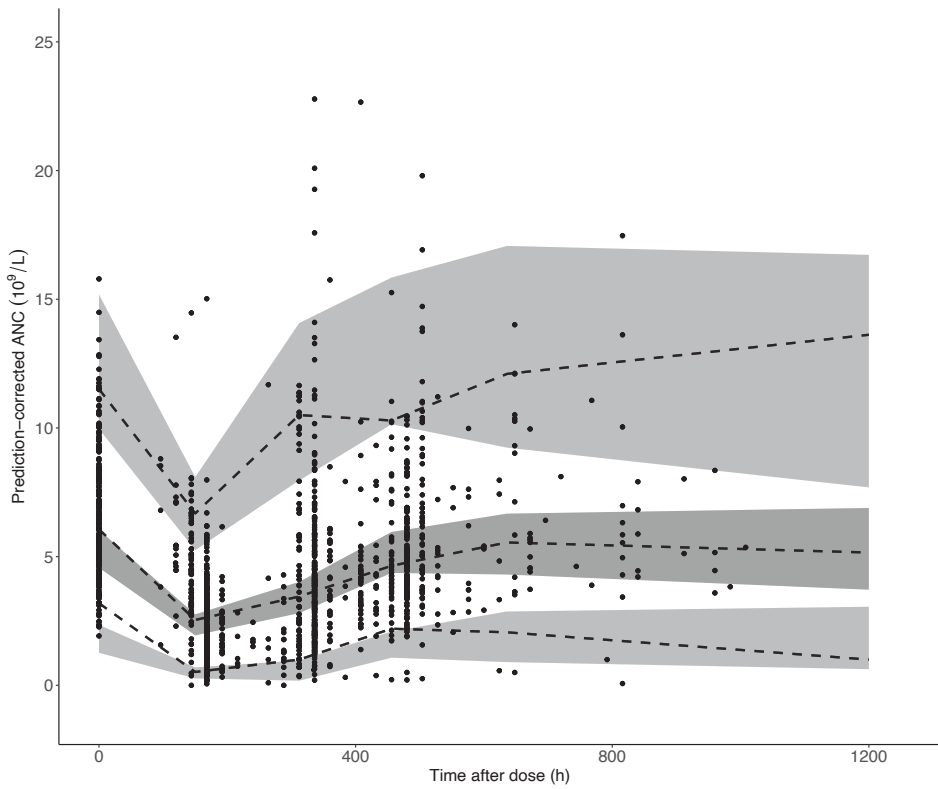


Figure S4. Visual predictive check for the threshold model. Observed ANCs are represented by the black points. The dashed lines represent the 5th, 50th and 95th percentile of the observed ANCs. The 95% confidence intervals for these percentiles are represented by the shaded gray areas.

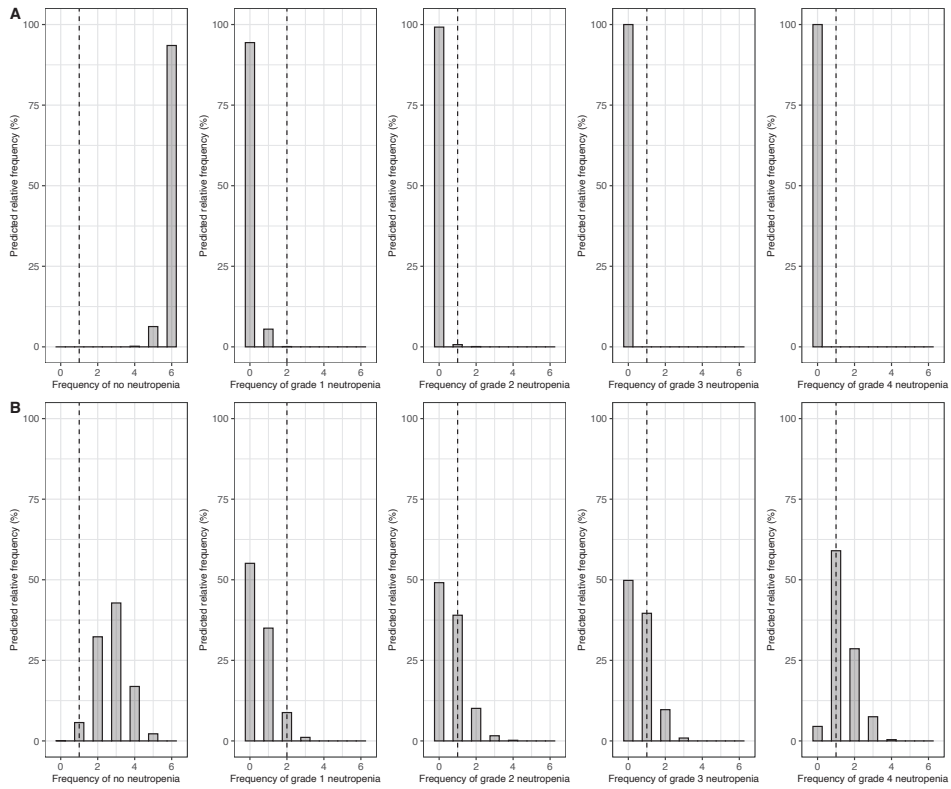


Figure S5. Frequencies of neutropenia found for the simulation of the study of McDonald et al. (1998)<sup>12</sup> in patients treated with 4 mg/m<sup>2</sup>/day pemetrexed for 5 consecutive days in A) the linear exposure-toxicity relationship and B) the threshold relationship. The panels from left to right represent the frequencies of no neutropenia, grade 1, grade 2, grade 3 and grade 4 neutropenia found in 6 patients. The vertical dashed line represents the value found in literature.

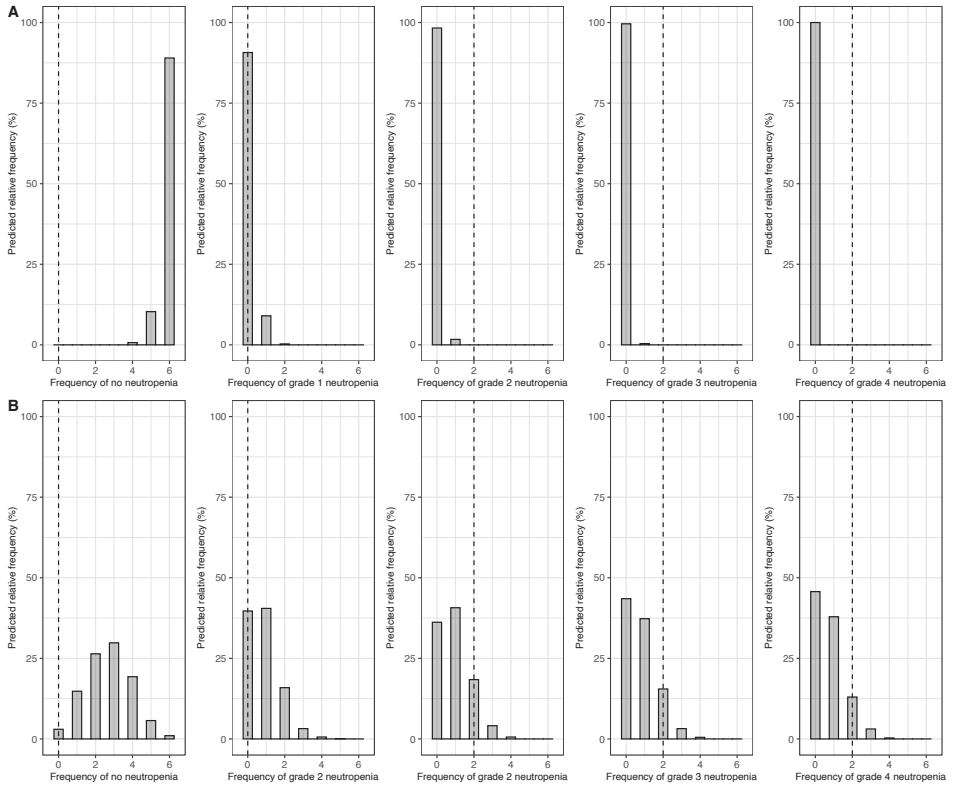


Figure S6. Frequencies of neutropenia found for the simulation of the study of Rinaldi et al. (1995)<sup>13</sup> in patients treated with 40 mg/m<sup>2</sup>/week pemetrexed for 4 consecutive weeks in A) the linear exposure-toxicity relationship and B) the threshold relationship. The panels from left to right represent the frequencies of no neutropenia, grade 1, grade 2, grade 3 and grade 4 neutropenia found in 6 patients. The vertical dashed line represents the value found in literature.

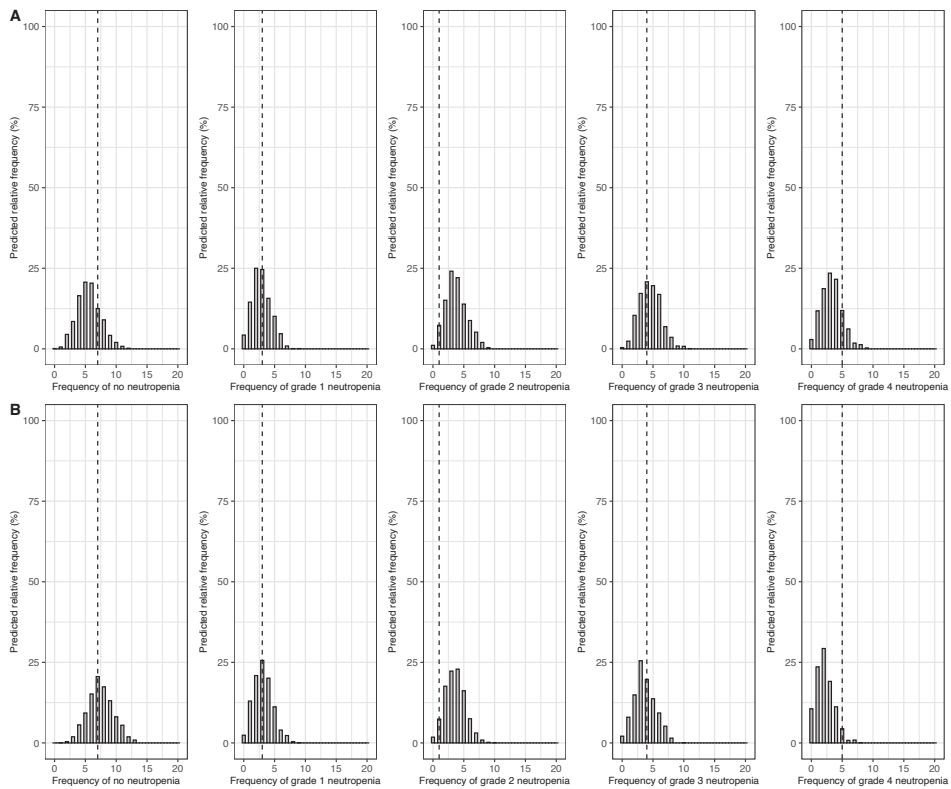


Figure S7. Frequencies of neutropenia found for the simulation of the study of Rinaldi et al. (1999)<sup>14</sup> in patients treated with 600 mg/m<sup>2</sup> pemetrexed in A) the linear exposure-toxicity relationship and B) the threshold relationship. The panels from left to right represent the frequencies of no neutropenia, grade 1, grade 2, grade 3 and grade 4 neutropenia found in 20 patients. The vertical dashed line represents the value found in literature.

**Final PKPD - NONMEM code**

```

$PROBLEM PKPD
$INPUT XX
$DATA XX IGNORE=@
$SUBROUTINES ADVAN13 TOL=9
$MODEL

; --- PK
COMP=(CENTRAL) ; 1 CENTRAL DOSING AND OBSERVATION COMPARTMENT
COMP=(PERI)    ; 2 PERIPHERAL PK
COMP=(PERI2)   ; 3 PERIPHERAL PK
; --- PD
COMP=(PROL)    ; 4 PROLIFERATION COMPARTMENT
COMP=(TRANS1) ; 5 TRANSIT COMPARTMENT
COMP=(TRANS2) ; 6 TRANSIT COMPARTMENT
COMP=(TRANS3) ; 7 TRANSIT COMPARTMENT
COMP=(ANC)     ; 8 NEUTROPHIL OBSERVATION COMPARTMENT

$ABBREV PROTECT

$PK
ALLOCL=(WT/70)**0.75 ;SCALING FOR base CL & Q
ALLOV=(WT/70)       ;SCALING FOR V

CLBASE = THETA(1) * ALLOCL
CLRENAL = THETA(2)
TVCL = CLBASE + (CLRENAL * (CKDEPI/75))
CL = TVCL * EXP(ETA(1))

V1 = THETA(3)*ALLOV*EXP(ETA(2))
Q = THETA(4)*ALLOCL
V2 = THETA(5)*ALLOV*EXP(ETA(3))
Q2 = THETA(6)*ALLOCL
V3 = THETA(7)*ALLOV*EXP(ETA(4))

D1=0.16667
S1=V1
S2=V2
S3=V3

```



$K_{10} = CL/V_1$

$K_{12} = Q/V_1$

$K_{21} = Q/V_2$

$K_{13} = Q_2/V_1$

$K_{31} = Q_2/V_3$

; --- BAS

BASINT=THETA(8)

BAS=BASINT \* EXP(ETA(5)) ; BASELINE NEUTROPHILS  $10^9/L$

; --- MTT

TVMTT= THETA(9)

MTT=TVMTT\*EXP(ETA(6)) ; MEAN TRANSIT TIME

; --- DRUG EFFECT

EMAX = THETA(10) \* EXP(ETA(7))

IC50 = THETA(11) \*(THETA(14))<sup>VIT</sup>

GAMMA = THETA(12)

; --- FP

FP=THETA(13)\*EXP(ETA(8))

; --- MASS TRANSIT

KTR=4/MTT

F4=BAS

F5=BAS

F6=BAS

F7=BAS

F8=BAS

\$DES

; --- PK

DADT(1)=-K10\*A(1)-K12\*A(1)-K13\*A(1)+K21\*A(2)+K31\*A(3)

DADT(2)=-K21\*A(2)+K12\*A(1)

DADT(3)=-K31\*A(3)+K13\*A(1)

C1=A(1)/V1

```

; --- PD
DRUG = 1-(EMAX*(C1**GAMMA)/((IC50**GAMMA)+(C1**GAMMA)))
FEEDB=(BAS/A(8))**FP
KPROL=KTR
KCIRC=KTR

DADT(4)=-KTR*A(4)+KPROL*A(4)*DRUG*FEEDB ; PROLIFERATION COMPARTMENT
DADT(5)=-KTR*A(5)+KTR*A(4) ; TRANSIT COMPARTMENT
DADT(6)=-KTR*A(6)+KTR*A(5) ; TRANSIT COMPARTMENT
DADT(7)=-KTR*A(7)+KTR*A(6) ; TRANSIT COMPARTMENT
DADT(8)=-KCIRC*A(8)+KTR*A(7) ; ANC

$ERROR
CC=A(1)/V1
A4=A(4)
A5=A(5)
A6=A(6)
A7=A(7)
A8=A(8)
IF(CMT.EQ.1)THEN
IPRED = CC
Y=IPRED+IPRED*ERR(1) ; PK ERROR MODEL
ENDIF
IF(CMT.EQ.8)THEN
IPRED = A8
Y=IPRED+IPRED*ERR(2) ; PD ERROR MODEL
ENDIF

$THETA
; --- PK
0.66 FIX ; 1 CLBASE
3.42 FIX ; 2 CLRENAL
6.70 FIX ; 3 V1
6.56 FIX ; 4 Q
8.01 FIX ; 5 V2
0.04 FIX ; 6 Q2
1.23 FIX ; 7 V3

```

; ---PD  
(0, 5.3) ; 8 BASINT  
103 FIX ; 9 TV MTT  
(0, 1.16) ; 10 EMAX  
(0, 0.03) ; 11 IC50  
20 FIX ; 12 GAMMA  
(0, 0.171) ; 13 FP  
(0, 3.66) ; 14 VS on IC50

\$OMEGA

; ---PK  
0.0441 FIX ; IIV CL  
\$OMEGA BLOCK(3)  
0.110 FIX ; IIV V1  
0.035 0.102 FIX ; IIV V2  
0.098 0.095 0.219 FIX ; IIV V3

\$OMEGA

; ---PD  
0.138 ; 5 IIV BAS  
0.0361 FIX ; 6 IIV MTT  
0.295 ; 7 IIV EMAX  
0.0839 ; 8 IIV FP

\$SIGMA

; --- PK  
0.0552 FIX ; PROP ERR PK  
; --- PD  
0.124 ; PROP ERR PD

## REFERENCES

1. Latz JE, Schneck KL, Nakagawa K, Miller MA, Takimoto CH. Population pharmacokinetic/pharmacodynamic analyses of pemetrexed and neutropenia: effect of vitamin supplementation and differences between Japanese and Western patients. *Clin Cancer Res.* 2009;15(1):346-354. <https://doi.org/10.1158/1078-0432.Ccr-08-0791>.
2. Simon R. Optimal two-stage designs for phase II clinical trials. *Control Clin Trials.* 1989;10(1):1-10. [https://doi.org/10.1016/0197-2456\(89\)90015-9](https://doi.org/10.1016/0197-2456(89)90015-9).
3. Latz JE, Rusthoven JJ, Karlsson MO, Ghosh A, Johnson RD. Clinical application of a semimechanistic-physiologic population PK/PD model for neutropenia following pemetrexed therapy. *Cancer Chemother Pharmacol.* 2006;57(4):427-435. <https://doi.org/10.1007/s00280-005-0035-2>.
4. Latz JE, Chaudhary A, Ghosh A, Johnson RD. Population pharmacokinetic analysis of ten phase II clinical trials of pemetrexed in cancer patients. *Cancer Chemother Pharmacol.* 2006;57(4):401-411. <https://doi.org/10.1007/s00280-005-0036-1>.
5. de Rouw N, Visser S, Koolen SLW, Aerts J, van den Heuvel MM, Derijks HJ, et al. A limited sampling schedule to estimate individual pharmacokinetics of pemetrexed in patients with varying renal functions. *Cancer Chemother Pharmacol.* 2020;85(1):231-235. <https://doi.org/10.1007/s00280-019-04006-x>.
6. Friberg LE, Henningsson A, Maas H, Nguyen L, Karlsson MO. Model of chemotherapy-induced myelosuppression with parameter consistency across drugs. *J Clin Oncol.* 2002;20(24):4713-4721. <https://doi.org/10.1200/jco.2002.02.140>.
7. Chabner BA, Young RC. Threshold methotrexate concentration for in vivo inhibition of DNA synthesis in normal and tumorous target tissues. *J Clin Invest.* 1973;52(8):1804-1811. <https://doi.org/10.1172/jci107362>.
8. de Rouw N, Boosman RJ, Huitema ADR, Hilbrands LB, Svensson EM, Derijks HJ, et al. Rethinking the application of pemetrexed for patients with renal impairment: a pharmacokinetic analysis. *Clin Pharmacokinet.* 2021;60(5):649-654. <https://doi.org/10.1007/s40262-020-00972-1>.
9. Worzalla JF, Shih C, Schultz RM. Role of folic acid in modulating the toxicity and efficacy of the multitargeted antifolate, LY231514. *Anticancer Res.* 1998;18(5a):3235-3239.
10. Akaike H. A new look at the statistical model identification. *IEEE Trans Automat Contr.* 1974;19(6):716-723. <https://doi.org/10.1109/TAC.1974.1100705>.
11. Dosne AG, Bergstrand M, Harling K, Karlsson MO. Improving the estimation of parameter uncertainty distributions in nonlinear mixed effects models using sampling importance resampling. *J Pharmacokinet Pharmacodyn.* 2016;43(6):583-596. <https://doi.org/10.1007/s10928-016-9487-8>.
12. McDonald AC, Vasey PA, Adams L, Walling J, Woodworth JR, Abrahams T, et al. A phase I and pharmacokinetic study of LY231514, the multitargeted antifolate. *Clin Cancer Res.* 1998;4(3):605-610.
13. Rinaldi DA, Burris HA, Dorr FA, Woodworth JR, Kuhn JG, Eckardt JR, et al. Initial phase I evaluation of the novel thymidylate synthase inhibitor, LY231514, using the modified continual reassessment method for dose escalation. *J Clin Oncol.* 1995;13(11):2842-2850. <https://doi.org/10.1200/jco.1995.13.11.2842>.
14. Rinaldi DA, Kuhn JG, Burris HA, Dorr FA, Rodriguez G, Eckhardt SG, et al. A phase I evaluation of multitargeted antifolate (MTA, LY231514), administered every 21 days, utilizing the modified continual reassessment method for dose escalation. *Cancer Chemother Pharmacol.* 1999;44(5):372-380. <https://doi.org/10.1007/s002800050992>.

# CHAPTER 4.3

# Cumulative pemetrexed dose increases the risk of nephrotoxicity

*Lung Cancer. 2020;146:30-35*

Nikki de Rouw  
René J. Boosman  
Heidi van de Bruinhorst  
Bonne Biesma  
Michel M. van den Heuvel  
David M. Burger  
Luuk B. Hilbrands  
Rob ter Heine  
Hieronymus J. Derijks

Author's contribution: R.J. Boosman contributed to the design of this study, performed the data management and supervised H. van de Bruinhorst who collected the data and conducted the data analysis. R.J. Boosman provided comments on the first draft of the manuscript.

# ABSTRACT

## Introduction

Pemetrexed is a pharmacotherapeutic cornerstone in the treatment of non-small cell lung cancer. As it is primarily eliminated by renal excretion, adequate renal function is essential to prevent toxic exposure. There is growing evidence for the nephrotoxic potential of pemetrexed, which even becomes a greater issue now combined immuno-chemotherapy prolongs survival. Therefore, the aim of this study was to describe the incidence of nephrotoxicity and related treatment consequences during pemetrexed-based treatment.

## Methods

A retrospective cohort study was conducted in the Jeroen Bosch Hospital, Den Bosch, The Netherlands. All patients that received at least 1 cycle of pemetrexed based therapy were included in the dataset. The primary outcome was defined as a  $\geq 25\%$  reduction in eGFR. Additionally, the treatment consequences of decreased renal function were assessed. Logistic regression was used to identify risk factors for nephrotoxicity during treatment with pemetrexed.

## Results

Of the 359 patients included in this analysis, 21% patients had a clinically relevant decline in renal function after treatment and 8.1% of patients discontinued treatment due to nephrotoxicity. Cumulative dose ( $\geq 10$  cycles of pemetrexed based therapy) was identified as a risk factor for the primary outcome measure (adjusted OR 5.66 (CI 1.73-18.54)).

## Conclusion

This study shows that patients on pemetrexed-based treatment are at risk of developing renal impairment. Risk significantly increases with prolonged treatment. Renal impairment is expected to become an even greater issue now that pemetrexed-based immuno-chemotherapy results in longer survival and thus longer treatment duration.

## INTRODUCTION

Pemetrexed is widely used as an anti-folate cytostatic agent for the treatment of non-small cell lung cancer (NSCLC), mesothelioma and thymoma.<sup>1-5</sup> Dependent on treatment indication, therapy generally exists of four cycles of induction therapy with pemetrexed and a platinum-agent, which can be combined with the recently approved programmed death-ligand 1 (PD-L1) targeting monoclonal antibody pembrolizumab.<sup>6</sup> Pemetrexed - and, if applicable, pembrolizumab - can be continued as maintenance treatment following the induction period.<sup>3, 6</sup>

Pemetrexed is primarily eliminated by renal excretion, with 70-90% of the dose recovered as the unchanged drug in urine within the first 24 hours after administration.<sup>4, 7</sup> Previous studies showed that pemetrexed pharmacokinetics are linearly correlated with creatinine clearance.<sup>8, 9</sup> Thus, to prevent high exposure, an adequate renal function is essential. Decreased creatinine clearance and higher exposure were shown to be associated with more severe hematologic toxicity.<sup>8, 10-13</sup> Due to these safety issues and based on the study of Mita *et al.* (2006), pemetrexed is currently contraindicated in patients with a creatinine clearance < 45 mL/min.<sup>4, 14</sup>

Cancer patients are already at increased risk of developing renal insufficiency, possibly due to volume depletion, advanced age of patients and the use of potentially nephrotoxic anti-cancer therapy.<sup>15-17</sup> For treatment in non-small cell lung cancer, the most common nephrotoxic anti-cancer drugs are platinum-agents, and possibly also the checkpoint-inhibitors.<sup>17-21</sup> In addition, there is now accumulating evidence for the nephrotoxic potential of pemetrexed itself. Several case reports describe incidents of (sub)acute kidney injury during or after pemetrexed therapy.<sup>22-29</sup> In the PARAMOUNT study, during pemetrexed maintenance, 7.8% of patients developed renal impairment (versus 2.3% in the placebo group) and 4% of patients discontinued therapy due to nephrotoxicity.<sup>30</sup> However, as with many registration studies, this represents only the incidence in a specific trial population. The available literature describing renal complications during pemetrexed therapy in daily practice consists mainly focusses on acute kidney injury.

The development of renal toxicity is potentially a major limitation for safe, long-term pemetrexed treatment because according to current recommendation pemetrexed dosing has to be terminated when CrCl falls below 45 mL/min. This is highly undesirable for all patients with positive clinical response to pemetrexed, but in particular to patients treated with pemetrexed-based immunotherapy who demonstrate longer survival and thus longer treatment durations.<sup>6</sup> Therefore, there is an urgent need for better knowledge on preventing and managing of pemetrexed-associated renal toxicity.

The aim of this study was to describe the incidence of nephrotoxicity and related treatment consequences during pemetrexed-based therapy. The secondary objective was to identify risk factors for the decrease in renal function.



## METHODS

### Study design and population

This retrospective cohort study was performed in the Jeroen Bosch Hospital, Den Bosch, The Netherlands and approved by the local medical research ethics committee. The medical ethics committee waived the necessity of acquiring informed consent. Through a system search in the hospital information systems (HiX, Chipsoft, version 6.1 and Centrasys, CSC, version 6.30.0.50-4.1) all consecutive patients who received at least 1 cycle of pemetrexed between January 1<sup>st</sup> 2014 and February 1<sup>st</sup> 2019 were identified.

### Data collection

All data used in this study were collected as part of routine care. For each patient the following patient demographics were obtained: Sex, ethnicity, age, weight and length at baseline, diagnosis, pre-treatment, number of neutropenic events and comorbidities and comedication affecting renal function (see appendix for details). Length and weight were used to calculate Body Surface Area (BSA, according to Du Bois and Du Bois' formula<sup>31</sup>) and Body Mass Index (BMI).

Regarding pemetrexed-based therapy, dates of the initial cycle (defined as baseline) and the last cycle of pemetrexed-based therapy were collected. In addition, pemetrexed dose and concomitant chemo- and/or immunotherapy at baseline, total number of cycles pemetrexed, and the date and reason of discontinuation of treatment were obtained. For patients still on treatment during data analysis, their last cycle before May 13<sup>th</sup> 2019 was considered as last cycle of therapy for analysis.

For the assessment of renal function, serum creatinine was used. Measurements of serum creatinine ( $\mu\text{mol/L}$ ) at baseline and at the end of therapy were collected. The cut-off date for the measurements at baseline was a maximum of 28 days prior to the initial chemotherapy cycle, or – only if not available – a maximum of 7 days after the initial chemotherapy cycle. The cut-off dates for the measurements at the end of therapy were a maximum of 28 days after the last cycle, or – only if not available – a maximum of 7 days prior to the last cycle. The estimated glomerular filtration rate (eGFR) ( $\text{mL}/\text{min}/1.73\text{m}^2$ ) was calculated using the Chronic Kidney Disease Epidemiology Collaboration equation (CKD-EPI).<sup>32</sup> Additionally, the occurrence of acute kidney injury (AKI) during therapy (as a reported diagnosis in the patient file by the physician) was investigated.

### Outcome

The primary outcome was defined as a  $\geq 25\%$  reduction in eGFR (in accordance with the Kidney Disease: Improving Global Outcomes (KDIGO) clinical practice guidelines<sup>33</sup>). The relative change in eGFR from baseline (bs) to end of therapy (eot) was calculated for each patient as:

$$\frac{(eGFR_{bs} - eGFR_{eot})}{eGFR_{bs}} * 100\%$$

To assess the treatment consequences of decreased renal function in patients with pemetrexed-based treatment, the incidence of treatment discontinuation due to nephrotoxicity and combined nephrotoxicity and hematologic toxicity was investigated. The secondary outcome was the identification of potential risk factors for nephrotoxicity during pemetrexed-based treatment.

#### *Statistical analysis*

Descriptive statistics were used to calculate the primary outcome measures. To identify risk factors for the development of renal impairment during pemetrexed-based therapy, the sample set was divided in cases (patients with  $\geq 25\%$  reduction in renal function) and non-cases. For both cases and controls, the prevalence of each variable was determined. All variables were expressed as categorical data. Within a variable, categories were divided based on equal group sizes. Multivariate logistic regression was used to calculate odds ratios for the various risk factors. The tested variables included: sex, age, body mass index (BMI), number of comorbidities and comedications affecting renal function, smoking status, pre-treatment, concomitant induction therapy and total number of cycles. Based on the first analysis, age and gender were included as potential confounding factors, resulting in adjusted odds ratios for all tested variables. A Bonferroni correction was applied to correct for multiple testing, resulting in an adjusted p-value for significance of  $p = 0.005$ . Accordingly, odds ratios were calculated with 99.5% confidence intervals (CI). All statistical analyses were performed using SPSS version 22.0 (IBM, Armonk, NY, USA). As an exploratory objective, the incidence of neutropenic events in both the cases and non-cases was calculated. A Fisher's exact test was applied to assess for significant difference.

## RESULTS

#### *Patient demographics*

The system search identified 386 patients who received at least one cycle of pemetrexed between January 1<sup>st</sup> 2014 and February 1<sup>st</sup> 2019. Due to missing data regarding pemetrexed therapy and/or serum creatinine measurements, 27 patients were excluded. The final analysis dataset consisted of 359 patients.

In Table 1 the baseline characteristics are presented. Gender was well balanced within the study population (54% male). The median age was 65 years. Approximately half of patients had a baseline eGFR of  $> 90$  mL/min/1.73m<sup>2</sup> (53%). The majority of patients was diagnosed with stage IV NSCLC (69%) and was treatment-naïve (73%). The number of received pemetrexed-based cycles had a wide range of 1-103, with a median of 4 cycles and median follow-up time of 3 months.

Table 1. patient demographics and results of risk factor analysis for development of renal impairment during pemetrexed-based treatment.

Parameter	Total n (%) 359 (100)	Cases n (%) 74 (21)	Controls n (%) 285 (79)	OR adjusted [99.5% CI]	p-value ( $< 0.005 =$ significant)
<b>Sex</b>					
Male	195 (54)	33 (45)	162 (57)	Reference	
Female	164 (46)	41 (55)	123 (43)	1.68 [0.79-3.59]	0.056
<b>Age (mean: 64.9, range 32-86 years)</b>					
0-60 years	104 (29)	17 (23)	87 (31)	Reference	
61-69 years	135 (38)	39 (53)	96 (34)	2.15 [0.86-5.41]	0.020
$\geq 70$ years	120 (33)	18 (24)	102 (36)	1.02 [0.35-2.92]	0.967
<b>Baseline eGFR (CKD-EPI)</b>					
$\geq 90$ mL/min/1.73m <sup>2</sup>	189 (53)	35 (47)	154 (54)	Reference	
$< 90$ mL/min/1.73m <sup>2</sup>	170 (47)	39 (53)	131 (46)	1.35 [0.59-3.09]	0.305
<b>BMI</b>					
$< 25$ kg/m <sup>2</sup>	185 (52)	32 (43)	153 (54)	Reference	
25-30 kg/m <sup>2</sup>	130 (36)	29 (39)	101 (35)	1.43 [0.63-3.24]	0.224
$> 30$ kg/m <sup>2</sup>	44 (12)	13 (18)	31 (11)	1.86 [0.63-5.52]	0.109
<b>Diagnosis</b>					
Mesothelioma	27 (7.5)	3 (11)	24 (8.4)	Reference	
NSCLC stage I-III	84 (23)	13 (18)	71 (25)	1.35 [0.19-9.55]	0.666
NSCLC stage IV	246 (69)	57 (77)	189 (66)	2.35 [0.38-14.59]	0.188
Other	2 (0.6)	1 (1.4)	1 (0.4)	n/a	n/a
<b>Pre-treatment</b>					
No pretreatment	261 (73)	56 (76)	205 (72)	Reference	
Pretreatment	98 (27)	18 (24)	80 (28)	0.81 [0.35-1.90]	0.483
<b>Smoking status</b>					
Never	20 (5.6)	2 (2.7)	18 (6.3)	Reference	
Past	129 (36)	31 (42)	98 (34)	3.00 [0.34-26.60]	0.157
Current ( $< 20$ cigarettes/day)	120 (33)	22 (30)	98 (34)	2.14 [0.24-19.38]	0.335
Current ( $\geq 20$ cigarettes/day)	68 (19)	16 (22)	52 (18)	2.97 [0.31-28.41]	0.177
Not known	22 (6.1)	3 (4.1)	19 (6.7)	1.61 [0.10-24.83]	n/a
<b>Number of comorbidities</b>					
None	80 (22)	12 (16)	68 (24)	Reference	
One	116 (32)	23 (31)	93 (33)	1.53 [0.50-4.62]	0.284
Two	107 (30)	24 (32)	83 (29)	1.81 [0.60-5.52]	0.134
Three or more	56 (16)	15 (20)	41 (14)	2.32 [0.67-8.08]	0.058

Table 1. Continued.

Parameter	Total n (%) 359 (100)	Cases n (%) 74 (21)	Controls n (%) 285 (79)	OR adjusted [99.5% CI]	p-value ( $< 0.005$ = significant)
<b>Number of comedications</b>					
None	152 (42)	27 (37)	125 (44)	Reference	0.658
One	128 (36)	25 (34)	103 (36)	1.15 [0.48-2.73]	0.085
Two or more	79 (22)	22 (30)	57 (20)	1.77 [0.70-4.51]	
<b>Concomitant induction therapy</b>					
No induction therapy	22 (6.1)	5 (6.8)	17 (6.0)	Reference	
Cisplatin	123 (34)	25 (34)	98 (34)	0.90 [0.19-4.32]	0.847
Carboplatin	179 (50)	35 (47)	144 (51)	0.85 [0.18-4.00]	0.775
Other	35 (9.7)	9 (12)	26 (9.1)	n/a	n/a
<b>Total number of cycles (median 4; range 1-103)</b>					
1-2	79 (22)	10 (14)	69 (24)	Reference	
3-4	144 (40)	18 (24)	126 (44)	0.96 [0.29-3.15]	0.921
5-9	68 (19)	15 (20)	53 (19)	1.98 [0.56-6.96]	0.130
$\geq 10$	68 (19)	31 (42)	37 (13)	5.66 [1.73-18.54]	$< 0.001$

CI: confidence interval, BMI: body mass index, CKD-EPI: Chronic Kidney Disease Epidemiology Collaboration equation, eGFR: estimated glomerular filtration rate, NSCLC: non-small cell lung cancer, OR: odds ratio

#### *Decrease in renal function and treatment consequences*

The mean eGFR (CKD-EPI) at baseline was  $87.8 \pm 15.4$  mL/min/1.73m<sup>2</sup>. In total, 21% of the patients (74 out of 359) had a clinically relevant decrease in eGFR of  $\geq 25\%$  from baseline to end of treatment. The mean absolute change of eGFR over treatment time was a decrease of 8.6 mL/min/1.73m<sup>2</sup> (mean eGFR at the end of therapy was  $79.2 \pm 22.5$  mL/min/1.73m<sup>2</sup>). This corresponds with a mean relative change of eGFR during therapy of -9.6%. As reported in the patient files by the physician, only 1.9% of patients had AKI.

Decrease in renal function can eventually lead to cessation of effective therapy. In our cohort 8.1% of patients discontinued treatment due to nephrotoxicity. In approximately one-third of these patients, nephrotoxicity was accompanied with hematotoxicity. From the patients with a clinically relevant decline in renal function (cases), 35.1% experienced  $\geq 1$  neutropenic event, compared to 13.7% in the controls ( $p < 0.001$ ).

#### *Risk factors for the development of renal impairment*

Table 1 summarizes the results of the analysed risk factors. The cumulative dose of pemetrexed ( $\geq 10$  cycles) was a significant risk factor (adjusted OR 5.66 (1.73-18.54),  $p$ -value  $< 0.001$ ). Figure 1 visualizes the number of cycles versus the relative change in eGFR. The graph shows a relation between the treatment duration and decrease in renal function. No significant effect was observed for the other tested variables.

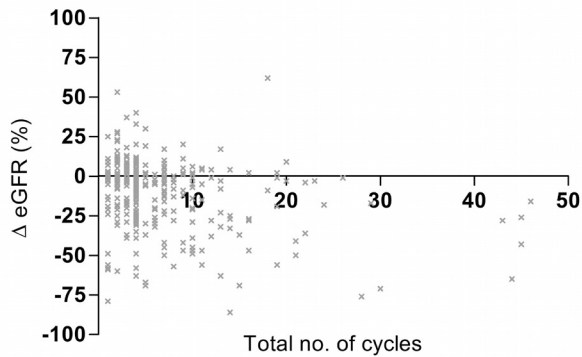


Figure 1. Total number of cycles versus relative change in eGFR n.b.: for clarity, the datapoint of 103 cycles is not visualized in the graph.

## DISCUSSION

To our knowledge this is the first study to investigate both the incidence and a broad panel of associated risk factors for renal impairment during pemetrexed-based therapy in a relatively large population in every day clinical practice. It confirms the nephrotoxic potential of pemetrexed. We demonstrated that, in clinical practice, approximately one-fifth of patients on pemetrexed-based therapy have a clinically relevant decline in eGFR. Additionally, around 8% of patients had to cease treatment due to nephrotoxicity. The risk of renal impairment increases with longer treatment duration ( $\geq 10$  cycles of pemetrexed-based treatment: adjusted OR 5.66 (1.73-18.54)) and is associated with an increased risk on hematotoxicity.

In the PARAMOUNT study (a phase III study of maintenance treatment with pemetrexed versus placebo), the investigators reported an incidence of 7.8% for renal toxicities and 4% of treatment discontinuation due to renal toxicity.<sup>34, 35</sup> Interestingly, the researchers also suggest the potential risk for a cumulative effect of pemetrexed on renal toxicity.<sup>35</sup> The incidence in our patient cohort is three times greater. Our patient population representing clinical practice has, when compared to the trial population, probably more heterogeneous performance score and more comorbidities and comedication affecting renal function. It is suggested that a physiologic decline in renal function in adults  $> 65$  years is 0.75 mL/min per year.<sup>36</sup> In our cohort, the difference between mean eGFR at baseline and end of treatment was 8.6 mL/min/1.73m<sup>2</sup> over a median follow-up time of three months. In the PARAMOUNT study, no effect on renal function was observed in the placebo group refuting the suggestion that the occurrence of clinically relevant decline in renal function might reflect the natural course. Therefore, the observed decline in renal function in our cohort can be attributable to treatment. In addition, it is generally known that cancer patients frequently suffer from sarcopenia, which may lead to overestimation of renal function<sup>37</sup> and thus, the actual prevalence of renal impairment may be even higher.

Visser *et al.* (2018) recently investigated the occurrence of renal impairment during pemetrexed maintenance therapy in clinical practice prospectively.<sup>38</sup> In their cohorts, 15-20% of patients ceased treatment due to nephrotoxicity, versus 8.1% in our study. Additionally, they report a very high incidence of AKI of 29.5% in their primary cohort, compared to approximately 2% in our population.<sup>38</sup> An explanation for these discrepancies is the possibility of underreporting in our study, as we only collected the AKI diagnoses that were reported by the physicians in the patient files. Our main objective focussed on gradual decline of renal function rather than acute injury.

As it stands, risk factors for pemetrexed-related nephrotoxicity have not been extensively studied. Visser *et al.* included a set of treatment-related factors associated with AKI and found baseline eGFR to be an important determinant. This finding was not confirmed in our study. In line with the findings of Langer *et al.* (2017) and Middleton *et al.* (2018), we also found an increasing risk of renal impairment with longer exposure to pemetrexed-based treatment.<sup>35, 39</sup> A significant effect was observed in the patient group that received > 10 cycles pemetrexed. The number of patients in this group was relatively small (n = 68), which is reflected in the large confidence interval. Nevertheless, there was a clear trend with increasing number of cycles, indicating an actual effect rather than a coincidental finding.

In our cohort, use of cisplatin in induction therapy was not associated with increased risk of renal impairment, despite its nephrotoxic potential. Extensive pre- and post-hydration schedules and administration of diuretics are nowadays used to minimize cisplatin nephrotoxicity, which may explain why cisplatin coadministration does not pose an additional risk. Another risk factor for nephrotoxicity is the use of radiocontrast agents.<sup>40</sup> Unfortunately, data on use of contrast was not available in the dataset. Theoretically, the amount of CT scans increases proportionally with the amount of cycles and are therefore difficult to distinguish. In the general population with normal renal function at baseline, the incidence of contrast-induced nephropathy is estimated to be low (1-2%)<sup>40</sup>, much lower than the incidence of nephrotoxicity in this study. Additionally, both cisplatin and radiocontrast are mainly associated with acute nephrotoxicity rather than chronic decline of renal function.<sup>19, 21, 40, 41</sup> Altogether, the significant effect of cumulative dose implies a possible causal relationship between pemetrexed and renal impairment.

A few limitations of the present study have to be taken into consideration. First, it was a retrospective study with its flaws. Not all data might have been captured by the electronic patient file. Despite this design we were able to confirm the findings of previous studies. Secondly, whereas the combination of pembrolizumab with a pemetrexed and platinum has now become the preferred first line treatment the number of patients with this combination in the study is very limited. It is expected that the number of cycles of pemetrexed per patients will increase because of the increased disease control because of combined chemoimmunotherapy.<sup>6</sup> Besides, the checkpoint-inhibitors also have nephrotoxic potential,<sup>18, 20</sup> but this mainly manifests as acute kidney injury. In the KEYNOTE-189 trial, acute kidney injury occurred more frequently in the pembrolizumab-combination group than in the placebo-combination group (5.2% vs. 0.5%).<sup>6</sup> Nevertheless, combining immunotherapy with chemotherapy may increase the risk for long term nephrotoxicity

as both agents have nephrotoxic potential and because patients have longer treatment duration, but we do not have data to support this synergistic toxicity. Thirdly, for assessing renal function, we calculated eGFR according to the CKD-EPI equation, which is not validated for eGFR > 90 mL/min. This could have led to incorrect calculation of the relative change of eGFR and thus, to misclassification of cases and controls. In order to assess the impact of using the CKD-EPI, a second analysis was performed using absolute serum creatinine (results not shown). This analysis yielded similar results on both the primary outcome and the risk factor analysis, indicating that inaccuracies in the calculation of eGFR had no significant impact on our conclusions.

One may argue that pemetrexed excretion interferes with creatinine clearance, as both are partially eliminated by active tubular secretion. The organic anion transporter 3 (OAT3) is involved in pemetrexed elimination, while organic cation transporter 2 (OCT2) is responsible for the active secretion of creatinine.<sup>42-44</sup> However, OAT3 was also shown to be involved in creatinine excretion in mice.<sup>45</sup> Nevertheless, we consider the possible effects of pemetrexed on creatinine secretion not relevant for our analysis as end of treatment serum creatinine measurements were not performed within 24 hours of pemetrexed administration. Pemetrexed has a relatively short half-life (3.5 hours), whereas up to 90% is excreted within the first 24 hours.<sup>9</sup>

In conclusion, this study shows that patients on pemetrexed-based treatment are at risk of developing clinically relevant renal impairment. Risk significantly increases with prolonged treatment, which suggests the cumulative dose of pemetrexed may be an important risk factor for the development of nephrotoxicity. Renal impairment is expected to become an even greater issue now that pemetrexed-based immuno-chemotherapy results in longer survival and thus longer treatment duration. Our data call for innovative interventions to allow safe and effective long-term treatment with pemetrexed. Also, further research is needed to investigate the incidence of renal impairment in patients using both pembrolizumab and pemetrexed, as well as the reversibility of renal impairment after discontinuing pemetrexed therapy.

## REFERENCES

- Baldwin CM, Perry CM. Pemetrexed: a review of its use in the management of advanced non-squamous non-small cell lung cancer. *Drugs*. 2009;69(16):2279-2302. <https://doi.org/10.2165/11202640-000000000-00000>.
- Hazarika M, White RM, Jr., Booth BP, Wang YC, Ham DY, Liang CY, et al. Pemetrexed in malignant pleural mesothelioma. *Clin Cancer Res*. 2005;11(3):982-992.
- Paz-Ares LG, de Marinis F, Dediu M, Thomas M, Pujol JL, Bidoli P, et al. PARAMOUNT: Final overall survival results of the phase III study of maintenance pemetrexed versus placebo immediately after induction treatment with pemetrexed plus cisplatin for advanced nonsquamous non-small-cell lung cancer. *J Clin Oncol*. 2013;31(23):2895-2902. <https://doi.org/10.1200/jco.2012.471102>.
- European Medicines Agency. Alimta: EPAR-Product information. 2017.
- Gubens MA. Treatment updates in advanced thymoma and thymic carcinoma. *Curr Treat Options Oncol*. 2012;13(4):527-534. <https://doi.org/10.1007/s11864-012-0211-7>.
- Gandhi L, Rodriguez-Abreu D, Gadgeel S, Esteban E, Felip E, De Angelis F, et al. Pembrolizumab plus chemotherapy in metastatic non-small-cell lung cancer. *N Engl J Med*. 2018;378(22):2078-2092. <https://doi.org/10.1056/NEJMoa1801005>.
- Rinaldi DA, Kuhn JG, Burris HA, Dorr FA, Rodriguez G, Eckhardt SG, et al. A phase I evaluation of multitargeted antifolate (MTA, LY231514), administered every 21 days, utilizing the modified continual reassessment method for dose escalation. *Cancer Chemother Pharmacol*. 1999;44(5):372-380. <https://doi.org/10.1007/s002800050992>.
- Latz JE, Chaudhary A, Ghosh A, Johnson RD. Population pharmacokinetic analysis of ten phase II clinical trials of pemetrexed in cancer patients. *Cancer Chemother Pharmacol*. 2006;57(4):401-411. <https://doi.org/10.1007/s00280-005-0036-1>.
- Ouellet D, Periclou AP, Johnson RD, Woodworth JR, Lalonde RL. Population pharmacokinetics of pemetrexed disodium (ALIMTA) in patients with cancer. *Cancer Chemother Pharmacol*. 2000;46(3):227-234. <https://doi.org/10.1007/s002800000144>.
- Ando Y, Hayashi T, Ujita M, Murai S, Ohta H, Ito K, et al. Effect of renal function on pemetrexed-induced haematotoxicity. *Cancer Chemother Pharmacol*. 2016;78(1):183-189. <https://doi.org/10.1007/s00280-016-3078-7>.
- Latz J, Adachi S, Symanowski J, Nakagawa K, Tamura T, Hanna N, et al. PD4-3-4: Correlation of pemetrexed (PEM) NSCLC exposure-response relationships (ERRs) to clinical study results from western and Japanese patient populations. *J Thorac Oncol*. 2007;2(8):S455-S456. <https://doi.org/10.1097/01.JTO.0000283390.06980.49>.
- Latz JE, Karlsson MO, Rusthoven JJ, Ghosh A, Johnson RD. A semimechanistic-physiologic population pharmacokinetic/pharmacodynamic model for neutropenia following pemetrexed therapy. *Cancer Chemother Pharmacol*. 2006;57(4):412-426. <https://doi.org/10.1007/s00280-005-0077-5>.
- Latz JE, Rusthoven JJ, Karlsson MO, Ghosh A, Johnson RD. Clinical application of a semimechanistic-physiologic population PK/PD model for neutropenia following pemetrexed therapy. *Cancer Chemother Pharmacol*. 2006;57(4):427-435. <https://doi.org/10.1007/s00280-005-0035-2>.
- Mita AC, Sweeney CJ, Baker SD, Goetz A, Hammond LA, Patnaik A, et al. Phase I and pharmacokinetic study of pemetrexed administered every 3 weeks to advanced cancer patients with normal and impaired renal function. *J Clin Oncol*. 2006;24(4):552-562. <https://doi.org/10.1200/jco.2004.00.9720>.
- Christiansen CF, Johansen MB, Langeberg WJ, Fryzek JP, Sørensen HT. Incidence of acute kidney injury in cancer patients: a Danish population-based cohort study. *Eur J Intern Med*. 2011;22(4):399-406. <https://doi.org/10.1016/j.ejim.2011.05.005>.
- Launay-Vacher V, Eteessami R, Janus N, Spano JP, Ray-Coquard I, Oudard S, et al. Lung cancer and renal insufficiency: prevalence and anticancer drug issues. *Lung*. 2009;187(1):69-74. <https://doi.org/10.1007/s00408-008-9123-5>.
- Perazella MA. Onco-nephrology: Renal toxicities of chemotherapeutic agents. *Clin J Am Soc Nephrol*. 2012;7(10):1713-1721. <https://doi.org/10.2215/cjn.02780312>.
- Cortazar FB, Marrone KA, Troxell ML, Ralto KM, Hoenig MP, Brahmer JR, et al. Clinicopathological features of acute kidney injury associated with immune checkpoint inhibitors. *Kidney Int*. 2016;90(3):638-647. <https://doi.org/10.1016/j.kint.2016.04.008>.



19. Goldstein RS, Mayor GH. Minireview. The nephrotoxicity of cisplatin. *Life Sci.* 1983;32(7):685-690. [https://doi.org/10.1016/0024-3205\(83\)90299-0](https://doi.org/10.1016/0024-3205(83)90299-0).
20. Perazella MA, Shirali AC. Nephrotoxicity of cancer immunotherapies: Past, present and future. *J Am Soc Nephrol.* 2018;29(8):2039-2052. <https://doi.org/10.1681/asn.2018050488>.
21. Saffirstein R, Winston J, Goldstein M, Moel D, Dikman S, Guttenplan J. Cisplatin nephrotoxicity. *Am J Kidney Dis.* 1986;8(5):356-367. [https://doi.org/10.1016/s0272-6386\(86\)80111-1](https://doi.org/10.1016/s0272-6386(86)80111-1).
22. Assayag M, Rouvier P, Gauthier M, Costel G, Cluzel P, Mercadal L, et al. Renal failure during chemotherapy: renal biopsy for assessing subacute nephrotoxicity of pemetrexed. *BMC Cancer.* 2017;17(1):770. <https://doi.org/10.1186/s12885-017-3705-7>.
23. Chauvet S, Courbebaisse M, Ronco P, Plaisier E. Pemetrexed-induced acute kidney injury leading to chronic kidney disease. *Clin Nephrol.* 2014;82(6):402-406. <https://doi.org/10.5414/cn107921>.
24. Fung E, Anand S, Bhalla V. Pemetrexed-induced nephrogenic diabetes insipidus. *Am J Kidney Dis.* 2016;68(4):628-632. <https://doi.org/10.1053/j.ajkd.2016.04.016>.
25. Glezerman IG, Pietanza MC, Miller V, Seshan SV. Kidney tubular toxicity of maintenance pemetrexed therapy. *Am J Kidney Dis.* 2011;58(5):817-820. <https://doi.org/10.1053/j.ajkd.2011.04.030>.
26. Michels J, Spano JP, Brocheriou I, Deray G, Khayat D, Izzedine H. Acute tubular necrosis and interstitial nephritis during pemetrexed therapy. *Case Rep Oncol.* 2009;2(1):53-56. <https://doi.org/10.1159/000208377>.
27. Sbitti Y, Chahdi H, Slimani K, Debbagh A, Mokhlis A, Albouzidi A, et al. Renal damage induced by pemetrexed causing drug discontinuation: a case report and review of the literature. *J Med Case Rep.* 2017;11(1):182. <https://doi.org/10.1186/s13256-017-1348-6>.
28. Vootukuru V, Liew YP, Nally JV, Jr. Pemetrexed-induced acute renal failure, nephrogenic diabetes insipidus, and renal tubular acidosis in a patient with non-small cell lung cancer. *Med Oncol.* 2006;23(3):419-422. <https://doi.org/10.1385/mo.23.3.419>.
29. Zattera T, Londrino F, Trezzi M, Palumbo R, Granata A, Tatangelo P, et al. Pemetrexed-induced acute kidney failure following irreversible renal damage: two case reports and literature review. *J Nephropathol.* 2017;6(2):43-48. <https://doi.org/10.15171/jnp.2017.07>.
30. Gridelli C, de Marinis F, Thomas M, Prabhask K, El Kouri C, Blackhall F, et al. Final efficacy and safety results of pemetrexed continuation maintenance therapy in the elderly from the PARAMOUNT phase III study. *J Thorac Oncol.* 2014;9(7):991-997. <https://doi.org/10.1097/jto.0000000000000207>.
31. Du Bois D, Du Bois EF. A formula to estimate the approximate surface area if height and weight be known. 1916. *Nutrition.* 1989;5(5):303-311; discussion 312-303.
32. Levey AS, Stevens LA, Schmid CH, Zhang YL, Castro AF, 3rd, Feldman HI, et al. A new equation to estimate glomerular filtration rate. *Ann Intern Med.* 2009;150(9):604-612. <https://doi.org/10.7326/0003-4819-150-9-200905050-00006>.
33. Kidney Disease: Improving Global Outcomes. Clinical practice guideline for the evaluation and management of chronic kidney disease. *Kidney Int Suppl.* 2013;3(1):1-150.
34. Pujol JL, Paz-Ares L, de Marinis F, Dediu M, Thomas M, Bidoli P, et al. Long-term and low-grade safety results of a phase III study (PARAMOUNT): maintenance pemetrexed plus best supportive care versus placebo plus best supportive care immediately after induction treatment with pemetrexed plus cisplatin for advanced nonsquamous non-small-cell lung cancer. *Clin Lung Cancer.* 2014;15(6):418-425. <https://doi.org/10.1016/j.clc.2014.06.007>.
35. Middleton G, Gridelli C, De Marinis F, Pujol JL, Reck M, Ramlau R, et al. Evaluation of changes in renal function in PARAMOUNT: a phase III study of maintenance pemetrexed plus best supportive care versus placebo plus best supportive care after induction treatment with pemetrexed plus cisplatin for advanced nonsquamous non-small-cell lung cancer. *Curr Med Res Opin.* 2018;34(5):865-871. <https://doi.org/10.1080/03007995.2018.1439462>.
36. Hommos MS, Glasscock RJ, Rule AD. Structural and functional changes in human kidneys with healthy aging. *J Am Soc Nephrol.* 2017;28(10):2838-2844. <https://doi.org/10.1681/asn.2017040421>.
37. Stevens LA, Coresh J, Greene T, Levey AS. Assessing kidney function-measured and estimated glomerular filtration rate. *N Engl J Med.* 2006;354(23):2473-2483. <https://doi.org/10.1056/NEJMra054415>.
38. Visser S, Huisbrink J, van 't Veer NE, van Toor JJ, van Boxem AJM, van Walree NC, et al. Renal impairment during pemetrexed maintenance in patients with advanced nonsmall cell lung cancer: a cohort study. *Eur Respir J.* 2018;52(4). <https://doi.org/10.1183/13993003.00884-2018>.

39. Langer CJ, Paz-Ares LG, Wozniak AJ, Gridelli C, de Marinis F, Pujol JL, et al. Safety analyses of pemetrexed-cisplatin and pemetrexed maintenance therapies in patients with advanced non-squamous NSCLC: retrospective analyses from 2 phase III studies. *Clin Lung Cancer*. 2017;18(5):489-496. <https://doi.org/10.1016/j.clcc.2017.04.003>.
40. Kidney Disease: Improving Global Outcomes. Clinical practice guideline for acute kidney injury. *Kidney Int Suppl*. 2012;2(1):1-138.
41. Stark JJ, Howel SB. Nephrotoxicity of cis-platinum (II) dichlorodiammine. *Clin Pharmacol Ther*. 1978;23(4):461-466. <https://doi.org/10.1002/cpt1978234461>.
42. Ikemura K, Hamada Y, Kaya C, Enokiya T, Muraki Y, Nakahara H, et al. Lansoprazole exacerbates pemetrexed-mediated hematologic toxicity by competitive inhibition of renal basolateral human organic anion transporter 3. *Drug Metab Dispos*. 2016;44(10):1543-1549. <https://doi.org/10.1124/dmd.116.070722>.
43. Kurata T, Iwamoto T, Kawahara Y, Okuda M. Characteristics of pemetrexed transport by renal basolateral organic anion transporter hOAT3. *Drug Metab Pharmacokinet*. 2014;29(2):148-153. <https://doi.org/10.2133/dmpk.dmpk-13-rg-042>.
44. Ciarimboli G, Lancaster CS, Schlatter E, Franke RM, Sprowl JA, Pavenstädt H, et al. Proximal tubular secretion of creatinine by organic cation transporter OCT2 in cancer patients. *Clin Cancer Res*. 2012;18(4):1101-1108. <https://doi.org/10.1158/1078-0432.Ccr-11-2503>.
45. Vallon V, Eraly SA, Rao SR, Gerasimova M, Rose M, Nagle M, et al. A role for the organic anion transporter OAT3 in renal creatinine secretion in mice. *Am J Physiol Renal Physiol*. 2012;302(10):F1293-1299. <https://doi.org/10.1152/ajprenal.00013.2012>.

## SUPPLEMENTAL MATERIAL

### Appendix A

*Comedications affecting renal function (C.A. Naughton 2008)*

- Vancomycine
- Aminoglycosides
- Ciprofloxacin
- Sulphonamides
- Cotrimoxazol
- NSAIDs (chronic use)
- Herpes antivirals ((val)aciclovir, (val)ganciclovir, foscarnet)
- Calcineurin inhibitors (tacrolimus, ciclosporin, pimecrolimus)
- Antidiuretics (thiazides, triamterene, loop diuretics)
- RAAS-inhibitors (ACE-inhibitors + ARB)
- Methotrexate
- Lithium
- HIV antivirals (tenofovir + protease inhibitors)
- Bisphosphonates iv
- Amphotericin B (conventional and liposomal)
- Allopurinol

Comorbidities:

- Hypertension
- Heart failure
- Other CVD
- Diabetes
- Gout
- COPD/asthma
- Liver disease
- Obesity
- Prior renal disease



# APPENDICES



CONCLUSIONS AND  
FUTURE PERSPECTIVES

SUMMARY

NEDERLANDSE SAMENVATTING

AUTHOR AFFILIATIONS

LIST OF PUBLICATIONS

DANKWOORD

CURRICULUM VITAE



# Conclusions and future perspectives





## CONCLUSIONS AND FUTURE PERSPECTIVES

Cancer drug dose optimization remains an important, yet often neglected part in current treatment paradigms. This thesis focuses on some of the gaps in knowledge regarding this frequently forgotten part of precision medicine in the treatment of non-small cell lung cancer (NSCLC). Several considerations, as outlined in **Table 1** should be taken into account with regard to these approaches. In **Figure 1** the steps and approaches of dose optimizations are illustrated, it is indicated how each chapter in this thesis is related to them.

Table 1. Key points to consider for dose optimizations.

<p><b>Knowledge regarding the therapeutic window</b></p> <p>There is often a delicate balance between efficacy and toxicity during therapy. Development of tools to obtain knowledge regarding the narrow therapeutic window is challenging.</p>
<p><b>Factors influencing or predicting exposure</b></p> <p>Dosing based on covariates or derived from pharmacokinetic measurement are promising strategies to enhance the proportion of patients dosed within the therapeutic range.</p>
<p><b>Toxicity of anticancer drugs</b></p> <p>The development of toxicity during therapy is multifactorial, sometimes additional strategies are necessary to ensure safe dosing.</p>

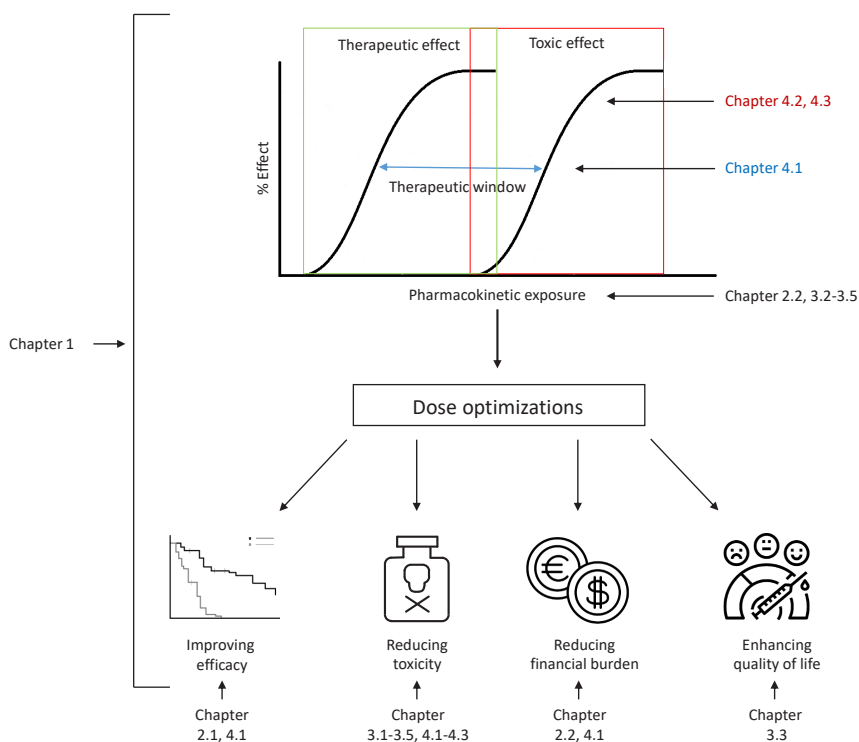


Figure 1. Graphical representation of the dose optimization steps and approaches as described in this thesis.

## KNOWLEDGE REGARDING THE THERAPEUTIC WINDOW

For most anticancer drugs, exposure has been related to both efficacy and toxicity of treatment<sup>1-3</sup>, thus the final goal in the clinical pharmacology of these drugs is to find that dose that balances between these parameters. Once knowledge regarding the width of this therapeutic window has been obtained, efforts can be made to ensure individuals are dosed within the therapeutic range. However, as highlighted in **Chapter 1**, for most drugs approved for the treatment of NSCLC, solid knowledge regarding this therapeutic window is lacking or ignored for dose optimizations.

For chemotherapeutic agents, a body surface area (BSA)-based dosing strategy is generally applied. However, this dosing strategy might be of limited value to attain a therapeutic range in the population. Especially for chemotherapeutic agents it is important to administer the right dose from the first dose onwards and, therefore, more accurate predictors for drug exposure are warranted. For carboplatin, a drug with an extensive renal clearance, inclusion of renal function measures in the dosing approach has been found to significantly decrease the variability in exposure of this drug<sup>4</sup>, and currently this predictor is used for dosing purposes.

For pemetrexed, it is assumed that efficacy is related to its exposure (partly based on its analogy with methotrexate). Renal function acts as important determinant for the systemic exposure to this drug. Nonetheless, dose optimization based on renal function is not readily performed. **Chapter 3.3** describes a prospective study, in which we compared a renal-based dosing of pemetrexed to the standard-of-care (BSA-based) dosing in patients with adequate renal function (estimated glomerular filtration rate (eGFR) > 45 mL/min). We showed a (non-statistical significant) trend between decreased renal function and increased exposure to pemetrexed using BSA-based dosing. Unfortunately, the study included few patients with a renal function below or above average (eGFR: 45-60 mL/min and > 120 mL/min, respectively) and thus, we added limited knowledge regarding the exposure to pemetrexed in these subpopulations. On the other hand, the results of our study indicated that for most patients with an adequate renal function, the current BSA-based dosing might be non-inferior to renal function based dosing with regard to pharmacokinetic exposure. For patients with an inadequate renal function (eGFR < 45 mL/min), however, we found that extrapolation of the approved dose might not be as straightforward as was initially thought and even cautious approaches might result in unwanted adverse effects (**Chapter 4.2**).

A few decades ago, chemotherapeutic agents were the only drugs available for treatment of cancer. Consequently, when the era of oral targeted therapies and immunotherapy commenced, clinical trial programs retained their dose-finding methods by dosing on the maximum tolerated dose. Currently, concerns have been raised for the ways these clinical trials are designed for these new drugs.<sup>5</sup> For example, flat exposure-response curves have been observed for most of the programmed cell death protein 1 (PD-1) and programmed cell death-ligand 1 (PD-L1) inhibitors in their current fixed dosing scheme.<sup>6</sup> Therefore, decreasing the dose might not influence efficacy or toxicity of therapy, however, lower fixed doses will substantially reduce the high healthcare costs associated with these drugs.<sup>7</sup> In addition, this knowledge might allow for a prolongation of the

dosing interval, reducing infusion-related costs and increasing quality of life by offering additional flexibility for patients.<sup>8</sup> Similarly, we showed in **Chapter 4.1** that the exposure to osimertinib in terms of trough concentrations is not related to efficacy in clinical practice at the approved dose. This has also been found in a previous study, assessing the exposure-response relationship in a clinical trial population.<sup>9</sup> For other oral tyrosine kinase inhibitors (TKIs) in this mutant epidermal growth factor receptor (EGFR)-targeting drug class, exposure-efficacy relationships are often absent in the current dosing schedule, while exposure-toxicity relationships are present.<sup>10-12</sup> This shows that EGFR inhibitors are currently dosed on the plateau of the exposure-efficacy curve and thus reduction in the approved dose might maintain efficacy while decreasing adverse events.

Generally speaking, the quest to obtain knowledge regarding the therapeutic window for anticancer drugs, is not always as straightforward as it seems. Tools to make predictions regarding the subgroups (e.g. patients with a higher or lower than average drug exposure) should be further explored. For instance, comparing the pharmacokinetics and pharmacodynamics of drugs within the same drug class could be valuable to manage the expectation regarding efficacy and toxicity.

A

## FACTORS INFLUENCING OR PREDICTING EXPOSURE

As highlighted in **Chapter 1**, the current dosing strategies for the SMIs and cytotoxic agents approved for treatment of NSCLC do not contribute to the fine balance between maximal efficacy and minimum toxicity for the individual patient. Therefore, it is necessary to find predictors for drug exposure, which can be used for dose optimizations. These predictors can be divided into two potentially synergistic approaches. On the one side, covariate-based dosing could be implemented with regard to patient characteristics including renal function (**Chapter 3.1-3.3**), age (**Chapter 3.5**), weight and/or co-medications (**Chapter 2.2**). On the other hand, PK-guided dosing in terms of therapeutic drug monitoring (TDM) or implementation of a test dose (**Chapter 3.4**) might prove helpful.

### *Covariate-based dosing*

Patients with renal impairment, elderly patients and patients with interacting co-medications are often excluded from clinical trials. However, these patients do reflect the general NSCLC population, thus, studies to assess the effects of these factors are warranted. In **Chapter 3.2**, we found for pemetrexed, that the implementation of renal function is able to reduce the interindividual variability in clearance of this drug. This effect is even more pronounced than found in earlier studies.<sup>13</sup> Since it has been postulated that exposure is related to both efficacy and toxicity (**Chapter 1**), dosing on renal function proves a promising dose optimization strategy for pemetrexed. Prospective trials should elucidate whether renal-function based dosing is indeed as effective and less toxic for patients with an above or below average renal function.

For elderly patients, it has been found that age-dependent physiological alterations might influence pharmacokinetic parameters. Dependent on drug characteristics, this may lead to sub- or supratherapeutic drug exposure. In **Chapter 3.5**, we investigated whether age has a statistical

significant and clinically relevant influence on pharmacokinetics of the hydrophilic drug gemcitabine. Our trial did not find that age should be included as a covariate contributing to dose optimization of gemcitabine. However, this cannot be generally extrapolated for other drugs and, therefore, pharmacokinetic studies in the elderly population remain a necessity.<sup>14</sup>

Many cancer patients suffer from co-morbidities, for which co-medication is administered. Drug-drug interactions with anticancer drugs can result in an increase or decrease of systemic exposure and thus might affect treatment outcome. However, interacting medication might also be used to boost the exposure of the drug. In **Chapter 2.2**, we showed the feasibility of a pharmacokinetic boosting agent (such as ritonavir) to increase the exposure to TKIs. Due to the rapid development of new TKIs, it is expected that the impact of TKI-treatment on the health care budget will quickly increase. Decreasing the dose and adding an affordable boosting drug, is an option to control drug cost. Since it is expected that the interpatient variability in CYP3A4 expression during inhibition is lowered, concomitant intake could also prove to be beneficial to reduce the pharmacokinetic variability of the boosted drug. In addition, in **Chapter 2.1**, we postulated that these combination strategies might not only be beneficial to increase systemic exposure, but might ameliorate tumor exposure of taxane-based chemotherapeutics by avoiding resistance mechanisms. In addition, some of these boosting agents might even have slight antitumor efficacy on its own.<sup>15</sup> Currently, the exact mechanisms of these synergistic effects are not fully known and should be further elucidated.

#### *PK-guided dosing*

Another way to predict exposure is by measurement of drug concentrations and subsequent dose adaptation. This strategy might allow for partial eradication of (un)known factors influencing the variability of drug exposure. TDM in oncology is able to reduce interindividual variability and is a promising tool to find the optimal, individual dose for many drugs.<sup>16</sup> Among other criteria, the presence of an exposure-response relationship and high interindividual variability in exposure to the drug are crucial factors favoring implementation of TDM.<sup>17</sup> However, in their approved dosing, clinically relevant exposure-response relationships were not present for all drugs currently nominated for TDM (**Chapter 4.1**). The combination of tailored lower doses and the implementation of TDM could be of value for such cases, especially if lower doses are cost-effective.

The best way to explore the pharmacokinetics of a drug in an individual is by administration of that drug. However, with regard to safety of the drug, a therapeutic dose might not always be suited for study purposes. Consequently, the pharmacokinetics of low test doses have frequently been reported to be a predictor of the pharmacokinetics of a therapeutic dose.<sup>18,19</sup> Therefore, we performed a proof-of-concept study to demonstrate the predictive performance of a test dose (**Chapter 3.4**). Although, we showed that a low test dose of pemetrexed is able to predict the pharmacokinetics of a therapeutic dose, we also found that renal function is superior in predicting the clearance of pemetrexed. Therefore, the highly invasive method (which might affect the quality-of-life) of administration of a test dose to optimize dosing for pemetrexed is not preferred.

Altogether, knowledge regarding factors which play major roles in the interindividual variability in exposure to drugs is essential. Dosing drugs with regard to these factors might allow to improve dosing inside the narrow therapeutic window of most drugs.

## TOXICITY OF ANTICANCER DRUGS

Toxicity of anticancer therapy is a major concern causing dose reductions, treatment delay or treatment discontinuations. In **Chapter 4.2**, we unraveled the relationship between the exposure to pemetrexed and neutropenia. We found that the time-above-threshold concentration of pemetrexed is driving the development of neutropenia. For methotrexate, a structural analogue to pemetrexed, this effect has already been observed.<sup>20</sup> As mentioned above, an adequate renal function will result in a sufficient clearance of pemetrexed, and thus, the exposure to pemetrexed (in terms of area under the concentration-time curve), might be a surrogate marker for the time-above-threshold concentration. However, this relationship might be distorted in case of decreased clearance of pemetrexed. As a result, we observed that an extremely lower dose was neutropenia-equivalent in this patient group when compared to patients with an adequate renal function. The prospective evaluation of prophylactic strategies (such as folinic acid or pegfilgrastim, which are used to prevent hematological toxicities to occur during methotrexate treatment<sup>21, 22</sup>) should be performed.

Combination treatment regimens (such as chemo-immunotherapy; as pointed out in **Chapter 3.1**) are becoming more standard of therapy and have shown to improve survival.<sup>23, 24</sup> Since this will inevitably lead to an increase in the number of cycles of chemotherapy, we need to prevent the introduction of a downward spiral in which the development of long-term adverse events will affect treatment efficacy (**Chapter 4.3**).

## FINAL REMARKS

Currently, the dosing guidelines in drug labels are often outdated and based on the limited research available during development. As a result, they often miss crucial dose adaptations for the general population or a fraction of these patients (e.g. patients with a decreased renal function or elderly). However, absence of solid evidence cannot simply lead to holding back effective therapies from those with characteristics outside the general population. For some drugs, justification of dose adaptations in clinical practice can already be substantiated by the strings of evidence found in the broad range of post-approval studies. This thesis focuses on different approaches for dose optimizations in the treatment of NSCLC and gives a foundation for further research. Introduction of a more extensive exploration of pharmacokinetic and pharmacodynamics relationships in clinical drug development programs should improve dose optimizations for drugs to come. In addition, we need to identify factors influencing efficacy, toxicity and quality of life and economic consequences of dosing strategies for the currently approved drugs. Only when these factors for dose optimizations are addressed, the full potential of precision medicine can be realized.

## REFERENCES

1. Groenland SL, Geel DR, Janssen JM, de Vries N, Rosing H, Beijnen JH, et al. Exposure-response analyses of anaplastic lymphoma kinase inhibitors crizotinib and alectinib in non-small cell lung cancer patients. *Clin Pharmacol Ther.* 2021;109(2):394-402. <https://doi.org/10.1002/cpt.1989>.
2. Joerger M, Huitema AD, Richel DJ, Dittrich C, Pavlidis N, Briasoulis E, et al. Population pharmacokinetics and pharmacodynamics of paclitaxel and carboplatin in ovarian cancer patients: a study by the European organization for research and treatment of cancer-pharmacology and molecular mechanisms group and new drug development group. *Clin Cancer Res.* 2007;13(21):6410-6418. <https://doi.org/10.1158/1078-0432.Ccr-07-0064>.
3. Jodrell DI, Egorin MJ, Canetta RM, Langenberg P, Goldbloom EP, Burroughs JN, et al. Relationships between carboplatin exposure and tumor response and toxicity in patients with ovarian cancer. *J Clin Oncol.* 1992;10(4):520-528. <https://doi.org/10.1200/jco.1992.10.4.520>.
4. Calvert AH, Newell DR, Gumbrell LA, O'Reilly S, Burnell M, Boxall FE, et al. Carboplatin dosage: prospective evaluation of a simple formula based on renal function. *J Clin Oncol.* 1989;7(11):1748-1756. <https://doi.org/10.1200/jco.1989.7.11.1748>.
5. Mathijssen RHJ, Sparreboom A, Verweij J. Determining the optimal dose in the development of anticancer agents. *Nat Rev Clin Oncol.* 2014;11(5):272-281. <https://doi.org/10.1038/nrclinonc.2014.40>.
6. Centanni M, Moes DJAR, Trocóniz IF, Ciccolini J, van Hasselt JGC. Clinical pharmacokinetics and pharmacodynamics of immune checkpoint inhibitors. *Clin Pharmacokinet.* 2019;58(7):835-857. <https://doi.org/10.1007/s40262-019-00748-2>.
7. Chatelut E, Hendriks JJMA, Martin J, Ciccolini J, Moes DJAR. Unraveling the complexity of therapeutic drug monitoring for monoclonal antibody therapies to individualize dose in oncology. *Pharmacology research & perspectives.* 2021;9(2):e00757-e00757. <https://doi.org/10.1002/prp2.757>.
8. Sehgal K, Costa DB, Rangachari D. Extended-interval dosing strategy of immune checkpoint inhibitors in lung cancer: Will it outlast the COVID-19 Pandemic? *Front Oncol.* 2020;10:1193-1193. <https://doi.org/10.3389/fonc.2020.01193>.
9. Brown K, Comisar C, Witjes H, Maringwa J, de Greef R, Vishwanathan K, et al. Population pharmacokinetics and exposure-response of osimertinib in patients with non-small cell lung cancer. *Br J Clin Pharmacol.* 2017;83(6):1216-1226. <https://doi.org/10.1111/bcp.13223>.
10. Kwok WC, Ho JCM, Tam TCC, Lui MMS, Ip MSM, Lam DCL. Efficacy of gefitinib at reduced dose in EGFR mutant non-small cell lung carcinoma. *Anticancer Drugs.* 2019;30(10):1048-1051. <https://doi.org/10.1097/cad.0000000000000849>.
11. Nakamura A, Tanaka H, Saito R, Suzuki A, Harada T, Inoue S, et al. Phase II study of low-dose afatinib maintenance treatment among patients with EGFR-mutated non-small cell lung cancer: North Japan Lung Cancer Study Group Trial 1601 (NJLCG1601). *The Oncologist.* 2020;25(10):e1451-e1456. <https://doi.org/10.1634/theoncologist.2020-0545>.
12. Lampson BL, Nishino M, Dahlberg SE, Paul D, Santos AA, Jänne PA, et al. Activity of erlotinib when dosed below the maximum tolerated dose for EGFR-mutant lung cancer: Implications for targeted therapy development. *Cancer.* 2016;122(22):3456-3463. <https://doi.org/10.1002/cncr.30270>.
13. Latz JE, Chaudhary A, Ghosh A, Johnson RD. Population pharmacokinetic analysis of ten phase II clinical trials of pemetrexed in cancer patients. *Cancer Chemother Pharmacol.* 2006;57(4):401-411. <https://doi.org/10.1007/s00280-005-0036-1>.
14. Mangoni AA, Jackson SHD. Age-related changes in pharmacokinetics and pharmacodynamics: basic principles and practical applications. *Br J Clin Pharmacol.* 2004;57(1):6-14. <https://doi.org/10.1046/j.1365-2125.2003.02007.x>.
15. Maksimovic-Ivanic D, Fagone P, McCubrey J, Bendtzen K, Mijatovic S, Nicoletti F. HIV-protease inhibitors for the treatment of cancer: Repositioning HIV protease inhibitors while developing more potent NO-hybridized derivatives? *Int J Cancer.* 2017;140(8):1713-1726. <https://doi.org/10.1002/ijc.30529>.
16. Mueller-Schoell A, Groenland SL, Scherf-Clavel O, van Dyk M, Huisinga W, Michelet R, et al. Therapeutic drug monitoring of oral targeted anti-neoplastic drugs. *Eur J Clin Pharmacol.* 2021;77(4):441-464. <https://doi.org/10.1007/s00228-020-03014-8>.

17. Groenland SL, Mathijssen RHJ, Beijnen JH, Huitema ADR, Steeghs N. Individualized dosing of oral targeted therapies in oncology is crucial in the era of precision medicine. *Eur J Clin Pharmacol*. 2019;75(9):1309-1318. <https://doi.org/10.1007/s00228-019-02704-2>.
18. Cano JP, Bruno R, Lena N, Favre R, Iliadis A, Imbert AM. Dosage predictions in high-dose methotrexate infusions. Part 1: Evaluation of the classic test-dose protocol. *Cancer Drug Deliv*. 1985;2(4):271-276. <https://doi.org/10.1089/cdd.1985.2.271>.
19. Kangarloo SB, Naveed F, Ng ESM, Chaudhry MA, Wu J, Bahlis NJ, et al. Development and validation of a test dose strategy for once-daily i.v. busulfan: importance of fixed infusion rate dosing. *Biol Blood Marrow Transplant*. 2012;18(2):295-301. <https://doi.org/10.1016/j.bbmt.2011.07.015>.
20. Chabner BA, Young RC. Threshold methotrexate concentration for in vivo inhibition of DNA synthesis in normal and tumorous target tissues. *J Clin Invest*. 1973;52(8):1804-1811. <https://doi.org/10.1172/jci107362>.
21. Ackland SP, Schilsky RL. High-dose methotrexate: a critical reappraisal. *J Clin Oncol*. 1987;5(12):2017-2031. <https://doi.org/10.1200/jco.1987.5.12.2017>.
22. Ellman MH, Telfer MC, Turner AF. Benefit of G-CSF for methotrexate-induced neutropenia in rheumatoid arthritis. *Am J Med*. 1992;92(3):337-338. [https://doi.org/10.1016/0002-9343\(92\)90088-S](https://doi.org/10.1016/0002-9343(92)90088-S).
23. Rodríguez-Abreu D, Powell SF, Hochmair MJ, Gadgeel S, Esteban E, Felip E, et al. Pemetrexed plus platinum with or without pembrolizumab in patients with previously untreated metastatic nonsquamous NSCLC: protocol-specified final analysis from KEYNOTE-189. *Ann Oncol*. 2021;32(7):881-895. <https://doi.org/10.1016/j.annonc.2021.04.008>.
24. Noronha V, Patil VM, Joshi A, Menon N, Chougule A, Mahajan A, et al. Gefitinib versus gefitinib plus pemetrexed and carboplatin chemotherapy in EGFR-mutated lung cancer. *J Clin Oncol*. 2020;38(2):124-136. <https://doi.org/10.1200/jco.19.01154>.





# Summary



## SUMMARY

In the current era of precision medicine in oncology, the tailoring of treatment of patients on the (molecular) characteristics of the tumor is widely performed. However, for many drugs, the full spectrum of precision medicine is not yet implemented in routine practice. The doses of drugs are still mostly based on the one-size-fits-all dosing approach. Nonetheless, the clinical pharmacology of these drugs suggests and warrants for the optimization of the current strategies. With the high incidence of non-small cell lung cancer (NSCLC), even minor improvements in the current dosing of the therapeutic options for this indication could have a high impact on the efficacy, toxicity and costs of treatment and the quality of life. In this thesis, parts of the knowledge gaps on dose optimizations for several therapeutic options of NSCLC are elucidated.

The aim of **Part I, Chapter 1** was to discuss the rationale of dose optimizations for the small-molecule inhibitors (SMIs), cytostatic agents and monoclonal antibodies in the treatment of NSCLC. For many of these therapeutic options, pharmacological knowledge becomes more abundant and often support the added value for dose optimizations with regard to treatment efficacy, toxicity, prescriber convenience and costs.

**Part II** described the rationale and impact of inhibition of the metabolic enzymes of SMIs and cytostatic agents.

In **Chapter 2.1**, the intratumoral expression of cytochrome P450 (CYP) 3A4, 3A5 and 2C8 in solid tumors was discussed. Although published data was conflicting, a trend towards higher CYP3A4 expression was observed in malignant tissue. As a result, it was advocated that higher CYP3A4 expression was associated with worse treatment outcomes after taxane therapy. Moreover, it was also shown that these therapies could induce intratumoral CYP3A4 expression during treatment. Concomitant intake of a CYP3A4 inhibitor (for example ritonavir) has been shown to decrease this potential resistance mechanism. In addition, it has been found that these inhibitors might yield additional antitumor efficacy by itself. These findings suggested a promising role for intratumoral CYP3A4 inhibition to counteract resistance mechanisms of therapies.

**Chapter 2.2** focused on the feasibility of the concomitant intake of SMIs and ritonavir. Erlotinib was set as an example-SMI in this open-label, single-arm, cross-over study. For the analysis, pharmacokinetic samples were drawn in nine patients during steady-state at 150 mg once daily (QD) erlotinib (control arm) and during steady-state at 75 mg QD erlotinib and 200 mg QD ritonavir (intervention arm). Exposure parameters for both dosing strategies were similar with a relative geometric mean of the systemic exposure over 24 h maximum plasma concentrations and trough concentrations of the intervention arm compared to the control arm of 99% (95% confidence interval (CI): 58-169%), 91% (95% CI: 55-149%) and 106% (95% CI: 59-193%), respectively. The findings of this study could serve as an example for other (expensive) therapies metabolized by CYP3A4.

Predictors of pharmacokinetics of the therapeutic options for NSCLC were described and evaluated in **Part III**. Both covariate-based as pharmacokinetically-guided dose optimizations were described in this part.

Although renal function is an important determinant for the systemic exposure of pemetrexed, dose individualization based on this parameter is not readily performed. In **Chapter 3.1**, the current position of the pemetrexed dosing paradigm was sketched. A contraindication for treatment exists for patients with a moderate to severe decreased renal function. Since pemetrexed itself might result in a deterioration of renal function, effective therapy is often withheld for patients crossing the renal function threshold. In general, individualized dosing of pemetrexed based on renal function could be of added value to maintain effective therapy while minimalizing the toxicities.

Moreover, in **Chapter 3.2**, the impact of renal function on the exposure of pemetrexed was assessed in a pharmacokinetic analysis. The pharmacokinetic data of 47 patients was best described by a three-compartment model with the estimated glomerular filtration rate (eGFR, assessed with the Chronic Kidney Disease–Epidemiology Collaboration (CKD-EPI) equation)) as a linear covariate on the clearance of pemetrexed. It was observed that renal function contributed more to the clearance of pemetrexed than initially thought (84% versus 50%). This finding highlighted the importance of the individual renal function on the pharmacokinetics of pemetrexed.

A multicenter randomized controlled trial was conducted and described in **Chapter 3.3**. In this study the superiority of an optimized, renal function-based dosing of pemetrexed was compared to the conventional body surface area (BSA)-based dosing in patients with an adequate renal function (eGFR > 45 mL/min). The individual exposure to pemetrexed was calculated and compared with a predefined pharmacokinetic target of 164 mg·h/L ( $\pm$  25%). In total, 37 patients were dosed following the optimized dosing strategy and 44 patients with the conventional BSA-based dosing. The results showed that 89% of patients in the optimized dosing arm and 84% of patients in the BSA-based dosing arm attained this target ( $p = 0.436$ ). The study concluded that the optimized dosing of pemetrexed does not yield an added value on the attainment of a pharmacokinetic endpoint, safety or quality of life in comparison with the conventional dosing strategy.

In addition to individualized dosing based on patient covariates, it has been postulated that pharmacokinetically-guided dosing based on a test dose could serve as a predictor for the pharmacokinetics of a therapeutic dose. Therefore, **Chapter 3.4** described a proof-of-concept study in ten patients in which we investigated the feasibility of a low test dose of pemetrexed to predict the pharmacokinetics of a therapeutic dose. The study showed that there is a statistical significant relationship between the clearance of the test dose and the clearance of a full dose of pemetrexed (Spearman's rho: 0.758,  $p = 0.02$ ). However, from our results it may be debated that renal function is a more precise and accurate predictor of pemetrexed clearance, therefore questioning the use of microdosing to perform dose individualization.

The impact of older age on the pharmacokinetic exposure of gemcitabine and its metabolite, 2',2'-difluorodeoxyuridine (dFdU) was described in **Chapter 3.5**. In this pharmacokinetic study, age was handled both as continuous and categorical (< 70 years versus ≥ 70 years) covariate. In addition, allometric scaling, gender, renal function and treatment indication were included as covariates based on previous analyses. This study indicated that elderly patients have a statistically non-significant 20% increase in the volume of distribution of the central compartment of gemcitabine. This effect was not considered to be clinically relevant and, therefore, this study concluded that dose adaptation in elderly based on pharmacokinetic considerations should not be performed.

**Part IV** addressed the relationships between exposure to drugs and the efficacy and/or toxicity of the therapy.

**Chapter 4.1** focused on the exposure-response analysis of osimertinib in epidermal growth factor receptor (EGFR)-mutated NSCLC. This study included a total of 145 NSCLC patients and a combined number of 513 osimertinib plasma concentration samples. The exposure-efficacy relationship was explored using a previously defined exploratory pharmacokinetic threshold of 166 µg/L. The exposure to osimertinib was not statistically significant associated with progression-free survival (PFS) with a hazard ratio of 0.65 (95% CI: 0.42-1.02;  $p = 0.06$ ). This trend in the relationship between higher osimertinib exposure and shorter PFS was explained by the presence of worse prognostic markers for the patient group with higher osimertinib exposure, compared to the group of patients with lower osimertinib exposure. Only the presence of an oncogenic driver mutation, other than the exon 19 del or L858R mutation was found to statistically significant decrease the PFS with a hazard ratio of 2.46 (95% CI: 1.20-5.03;  $p = 0.01$ ). No relationship between osimertinib exposure and toxicity was observed. This study indicated that plasma concentrations of osimertinib is not a predictor for treatment outcome. Moreover, it postulated that lower doses of osimertinib might potentially be equivalently effective compared to the current approved dosing.

Patients with renal dysfunction, treated with pemetrexed, are more prone for the development of hematological toxicities. In an earlier study, a linear relationship between the exposure to pemetrexed and the inhibition of the proliferation rate of neutrophils has been described. Based on these findings, we studied a renal function-based dosing strategy in patients with impaired renal function. However, because of unexpected toxicities in these patients, the study was prematurely halted. **Chapter 4.2** described the analysis of the pemetrexed exposure-neutropenia relationship. This pharmacokinetic analysis was based on the data of the halted clinical study ( $n = 3$ ) and supplemented with data from a phase I study ( $n = 106$ ). In our study, we found that the development of neutropenia during treatment with pemetrexed is most likely driven by a threshold toxicity concentration relationship. This found exposure-toxicity relationship is different than the earlier assumed (linear) relationship. The observed threshold concentration for patients in the current clinical practice was 0.11 mg/mL. Moreover, this study also indicated that a neutropenia equivalent dose in patients with renal dysfunction is substantially lower than the current approved dose. Therefore, we postulated that the approved dose of pemetrexed in patients with impaired renal function could only be given when combined with prophylactic strategies for toxicity.

In **Chapter 4.3**, the relationship between pemetrexed exposure and the development of nephrotoxicity is described. In this retrospective analysis, 359 patients were included. In total 21% of the patients had a clinically relevant decline of their renal function and 8.1% of the patients were forced to discontinue pemetrexed treatment due to nephrotoxicity. The cumulative dose of pemetrexed ( $\geq 10$  cycles of therapy) was identified as risk factor for nephrotoxicity (adjusted odds ratio: 5.66 (95% CI: 1.73-18.54)). This study showed the risks of prolonged treatment with pemetrexed, which becomes more important since combination therapies with pemetrexed are becoming standard of care.

In conclusion, this thesis described several studies, which aimed to improve the dosing strategies for the treatment of NSCLC. It was concluded that for many drugs a rationale for dose optimization is present. The landscape of the therapeutic window should first be assessed, followed by the identification of predictors for the systemic exposure of the drug. Finally, based on this information, efforts could be made to ensure that the individual patient is dosed the most optimal dosing with regard to efficacy, toxicity, quality of life and financial burden. Implementation of these considerations might prove valuable in the quest to optimize precision medicine in clinical practice.







# Nederlandse samenleving



## NEDERLANDSE SAMENVATTING

In het huidige tijdperk van de precisiegeneeskunde in de oncologie worden patiënten al vaak op maat behandeld op basis van de (moleculaire) karakteristieken van de tumor. Echter, hiermee wordt niet de volle potentie van de precisiegeneeskunde benut in de huidige klinische praktijk. Geneesmiddelen worden namelijk vaak nog gedoseerd in een dosering die voor iedere patiënt hetzelfde is. Desalniettemin wijst de klinische farmacologie van veel anti-kankergeneesmiddelen erop dat de huidige doseerstrategieën geoptimaliseerd kunnen worden. Mede omdat niet-kleincellig longkanker (NSCLC) veel voorkomt, zullen kleine veranderingen in de huidige doseerstrategieën een grote impact kunnen hebben op de effectiviteit, toxiciteit en kosten van de behandeling en de kwaliteit van leven van de individuele patiënt. In dit proefschrift worden enkele hiaten in kennis met betrekking tot het optimaliseren van de doseerstrategieën van de behandeling van NSCLC besproken.

Het doel van **Deel 1, Hoofdstuk 1** was om de rationale achter de optimalisatie van de doseringen van de verschillende geneesmiddelen bij de behandeling van NSCLC (orale doelgerichte therapieën, klassieke chemotherapieën en monoclonale antilichamen) te bespreken. Voor vele van deze behandelopties is er al veel kennis beschikbaar en daarmee wordt het steeds duidelijker dat het optimaliseren van de doseringen bij kan dragen aan de effectiviteit en de toxiciteit en kosten van deze behandelingen kan verminderen.

**Deel 2** beschreef de rationale achter en het effect van het remmen van metaboliserende enzymen van de orale doelgerichte therapieën en chemotherapie.

In **Hoofdstuk 2.1** werd de intratumorale expressie van de cytochroom P450 (CYP) 3A4, 3A5 en 2C8 enzymen besproken. In de literatuur werden verschillende resultaten gevonden, maar over het algemeen lijkt de CYP3A4 expressie verhoogd te zijn in tumorweefsel ten opzichte van het gezonde weefsel. Een hogere CYP3A4 expressie leek ook geassocieerd te zijn met slechtere uitkomsten van therapieën met taxanen. Daarnaast leken de taxanen zelf een verhogend effect te hebben op de CYP3A4 expressie. Gelijktijdige inname van een CYP3A4-remmer (bijvoorbeeld ritonavir) zou dus een belangrijke rol kunnen spelen om dit potentiële resistentiemechanisme te ondervangen. Daarnaast werd gevonden dat deze CYP3A4-remmers ook nog via andere mechanismen de groei van de tumor kunnen verminderen. Kortom, deze bevindingen lieten zien dat de remming van intratumorale CYP3A4 waardevol kan zijn om resistentiemechanismen te doorbreken.

**Hoofdstuk 2.2** richtte zich op de gelijktijdige inname van orale doelgerichte therapieën en ritonavir. In deze studie werd erlotinib als een voorbeeld voor de orale doelgerichte therapieën gebruikt. Bij negen patiënten werd bloed afgenomen op twee tijdstippen: na inname van 150 mg iedere dag (QD) erlotinib (controle dosering) en na inname van 75 mg QD erlotinib en 200 mg QD ritonavir (interventie dosering). De blootstellingsparameters van beide doseerstrategieën was nagenoeg gelijk met een relatief geometrisch gemiddelde van de oppervlakte onder de plasmaconcentratie-tijd curve (AUC) over 24 uur, de topspiegel en de dalspiegel van 99%, 91% en

106%, respectievelijk. Deze resultaten suggereerden dat het verhogen van de blootstelling met ritonavir een veelbelovende strategie is om de dosering van erlotinib en daarmee de kosten van de therapie te verlagen. Deze strategie zou wellicht ook geïmplementeerd kunnen worden voor andere dure therapieën die via CYP3A4 gemetaboliseerd worden.

Voorspellers van de farmacokinetiek van de behandelopties voor NSCLC werden beschreven en geëvalueerd in **Deel III**. Zowel covariaat-gebaseerde als farmacokinetiek-geleide optimalisaties van de doseringen werden hier onderzocht.

Alhoewel de nierfunctie een belangrijke determinant is voor de systemische blootstelling van pemetrexed, wordt een individualisering op basis van deze parameter nog niet uitgevoerd. In **Hoofdstuk 3.1** werd de huidige doseerstrategie van pemetrexed geschetst. Op dit moment bestaat er een contra-indicatie voor behandeling van patiënten met een matige tot slechte nierfunctie. Gezien pemetrexed zelf ook een negatief effect op de nierfunctie heeft, wordt effectieve therapie vaak onthouden voor patiënten die tijdens therapie een vermindering in de nierfunctie ondervinden. Samengevat, kan een geïndividualiseerde dosering op basis van de nierfunctie van toegevoegde waarde zijn om deze effectieve therapeutische optie te behouden en de kans op bijwerkingen te verminderen.

In **Hoofdstuk 3.2** werd het effect van de nierfunctie op de blootstelling aan pemetrexed in een farmacokinetische analyse onderzocht. De farmacokinetische data van 47 patiënten werd het best beschreven door een drie-compartiment model met de geschatte glomerulaire filtratie snelheid (eGFR, bepaald met de Chronic Kidney Disease-Epidemiology Collaboration (CKD-EPI) formule) als een lineaire covariaat op de klaring van pemetrexed. Het effect van nierfunctie op de klaring van pemetrexed was hoger dan aanvankelijk gedacht (84% versus 50%). Met deze bevinding werd het belang van de individuele nierfunctie op de farmacokinetiek van pemetrexed onderstreept.

Een gerandomiseerde studie in meerdere ziekenhuizen in Nederland werd uitgevoerd en beschreven in **Hoofdstuk 3.3**. In dit onderzoek werd de meerwaarde van een geoptimaliseerde, op nierfunctie-gebaseerde dosering met pemetrexed ten opzichte van de conventionele lichaamsoppervlakte (BSA)-gebaseerde dosering onderzocht in patiënten met een adequate nierfunctie (> 45 mL/min). De blootstelling aan pemetrexed werd per patiënt berekend en vergeleken met een eerder vastgestelde streefwaarde voor de farmacokinetische blootstelling van 164 mg·h/L (± 25%). In totaal werden er 37 patiënten gedoseerd met de geoptimaliseerde dosering en 44 patiënten geïnccludeerd in de BSA-gebaseerde doseringsarm. In de geoptimaliseerde arm was de blootstelling pemetrexed in 89% van de patiënten binnen het farmacokinetische target en in de BSA-gebaseerde doseringsarm was dit 84% ( $p = 0.436$ ). Een geoptimaliseerde dosering op basis van nierfunctie in patiënten met een adequate nierfunctie had geen toegevoegde waarde op basis van een farmacokinetisch eindpunt, op veiligheid of op de kwaliteit van leven in vergelijking met de conventionele doseerstrategie.

Naast het doseren op basis van individuele covariaten zou de dosering ook geoptimaliseerd kunnen worden op basis van de farmacokinetiek van het middel in de individuele patiënt. Hierbij zou een testdosering toegediend kunnen worden die als voorspeller voor een therapeutische dosering fungeert. In **Hoofdstuk 3.4** werd dit in tien patiënten geëvalueerd, waarbij de farmacokinetiek van een zeer lage test dosis werd vergeleken met de farmacokinetiek van pemetrexed na een therapeutische dosering. De studie liet een statistisch significante relatie zien tussen de klaring van de test dosis en de klaring van de volledige dosering van pemetrexed (Spearman's rho: 0.758,  $p = 0.02$ ). Desalniettemin, bleek nierfunctie een betere voorspeller te zijn van de farmacokinetiek van pemetrexed. Gezien deze strategie minder invasief is voor de patiënt, verdient deze de voorkeur boven de toediening van de test dosis.

Het effect van een oudere leeftijd op de farmacokinetische blootstelling van gemcitabine en haar metaboliet, 2',2'-difluorodeoxyuridine (dFdU) werd beschreven in **Hoofdstuk 3.5**. In deze farmacokinetische studie werd leeftijd zowel als continue als categorische (< 70 jaar versus  $\geq 70$  jaar) covariaat onderzocht. Allometrische schaling, geslacht, nierfunctie en tumortype werden – gebaseerd op voorgaande analyses – ook geïncorporeerd als covariaat. De studie liet een niet-statistisch significante toename van 20% zien van het verdelingsvolume van het centrale compartiment van gemcitabine in ouderen. Dit effect was niet klinisch relevant en dosisaanpassingen op basis van farmacokinetische redenen zijn daarom niet nodig in de oudere populatie.

**Deel IV** richtte zich op de relatie tussen blootstelling aan geneesmiddelen en de effectiviteit en/of toxiciteit van de behandeling.

**Hoofdstuk 4.1** richtte zich op de blootstelling-respons relatie van osimertinib in epidermal growth factor receptor (EGFR)-gemuteerde NSCLC. In deze studie werden in totaal 145 patiënten met NSCLC geïncorporeerd, waarbij een gecombineerd aantal van 513 osimertinib plasmaconcentraties gemeten waren. De blootstellings-effectiviteit relatie werd onderzocht met behulp van een vooraf vastgestelde farmacokinetische streefwaarde van 166  $\mu\text{g}/\text{L}$ . De blootstelling van osimertinib was niet statistisch significant gerelateerd met de progressie-vrije overleving (PFS) met een hazard ratio van 0,65 (95% betrouwbaarheidsinterval (BI): 0,42-1,02;  $p = 0.06$ ). De trend in de relatie tussen de hogere osimertinib blootstelling en een verminderde PFS kon verklaard worden door de aanwezigheid van slechtere prognostische markers in de groep met hogere blootstelling in vergelijking met de groep met een lagere osimertinib blootstelling. De aanwezigheid van een oorzakelijke mutatie in een oncogen, anders dan de exon 19 deletie of L858R mutatie, werd geassocieerd met een statistisch significante vermindering van de PFS met een hazard ratio van 2,45 (95% BI: 1,20-5,03;  $p = 0.01$ ). Er werd geen relatie gevonden tussen de blootstelling aan osimertinib en de klinisch relevante bijwerkingen. De studie suggereerde dat de plasmaconcentraties van osimertinib geen voorspeller is voor de behandeluitkomsten. Bovendien zou het toedienen van lagere doseringen van osimertinib even effectief kunnen zijn als de huidige doseringen.

Het is bekend dat patiënten met een verminderde nierfunctie, die behandeld worden met pemetrexed, meer risico lopen op de ontwikkeling van hematologische bijwerkingen. In een eerdere studie werd een lineaire relatie gevonden tussen de blootstelling aan pemetrexed en de remming van de proliferatie van neutrofielen. Op basis van deze bevindingen hebben wij vervolgens een nierfunctie-gebaseerde doseringsstrategie onderzocht in patiënten met een verminderde nierfunctie. Helaas werden er bij deze doseerstrategie veel onverwachte bijwerkingen gezien en werd deze studie gepauzeerd. In **Hoofdstuk 4.2** werd de analyse van de pemetrexed blootstelling-neutropenie relatie beschreven. Deze farmacokinetische analyse werd gebaseerd op onze vroegtijdig stopgezette studie (n = 3) en aangevuld met data van een fase I studie (n = 106). Onze studie liet zien dat neutropenie hoogstwaarschijnlijk gedreven wordt door een toxiciteit drempelwaarde concentratie. Deze relatie is dus wezenlijk anders dan de eerder beschreven lineaire relatie. Voor patiënten in de huidige klinische praktijk werd een drempelwaarde concentratie van 0,11 mg/mL pemetrexed gevonden. Daarnaast voorspelde deze studie dat een dosering die tot eenzelfde neutropene response leidt in patiënten met een verminderde nierfunctie substantieel lager is dan de geregistreerde dosering. Toediening van de geregistreerde dosering pemetrexed in patiënten met een verminderde nierfunctie zal alleen mogelijk zijn als deze gecombineerd wordt met profylactische strategieën tegen de hematologische bijwerkingen.

In **Hoofdstuk 4.3** werd de relatie tussen de blootstelling aan pemetrexed en de ontwikkeling van nierschade beschreven. In deze retrospectieve studie werden 359 patiënten geïncludeerd. In totaal werd bij 21% van deze patiënten een klinisch relevante vermindering van de nierfunctie gevonden en moest de therapie gestopt worden bij 8,1% van de patiënten doordat hun nierfunctie te ver achteruitgegaan was. Een cumulatieve dosering van pemetrexed ( $\geq 10$  cycli) werd geïdentificeerd als een risicofactor voor nierschade (adjusted odds ratio van 5,66 (95% BI: 1,73-18,54)). De studie liet zien dat herhaalde blootstelling aan pemetrexed risicovol is. Dit is vooral belangrijk omdat pemetrexed steeds vaker en langer gebruikt wordt als combinatietherapie bij de behandeling van NSCLC.

Samenvattend, beschrijft dit proefschrift verscheidene studies die zich richten op de verbetering van doseerstrategieën bij de behandeling van NSCLC. Voor vele van de geneesmiddelen is een rationale voor deze optimalisatie aanwezig. Eerst dient het speelveld voor de optimalisaties volledig in kaart gebracht te worden door het therapeutische venster van de individuele therapieën vast te stellen. Daarna kunnen voorspellers voor de blootstelling en de uitkomsten van de behandelingen onderzocht worden. Ten slotte, als deze informatie bekend is, kunnen de daaruit volgende dosis optimalisaties geïmplementeerd worden om een optimale balans in effectiviteit, toxiciteit, kwaliteit van leven en kosten te vinden.







# Author affiliations



## AUTHOR AFFILIATIONS

<b>Joachim G.J.V. Aerts</b>	Department of Pulmonary Medicine, Erasmus Medical Center, Rotterdam, The Netherlands
<b>Paul Baas</b>	Department of Thoracic Oncology, The Netherlands Cancer Institute - Antoni van Leeuwenhoek, Amsterdam, The Netherlands
<b>Jos H. Beijnen</b>	Department of Pharmacy & Pharmacology, The Netherlands Cancer Institute - Antoni van Leeuwenhoek, Amsterdam, The Netherlands  Department of Pharmaceutical Sciences, Utrecht University, Utrecht, The Netherlands
<b>Bonne Biesma</b>	Department of Pulmonary Diseases, Jeroen Bosch Hospital, 's-Hertogenbosch, The Netherlands
<b>Heidi van de Bruinhorst</b>	Utrecht University, School of Pharmacy, Utrecht, The Netherlands
<b>David M. Burger</b>	Department of Pharmacy, Radboud Institute for Health Sciences, Radboud University Medical Center, Nijmegen, The Netherlands
<b>Jacobus A. Burgers</b>	Department of Thoracic Oncology, The Netherlands Cancer Institute - Antoni van Leeuwenhoek, Amsterdam, The Netherlands
<b>Sander Croes</b>	Department of Clinical Pharmacy & Toxicology, Maastricht University Medical Centre, Maastricht, The Netherlands
<b>Marie-Rose B.S. Crombag</b>	Department of Hospital Pharmacy, Erasmus Medical Center, Rotterdam, The Netherlands
<b>Hieronymus J. Derijks</b>	Department of Pharmacy, Radboud Institute for Health Sciences, Radboud University Medical Center, Nijmegen, The Netherlands  Department of Pharmacy Jeroen Bosch Hospital, 's-Hertogenbosch, The Netherlands
<b>Anne-Marie C. Dingemans</b>	Department of Pulmonary Diseases, GROW - School for Oncology and Developmental Biology, Maastricht University Medical Centre, Maastricht, The Netherlands  Department of Pulmonary Medicine, Erasmus Medical Center, Rotterdam, The Netherlands
<b>Thomas P.C. Dorlo</b>	Department of Pharmacy & Pharmacology, The Netherlands Cancer Institute - Antoni van Leeuwenhoek, Amsterdam, The Netherlands
<b>Daphne W. Dumoulin</b>	Department of Pulmonary Medicine, Erasmus Medical Center, Rotterdam, The Netherlands
<b>Maarten van Eijk</b>	Department of Pharmacy & Pharmacology, The Netherlands Cancer Institute - Antoni van Leeuwenhoek, Amsterdam, The Netherlands
<b>Nielka P. van Erp</b>	Department of Pharmacy, Radboud Institute for Health Sciences, Radboud University Medical Center, Nijmegen, The Netherlands
<b>Cornedine J. de Gooijer</b>	Department of Thoracic Oncology, The Netherlands Cancer Institute - Antoni van Leeuwenhoek, Amsterdam, The Netherlands
<b>Stefanie L. Groenland</b>	Department of Medical Oncology and Clinical Pharmacology, The Netherlands Cancer Institute - Antoni van Leeuwenhoek, Amsterdam, The Netherlands

<b>Rob ter Heine</b>	Department of Pharmacy, Radboud Institute for Health Sciences, Radboud University Medical Center, Nijmegen, The Netherlands
<b>Lizza E.L. Hendriks</b>	Department of Pulmonary Diseases, GROW - School for Oncology and Developmental Biology, Maastricht University Medical Centre, Maastricht, The Netherlands.
<b>Michel M. van den Heuvel</b>	Department of Pulmonology, Radboud University Medical Center, Nijmegen, The Netherlands
<b>Luuk B. Hilbrands</b>	Department of Nephrology, Radboud University Medical Center, Nijmegen, The Netherlands
<b>Alwin D.R. Huitema</b>	Department of Pharmacy & Pharmacology, The Netherlands Cancer Institute - Antoni van Leeuwenhoek, Amsterdam, The Netherlands  Department of Pharmacology Princess Máxima Center for Pediatric Oncology, Utrecht, The Netherlands  Department of Clinical Pharmacy, University Medical Center Utrecht, Utrecht University, Utrecht, The Netherlands
<b>Merel Jebbink</b>	Department of Thoracic Oncology, The Netherlands Cancer Institute - Antoni van Leeuwenhoek, Amsterdam, The Netherlands
<b>Adrianus J. de Langen</b>	Department of Thoracic Oncology, The Netherlands Cancer Institute - Antoni van Leeuwenhoek, Amsterdam, The Netherlands
<b>Ron H.J. Mathijssen</b>	Department of Medical Oncology, Erasmus Medical Center, Rotterdam, The Netherlands
<b>Pim Moeskops</b>	Quantib, Rotterdam, The Netherlands
<b>Vincent van der Noort</b>	Department of Biometrics, The Netherlands Cancer Institute - Antoni van Leeuwenhoek, Amsterdam, The Netherlands
<b>Berber Piet</b>	Department of Pulmonary Diseases, Radboud University Medical Center, Nijmegen, The Netherlands
<b>Melinda A. Pruis</b>	Department of Pulmonary Medicine, Erasmus Medical Center, Rotterdam, The Netherlands  Department of Medical Oncology, Erasmus Medical Center, Rotterdam, The Netherlands
<b>Nikki de Rouw</b>	Department of Pharmacy, Radboud Institute for Health Sciences, Radboud University Medical Center, Nijmegen, The Netherlands  Department of Pharmacy, Jeroen Bosch Hospital, 's-Hertogenbosch, The Netherlands
<b>Alfred H. Schinkel</b>	Division of Pharmacology, The Netherlands Cancer Institute - Antoni van Leeuwenhoek, Amsterdam, The Netherlands
<b>Egbert F. Smit</b>	Department of Thoracic Oncology, The Netherlands Cancer Institute - Antoni van Leeuwenhoek, Amsterdam, The Netherlands
<b>Neeltje Steeghs</b>	Department of Medical Oncology and Clinical Pharmacology, The Netherlands Cancer Institute - Antoni van Leeuwenhoek, Amsterdam, The Netherlands

---

<b>Elin M. Svensson</b>	Department of Pharmacy, Radboud Institute for Health Sciences, Radboud University Medical Center, Nijmegen, The Netherlands
	Department of Pharmaceutical Biosciences, Uppsala University, Uppsala, Sweden
<b>Wouter B. Veldhuis</b>	Department of Radiology, University Medical Center Utrecht, Utrecht University, Utrecht, The Netherlands
<b>Bianca A.M.H. van Veggel</b>	Department of Thoracic Oncology, The Netherlands Cancer Institute - Antoni van Leeuwenhoek, Amsterdam, The Netherlands
<b>Anthonie J. van der Wekken</b>	Department of Pulmonary Diseases, University of Groningen, University Medical Center Groningen, Groningen, The Netherlands

---



# List of publications





## LIST OF PUBLICATIONS

### Published

1. **Boosman RJ**, Crombag MBS, van Erp NP, Beijnen JH, Steeghs N, Huitema ADR. Is age just a number? A population pharmacokinetic study of gemcitabine. *Cancer Chemother Pharmacol*. 2022 [Epub ahead of print].
2. **Boosman RJ**, de Gooijer CJ, Groenland SL, Burgers JA, Baas P, van der Noort V, Beijnen JH, Huitema ADR, Steeghs N. Ritonavir-boosted exposure of kinase inhibitors: an open label, single-arm pharmacokinetic proof-of-concept trial with erlotinib. *Pharm Res*. 2022 [Epub ahead of print].
3. **Boosman RJ**, Burgers JA, Smit EF, Steeghs N, van der Wekken AJ, Beijnen JH, Huitema ADR, ter Heine R. Optimized dosing: the next step in precision medicine of non-small cell lung cancer. *Drugs*. 2022;82(1):15-32.
4. de Rouw N, de Boer M, **Boosman RJ**, van den Heuvel MM, Burger DM, Lieveerse JE, Derijks HJ, Frederix GWJ, ter Heine R. The pharmaco-economic benefits of pemetrexed dose individualization in lung cancer patients. *Clin Pharmacol Ther*. 2022 [Epub ahead of print].
5. van Ewijk-Beneken Kolmer EWJ, Teulen MJA, **Boosman RJ**, de Rouw N, Burgers JA, ter Heine R. Highly sensitive quantification of pemetrexed in human plasma using UPLC-MS/MS to support microdosing studies. *Biomed Chromatogr*. 2022;36(2):e5277.
6. de Rouw N, Derijks HJ, Hilbrands LB, **Boosman RJ**, Piet B, Koolen SLW, Burgers JA, Dingemans AC, van den Heuvel MM, Hendriks LEL, Aerts JGJV, Croes S, Mathijssen RHJ, Huitema ADR, Burger DM, Biesma B, ter Heine R. Hyperhydration with cisplatin does not influence pemetrexed exposure. *Br J Clin Pharmacol*. 2022;88(2):871-876.
7. **Boosman RJ**, Dorlo TPC, de Rouw N, Burgers JA, Dingemans AC, van den Heuvel MM, Hendriks LEL, Biesma B, Aerts JGJV, Croes S, Mathijssen RHJ, Huitema ADR, ter Heine R. Toxicity of pemetrexed during renal impairment explained - implications for safe treatment. *Int J Cancer*. 2021;149(8):1576-1584.
8. de Rouw N, **Boosman RJ**, Huitema ADR, Hilbrands LB, Svensson EM, Derijks HJ, van den Heuvel MM, Burger DM, ter Heine R. Rethinking the application of pemetrexed for patients with renal impairment: A pharmacokinetic analysis. *Clin Pharmacokinet*. 2021;60(5):649-654.
9. de Rouw N, **Boosman RJ**, van de Bruinhorst H, Biesma B, van den Heuvel MM, Burger DM, Hilbrands LB, ter Heine R, Derijks HJ. Cumulative pemetrexed dose increases the risk of nephrotoxicity. *Lung Cancer*. 2020;146:30-35.

10. **Boosman RJ\***, van Eijk M\*, Schinkel AH, Huitema ADR, Beijnen JH. Cytochrome P450 3A4, 3A5, and 2C8 expression in breast, prostate, lung, endometrial, and ovarian tumors: relevance for resistance to taxanes. *Cancer Chemother Pharmacol.* 2019;84(3):487-499.
11. **Boosman RJ**, Burgers JA. Optimisation of chemotherapy in the era of immunotherapy. *Eur Respir J.* 2018;52(4):1801698.
12. Manka P, Coombes JD, **Boosman RJ**, Gauthier K, Papa S, Syn WK. Thyroid hormone in the regulation of hepatocellular carcinoma and its microenvironment. *Cancer Lett.* 2018;419:175-186.
13. Visser CJ, Weggemans OAF, **Boosman RJ**, Loos KU, Frijlink HW, Woerdenbag HJ. Increased drug load and polymer compatibility of bilayered orodispersible films. *Eur J Pharm Sci.* 2017;107:183-190.

#### Submitted

1. **Boosman RJ\***, de Rouw N\*, Burgers JA, Huitema ADR, Dingemans AC, Derijks HJ, Burger DM, Piet B, Hendriks LEL, Biesma B, Pruis MA, Dumoulin DW, Croes S, Mathijssen RHJ, van den Heuvel MM, ter Heine R. Optimized versus standard dosing of pemetrexed – a randomized controlled trial. *Submitted.*
2. **Boosman RJ**, de Rouw N, Huitema ADR, Burgers JA, ter Heine R. Prediction of the pharmacokinetics of pemetrexed with a low test dose: a proof-of-concept study. *Submitted.*
3. **Boosman RJ\***, Jebbink M\*, Veldhuis WB, Groenland SL, van Veggel BAMH, Moeskops P, de Langen AJ, Beijnen JH, Smit EF, Huitema ADR, Steeghs N. Exposure-response analysis of osimertinib in EGFR mutation positive non-small cell lung cancer patients in a real-life setting. *Submitted.*

#### In preparation

1. **Boosman RJ**, Bol K, Huitema ADR. Population pharmacokinetic modelling of MCLA-117, a bispecific monoclonal antibody for the treatment of acute myeloid leukemia. *In preparation.*

\*These authors contributed equally and thus share first authorship





# Dankwoord



## DANKWOORD

Bijna vier jaar geleden begon het avontuur in het AvL, waarvan dit proefschrift het resultaat is. In die periode heb ik ontzettend veel geleerd, gelachen en een ontzettend fijne tijd gehad. Eén van de eerste dingen die ik leerde was dat je onderzoek nooit alleen doet. Zonder de hulp en inzet van velen was het onderzoek niet geworden wat het nu is. Ik wil daarbij een aantal mensen in het bijzonder benoemen.

Allereerst wil ik alle **patiënten** bedanken die mee hebben gedaan aan de klinische studies die beschreven zijn in dit proefschrift. Het is bewonderingswaardig hoe veel van hen met altruïstische motieven bij wilden dragen aan de wetenschap om hun medemens te helpen. Zonder hen was het onmogelijk geweest om deze onderzoeken uit te voeren.

**Alwin**, ik kan mij geen betere promotor voorstellen. Je bent een inspiratiebron die problemen op een gestructureerde manier aanpakt en bijna altijd wel een idee heeft om tot een verbetering te komen. Ik ben je super dankbaar voor de kansen die je mij hebt gegeven, dat je in mij geloofde en daarbij ook als mentor wilde optreden. Jouw enthousiasme werkte veelal aanstekelijk en leidde er vaak toe dat ik vol frisse moed weer jouw kantoor verliet.

**Rob**, ik heb er super veel respect voor hoe jij alle ballen in de lucht kan houden. Jouw razendsnelle feedback, waarin jij zelfs kritischer was dan Alwin (ja, het bestaat echt), hebben het niveau van de manuscripten zeker naar een hoger niveau getild. Nikki en ik hebben jou wel vaker dan eens de bijnaam 'word-wizard' gegeven en dat is niet voor niets. Jij hebt het vermogen om mensen op de juiste manier te enthousiasmeren voor het doen van onderzoek. Ik ben jou dankbaar dat jij dit effect ook op mij hebt gehad, mede dankzij jou kijk ik terug op een ontzettend leerzame ervaring die ik voor geen goud wilde missen.

**Neeltje**, als enige arts in mijn promotieteam zorgde jij ervoor dat de kliniek en het onderzoek met elkaar verweven werden. Ook al was jouw agenda altijd bomvol, jij maakte altijd tijd voor mij vrij als ik eventjes wilde sparren. Bedankt voor de goede begeleiding en alle inzichten die jij hebt geboden de afgelopen jaren.

**Jos**, jouw commentaar op manuscripten zorgde er altijd weer voor dat een eventuele tunnelvisie doorbroken werd. Met jouw kritische oog wist jij feilloos de zwakke punten te vinden en aanwijzingen te geven hoe dit verbeterd kon worden. Bedankt voor het vertrouwen dat jij vanaf de start van het onderzoek in mij had.

Beste leden van de **leescommissie**, ik wil jullie bedanken voor het lezen en beoordelen van mijn proefschrift.



**Frans**, jij maakte het voor mij mogelijk om de opleiding tot klinisch farmacoloog naast mijn onderzoek te doen. In de afgelopen vier jaar heb ik gezien hoe jij deze opleiding opnieuw hebt ingericht en hoe dit heeft geleid tot een ontzettend fijn leerklimaat. Dank voor al jouw goede zorgen!

**Sjaak**, als lokale hoofdonderzoeker op de IMPROVE studie in het AvL, verdien jij toch een apart plekje in mijn dankwoord. Ik kon altijd bij jou terecht voor vragen, super bedankt voor de goede en nauwe samenwerking. Ook wil ik alle andere **(long)oncologen** bedanken voor de fijne samenwerking en jullie inzet voor alle studies.

**Hilde, Niels, Bas** en alle andere **analisten**, zonder jullie was mijn proefschrift nooit op tijd afgekomen. Dank jullie wel dat jullie altijd voor mij klaar stonden, voor de sparmomentjes met betrekking tot de TDM en de welwillendheid om mijn samples zo snel te meten.

Ook zou ik graag de **coauteurs** van alle stukken willen bedanken voor hun kritische feedback en alle leuke discussies met betrekking tot de resultaten. Daarnaast ben ik ook dankbaar voor iedereen die op een andere manier heeft bijgedragen aan het onderzoek. In het bijzonder **Marianne**, voor al jouw hulp bij alle longkanker studies. **Carla**, voor jouw ondersteuning als CRA. Het **Trialbureau** voor de administratieve ondersteuning. De **planning farmacologie** voor het altijd mee willen denken met betrekking tot de planning van de individuele patiënt. De **verpleegkundig specialisten, researchverpleegkundigen** en **kinetiekverpleegkundige** van de Clinical Trial Unit en de **verpleegkundigen** van de dagbehandeling voor de prettige samenwerking de afgelopen jaren.

**Nikki**, zonder jou was het team niet compleet. Ik sta nog steeds versteld van jouw efficiëntie, intelligentie en het feit dat je jouw promotietraject tegelijkertijd met jouw opleiding tot ziekenhuisapotheker hebt volbracht. In de afgelopen jaren hebben wij een hechte band opgebouwd, waarbij we naast werk-gerelateerde adviezen ook privé situaties konden bespreken. Super bedankt voor alles!

**Kimberley**, ik ben super blij dat wij elkaar in het AvL hebben ontmoet, in de afgelopen jaren heb je mij geleerd dat er meer is dan alleen maar werk. Ik ben dankbaar dat wij vrienden geworden zijn en hoop jou en de kattenbende nog vaak te zien! Daarnaast wil ik je ook ontzettende bedanken dat je als paranimf naast mij wil staan tijdens mijn verdediging.

**Laura**, dankjewel dat jij mij wil bijstaan als paranimf. Ook onze vriendschap vindt zijn oorsprong in het AvL. Ik heb je leren kennen als een ontzettend goede apotheker met veel doorzettingsvermogen. Ik weet zeker dat jij heel binnenkort een opleidingsplek tot ziekenhuisapotheker bemachtigt en wens je nu alvast heel veel plezier.

**Lisa**, dankjewel dat jij zo af en toe mijn klankbord wilde zijn in de vroege ochtenden en tijdens de thee/koffie momenten, jouw manier van denken leidde altijd tot nieuwe inzichten. Ik ben ontzettend blij dat wij vrienden zijn geworden!

(Oud)-kamergenootjes, **Kimberley, Laura, Marit, Steffie, Willeke, Alaa** en **Pia**; door jullie ging ik altijd met heel veel plezier naar het AvL. De sfeer in onze 'James Bond' kamer (maar ook op de kamer-etentjes) was altijd superfijn, dank voor dit alles!

Alle **OIO's van H3**, bedankt voor de borrels, goede gesprekken, OIO-weekenden en Renesse retreats. De afgelopen jaren konden we helaas niet veel sociale activiteiten plannen, maar hopelijk halen we dit snel weer in.

Ook alle **vrienden** en **familie** wil ik bedanken voor hun steun tijdens de afgelopen vier jaar. In het bijzonder de **Farmacie Hulplijn: Zizi, Nathalie, Laura, Iris** en **Hans**; we zien elkaar nu veel minder dan tijdens de colleges en practica van de studie. Toch kan ik altijd bij jullie terecht voor een goed gesprek en ben ik dankbaar voor de welkome afleiding tijdens mijn PhD-traject. Ik heb genoten van onze escape rooms, etentjes, borrels, dubbel dates, wandelingen en kano-avonturen. **Jia Shu** en **Sinja**, ook jullie wil ik ontzettend bedanken. Ook al wonen we niet meer samen, ik ben super blij dat we elkaar nog wekelijks spreken en zo een goede band hebben.

**Papa** en **Mama**, bedankt voor jullie onvoorwaardelijke steun. Ook al staan er veel moeilijke woorden in de samenvattingen van de artikelen, jullie deden altijd je best om het te begrijpen. Ik ben er trots op dat ik zulke lieve ouders heb die zoveel voor mij over hebben. **Daphne** en **Jasper**, dank jullie wel voor jullie aanmoedigende woorden de afgelopen jaren.

Hey **Goes** (alias **Stefan**), ik weet dat jij al eens hebt gezegd dat ik jou niet hoeft te bedanken omdat jij niet hebt bijgedragen aan mijn proefschrift. Wat mij betreft is dat maar gedeeltelijk waar. Jouw enthousiasme, humor, onvoorwaardelijke steun en vermogen om mij echt gehoord te laten voelen hebben mij ontzettend geholpen met de laatste loodjes. Heel erg bedankt voor al jouw hulp en op naar ons volgende avontuur!



# Curriculum vitae



## CURRICULUM VITAE

René Boosman was born on July 23rd, 1994 in Assen, The Netherlands. After his high school graduation from the dr. Nassau College in Assen, he started the study Pharmacy at the University of Groningen in 2012. As part of his Masters' program, he performed a scientific internship at the department of Hepatology and Gastroenterology of the Essen University Hospital in Essen, Germany, focusing on the effects of thyroid hormone on the fibrotic responses of hepatic stellate cells. After his *summa cum laude* graduation in 2018, he started his PhD research at the department of Pharmacy & Pharmacology of the Netherlands Cancer Institute - Antoni van Leeuwenhoek Hospital, under the supervision of prof. dr. Alwin Huitema, prof. dr. Jos Beijnen, dr. Rob ter Heine and dr. Neeltje Steeghs. This PhD mainly focused on the dose optimizations of the therapeutic options used in the treatment of non-small cell lung cancer. During his PhD, he also trained as a clinical pharmacologist. As of January 2022, he started as a resident in the Onze Lieve Vrouwe Gasthuis (OLVG hospital) in Amsterdam, to become a hospital pharmacist.



